Cell/Cell and Cell/ECM interaction at the Nano-scale for Orthopaedic tissue engineering

By
Najla Ali M. Alburae

BSc in Biology
MSc in Histology and cytology
MRes in Cellular and molecular bioscience (Nanomedicine)

Thesis submitted for the degree of Doctor of Philosophy
Institute for Cellular medicine
Newcastle University, UK
March 2015

Declaration

I declare that this thesis is the result of my own work which has been mainly undertaken during my period of registration for the degree of Doctor of Philosophy at Newcastle University.

Najla A. Alburae

March 2015

Acknowledgment

There are number of people whom without them this thesis might not be completed, and to whom I am grateful.

I would like to express my sincere gratitude to my supervisor Dr. Mark Andrew Birch for being very supportive and patient.

I will also heartily thank my mother for her lovely prayers and to my father for guiding me through life. My thanks are extended to my brothers and sisters for their encouragements, and my nephews the hope of the future; you are all the greatest gifts God have given me.

My sincere thanks go to my friends whom have been there for me when needed: Rahma Alshamrani, Fouz Alahmadi, Najat Alahmadi, Jwahir Alzamil, Reham Alashari, Fatema Alatwai, Patience Cole Ezea, Iman Salem, Kathleen Wright, Deepak Kalaskar, Sotiria Toumpaniari, Ferreira Duarte Ana Marina, Elena Mancuso, Simon Partridge, and Shane Walsh.

My love and respect goes to my lovely fiancé, Abdulsalam Ghaleb for finding me the light whenever it was far away.

Finally, I would like to extend my appreciation to King Abdulaziz University for giving me the chance to continue my studies.

Abstract

Tissue engineering involves the use of cells, growth factors/cytokines, and scaffolds to regenerate damaged tissue. The choice of cells, scaffold and their delivery is crucial to the successful outcome of the treatment and this is particularly the case in bone and cartilage where the repair tissue has to recreate a structural hierarchy to restore long lasting function. One approach to deliver high numbers of cells to a defect site is as cell aggregates or spheroids. Experiments are described here that aim to understand how mesenchymal stem cells (MSCs) and osteoblastic cells behave in a cell aggregate and how this could be refined by the inclusion a self -assembling hydrogel to influence cell-cell and cell-extracellular matrix (ECM) interactions. Forming cellular spheroids in vitro can be achieved using various methods, including hanging drop, static suspension culture, encapsulation/entrapment, and low adherence multi-well. Extensive analysis identified that the most efficient and reproducible method for the formation of spheroids using rat osteoblasts and human MSCs was through their culture at a specific concentration in polyHEMA coated plates. Both viability and ability of cells to differentiate was investigated. The MTT assay was used to assess cells viability while their ability to differentiate was assessed by measuring alkaline phosphatase activity as well as measuring gene osteogenic markers expression via qRT-PCR. Analysis of cell differentiation under these conditions revealed that alkaline phosphatase activity appeared more elevated in 2D cultures compared to 3D. However, it was noted that there were contrasting results between the two types of cells with expression of osteogenic genes higher when MSCs were grown in osteogenic media while with calvarial significant expression was also observed when grown in normal media. Because of the distinct regulatory cues given by cell-cell contact in the spheroid, analysis was performed for connexin (Cx)-43, a gap junction protein and members of the ephrin/Eph family. Cx-43

was immunolocalised to gap junction structures in cells after osteogenic treatment on a flat substrate but this was more difficult to assess in the 3D spheroids. Analysis of transcript patterns reflected the increased abundance of Cx-43 in cells treated with osteogenic supplements and parallel changes in expression of Ephrin B1 and Ephrin B2. Experiments were also performed including a Puramatrix hydrogel nanofibers scaffold that could encase the cells in an ECM-like environment, provide mechanical support and protect them and manipulate cell-cell interactions. The results obtained in this study concluded that calvaria cells viability and hence proliferation increased when grown embedded within 0.25% Puramtrix while mesenchymal stem cells increased when embedded in 0.5% Puramatrix. Similarly, alkaline phosphatase activity was higher in cells embedded within 0.25% Puramatrix while mesenchymal stem cells favoured 0.5%. On the other hand, osteogenic gene expression of both cells was enhanced with the use of Puramatrix scaffold.

List of abbreviations

BMPs	Bone Morphogenetic Proteins
DAPI	4',6-diamidino-2-phenylindole
DEPC	Diethylpyrocarbonate
DMEM	Dulbecco's modified Eagle's medium
dNTPs	Deoxynucleotidetriphosphates
DPBS	Dulbecco s Phosphate Buffered Saline
DTT	Dithiothreitol
EBs	Embryoid bodies
ECM	Extracellular matrix
ESs	Embryonic stem cells
FBS	Fetal bovine serum
GPI	Glycosylphosphatidylinisotol
MCP-1	Monocyte chemoattractant protein 1
MSCs	Mesenchymal stem cells
PCR	polymerase chain reaction
Poly-HEMA	Poly (2-hydroxyethyl methacrylate)
qRT-PCR	Quantitative reverse transcription polymerase chain reaction
SDF-1	Stromal cell-derived factor-1
SDS	Sodium dodecyl sulfate
TAE	Tris-acetate-EDTA

List of tables

Table 1.1: Natural and synthetic materials available to be used as scaffolds…… 3

Table 1.2: Parameters to optimize biomaterials for tissue regeneration…… 5

Table 1.3: Eph receptors and ephrin ligands specifities arranged depending on their affinity……..…….. 19

Table 2.1: thermal cycles for genes amplification…….……. 31

Table 2.2: list of rat primers used for qRT-PCR analysis…….. 32

Table 2.3: list of human primers used for qRT-PCR analysis…….……. 33

List of figures

Figure 1.1: Tissue engineering three key elements …….. 1

Figure 1.2: A mummy skull with a golden plate used to repair a defect at the front of the skull……. 2

Figure 1.3: An amputated toe replaced with a wooden one…….. 2

Figure 1.4: Examples of different structures of self -assembled peptides……. 6

Figure 1.5: Puramatrix molecular model…… 8

Figure 1.6: (A) self-assembled Puramatrix 1% (B) Puramatrix SEM image shows the formation of nanofibers (10-20 nm) …… 8

Figure 1.7.: Molecular model of DAR 16-IV……..... 9

Figure 1.8: (A) cells grown in a designed pattern coated with molecular carpet peptides (B) Molecular model of RADSC-14 which forms a monolayer on surface and attract specific molecules…… 10

Figure 1.9: 3D culture methods……..…… 11

Figure 1.10: 3D culture methods……..…… 14

Figure 1.11: Bone remodeling three phases which involves bone resorption and formation…….. 15

Figure 1.12: Osteoclast – osteoblast interaction in bone remodelling…… 16

Figure 1.13: Eph receptors and ephrin ligands structure…… 18

Figure 1.14: Eph/ephrin signaling in bone homeostasis…….……... 20

Figure 2.1: Illustration of a hemocytometer slide……. 23

Figure 2.2: Represents the chemical structure of MTT and its reduction by mitochondrial enzymes in viable cells to formazan……..... 25

Figure 2.3: Represents the chemical structure of a p-nitrophenol molecule ……... 26

Figure 2.4: drawing of RNA extraction steps ……. 28

Figure 2.5: Measuring RNA using Nanodrop instrument …… 29

Figure 2.6: Cell block preparation with a collodion bag…… 35

Figure 2.7: Schematic of direct and indirect Immunofluorescence methods……..... 36

Figure 3.1: 3D optimization plan…… 39

Figure 3.2: Shows an uneven polyHEMA coating that led to cells attaching in some areas, while some formed spheres…… 46

Figure 3.3: Calvarial cells grown on the surface of a 96u rounded bottom plate ….. 47

Figure 3.4: Low density of calvarial cells grown on the surface of a 96u rounded bottom plate at 7days …… 47

Figure 3.5: Calvarial cells grown under osteogenic conditions on the surface of a 96u rounded bottom plate at day 14 …… 48

Figure 3.6: Calvarial cells grown under osteogenic conditions on the surface of a 96u rounded bottom plate at day 21 …… 48

Figure 3.7: Calvarial cells grown on the surface of a 24 well in a serum free media after 24hr …… 49

Figure 3.8: High densities of calvarial cells grown on the surface of a 24 well in a serum free media at 7days …… 49

Figure 3.9: Calvarial cells grown on the surface of a 24 well in a serum free media at 14days under osteogenic conditions …… 50

Figure 3.10: Calvarial cells grown using hanging drop technique after 24hr …….. 50

Figure 3.11: Calvarial cells grown after 48hr using hanging drop technique …… 51

Figure 3.12: Calvarial cells grown at 21days using hanging drop technique …… 52

Figure 3.13: Calvarial cells grown after 24hrin normal media mixed with methylcellulose ……. 52

Figure 3.14: Calvarial cells at 21days grown in osteogenic media mixed with methylcellulose ……. 53

Figure 3.15: Calvarial cells grown after 48hr on the surface of 24 well plate coated with polyHEMA ……. 53

Figure 3.16: Calvarial cells grown on the surface of a 24 well plate coated with polyHEMA after 14days …… 54

Figure 3.17: Shows the surface of high concentration [40mg/ml] polyHEMA coating which was broken after 14 days …… 54

Figure 3.18: Calvarial cells grown after 24hr on the surface of 24 well plate coated with 2% agar ……..… 55

Figure 3.19: Calvarial cells grown after 24hr on the surface of 24 well plate coated with 0.5% agar …….……..… 55

Figure 3.20: Calvarial cells grown after 14 days shows the formation of large spheroid by time at high cells density …… 56

Figure 3.21: Calvarial cells grown after 14 days shows cells suspended in the media while most of the cells attached to the surface of the well……..……. 56

Figure 3.22: shows MTT Viability assay results for cells grown in normal media with cell density approximately 14 x10^6 …… 60

Figure 3.23: shows MTT Viability assay results for cells grown in osteogenic media with cell density approximately 14 x10^5……..... 61

Figure 3.24: shows MTT Viability assay results for cells grown in normal media with cell density approximately 6 x10^5……..... 62

Figure 3.25: is a graph that represents MTT Viability assay results for cells grown in osteogenic media with cell density approximately 6 x10^5 .the vertical axis represents absorbance while horizontal axis represents time. ……..... 63

Figure 3.26: shows MTT Viability assay results for cells grown in normal media with cell density approximately 3.5 x10^5……..... 64

Figure 3.27: shows MTT Viability assay results for cells grown in osteogenic media with cell density approximately 3.5 x10^5……. 65

Figure 3.28: shows MTT Viability assay results for cells grown in normal media with cell density approximately 0.5 x10^5…….. 66

Figure 3.29: shows MTT Viability assay results for cells grown in osteogenic media with cell density approximately 0.5 x10^5……..... 67

Figure 3.30: shows (a) spheroids generation on plates coated with poly-HEMA (b) Spheroids diameter measurement ……. 69

Figure 3.31: Data represents the mean ± standard error of the mean statistical significant determined using Kruskal-Wallis test. P value ≤ 0.05 was considered significant (a) number of spheroids. (b) Spheroids diameter …… 70

Figure 4.1: Immunofluorescent staining of Cx43 in rat calverial cells monolayers grown for 7 days under normal conditions. Cx43 [green] localize around the nucleus [blue] and at the cell membrane ……..... 82

Figure 4.2: Immunofluroescent staining of Cx43 in rat calverial cells monolayers grown for 7 days under osteogenic conditions. Cx43 [green] localize at the cell membrane …….. 83

Figure 4.3: Immunofluorescent staining of Cx43 in rat calvarial cells 3D grown for 7 days (a) Normal media (b) osteogenic media. Cx43 [green] while nucleus is stained with DAPI [blue]…….. 84

Figure 4.4: Immunofluorescent staining of Cx43 in human mesenchymal stem cells 3D grown for 7 days (a) Normal media (b) osteogenic media. Cx43 [green] while nucleus is stained with DAPI [blue]……... 85

Figure 4.5: laser confocal images of Cx43 in rat calvarial cells 3D grown for 7 days (a) Normal media (b) osteogenic media. Cx43 [green] while nucleus is stained with DAPI [blue]……..…… 86

Figure 4.6: laser confocal images of Cx43 in human mesenchymal stem cells 3D grown for 7 days (a) Normal media (b) osteogenic media. Cx43 [green] while nucleus is stained with DAPI [blue]……. 87

Figure 4.7: laser confocal microscopy series images of a spheroid. Cx43 [green] while nucleus is stained with DAPI [blue]……..... 88

Figure 4.8: a Z -section confocal microscope image of spheroids with a thickness (a) 52.2µm and (b) 97.49µm ……..... 89

Figure 4.9: spheroid section stained with H&E (a) lower and (b) higher 90

magnification…….

Figure 4.10: spheroid section stained withantiCx43 antibody (a) nucleus stained blue using DAPI (b) Cx43……..... 91

Figure 4.11: SEM image of rat calvarial cells spheroids pellet (a) normal media (b) osteogenic media ……..... 93

Figure 4.12: SEM image of rat calvarial cells spheroids after 24hr grown in normal media (a) lower magnification (b) and (c) higher magnification illustrates communication between spheroids …… 94

Figure 4.13: SEM image of rat calvarial cells spheroids after 24hr grown in osteogenic media (a) lower and (b) higher magnification illustrates small spheres in contact with a larger sphere…… 95

Figure 4.14: SEM image of rat calvarial cells spheroids at 7days grown in normal media (a) lower and (b) higher magnification illustrates a compact sphere…….. 96

Figure 4.15: SEM image of rat calvarial cells spheroids at 7days grown in osteogenic media (a) lower and (b) higher magnification illustrates spheres that dissociate ……..…….. 97

Figure 4.16: SEM image of human mesenchymal stem cells spheroids after 24hr grown in (a) normal media and (b) osteogenic media……... 98

Figure 4.17: SEM image of human mesenchymal stem cells spheroids at 7days grown in (a) normal media and (b) osteogenic media……..... 99

Figure 4.18: SEM image of spheroids with amorphous coating believed to be 100

polyHEMA from the surface of the culture plates …….....

Figure 4.19 Graph shows the viability of calvarial rat cells after 24hr…….. 102

Figure 4.20 Graph shows the viability of human MSCs after 24hr……. 102

Figure 4.21 Graph shows the viability of rat calvarial cells at 72hr…….. 103

Figure 4.22 Graph shows the viability of human MSCs at 72hr……..... 103

Figure 4.23 Graph shows the viability of rat calvarial cells at 7days……..… 104

Figure 4.24 Graph shows the viability of human MSCs at 7days.…… 104

Figure 4.25 Graph shows the alkaline phosphatase activity level of rat calverial cells after 24hr…..... 106

Figure 4.26 Graph shows the alkaline phosphatase activity level of human MSCs after 24hr ……..…….. 106

Figure 4.27 Graph shows the alkaline phosphatase activity level of rat calverial cells at 72hr……..... 107

Figure 4.28 Graph shows the alkaline phosphatase activity level of human MSCs at 72hr……..... 107

Figure 4.29 Graph shows the alkaline phosphatase activity level of rat calverial cells at 7days……..…….... 108

Figure 4.30 Graph shows the alkaline phosphatase activity level of human MSCs at 7days……..... 108

Figure 4.31 ALP relative level expression in rat calvarial cells after 24hr …… 110

Figure 4.32 ALP relative level expression in MSCs after 24hr …….. 110

Figure 4.33 ALP relative level expression in rat calvarial cells at 72hr, the data represents the mean ± standard error of the mean, a statistical significant was considered when P value ≤ 0.05……. 111

Figure 4.34 ALP relative level MSCs at 72hr……. 111

Figure 4.35 ALP relative level Rat cells at 7days……. 112

Figure 4.36 ALP relative level MSCs cells at 7days……..…….. 112

Figure 4.37 RUNX 2 relative level expression in rat cells after 24hr……. 114

Figure 4.38 RUNX 2 relative level expression in MSCs after 24hr……..…. 114

Figure 4.39 RUNX 2 relative level expression in rat cells at 72hr……..…. 115

Figure 4.40 RUNX 2 relative level expression in MSCs at 72hr……..… 115

Figure 4.41 RUNX 2 relative level expression in rat cells at 7days……..…… 116

Figure 4.42 RUNX 2 relative level expression in MSCs at 7days……..… 116

Figure 4.43 SP7 relative level expression in rat cells after 24hr……..…..…… 118

Figure 4.44 SP7 relative level expression in MSCs after 24hr……...…… 118

Figure 4.45 SP7 relative level expression in rat cells at 72hr……...…….. 119

Figure 4.46 SP7 relative level expression in MSCs at 72hr…… 119

Figure 4.47 SP7 relative level expression in Rat cells at 7days……..…… 120

Figure 4.48 SP7 relative level expression in MSCs at 7days ……..… 120

Figure 4.49 CX43 relative level expression in rat cells after 24hr …….. 122

Figure 4.50 CX43 relative level expression in MSCs after 24hr……... 122

Figure 4.51 CX43 relative level expression in rat cells at 72hr……..… 123

Figure 4.52 CX43 relative level expression in MSCs at 72hr…… 123

Figure 4.53 CX43 relative level expression in rat calvarial cells at 7days…..…..…. 124

Figure 4.54 CX43 relative level expression in MSCs at 7days…….…….. 124

Figure 4.55 Ephrin B1 relative level expression in rat calvarial cells after 24hr..... 126

Figure 4.56 Ephrin B1 relative level expression in MSCs after 24hr……. 126

Figure 4.57 Ephrin B1 relative level expression in rat cells at 72hr.…….……. 127

Figure 4.58 Ephrin B1 relative level expression in MSCs at 72hr……...…..…. 127

Figure 4.59 Ephrin B1 relative level expression in rat cells at 7days……...…. 128

Figure 4.60 Ephrin B1 relative level expression in MSCs at 7days…….…….. 128

Figure 4.61 Ephrin B2 relative level expression in Rat cells after 24hr……...…. 130

Figure 4.62 Ephrin B2 relative level expression in MSCs after 24hr……...……..… 130

Figure 4.63 Ephrin B2 relative level expression in rat cells at 72hr……..... 131

Figure 4.64 Ephrin B2 relative level expression in MSCs at 72hr……...…….. 131

Figure 4.65 Ephrin B2 relative level expression in Rat cells at 7days.……..…. 132

Figure 4.66 Ephrin B2 relative level expression in MSCs at 7days……..…….. 132

Figure 4.67 Ephrin B4 relative level expression in Rat cells after 24hr……..……... 134

Figure 4.68 Ephrin B4 relative level expression in MSCs after 24hr……..… 134

Figure 4.69 Ephrin B4 relative level expression in rat cells at 72hr……...…..….. 135

Figure 4.70 Ephrin B4 relative level expression in MSCs at 72hr……...…..…… 135

Figure 4.71 Ephrin B4 relative level expression in rat cells at 7days……...…….. 136

Figure 4.72 Ephrin B4 relative level expression in MSCs at 7days……..……. 136

Figure 5.1: Flowchart of puramatrix hydrogel scaffold preparation…….. 142

Figure 5.2: Rat calvarial cells grown after 24hr on 0.1% Puramatrix in normal media, cells adhered while others formed clusters ……..... 146

Figure 5.3: Rat calvarial cells grown after 24hr on 0.25% Puramatrix in normal media, cells formed cluster,s note that the hydrogel breakage is clearer than 0.1%..... 147

Figure 5.4: Rat calvarial cells grown after 24hr on 0.5% Puramatrix in normal media, cells formed clusters and some communicates with each other ……. 148

Figure 5.5: Rat calvarial cells grown after 24hr on 1% Puramatrix in normal media, some cells formed clusters and some adhered to the hydrogel scaffold …..... 149

Figure 5.6: Rat calvarial cells grown at 7days on 0.1% Puramatrix in normal media, most of the cells adhered to the plate surface with few clusters..... 150

Figure 5.7: Rat calvarial cells grown at 7days on 0.25% Puramatrix in normal media, most of the cells adhered to the plate surface with few clusters …… 151

Figure 5.8: Rat calvarial cells grown at 7days on 0.5% Puramatrix in normal media, most of the cells adhered to the plate surface with few cellular clusters 152

contacting each other.....

Figure 5.9: Rat calvarial cells grown at 7days on 1 % Puramatrix in normal media, few cells adhering to the surface with cellular clusters ……..... 153

Figure 5.10: Rat calvarial cells grown after 24hr on MAPTrix hydrogel cells adhered to the surface of the scaffold ……..... 154

Figure 5.11: Rat calvarial cells grown at 7days on MAPTrix hydrogel cells adhered to the surface of the scaffold ……..... 155

Figure 5.12: shows hydrogel drops of puramatrix (a) 0.1% (b) 0.25% (c) 0.5%..... 156

Figure 5.13: Shows hydrogel drops of Puramatrix (a) 0.1% low magnification (b) 0.1% high magnification (c) 0.25% low magnification (d) high magnification (e) 0.5% low magnification (f) high magnification …… 157

Figure 5.14: Shows SEM images of Puramatrix hydrogel where nanofibers are more dense at higher peptide concentrations (a) 0.1% (b) 0.25% (c) 0.5% (d) 1% ... 159

Figure 5.15: Shows SEM images of rat calvarial cells grown on the surface of 0.1% Puramatrix hydrogel ……..... 160

Figure 5.16: Shows SEM images of rat calvarial cells grown on the surface of 0.25% Puramatrix hydrogel, some cells formed clusters and some adhered to the surface……. 161

Figure 5.17: Shows SEM images of rat calvarial cells grown on the surface of 0.5% Puramatrix hydrogel, few clusters and most of the cells adhered to the surface forming monolayer..... 162

Figure 5.18: Shows SEM images of rat calvaria cells grown on the surface of 1% Puramatrix hydrogel, cellular clusters formed and few of the cells adhered to the surface of the scaffold……..…. 163

Figure 5.19 Graph shows the viability of encapsulated calvarial rat cells after 24hr. 165

Figure 5.20 Graph shows the viability of encapsulated human MSCs after 24hr…... 165

Figure 5.21 Graph shows the viability of encapsulated calvaria rat cells at 72hr..... 166

Figure 5.22 Graph shows the viability of encapsulated human MSCs at 72hr..... 166

Figure 5.23 Graph shows the viability of encapsulated calvaria rat cells at 7days..... 167

Figure 5.24 Graph shows the viability of encapsulated human MSCs at 7days…... 167

Figure 5.25 Graph shows the alkaline phosphatase activity level of encapsulated calvaria cells after 24hr……..... 170

Figure 5.26 Graph shows the alkaline phosphatase activity level of encapsulated human MSCs after 24hr……...…... 170

Figure 5.27 Graph shows the alkaline phosphatase activity level of encapsulated calvarial cells at 72hr……..…… 171

Figure 5.28 Graph shows the alkaline phosphatase activity level of encapsulated human MSCs at 72hr……..……. 171

Figure 5.29 Graph shows the alkaline phosphatase activity level of encapsulated calvarial cells at 7days……..…..... 172

Figure 5.30 Graph shows the alkaline phosphatase activity level of encapsulated human MSCs at 7days ……...……..... 172

Figure 5.31 ALP relative expression level in encapsulated calvarial cells after 24hr 174

Figure 5.32 ALP relative expression level in encapsulated MSCs after 24hr..... 174

Figure 5.33 ALP relative expression level in encapsulated calvarial cells at 72hr…. 175

Figure 5.34 relative expression level in encapsulated MSCs at 72hr……..... 175

Figure 5.35 ALP relative expression level in encapsulated calvarial cells at 7days... 176

Figure 5.36 ALP relative expression level in encapsulated MSCs at 7days…...…… 176

Figure 5.37 RUNX 2 relative expression level in encapsulated calvarial cells after 24hr ……..…….. 178

Figure 5.38 RUNX 2 relative expression level in encapsulated MSCs after 24hr….. 178

Figure 5.39 RUNX 2 relative expression level in encapsulated calvarial cells at 72hr……. 179

Figure 5.40 RUNX 2 relative expression level in encapsulated MSCs at 72hr…..…. 179

Figure 5.41 RUNX 2 relative expression level in encapsulated calvaria cells at 7days……..……. 180

Figure 5.42 RUNX 2 relative expression level in encapsulated MSCs at 7days...…. 180

Figure 5.43 SP7 relative expression level in encapsulated calvarial cells after 24hr. 182

Figure 5.44 SP7 relative expression level in encapsulated MSCs after 24hr…….…. 182

Figure 5.45 SP7 relative expression level in encapsulated calvaria cells at 72hr…... 183

Figure 5.46 SP7 relative expression level in encapsulated MSCs at 72hr ……..… 183

Figure 5.47 SP7 relative expression level in encapsulated calvaria cells at 7days 184

Figure 5.48 SP7 relative expression level in encapsulated MSCs at 7days…… 184

Figure 5.49 CX43 relative expression level in encapsulated calvarial cells after 24hr……. 186

Figure 5.50 CX43 relative expression level in encapsulated MSCs after 24hr..... 186

Figure 5.51 CX43 relative expression level in encapsulated calvarial cells at 72hr... 187

Figure 5.52 CX43 relative expression level in encapsulated MSCs at 72hr……... 187

Figure 5.53 CX43 relative expression level in encapsulated calvarial cells at 7days. 188

Figure 5.54 CX43 relative expression level in encapsulated MSCs at 7days……. 188

Figure 5.55 Ephrin B1 relative expression level in encapsulated calvarial cells after 24hr……. 190

Figure 5.56 Ephrin B1 relative expression level in encapsulated MSCs after 24hr... 190

Figure 5.57 Ephrin B1 relative expression level in encapsulated calvarial cells at 72hr……. 191

Figure 5.58 Ephrin B1 relative expression level in encapsulated MSCs at 72hr..... 191

Figure 5.59 Ephrin B1 relative expression level in encapsulated calvarial cells at 7days……... 192

Figure 5.60 Ephrin B1 relative expression level in encapsulated MSCs at 7days..... 192

Figure 5.61 Ephrin B2 relative expression level in encapsulated calvarial cells after 24hr……. 194

Figure 5.62 Ephrin B2 relative expression level in encapsulated MSCs after 24hr 194

Figure 5.63 Ephrin B2 relative expression level in encapsulated calvarial cells at 72hr……. 195

Figure 5.64 Ephrin B2 relative expression level in encapsulated MSCs at 72hr..... 195

Figure 5.65 Ephrin B2 relative expression level in encapsulated calvarial cells at 7days……..……..... 196

Figure 5.66 Ephrin B2 relative expression level in encapsulated MSCs at 7days….. 196

Figure 5.67 Ephrin B4 relative expression level in encapsulated calvaria cells after 24hr…… 198

Figure 5.68 Ephrin B4 relative expression level in encapsulated MSCs after 24hr... 198

Figure 5.69 Ephrin B4 relative expression level in encapsulated calvarial cells at 72hr……. 199

Figure 5.70 Ephrin B4 relative expression level in encapsulated MSCs at 72hr..... 199

Figure 5.71 Ephrin B4 relative expression level in encapsulated calvarial cells at 7days……... 200

Figure 5.72 Ephrin B4 relative expression level in encapsulated MSCs at 7days..... 200

Table of contents

Declaration …….. i

Acknowledgment …… ii

Abstract …….. iii

List of abbreviations ……..... vi

List of tables …….. vii

List of figures …….. viii

Table of contents …….. xxiii

Chapter 1: literature review ……..…. 1

1.1 Introduction ……..……. 1

1.2 Biomaterials in orthopaedics ……..……..……. 2

1.3 Self- assembly peptides …… 7

1.4 Three dimensional (3D) cultures…… 10

1.5 Bone signalling……..……. 15

1.5.1 Bone remodelling……. 15

1.5.2 Eph/ephrin signaling in bone…… 17

1.6 Project aims……. 21

Chapter 2: General materials and methods……. 22

2.1 Materials and methods …… 22

2.1.1 Cell culture ……..……..…… 22

2.1.2 Cell counting and viability determination using a hemocytometer…… 23

2.1.3 Cell viability and proliferation assay…….. 24

2.1.4 Alkaline phosphatase assay ……...……...……. 26

2.1.5 RNA extraction and cDNA synthesis ……..……..……. 27

2.1.5.1 RNA isolation……. 27

2.1.5.2 RNA quantity and quality assessment…… 29

2.1.5.3 RNA integrity assessment…… 30

2.1.5.4 First-Strand cDNA synthesis……. 30

2.1.6 Quantitative real time polymerase chain reaction (qRT-PCR) ……..….. 31

2.1.7 Scanning electron microscopy [SEM]…… 33

2.1.8 Histology and immunoflourescent studies…… 34

2.1.8.1 Samples preparation for histological studies……. 34

2.1.8.2 Immunoflourescent staining……. 36

2.1.9 Statistical analysis…….. 37

Chapter 3: Investigating spheroids generation using different approaches.. 38

3.1 Introduction …… 38

3.2 Materials and methods …… 40

3.2.1 Stock solutions preparation ……..…….. 40

3.2.1.1 Methylcellulose stock solutions ……..……. 40

3.2.1.2 Poly-HEMA stock solutions ……...…… 40

3.2.1.3 Agar stock solutions ……...…… 40

3.2.2 Cell culture…… 40

3.2.2.1 Rat calvarial cell culture…….. 41

3.2.2.2 Multicellular spheroid culture……. 41

3.2.2.3 Evaluation of cell viability and number using the MTT assay…… 43

3.2.2.4 Image analysis……. 43

3.3 Results …… 44

3.3.1 Efficiency of spheroid formation……... 44

3.3.1.1 96 round -bottom plates……. 44

3.3.1.2 Serum free media…….. 44

3.3.1.3 Hanging drop method……. 44

3.3.1.4 Methylcellulose cell entrapment…….. 45

3.3.1.5 PolyHEMA coated dish…….. 45

3.3.1.6 Liquid overlay technique……. 46

3.3.2 Cell viability and number……. 57

3.3.2.1 96 U plate…… 57

3.3.2.2 Serum free media……. 57

3.3.2.3 Methylcellulose cells entrapment…….……. 58

3.3.2.4 PolyHEMA coated dish……. 58

3.3.2.5 Liquid overlay technique……. 59

3.3.3 Analysis of spheroid size and number in different culture environments 68

3.4 Discussion ……... 71

Chapter 4: Investigating cell gene expression and communication in 2D and 3D cultures…… 77

4.1 Introduction …… 77

4.2 Materials and methods …… 78

4.2.1 Cell culture ……..…….. 78

4.2.1.1Poly-HEMA stock solution……. 78

4.2.1.2 Preparation of Poly-HEMA Coated Plates…… 78

4.2.1.3 Rat calvarial cell culture …… 78

4.2.1.4 Human mesenchymal stem cells cell culture ……. 78

4.2.2 Histology and Immunofluorescent studies……... 78

4.2.2.1 Hematoxylin and eosin staining ……. 78

4.2.2.2 Immunofluorescent staining …….. 79

4.2.3 Scanning electron microscopy [SEM] …….. 79

4.2.4 Evaluation of cell viability and proliferation using MTT assay ……... 79

4.2.5 Alkaline phosphatase assay ……. 79

4.2.6 RNA isolation and quantitative real time polymerase chain reaction ….. 79

4.2.7 Statistical analysis ……. 80

4.3 Results …… 81

4.3.1 Connexin 43 localisation in 2D and 3D culture …… 81

4.3.2 Morphological analysis of spheroids …… 92

4.3.3 Cell Viability in 2D and 3D …… 101

4.3.4 Alkaline phosphatase assay ……. 105

4.3.5 Changes in gene expression between 2D and 3D culture …… 109

4.4 Discussion ……... 137

Chapter 5: In vitro osteogenic differentiation of cells encapsulated within a nanofiberous environment……..……..…….. 140

5.1 Introduction …… 140

5.2 Materials and methods …… 141

5.2.1 Cell culture …….. 141

5.2.1.1. Rat calvaria cell culture …… 141

5.2.1.2 Human mesenchymal stem cells cell culture …….. 141

5.2.2 Hydrogel scaffold preparation …… 141

5.2.2.1 Self-assembling peptide nanofibres …….. 141

5.2.2.2 Mussel adhesive protein …… 142

5.2.3 Scanning electron microscopy [SEM] …….. 143

5.2.4 Evaluation of cell viability using the MTT assay ……. 143

5.2.5 Alkaline phosphatase assay …… 143

5.2.6 RNA isolation and quantitative real time polymerase chain reaction…... 144

5.2.7 Statistical analysis …… 144

5.3 Results …….. 145

5.3.1 Morphological observations …… 145

5.3.2 SEM morphology study …… 158

5.3.3 Cells viability in the hydrogel environment ……. 164

5.3.4 Alkaline phosphatase activity assay ……. 168

5.3.5 Modulation of gene expression by cells interacting with the hydrogel 173

matrix …….

5.4 Discussion ……. 201

Chapter 6: Final conclusions and future work……..… 204

References …… 209

Appendix A …….. 227

Appendix B…….. 229

Chapter 1: Literature review

1.1 Introduction

The term tissue engineering emerged in 1987; it was coined by Professor Y. C. Fung at University of California (Lanza, Langer et al. 2007). Tissue engineering is defined as "the use of a synthetic or natural biodegradable material, which has been seeded with living cells when necessary, to regenerate the form and/or function of a damaged or diseased tissue or organ in a human patient" (Lanza, Langer et al. 2007). As indicated in the definition tissue engineering may involve three elements cells, nutrients [growth factors and cytokines], and scaffolds (TAKEI 2005) [figure1.1]. These scaffolds can be made either from synthetic or natural materials or a combination of the two (Khang, Kim et al. 2007).

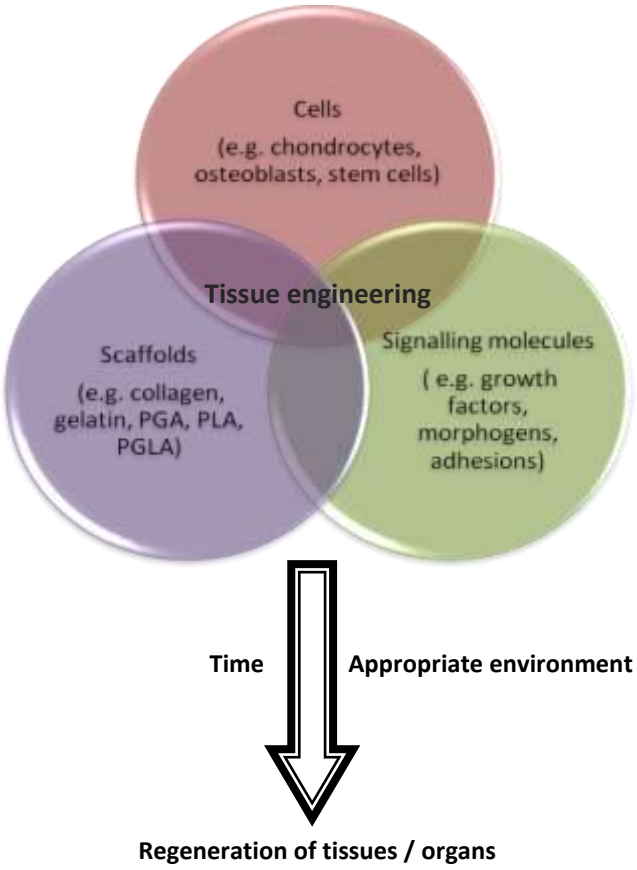

Figure 1.1: *Tissue engineering three key elements (Khang, Kim et al. 2007)*

1.2 Biomaterials in orthopaedics

The use of biomaterials in orthopaedics started thousands of years ago 3000 BC (Pietrzak 2008). Where raw materials such as wood and gold were commonly used to repair or restore bone defects (Pietrzak 2008) [figures 1.2 and 1.3].

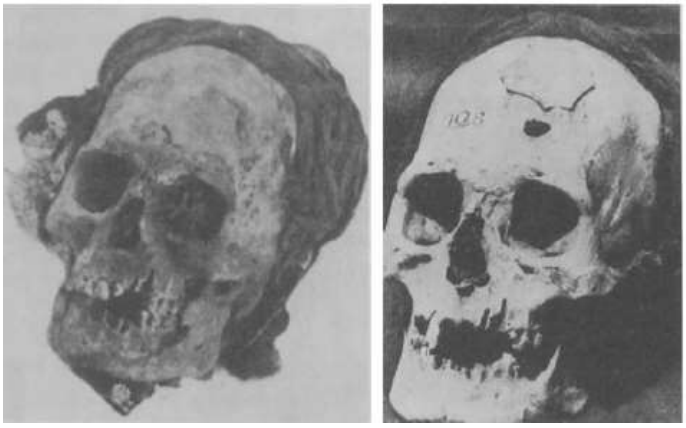

Figure 1.2: *A mummy skull with a golden plate used to repair a defect at the front of the skull [cranioplasty] (Pietrzak 2008)*

Figure 1.3: *An amputated toe replaced with a wooden one (Pietrzak 2008)*

Since then significant progress has been made using different materials in artificial implants, commonly metals, ceramics, and polymers particularly in orthopaedic field (Yarlagadda, Chandrasekharan et al. 2005). Today, there are several biomaterials that have the potential to be used as scaffolds in tissue engineering for both bone and cartilage repair [table 1.1] (Haasper, Zeichen et al. 2008).

Table 1.1: *Illustrates the different types of natural and synthetic materials available to be used as scaffolds in orthopaedic tissue engineering for both cartilage and bone (Haasper, Zeichen et al. 2008)*

Biological materials	Synthetic materials
• perichondrium • SIS (small intenstinal submucosa) • collagen (I) sponge • collagen (I)-GAG (glycosaminoglykan) • collagen (II)-GAG • collagen (III)-GAG • fibrin • hyaluronan • gelatin • alginate • agarose • chitosan • periost • DBM (demineralized bone matrix) • allogeneic/xenogenic bone	• PL (Polylactic acid) • PGLA (Polyglycolicacid and copolymers) • CF-PU-PLLA (Carbonfibre-Polyurethane-Poly • (L-lactide)-Graft) • CF-Polyester (Polyester-Carbonfibre) • PU (Polyurethane) • PLLA (Capralactone (Poly-L-Lactide/epsilon- • Caprolactone) • PLLA-PPD (Poly- L-Lactic Acid and Poly- p-Dioxanol) • PVA-H (Polyvinylalcohol-Hydrogel) • ß-TCP (Tricalcium phosphate) • CDHA (Calcium-deficient hydroxyapatite)

Materials are classified according to their origin into natural and synthetic (Mark 2004). Natural materials include those that can be found in the extracellular matrix [ECM] such as collagen and laminin (Saha, Pollock et al. 2007), alginate (Hutmacher, Goh et al. 2001). Whereas polyethylene glycol (PEG), poly 2-hydroxyethylmethacrylate (PHEMA), are examples of synthetic materials (Lee 2005). Both materials have drawbacks, the former can be expensive with a potential for contamination and may cause unfavourable immune responses (Saha, Pollock et al. 2007). whilst the synthetic materials are less expensive and more reproducible compared to the natural materials, they may also cause immune reaction (Yarlagadda, Chandrasekharan et al. 2005).

Despite the presence of a wide range of materials, there is still a need to find the optimal material that can fully replace both structural and biochemical parameters to resemble the original tissue (Kutz 2009). [Table1.2]. Both natural and synthetic materials are usually used to achieve the structural parameter only, while the biochemical parameters are integrated through cells or immobilized signals (Kutz 2009).

Table 1.2: *In tissue engineering several parameters are taken into consideration to optimize biomaterials for tissue regeneration and in particular two main categories: structural and biochemical. Optimizing structural parameters includes the physical, mechanical, and chemical properties. While biochemical parameter optimization are incorporated through immobilized signals, diffusible signals, and/or living components.(Meilander and Bellamkonda 2004)*

Structural components	Biochemical components
Physical properties • Shape • Size • Pore features • Three-dimensional • Surface topography	Immobilized signals • ECM proteins • Adhesive peptides • Growth factors
Mechanical properties • Reinforced composites • Mechanical loading • Electrical stimuli	Diffusible signals • One- component system • Two-component system • Gene delivery
Chemical properties • Hydrophobicity • Charge • Biodegradation	Living components • Cell seeding • Differentiated cells • Scaffold pre-vascularization • Cells for neuro-regeneration • Combination therapy • Stem cells • Commercial, cell-based products

This led scientists to draw attention to what is called “smart biomaterials”, which refers to biomaterials that behave at the structural or functional levels by responding to changes in the surrounding environment (Fairman and Akerfeldt 2005). For instance, a sequence of amino acids/peptides in a specific arrangement responds to changes in temperature or pH or the presence of particular ions, resulting in the formation of different structures [figure 1.4] (Fairman and Akerfeldt 2005).

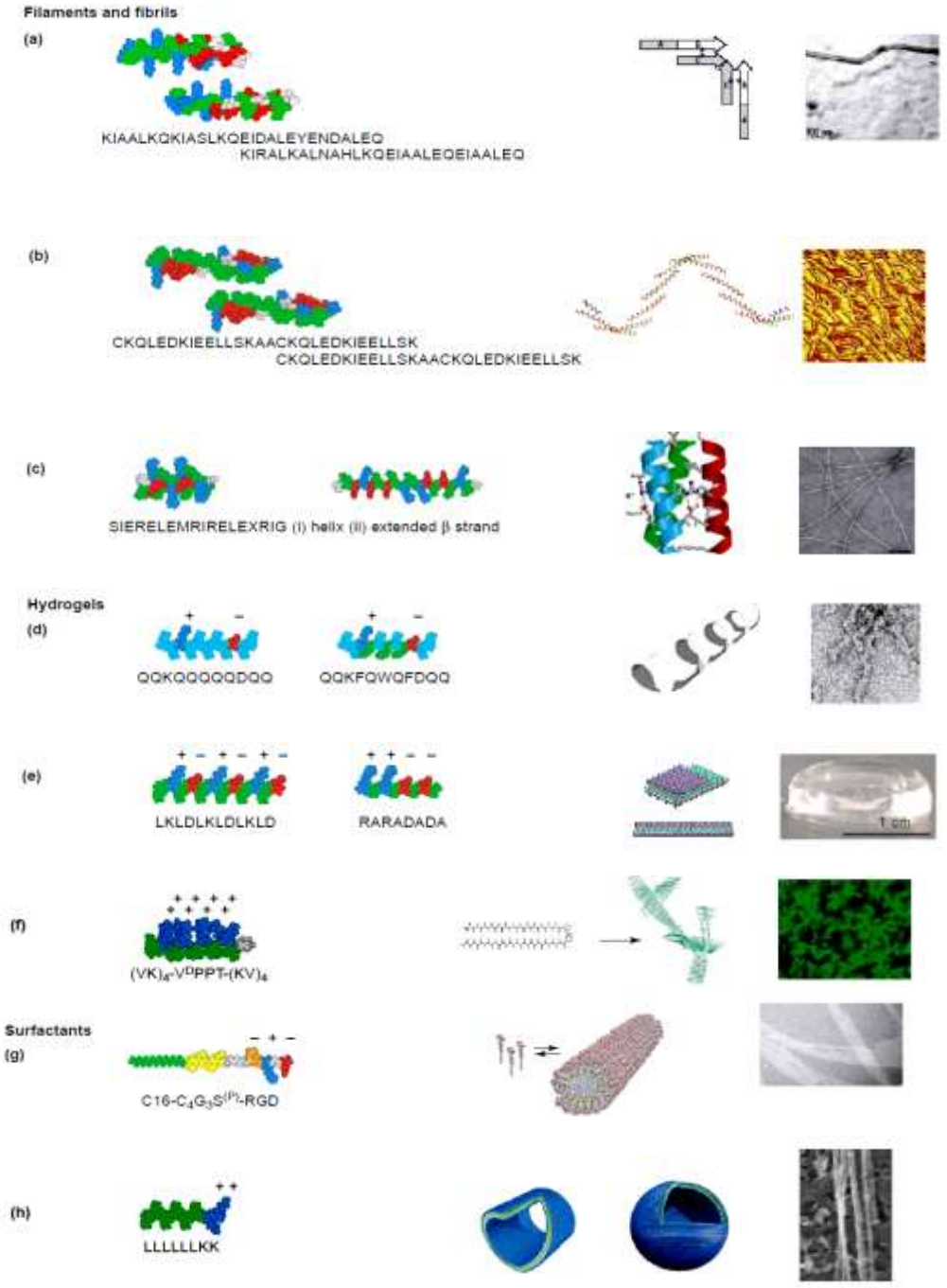

Figure 1.4: *Examples of different structures of self -assembled peptides (Fairman and Akerfeldt 2005)*

Consequently, this directs the attention of researchers towards self-assembling peptide systems as a highly controllable and functional biomaterial scaffold.

1.3 Self- assembly peptides:

The molecular self-assembly process can be defined as "the spontaneous organization of molecules under thermodynamic equilibrium conditions into structurally modified arrangements due to non-covalent interactions" (Aggeli, Boden et al. 2001). Even though the first scientist who suggested exploitation of these events in order to fabricate new devices was Eric Drexler in 1981 (Rajagopal and Schneider 2004), it is only recently that self-assembly peptide based materials emerged as a new method to fabricate at the nanoscale from the bottom-up approach (Ryadnov 2007) giving the opportunity for three dimensional assembly (Lu and Lieber 2007).

Inspired by naturally self- assembled systems such as DNA, protein folding, and lipids (Rajagopal and Schneider 2004) materials have been designed to assemble spontaneously governed by non- covalent forces including ionic bonding, hydrophobic effects, hydrogen bonds, and Van der Waals interactions (Mirkin and Niemeyer 2007).

According to (Aggeli, Boden et al. 2001) self-assembly peptides can be classified into three types:

1) Self -assembling peptides type I: also known as "Molecular Lego" for the reason that they assemble in a specific order like Lego bricks (Zhang 2003). The assembly process in this system is driven by the intermolecular forces based on the presence of alternating charged amino acids [figure 1.5] (Zhang 2003). When introducing the deigned peptide to a physiological solution it assembled spontaneously forming a hydrogel [figure 1.6A] build of nanofibers [figure 1.6B]

which can be used as scaffolds to support cell attachment, proliferation, and differentiation (Aggeli, Boden et al. 2001). Hence most of the peptide materials that have been studied thus far are of this type (Aggeli, Boden et al. 2001).

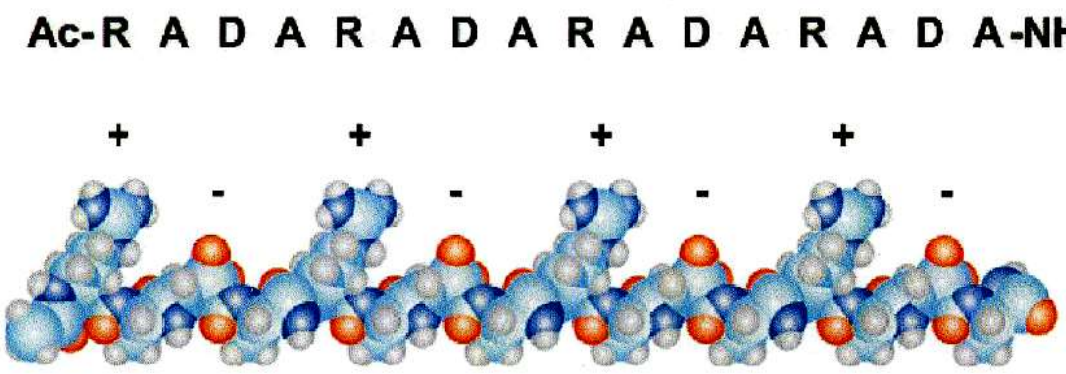

Figure 1.5: *Puramatrix molecular model (TAKEI 2005)*

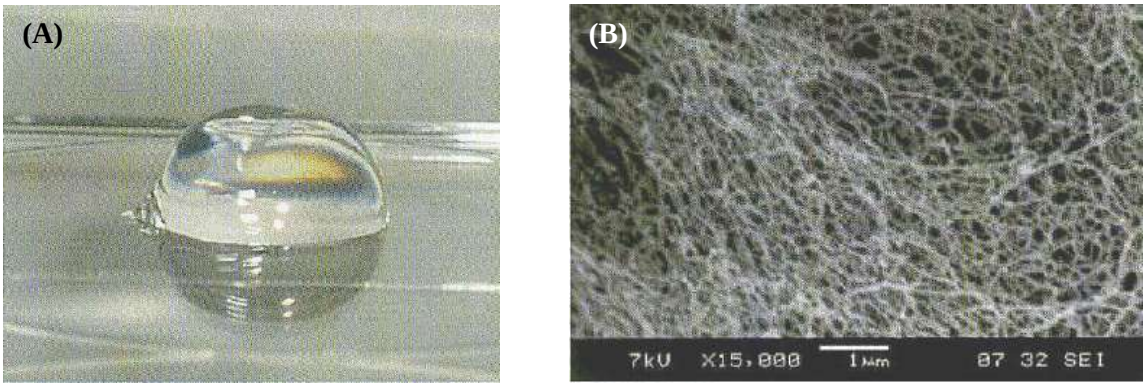

Figure 1.6: *(A) self-assembled Puramatrix 1% (B) Puramatrix SEM image shows the formation of nanofibers (10-20 nm) (TAKEI 2005)*

2) Self -assembling peptides type II: also called "molecular switch" , due to their ability to change molecular structure based on the surrounding environment (Aggeli, Boden et al. 2001). For example, DAR 16-IV which consist of 16 amino acids that form a β-sheet structure at a specific temperature (Aggeli, Boden et al. 2001). However, it undergoes a conformational transformation from the β to α helical structure at different temperature and pH (Zhang 2003). This type of

material can be useful in protein-protein interactions and disease caused by protein folding disruption studies (Zhang 2003). Where it was found that the structural transformation of DAR 16-IV is similar to that seen in diseases associated with accumulation of β sheet structures such as Alzheimer (Zhang and Rich 1997).

Figure 1.7.: *Molecular model of DAR 16-IV (Zhang 2003)*

3) Self-assembling peptide III: With this type of peptide the molecules self-assemble on a surface forming a layer that is a few millimeters thick , and for that reason it's called "molecular paint" or "molecular carpet" [figure 1.8] (Zhang 2003). This kind of peptide consists of three parts, the first part is the ligand that can be recognized by the cell surface or other molecules, the second part forms a linker while the third is the surface anchor (Zhang 2003). Due to the presence of regions that the cell surface or other molecules can be attach to, this type of peptide is also known as "molecular Velcro" (Aggeli, Boden et al. 2001). Accordingly, it is a useful tool in cell-cell behaviour and communication studies (Zhang 2003).

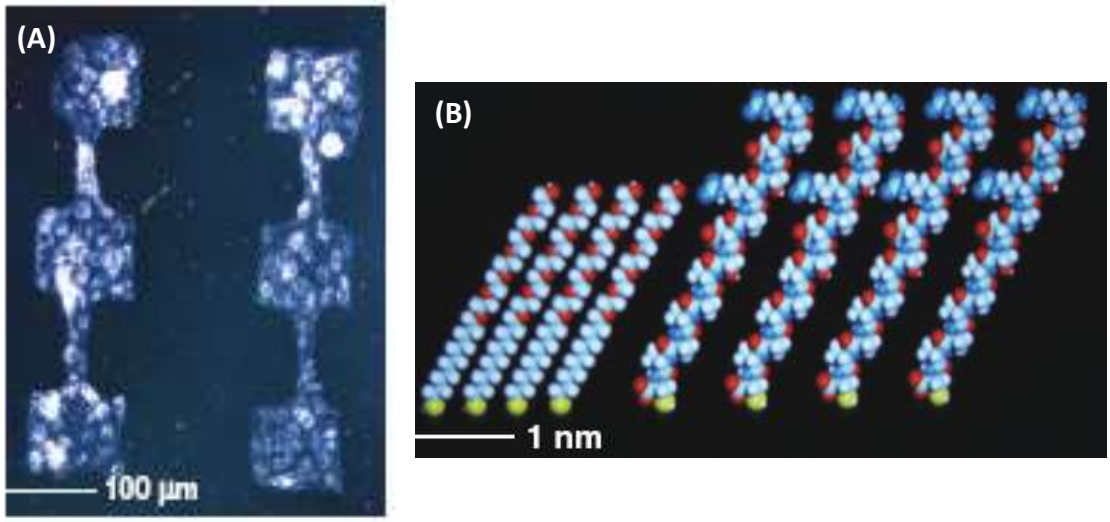

Figure 1.8: *(A) cells grown in a designed pattern coated with molecular carpet peptides (B) Molecular model of RADSC-14 which forms a monolayer on surface and attract specific molecules (Zhang 2003)*

Self-assembly peptides can be used as scaffolds in 3D cell culture (Fichman and Gazit 2014); providing nanoscale features which are important to determine cell behaviour and interaction with the substrate (Haycock 2011).

1.4 Three dimensional (3D) cultures:

Cell shape and relationships with neighbouring cells are fundamental parts of controlling cell activity. Examples of this are clear in development and tissue formation. More often than not embryonic stem cells [ESs] differentiate in two ways, either directly from pluripotent cells or via a non-adherent spheroids cellular aggregation forming what is known as embryoid bodies [EBs] (Rungarunlert, Techakumphu et al. 2009). The formation of these spheroids enables cell-cell interaction, which influences the course of ESC differentiation (Rungarunlert, Techakumphu et al. 2009). The earliest records in spheroids formation was on cancer research in the 80's (Sutherland, Carlsson et al. 1981). It was reported that cells have the ability to reorganized and spontaneously formed 3D spheroids (Pallua and Suschek 2010). To stimulate cell aggregation in vitro, a wide

range of 3D culture systems are available varying from simple and cheap to a more complicated or rather expensive methods. The methods include the conventional "hanging drop" method, static suspension, the use of low adherence 96 multi-well round bottom plate, bioreactors, and finally cell encapsulation/entrapment using a semi solid medium such as methylcellulose or alginate [figure 1.9] (Rungarunlert, Techakumphu et al. 2009).

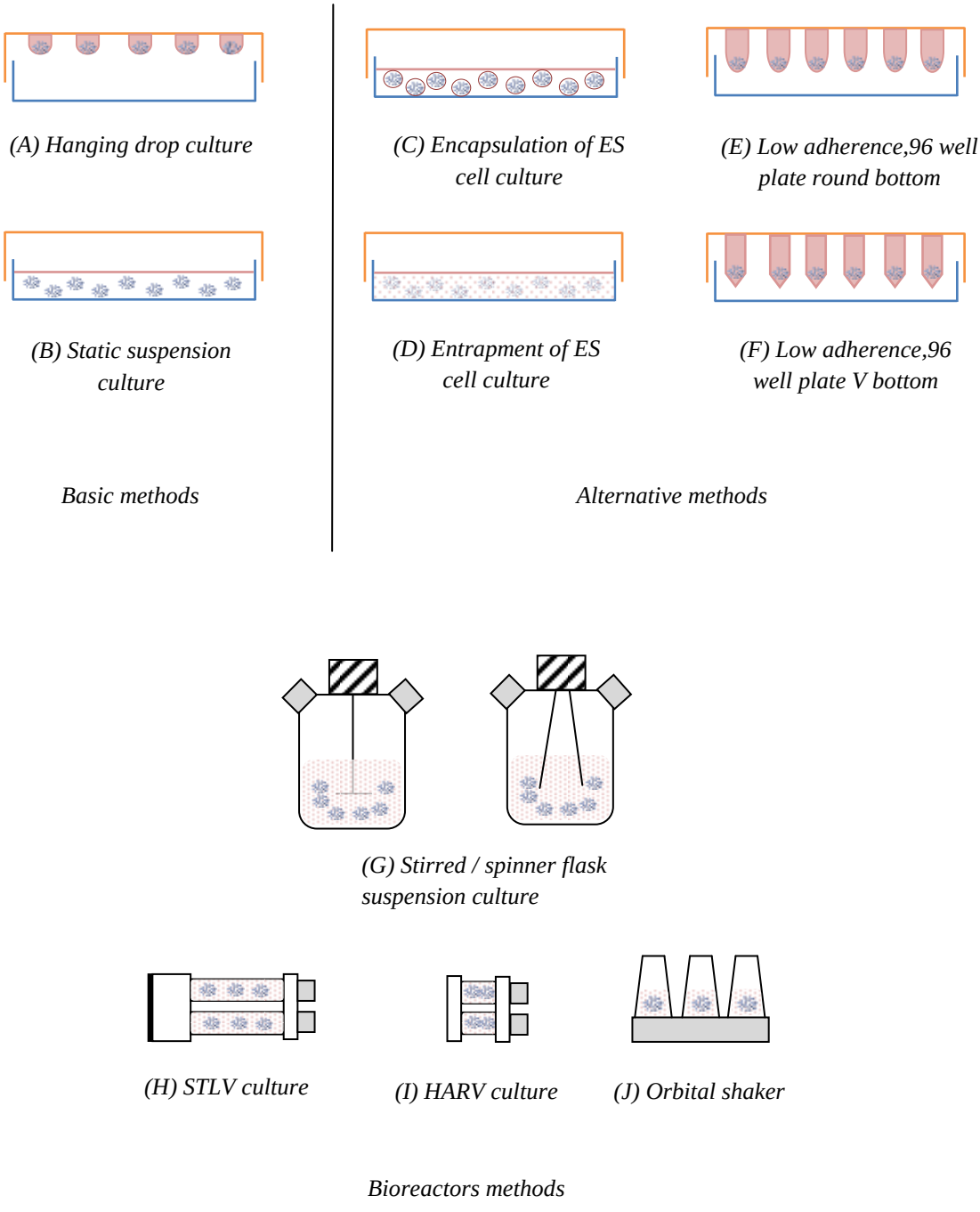

Figure 1.9: *An overview of the common 3D culture methods adapted from (Rungarunlert, Techakumphu et al. 2009)*

Nowadays, most researchers are aware of the limitation of the traditional 2D cell culture (Gelain, Bottai et al. 2006). 3D culture systems can be considered more effective compared to the 2D culture systems (Baharvand, Hashemi et al. 2006), because they better resemble the natural in vivo 3D environment (Zhang, Chai et al. 2006). A 3D culture system plays an important role in helping and understand cellular development, communication, and signal transduction (Gelain, Horii et al. 2007). Previous studies have shown that cellular function, particularly cell signaling is different in a 2D culture compared to a 3D culture (Cukierman, Pankov et al. 2002). For example, specific extra cellular matrix [ECM] protein production may be reduced by cells grown in a 2D culture system (Gelain, Bottai et al. 2006). This may be due to the fact that in a 2D culture, cells are attached to the plate surface from one side and communicate with the adjacent cells from the other side, but the remaining parts are exposed to the culture media (Gelain, Horii et al. 2007). So, in 2D culture an interaction between cell and the plastic surface is prevail rather than cell/cell and cell/ECM interaction which form normal cell function basis (Achilli, Meyer et al. 2012). In contrast, in a 3D culture cells are surrounded with the extracellular matrix [ECM] and other cells mimicking the in vivo environment (Gelain, Bottai et al. 2006).

It is well known that tissues are composed of heterogeneous cell population with interactions between stroma, vessels, and nerves (Fennema, Rivron et al. 2013). Moreover, studies have found that osteogenic differentiation increased (Rouwkema, de Boer et al. 2006) as well as Wnt signalling pathway activation in heterotypic cell communication (Saleh, Whyte et al. 2011). This complex interplay require a 3D environment, here the use of spheroids as a tool to investigate intercellular and cell/ECM

interactions is vital (Fennema, Rivron et al. 2013). For instance, lack of vascular network limits the size of tissue engineering constructions, so, a 3D process in which vascular structure develops within another tissue may be the answer to the problem (Fennema, Rivron et al. 2013). In a recent study by (Rivron, Raiss et al. 2012) spheroids have been used to engineer pre-vascularized bone which helped in improving the survival of implanted cells (Fennema, Rivron et al. 2013). Furthermore, bone defects e.g. osteoporosis and tumour resection are major clinical problems where conventional methods such as transplantation and bone filling material is insufficient (Langenbach, Naujoks et al. 2013). Alternatively, bone tissue engineering promises new therapeutic opportunities via combination of cells, growth factors, and scaffolds (Langenbach, Naujoks et al. 2013).

Different biomaterial scaffolds can be used to form a 3D environment replicating the ECM to provide both physical structure and chemical compositions (Bajaj, Schweller et al. 2014). The choice of biomaterial type depends on the cell type used in the study, where different requirements are needed such as the mechanical properties and growth factors (Dhandayuthapani, Yoshida et al. 2011).

Scaffolds are divided mainly into two application categories: functional implants for regenerative and clinical applications, and in vitro 3D scaffolds for laboratory applications (Karamuk 2001). The characteristics of both scaffolds differ, where in the case of the implantable scaffolds it should match the defect size; promote cell growth, and biodegrade with no harmful effects. Whereas in the case of scaffolds used in the laboratory, supporting desired cell growth and differentiation are more important. Thus, there are different factors that should be considered when choosing a 3D cell culture system [figure 1.10] (3DBiomatrix 2012)

Figure 1.10 : Diagram showing four main factors that should be considered when choosing a 3D cell culture environment; which include cell type, research needs, specific application, and budget. (3DBiomatrix 2012)

Numerous studies have used 3D scaffolds to investigate different cell types and their growth and differentiation, such as neural progenitor cells (Ortinau, Schmich et al. 2010), cardiomyocytes (Mihic, Li et al. 2014), lung progenitor cells (Ling, Liu et al. 2014), and mesenchymal stem cells (Karadzic, Vucic et al. 2014). The interest of this study is towards osteogenesis and bone signalling.

1.5 Bone signaling:

1.5.1 Bone remodeling:

Bone tissue originates from mesenchymal stem cells [MSCs] that also give rise to chondrocytes, myoblasts, and adipocytes (Triffitt, Oreffo et al. 2001). Bone is composed of two contents cells and matrix (Firestein, Budd et al. 2008). The latter consists of 10% water, 70% inorganic component, and 20% organic component with 90% of this being collagen type I (Nakamura 2007). As regards to cells three types are present bone forming cells [osteoblasts], mechanically sensitive cells [osteocytes], and bone resorbing cells [osteoclasts] (Firestein, Budd et al. 2008). Osteoblasts are active cells that produce bone matrix along with other molecules which play a role in bone remodeling, activation and differentiation of osteoclasts (Firestein, Budd et al. 2008). Inactive osteoblasts can become osteocytes which are buried in bone matrix or if they remain at the surface of the bone termed as bone lining cells (Nakamura 2007).

Bone can be renewed where old bone matrix is replaced with new in a process known as bone remodeling (Nakamura 2007). In 3 stages initiation, transition, and termination [see figure 1.11] bone remodeling is regulated by the communication of different cells including, bone vascular endothelial, marrow stromal cells, bone lining cells, osteoblasts, and osteoclasts (Matsuo and Irie 2008).

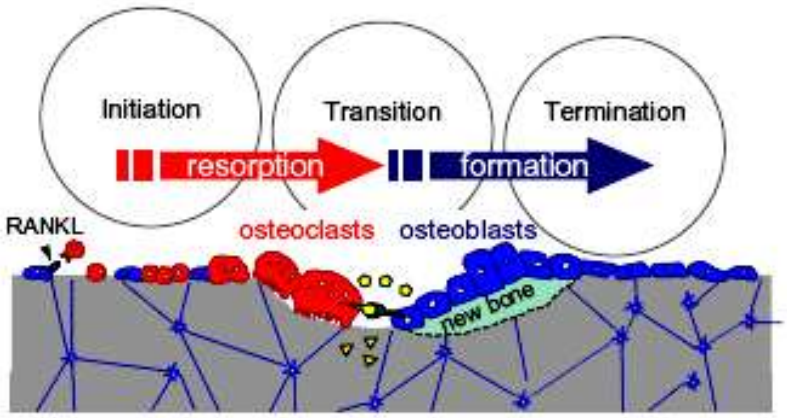

Figure 1.1: *Bone remodeling three phases which involves bone resorption and formation (Matsuo and Irie 2008)*

In the initiation phase, recruitment of osteoclasts occurs through chemokines produced by stromal cells and vascular endothelial cells [e.g. SDF1], and osteoblasts [e.g. MCP-1] (Matsuo and Irie 2008). Osteoclasts are directed to the bone surface that require repair by bone sensory cells the osteocytes which determine the surface that will be resorbed (Matsuo and Irie 2008).It has been suggested that osteoclast differentiation occurs beneath the bone lining cells (Matsuo and Irie 2008).

The second stage is the transition phase and as the name suggests it involves the transition from bone resorption to bone formation (Matsuo and Irie 2008). Coupling plays a vital role in this stage, where bone formation by osteoblasts is activated by osteoclasts either by a direct cell – cell contact [e.g. Eph/ephrin pathway] or indirectly by stimulating the production of growth factors [e.g. TGF-β], and bone morphogenetic proteins [BMPs] (Matsuo and Irie 2008).

In the last phase bone formation continues and may last for approximately three months, unlike bone resorption that lasts for only a short period (Matsuo and Irie 2008).

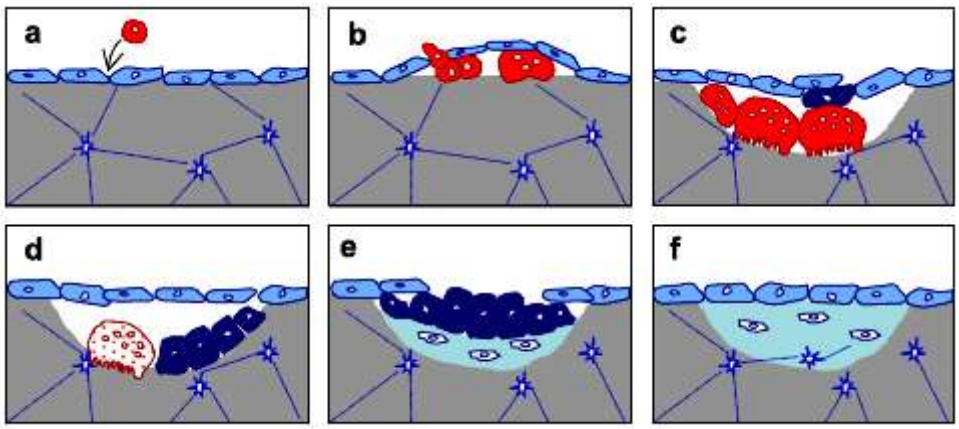

Figure 1.12: *Osteoclast – osteoblast interaction in bone remodeling*

a + b initiation phase [bone lining cells blue] [osteoclast red]

c + d transition phase [bone lining cells blue] [osteoblast dark blue] [osteoclast red]

e + f termination phase (Matsuo and Irie 2008)

1.5.2 Eph/ephrin signaling in bone:

Over the last few years signaling via Eph/ephrin proteins has attracted the attention of many researchers, because of their involvement in diseases such as cancer and osteoporosis (Edwards and Mundy 2008). In addition, they play an important role in cell migration (Holder and Klein 1999), immune regulation (Edwards and Mundy 2008), and bone homeostasis (Edwards and Mundy 2008). Ephrins were first identified in erythropoietin producing hepatocellular carcinoma cell line (Edwards and Mundy 2008). Eph/ephrins signaling involves two classes a GPI linked protein [class A], and transmembrane protein [class B] (Holder and Klein 1999). Eph receptors consist of 8 receptors type A and 6 type B, while ephrin ligands consist of 5 types A and 3 type B (Jensen 2000). Generally, a B type ligand binds to a B type receptor, and A ligand to A receptor (Kullander and Klein 2002). However, there are some exceptions, for example Eph A4 can bind to both A and B type ligands (Kullander and Klein 2002) [see table 1.15]. Furthermore, Eph receptors can act as ligands and vice versa (Kullander and Klein 2002). Additionally, since both Eph receptors and ephrin ligands are bound to the membrane, signaling through Eph/ephrin requires cell – cell contact (Kullander and Klein 2002).

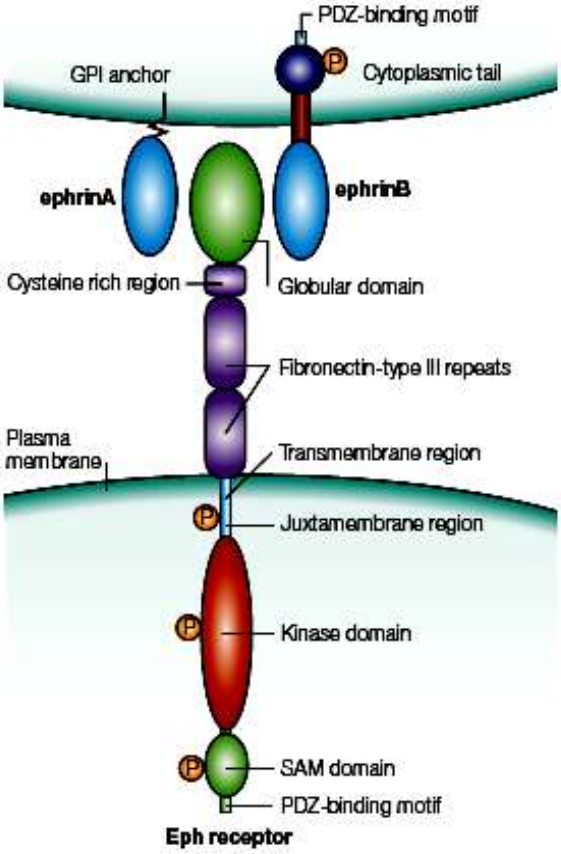

Figure 1.13: *Eph receptors and ephrin ligands structure (Kullander and Klein 2002)*

Table 1.3: *Eph receptors and ephrin ligands specificities arranged depending on their affinity, based on structure and function ephrins are divided into two groups ephrin-A and ephrin-B. EphA receptors bind to ephrin-A ligands and Eph-B receptors bind to ephrin-B ligands with few exceptions shown in the table (Jensen 2000)*

Eph receptors	ephrin ligands
Eph A1	ephrin A1
Eph A2	ephrin A3, A1, A5, A4, A2
Eph A3	ephrin A5, A2, A3,A1,A4, and B1(weak)
Eph A4	ephrin A5, A1, A3, A2, B2, B3, A4
Eph A5	ephrin A5, A1, A2, A3, A4
Eph A6	ephrin A2, A1, A3, A4, A5
Eph A7	ephrin A2, A3, A1, A4, A5
Eph A8	ephrin A5, A3, A2
Eph B1	ephrin B2, B1, A3, A1(?), A4(?), B3(?)
Eph B2	ephrin B1, B2, B3
Eph B3	ephrin B1, B2, B3
Eph B4	ephrin B2, B1,
Eph B5	Unknown
Eph B6	Unknown

In general bone cells express ephrin B1, ephrin B2, Eph B2, Eph B3, Eph B4, Eph B6, and Eph A4 (Xing, Kim et al. 2010). Osteoclasts express ephrin B1 and B2 ligands but not receptors (Kwan Tat, Pelletier et al. 2009), whereas osteoblasts express Eph B4 and ephrin B2 (Edwards and Mundy 2008). Eph/ephrin in bone involves what is known as bidirectional signaling, where cell expressing Eph receptors [forward signaling] interact with cell expressing ephrin ligands [reverse signaling] (Mundy and Elefteriou 2006). Most studies have focused on Eph B4 / ephrin B2 interactions while ephrin B1 was the focus for others.

In the Eph B4 / ephrin B2 interactions in bone, for ephrin B2 reverse signaling to be activated the inhibition of Fos and NFATC1 are required (Mundy and Elefteriou 2006). On the other hand, Eph B4 forward signaling depends on Rho inactivation in osteoblasts (Mundy and Elefteriou 2006). It worth mentioning that Rho can be activated via Eph A receptor leading to the formation of lamellipodia and filopodia, and resulting in changes in movement and cell shape (Edwards and Mundy 2008).

Eph B4 increases bone formation and decreases bone resorption (Mundy and Elefteriou 2006), whereas the stimulation of Eph B4 forward signaling is through ephrin B2 (Edwards and Mundy 2008). In addition, ephrin B1 is important for bone marrow stromal cells differentiation, osteoblasts differentiation, osterix expression stimulation, and bone formation (Xing, Kim et al. 2010). Moreover, ephrin B2 interacts with connexin 43 and thereby regulates cellular communication via gap junctions (Kwan Tat, Pelletier et al. 2009).

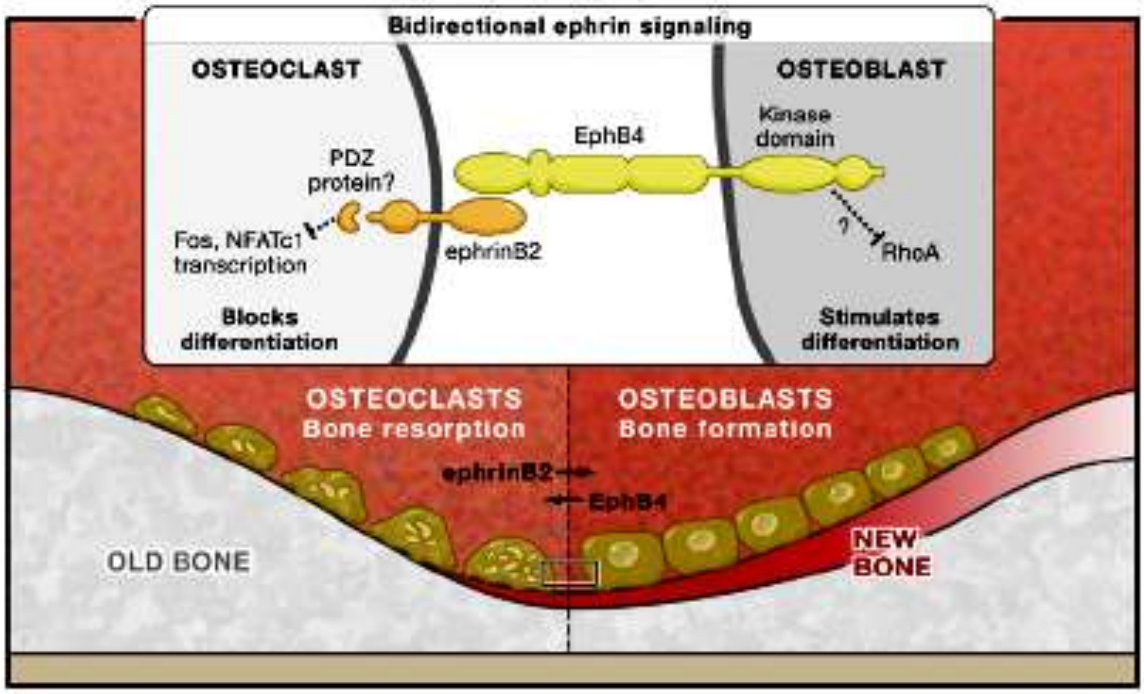

Figure 1.14: *Eph/ephrin signaling in bone homeostasis (Mundy and Elefteriou 2006)*

1.6 Project aims

The main aim of this study was to examine cell behaviour in a 3D environment where cell/cell and cell/ECM communication could be explored. This included investigating RAD-16 peptide that self assembles forming a hydrogel scaffold for cells and allowing the presentation of cell interaction motifs. This allowed investigation of the role of 3D interactions in the control of MSC differentiation.

Specific objectives were the following:

1) To optimize in vitro spheroid culture conditions in order to evaluate differentiation of marrow-derived mesenchymal cells in 3D.

2) To determine cell viability in 2D and 3D culture using the MTT assay. Also cell differentiation to osteoblasts will be assessed via alkaline phosphatase enzyme activity measurement, and through quantifying osteoblastic gene expression using qRTPCR.

3) To investigate cell response to RAD-16 self-assembly peptide assessing cell viability and ability to differentiate into osteoblasts.

Chapter 2: Materials and Methods

2.1 Materials and methods:

All materials and reagents were purchased from Sigma-Aldrich company, Ltd Ayrshire, UK unless otherwise specified.

2.1.1 Cell culture

Tissue culture was carried out in an aseptic environment using a class II laminar flow hood which had been decontaminated with 70% ethanol. Two cell types were used in this study, rat calvaria-derived osteoprogenitor cells and human mesenchymal stem cells, both were grown as monolayer [2D] and aggregates (spheroids) [3D] under normal and osteogenic conditions. The normal media for routine culture was Dulbecco's Modified Eagle Medium [DMEM/Gibco BRL, UK] supplemented with 10% fetal bovine serum [FBS], 10% 2mML-Glutamine, 100µg/ml streptomycin and 100U/ml penicillin. To promote osteogenic differentiation the media was supplemented with 5mM of β-Glycerophosphate disodium salt hydrate, 100 µg/ml of 2-Phospho-L-ascorbic acid trisodium salt and 10nM of dexamethasone. Dexamethasone is a synthetic glucocorticoid that has been shown in previous studies to induce the osteoblastic phenotype and thus bone formation (Atala and Lanza 2001). β-Glycerophosphate is added as a source of phosphate to promote the matrix mineralization process (Atala and Lanza 2001). While ascorbic acid works as a cofactor for proline hydroxylation which is important in collagen triple helix stabilization (Atala and Lanza 2001). After seeding; the cells were incubated at 37º C in a 5% co_2 atmosphere for 24hour, 72hour, and 7 days. Cultures were observed using a phase contrast inverted microscope.

2.1.2 Cell counting and viability determination using a hemocytometer:

The number of cells in culture can be determined using either a hemocytometer or coulter counter, in this study a haemocytometer was used. A hemocytometer is a thick glass slide with two chambers; each one is divided with gridlines into nine squares each of which is 1mm square (Adams 2003).

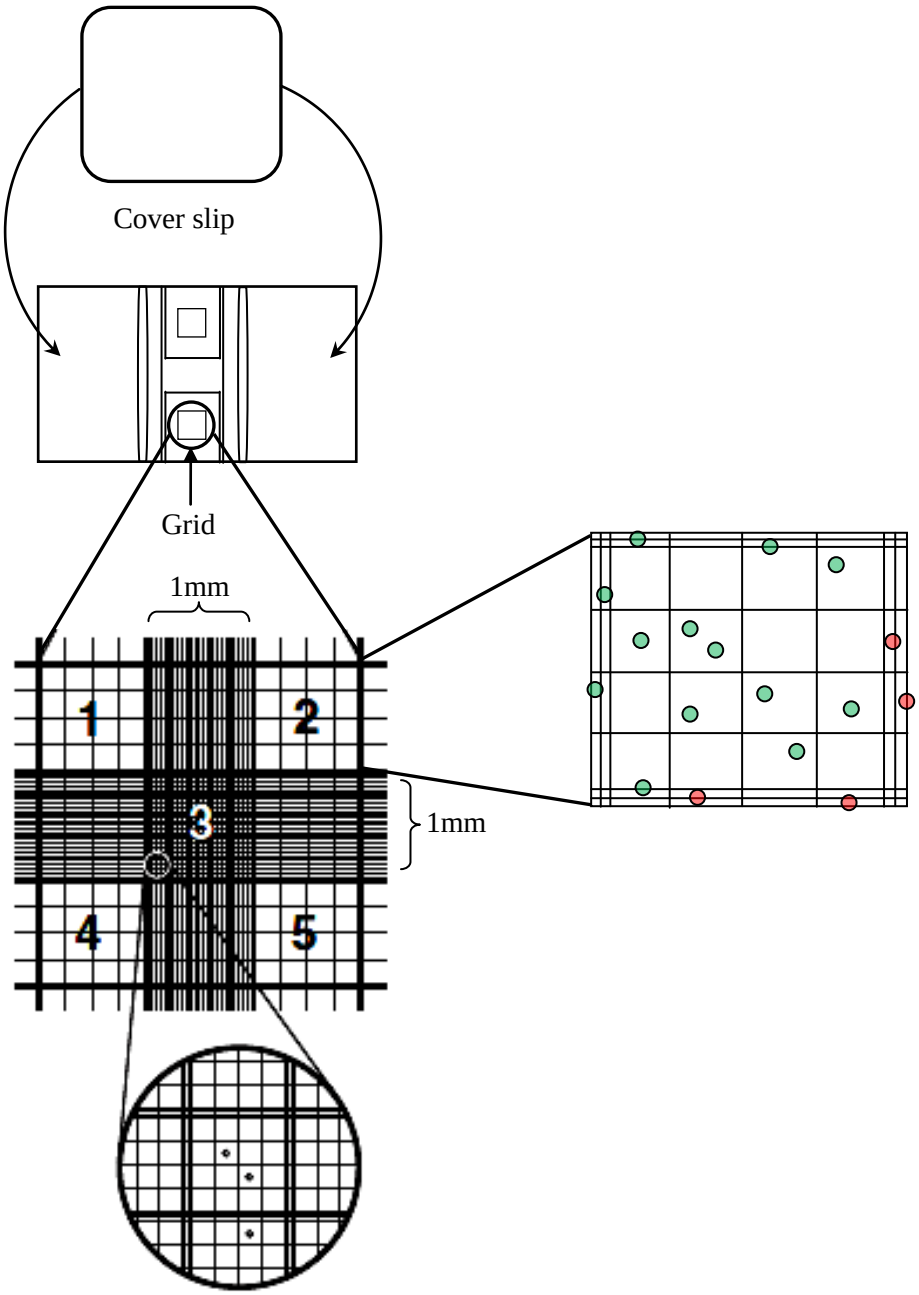

Figure 2.1: *Illustration of a hemocytometer slide. After placing the coverslip on the slide, a cell suspension is loaded and cells are counted in each square. Cells touching the middle line on the top and left are included in the counting (green) while those touching right and bottom are excluded from the count (red) (Phelan 2007; Ortinau, Schmich et al. 2010)* (Martin 1994)

To determine the number and viability of cells per millilitre, first both coverslip and hemocytometer were cleaned with 70% [v/v] ethanol then after cell trypsinzation a 100µl of the cell suspension and a 100µl of Trypan blue dye were mixed, using a sterile pipette and about 10µl of cell suspension was loaded and cells in 4 squares were counted. To determine the percentage of viability the number of viable cells [nonstained] was divided by the total number of cells and multiplied by 100 (Adams 2003)

$$\text{viability precentage} = \frac{number\ of\ viable\ cells}{total\ number\ of\ cells} x\ 100$$

Then the following equation was used:

Cells/ml = average count per square x dilution factor x 10^4

2.1.3 Cell viability and proliferation assay:

Measuring cell viability and proliferation is important in cell- based studies (Kresse 2003). A decrease in cell viability reflects a reduction in cell growth, while an increase in cell viability which assesses healthy cells indicates cell proliferation (Kresse 2003). Several viability assays are available which are based on measuring the metabolic activity [e.g., MTT, XTT, WST-1] or by examining cell membrane integrity using a dye that stains dead cells [e.g., trypan blue] (Kresse 2003).

In this study cell viability and proliferation were measured using an MTT assay which is a colorimetric assay that measures the 3-(4,5-dimethythiazol-2-yl)-2,5-diphenyl tetrazolium bromide (MTT- yellow coloured) reduction by the succinate dehydrogenase enzyme produced by active mitochondria in live cells resulting in the formation of

formazan (dark purple insoluble crystals) (Chapdelaine 1989). The insoluble formazan can be solubilized using an organic solvent e.g. isopropanol or DMSO and measured at 570nm OD using a colorometric plate reader (Chapdelaine 1989).

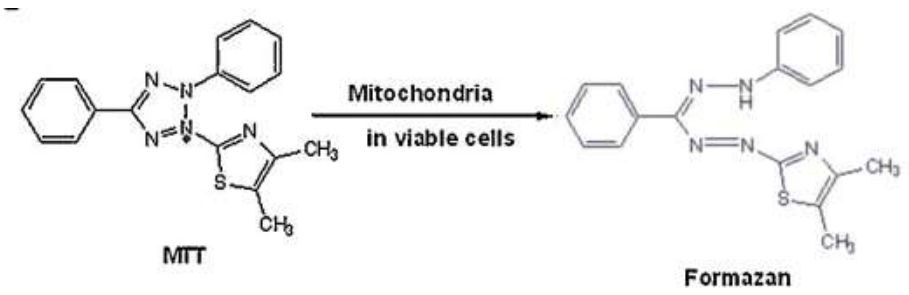

Figure 2.2: *Represents the chemical structure of MTT and its reduction by mitochondrial enzymes in viable cells to formazan (Duval, Clarot et al. 2012)*

Cell proliferation and viability were assessed as described by (Wirth, Comte et al. 2005). First, the media were discarded from the wells and 200µl of MTT solution with a final concentration of 1mg/ml was placed in each well.(24 well plate) the cells were then incubated for 4h at 37ºC. Thereafter, media were removed and 100µl of isopropanol was added to solubilize the formazan crystals completely; the plates were placed on a shaking plate for 30 min at room temperature. Using a microplate reader the plates were read at 570nm OD. Next, the absorbance values were blanked against isopropanol absorbance and cell viability was measured following the equation below:

$$Cell\ viability\ (\%) = \frac{A_s - A_b}{A_c - A_b}\ x100$$

Where:

A_s = Sample absorbance

A_b = Blank absorbance

A_c = Control absorbance

2.1.4 Alkaline phosphatase activity

Alkaline phosphatase is an enzyme that is found in most tissues but is extensively in placenta, kidney and bone (Wilson and Walker 2000). To assess alkaline phosphatase activity a colorimetric assay with 4-nitrophenylphosphate (PNPP) was used where alkaline phosphatase cleaves this colourless substrate to a yellow product known as p-nitrophenol.

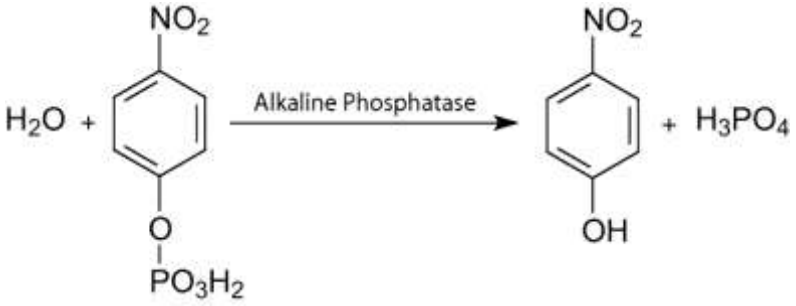

Figure 2.3: *Represents the chemical structure of a p-nitrophenol molecule which is hydrolysed by alkaline phosphatase developing a yellow end product (Sigma)*

First the media were removed and the cells were fixed in 4% (w/v) paraformaldehyde in PBS for 10 min, followed by washing with 50mM HEPES buffer (pH = 8). Then 200µl of alkaline phosphatase colorimetric substrate (pNPP) was added and left at room temperature for about 30 min. The absorbance of the end product was measured at 405nm.

The alkaline phosphatase enzyme activity was calculated via interpolation of a standard curve which was generated by making a serial dilution from a concentrated solution containing 1ml of 50mM HEPES buffer (pH = 8) and 20µl of 10mM p-nitrophenol standard to give a concentration range of 0.2, 0.1, 0.05, 0.025, 0.0125 and 0.00625µM/ml, respectively.

2.1.5 RNA extraction and cDNA synthesis

2.1.5.1 RNA isolation:

RNA isolation can be performed using different methods either by disrupting both plasma membrane and subcellular organelles with chaotropic agents such as Sodium docedyl sulphate (SDS), N-Lauryl sarcosine, urea, chloroform, guanidinium salts, or phenol (Farrell Jr 2010). or by solubilizing the plasma membrane gently maintaining organelle integrity using non-ionic lysis buffer (Farrell Jr 2010). In this study RNA was isolated using Guanidinium thiocyanate-phenol-chloroform extraction method with the TRIzol reagent which disrupts the cell and dissolves cell components but maintains RNA integrity.

For this study TRIzol® reagent (Invitrogen) was used according to the manufacturers protocol. Media were removed and cells were washed with PBS (Lonza), then 1ml TRIzol per 10 cm^2 of culture dish surface area was added to lyse the cells. After 5 min at room temperature the viscous solution was pipetted up and down several times for complete nucleoprotein dissociation. 0.2ml of chloroform per 1ml of TRIzol was then added and mixed vigorously for 15 s and incubated at room temperature for 2-3 min. The samples were spun at 13,000 xg for 15 min and 3 layers were formed [see figure 2.4]. The colourless aqueous upper phase that contains the RNA was transferred to a new tube for subsequent analysis. RNA was precipitated by adding 0.5ml of ice cold isopropanol

(Fisher) followed by incubation at room temperature for 10 min RNA was collected by centrifugation at 12,000 xg 4Cº for 10 min and the RNA pellet formed on the base side of the tube. Afterward the supernatant was removed leaving the RNA pellet which was washed by adding 1ml of 70% ethanol and then the samples were vortexed briefly and then centrifuged again for 5 minutes at 7500xg 4Cº. After removing the supernatant the pellet was air dried for about 5-10 min, never allowing the RNA pellet to dry completely. Then the pellets were re-suspended in 20-50µl RNase free water followed by incubating in a water bath at 65ºC for 5 min and samples were then ready to be quantified.

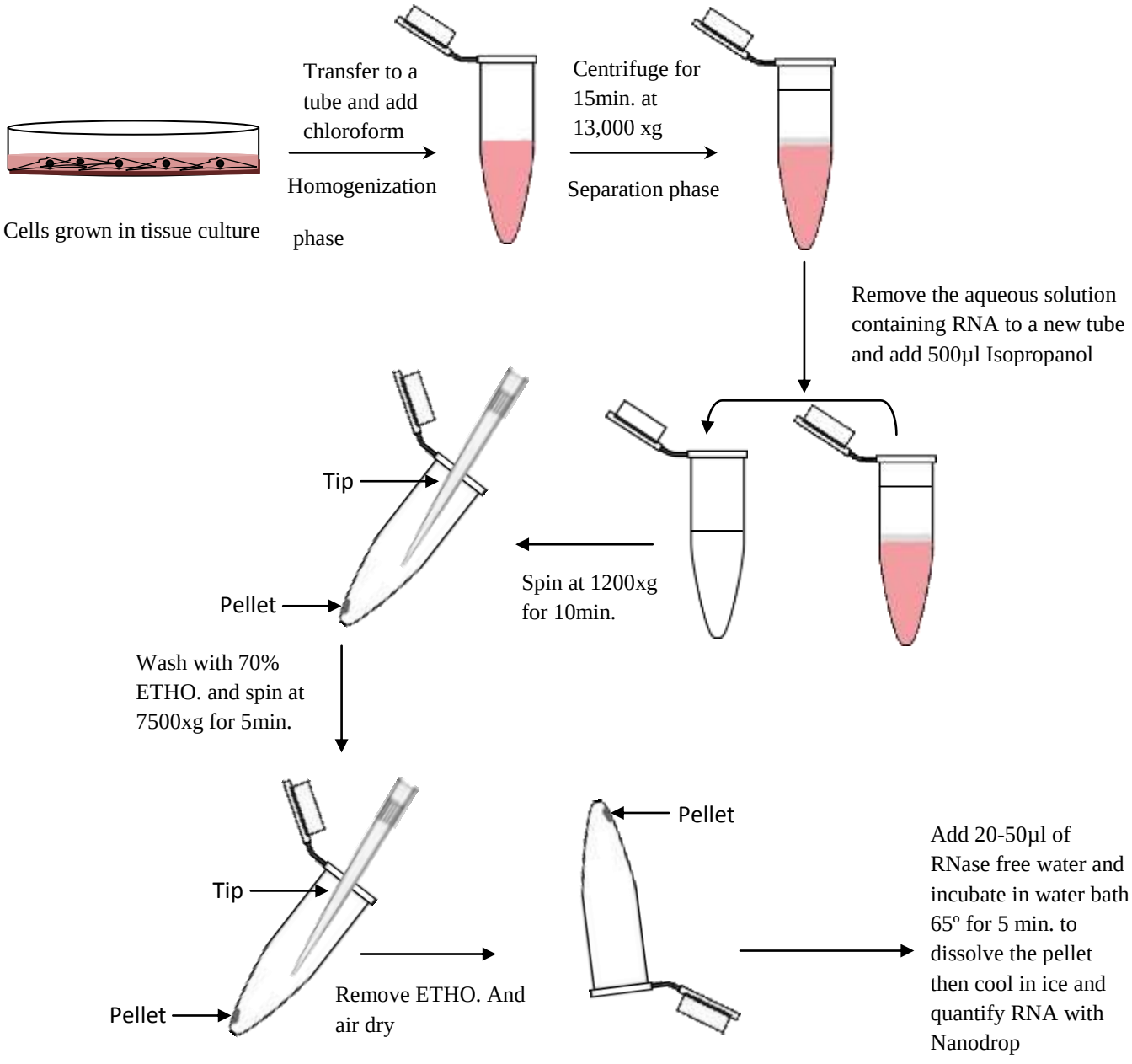

Figure 2.4: *schematic of RNA extraction steps*

2.1.5.2 RNA quantity and quality assessment:

Different methods may be used for RNA quantification including UV absorbance, micro capillary electrophoresis, and fluorescence based quantification (Aranda, Dineen et al. 2009). In this study RNA concentration and purity was measured using a Nano-drop 1000 spectrophotometer (Thermo scientific) following the manufacturers protocol. Briefly, with the arm open a 1µl of the sample was placed into the lower measurement pedestal and the upper pedestal was lowered, after closing a closed liquid cell is automatically formed between both lower and upper pedestal and a spectral measurement is made [see Figure 2.5] . The ratio between 260/280 nm readings provide an estimation of nucleic acid purity, where values of 1.8 and 2 is accepted as pure DNA and RNA respectively (Roskams and Rogers 2002). Subsequently, samples were ready for cDNA synthesis.

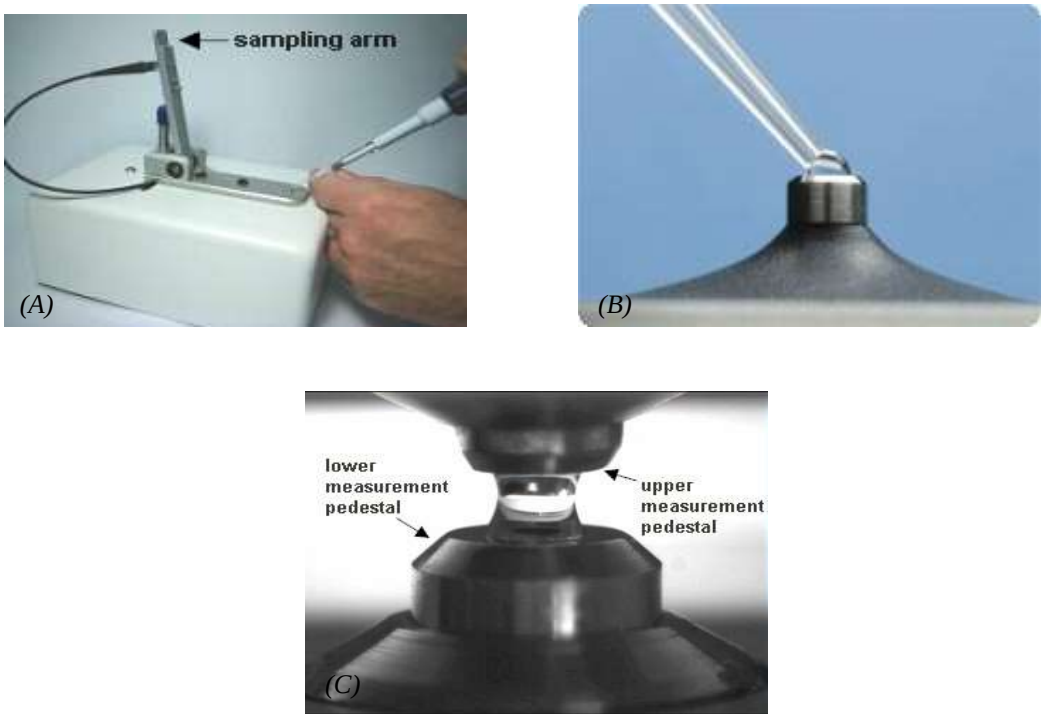

Figure 2.5: *Measuring RNA using the Nanodrop instrument (A) pipette the sample into the lower measurement pedestal, with the sampling arm open. (B) 1µl of the sample. (C) when the sampling arm is closed the spectral measurement is initiated using the operating software on the PC, automatically the sample column is drawn between the upper and the lower measurement pedestals.*

2.1.5.3 RNA integrity assessment:

RNA integrity was assessed by running it on a 1.2% agarose gel formed by melting 0.6g of electrophoresis grade agarose in 50 ml of 1x TAE buffer 2 µl of 10 mg/ml ethidium bromide (EtBr) stock solution was also added to the molten agarose. The gel was poured in a casting frame and the comb was inserted and left to solidify for about [20-30 min]. Once the gel was set the comb was removed and the gel placed in 1x TAE buffer 1 µl 8x loading dye and 6 µl diH_2O with 2 µl of each RNA sample was loaded into each well of the solidified gel, and a DNA ladder 2kb was also loaded. The gel was run at 100v for approximately 30-40 min. Then the nucleic acids were visualized using UV illumination. Two distinct bands should appear if the RNA is intact.

2.1.5.4 First-Strand cDNA synthesis:

cDNA was prepared from approximately 1µg of RNA using SuperScript III first-strand cDNA synthesis kit (Invitrogen) following the manufacturer's protocol. In brief, the samples were mixed with 1µl of 50µM Oligo (dT) (Promega) and 2 µl of 10mM dNTP mix and heated in a water bath at 65ºC for 5 min. After that the samples were incubated for at least 1 minute on ice followed by centrifugation and adding 4µl 5x First-Strand Buffer, 1µl 0.1M DTT, 1µl Recombinant RNase Inhibitor (40units/µl), and 1µl of SuperScript III Reverse Transcriptase (200 units/µl). Then cDNA synthesis was performed in a 20µl reaction volume by incubating for 60 min at 50ºC using a Thermo-cycler, and samples were then used for qPCR amplification.

2.1.6 Quantitative reverse transcriptase-polymerase chain reaction (qRT-PCR):

Once cDNA was obtained, qRT-PCR assays for multiple genes [listed in table 2.2 and 2.3] were performed with a Real –Time PCR system, ABI Prism 7900HT (Applied Biosystem) using SYBR Advantage qPCR Premix (Clontech) following manufacture recommendations. The PCR reaction mixture was prepared by mixing 10µl of x2 SYBR Advantage qPCR Premix, 0.4µl of 10µM PCR forward primer, 0.4µl of 10 µM PCR reverse primer, 2µl of cDNA template, and 7.2µl of free nuclease water to achieve a total volume of 20µl in each well of a 96well plate. The plate was then placed in the ABI Prism 7900HT, the thermal profile used is shown in table 2.1.

Table 2.1: *thermal cycles for genes amplification*

Procedure	Temperature	Time
Hot start	50 Cº	2 minutes
x40	95 Cº	10 minutes
	95 Cº	15 seconds
	60 Cº	1 minute
Dissociation curve	95 Cº	15 seconds
	60 Cº	15 seconds
	95 Cº	15 seconds

GAPDH expression levels were used in normalizing Ct values obtained for each gene.

For qPCR assay specificity, a verification melt curve was generated and analysed where one defined peak suggests a clean amplification of a single product, while multiple peaks suggest the presence of more than one product which may be caused by primer dimer or non-specific amplification. The genes explored in this study are shown in table 2.2 and table 2.3.

Table 2.2: *list of rat primers [Sigma] used for qRT-PCR analysis*

Gene	Forward primer	Reverse primer
GAPDH	CTGCACCACCAACTGCTTAC	CAGAGGTGCCATCCAGAGTT
Runx2	CCGTGTCAGCAAAACTTCTTT	CTCACGTCGCTCATCTTGC
ALP	GCACAACATCAAGGACATCG	TCAGTTCTGTTCTTGGGGTACAT
Osterix	GGACAGCCAACCCTAGCC	TGGAGCCACCAAACTTGC
CX 43	AGCCTGAACTCTCATTTTTCCTT	CCATGTCTGGGCACCTCT
Pannexin 3	ATCTCTCTGGCCTCACAAGG	CAGCACTGGCAGATACATGG
Ephrin B1	GCCAAGCAAAGAGTCAGACA	TCTTGCTGGTTCACAGTCTCAT
Ephrin B2	TCCTCATGAAAGTTGGACAAGA	CTGGACGTCTTGTTGGATCA
Ephrin B4	CTGCGGAACATCTGACTCG	TGATGTTAACTTTCCCTGTTGC

Table 2.3: *list of human primers [Sigma] used for qRT-PCR analysis*

Gene	Forward primer	Reverse primer
GAPDH	AGCCACATCGCTCAGACAC	GCCCAATACGACCAAATCC
Runx2	GTGCCTAGGCGCATTTCA	GCTCTTCTTACTGAGAGTGGAAGG
ALP	CCTGCCTTACTAACTCCTTAGTGC	CGTTGGTGTTGAGCTTCTGA
Osterix	CATCTGCCTGGCTCCTTG	CAGGGGACTGGAGCCATA
CX 43	TTTCAATGGCTGCTCCTC	TGCTCACTTGCTTGCTTGTT
Pannexin 3	GCTGATGTCCCTGGCATT	GAGAAGCAGCTGATCGGAGA
Ephrin B1	TCATGAAGGTTGGGCAAGA	GTGTTGTCTGCCTCCTTGCT
Ephrin B2	TCTTTGGAGGGCCTGGAT	GATCCAGCAGAACTTGCATCT
Ephrin B4	CCCCAGACTGTCCCACCT	GCATTCCGGTCTTTCTGC

2.1.7 Scanning electron microscopy [SEM]:

An electron microscope is an instrument that uses a beam of electrons to examine objects. SEM is used to observe the surface topography, chemical composition [via EDX], crystalline structure, and the size and shape of a sample (Bogner, Jouneau et al. 2007) (Vernon-Parry 2000).

In order to study specimen topography, first, cell culture media were removed gently. Then, samples were washed with PBS followed by fixation in 2%(w/v) gluteraldehyde in Sorensons phosphate buffer for 30 min. They were washed with PBS and dehydrated using an ascending grade of ethanol [25%, 50%, and 75%] for 30 min then 100% ethanol x2 changes for 1 h. Samples were then finally dehydrated using Hexmethyldisilazane [HDMS] in a fume hood overnight at room temperature. Following this, samples were mounted on aluminium stubs with carbon discs (Agar Scientific, UK) and coated with 15nm of gold using a Polaron SEM coating unit (Bozzola 1998).

2.1.8 Histology and immunoflourescent studies:

2.1.8.1 Samples preparation for histological studies:

For 2D histological studies, cells were grown on a slide/cover glass which was placed in a petri dish and cells were left to grow for 7 days. After removing the media and washing with PBS, samples were fixed in 4% paraformaldehyde in PBS [w/v].

For analysis of 3D specimens, samples were first gently washed with PBS gently and the spheroids fixed for 10 min with 4% paraformaldehyde in PBS [w/v]. They were then placed in collodion bag which was made following (Shidham and Atkinson 2007). Briefly, a conical Pyrex tube was filled with collodion solution and left to dry in a fume hood for about 10 minutes. The dried layer that forms at the top of the tube was punctured and the extra collodion solution was placed in a container for reuse. Once it had completely dried and coated the wall of the tube, PBS was added to wash the bag and then the spheroids were placed inside and the bag was released from the tube. The collodion bag containing the spheroids were rolled and wrapped in a tissue paper then placed in a histology processing cassette.

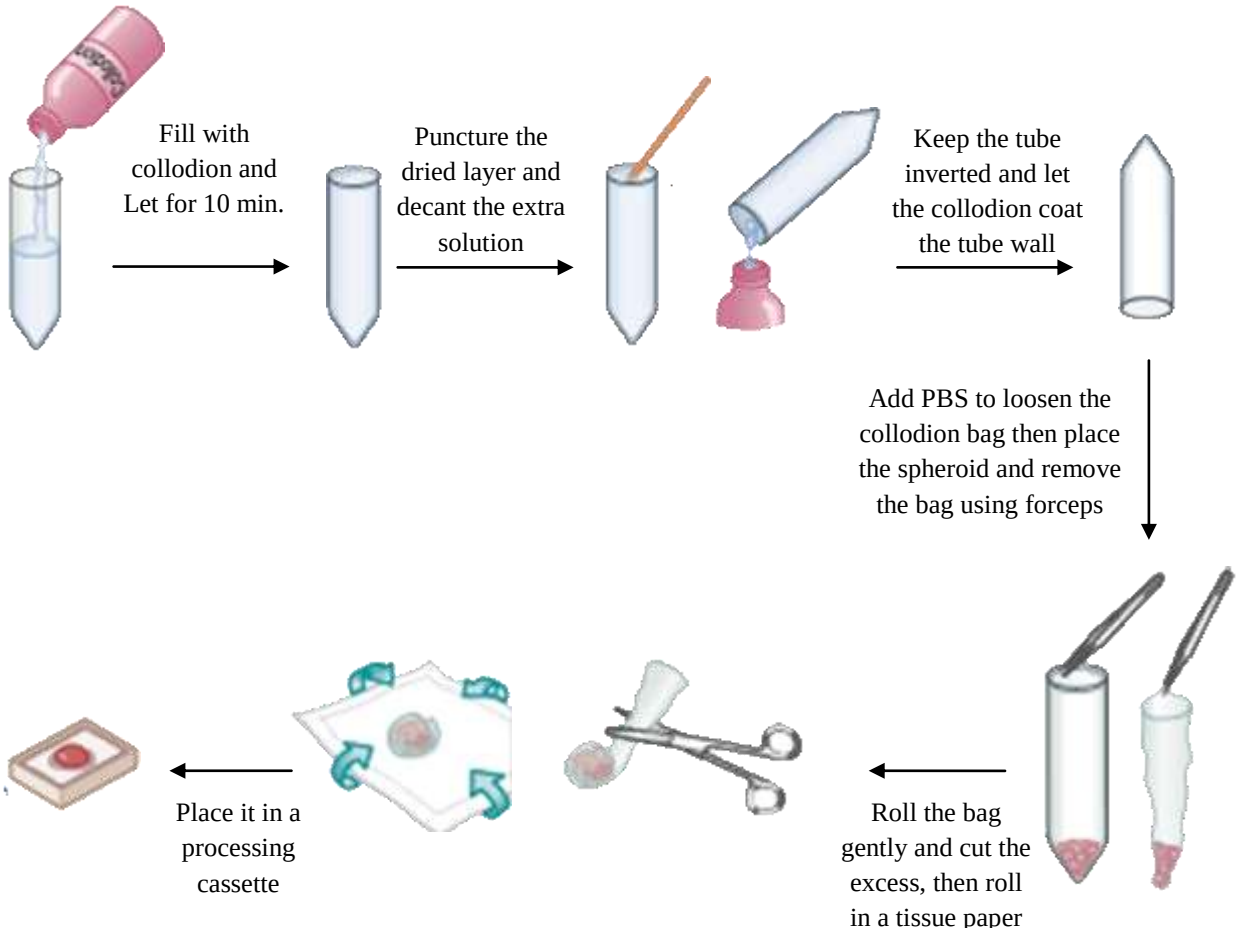

Figure 2.6: *Cell block preparation with a collodion bag (Shidham and Atkinson 2007)*

The samples were embedded in paraffin wax, they were then sectioned [5 μm thick] using a Leica microtome (Leica Microsystems Ltd., U.K.) and the sections were placed on poly-L-lysine-coated slides which were left to dry at room temperature.

Haematoxylin and Eosin (H&E), a routine stain was used, which stains nuclei bluish-purple and cytoplasm pink. First, sections were deparaffinised in xylene for 10 minutes followed by rehydrating with ethanol 100% and 95% respectively for 3 minutes at each concentration. After rinsing in dH_2O sections were treated with Harris's haematoxylin for

5 minutes then washed in dH_2O then in Scott's water for 2minutes. Staining with eosin was followed for 1 minute, then washing in dH_2O. Finally, dehydrating through a series of ascending concentrations of ethanol [50% - 70% - 95% - 100% - 100%] for 2 minutes, followed by clearing in xylene for 2 minutes. Sections were then mounted in DPX and stored in a cool dry place.

2.1.8.2 Immunoflourescent staining:

Immunofluorescence (IF) is a technique where antibodies are chemically conjugated to a fluorescent dye such as tetramethyl rhodamine isothiocyanate (TRITC) or fluorescein isothiocyanate (FITC). Two methods are available direct and indirect binding of antibodies to the antigen of interest allowing detection through fluorescence techniques. The fluorescence can then be quantified using an array scanner or automated imaging instrument, or flow cytometer, or visualized using fluorescence or confocal microscopy (Robinson, Sturgis et al. 2009).

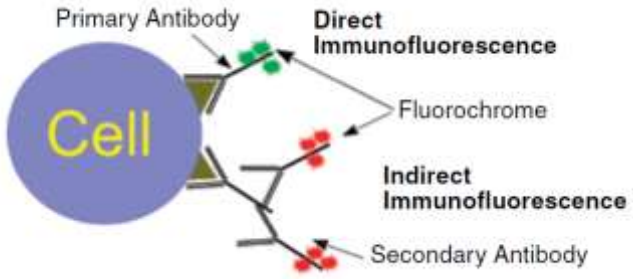

Figure 2.7: *Schematic of direct and indirect Immunofluorescence methods (Robinson, Sturgis et al. 2009)*

For monolayer [2D] cells were grown on a coverslip and left to grow for 7 days. Whereas in the case of the spheroids [3D] cells were grown on the coated surface of the

24 well plate, the spheres then were moved gently to a new non-coated well. In both cases [2D and 3D] the media were aspirated and cells were washed then fixed in 4% [w/v] paraformaldehyde in PBS for 20 min, then washed three times in PBS/0.1% Tween 20 [v/v] for permeabilization. Non-specific binding of antibodies was blocked by 3% (v/v) goat serum in PBS/0.1% Tween 20 [v/v] for 20 min. Sections were incubated for one hour at room temperature with a primary monoclonal anti-connexin 43 antibody [1:100 dilution]. Followed by washing three times with PBS/0.1% Tween 20 [v/v], and incubating with FITC secondary antibody [1:200 dilution] for 45 minutes in the dark. Sections were rinsed with PBS/0.1% Tween 20 [v/v] then mounted with 'Vectashield with DAPI' (Vector Laboratories Ltd., Peterborough U.K.) and incubated overnight at 4°C in the dark. The stained specimens in this study were visualized using both fluorescence and confocal microscopy.

2.1.9 Statistical analysis:

Data management and analysis was performed using SPSS 17.0 (Statistical Product and Service Solutions 17.0, Chicago, IL, USA). Variables were tested first to verify if they follow a Gaussian distribution. Since the analysis showed that our data were not normally distributed a non-parametric test, a Kruskal-Wallis one-way analysis of variance was conducted. The variance was then subjected to a multi-comparison analysis Mann – Whitney U test to determine the significance. Results were presented as mean ± standard error, and a p-value of < 0.05 was considered significant.

Chapter 3: Investigating spheroids generation using different approaches

3.1 Introduction

Due to the limitations of traditional monolayer cell culture (Gelain, Bottai et al. 2006), three dimensional cell culture have been developed that are considered to be more effective at mimicking the in vivo scenario and are therefore more representative at modelling cell activity (Baharvand, Hashemi et al. 2006).

Different 3D culture methods are available to study cell aggregation and the formation of spheroids in vitro, which can be classified in to scaffold and non-scaffold based methods (Riss 2014). The latter includes serum free media (Pease, Brewer et al. 2012), the hanging drop method (Yusuf, Gopurappilly et al. 2013), rounded bottom 96 well plate (Kawai, Hayashi et al. 2001), agar (Kang, Jenabi et al. 2007), methylcellulose (Baum, Hlushchuk et al. 2007), poly (2-hydroxyethyl methacrylate) [PolyHEMA] (Le Beyec, Xu R Fau - Lee et al. 2007), rotating spinner flasks (Lin and Chang 2008), micro-patterned surfaces (Wang, Itaka et al. 2009), and magnetic levitation (Souza, Molina et al. 2010). The quantity and quality of these spheroids is affected by different factors including spheroid culture method choice, culture media, and viability (Atala and Lanza 2001).

Accordingly in this chapter we aimed to optimize *in vitro* spheroid culture conditions for the cells in this study by testing different simple methods to identify which of these methods is the most appropriate and reproducible. Figure 3.1 summarizes the optimization plan.

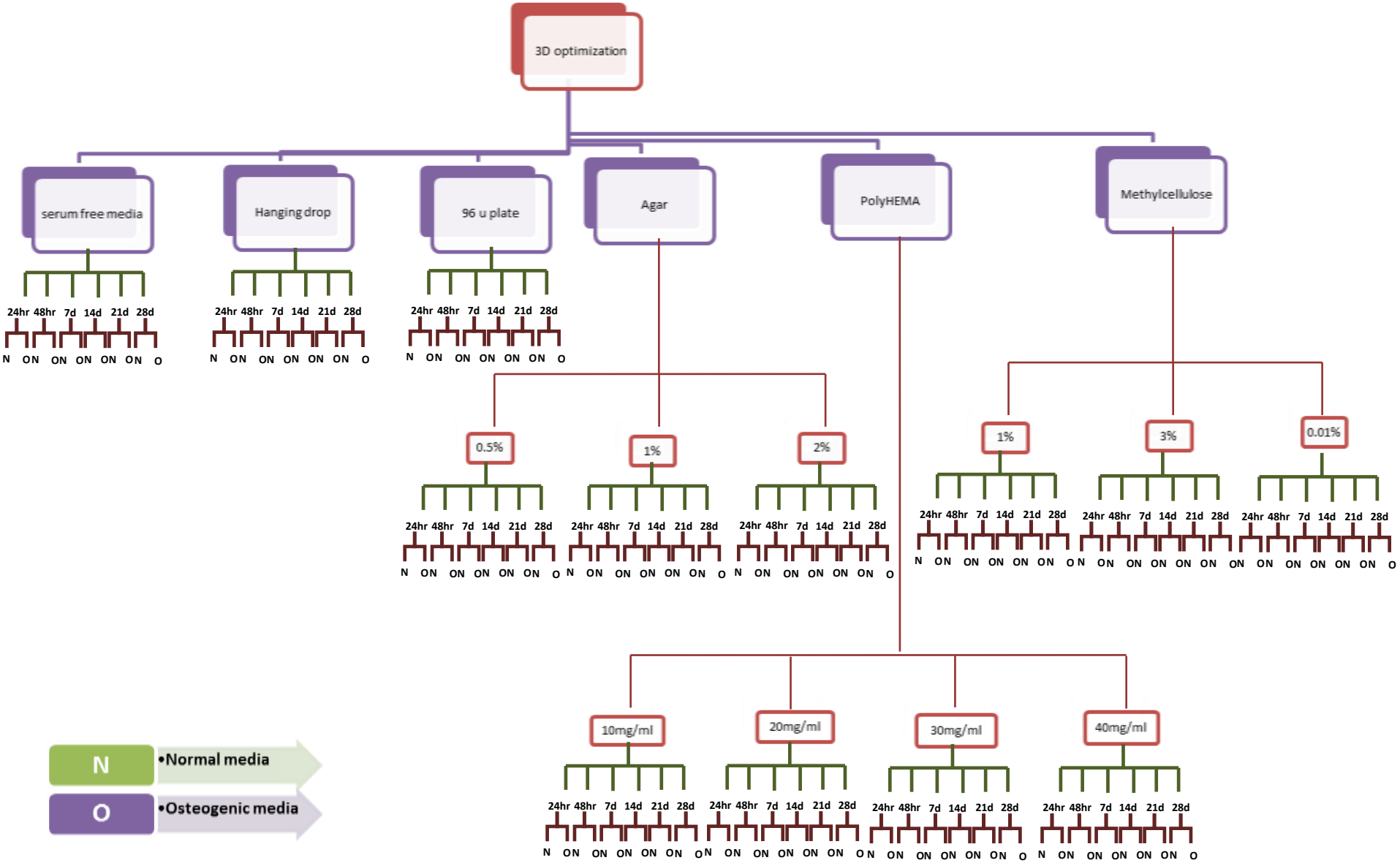

Figure 3.1: *3D optimization plan*

3.2 Materials and methods:

All materials and reagents were purchased from Sigma-Aldrich company, Ltd Ayrshire, UK unless otherwise specified.

3.2.1 Stock solutions preparation:

3.2.1.1 Methylcellulose stock solutions: Methylcellulose stock solutions were prepared as described in (Longati, Jia et al. 2013). Briefly, methylcellulose powder was autoclaved then dissolved in DMEM media [w/v]. Three concentrations were made 0.01% (Baum, Hlushchuk et al. 2007) [w/v], 1% [w/v] (Dang, Kyba et al. 2002), and 3% [w/v].

3.2.1.2 PolyHEMA stock solutions: Poly-HEMA crystals was dissolved in 95% ethanol by placing the tube in a shaker at room temperature overnight; four concentrations were prepared 10mg/ml (Zhang, Xu et al. 2010), 20mg/ml (Dhawan, Jeffreys et al. 2008), 30mg/ml, and 40mg/ml.

3.2.1.3 Agar stock solutions: three concentrations were prepared 0.5% [w/v] (Kunz-Schughart and Freyer 2002) , 1% [w/v] (Yu, Dillon et al. 1999), and 2% [w/v] (Ulrich, Jain et al. 2010) by dissolving the agar in phenol red-free media or PBS.

3.2.2 Cell culture:

Tissue culture was carried out following protocols described in section 2.1.1.

3.2.2.1 Rat calvarial cell culture:

Rat calvarial cells were isolated by Dr. Mark Birch; and preserved in 10% dimethylsulfoxide [DMSO] with bovine serum, they were then stored in liquid nitrogen. A cryovial containing frozen cells was placed in a water bath at 37º C and the cells were thawed quickly by swirling the vial gently. The outside of the vial was then dried, the vial transferred to a class II tissue culture hood and wiped with 70% ethanol. DMEM/10% FCS media was added slowly and the cells transferred to a T75-flask and grown until they were ready to be used [80-90% confluent, passage 3-4].

In this experiment cells were grown for 24 h, 48 h 7 d, 14 d, 21 d, and 28 d in normal Dulbecco`s modified Eagle`s medium [DMEM] supplemented with 10% foetal bovine serum [FBS], 10％ 2mM L-Glutamine, 100 µg/mL streptomycin and 100 U/mL penicillin. To promote osteogenic differentiation, the media was replaced after 24h with growth media supplemented with 5mM of Glycerol 2-phosphate disodium salt hydrate, 100 µg/ml of 2-Phospho-L-ascorbic acid, and 10nM dexamethasone. Cells were seeded at four densities of approximately 14 $x10^5$, 6 $x10^5$, 3.5 $x10^5$, and 0.5 $x10^5$ cells/ml.

3.2.2.2 Multicellular spheroid culture:

- ***96 U plate:***

  160µl of cells suspension were dispensed into the well and left to grow.

- ***Serum free media:***

  1000µl of cells suspension in a free serum media were dispensed in to the well of a 24 well plate and left to grow.

- ***Hanging drop method:***

  In this method drops of 20µl of cell suspension were placed on the inside of the lid of a 60mm Petri dish filled with sterile PBS or media (Del Duca, Werbowetski et al. 2004). The lid was then inverted over the dish so the drops are hanging from the lid [see figure 3.1]

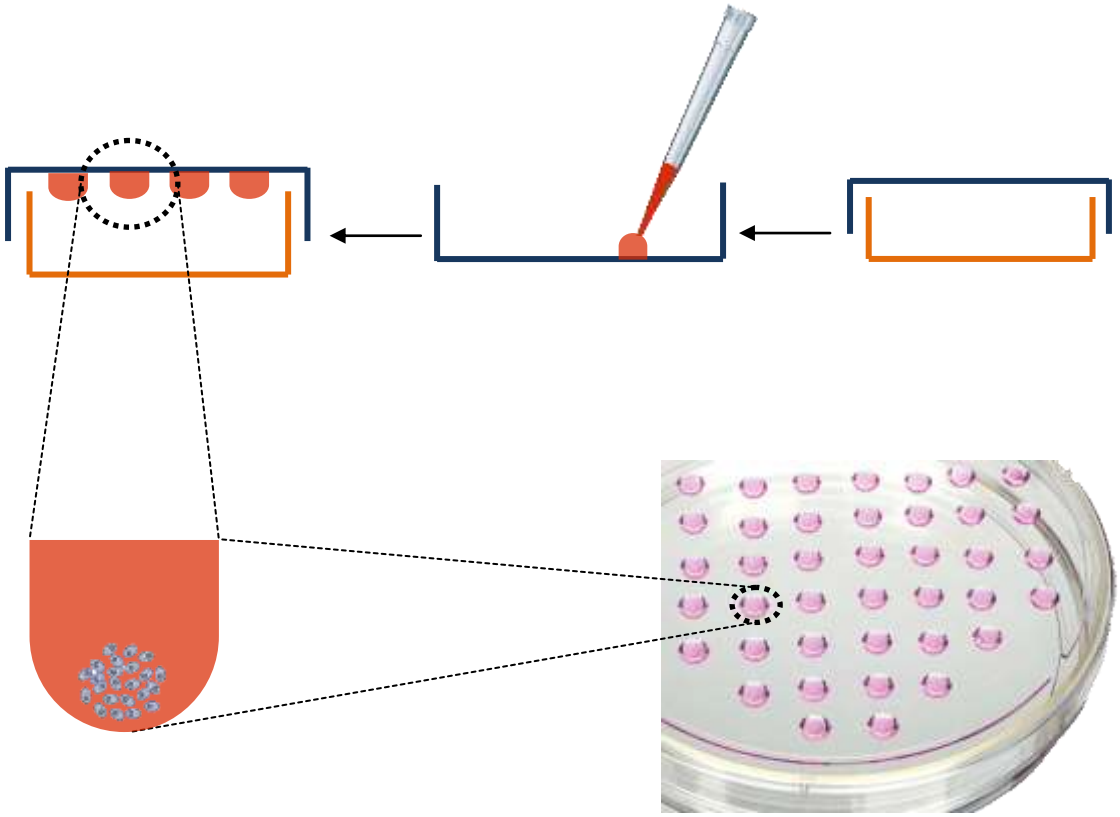

Figure 3.1 *Represents drawing of hanging drop technique. The lid of the petri dish was removed to place drops of cells suspension. The petri dish was filled with PBS to prevent drops drying. The lid was then placed again carefully.*

- ***Methylcellulose cells entrapment:***

  This method was performed according to the method of (Kubota, Preisler et al. 1981). The cell suspension was mixed in 0.01% - 1% - 3% methylcellulose media and this was then dispensed in a 24 well plate.

- ***PolyHEMA coated dish:***

  A 24 well plate was coated with 50µl of polyHEMA solution and left to dry overnight at room temperature. The coated plates were sterilized using UV light before seeding the cells.

- ***Liquid overlay technique:***

  400 µl of each agar solution [0.5%, 1%, and 2%] concentration was placed in a 24 well plate and left to solidify. Cells were then seeded onto this surface and placed in the incubator.

3.2.2.3 Evaluation of cell viability and number using the MTT assay:

Cellular spheres were collected in an eppendorf tube and spun to form a pellet. The media was then discarded and MTT assay was performed as described in section 2.1.3.

3.2.2.4 Image analysis:

The morphological appearance of the cells was observed and images were taken using an inverted light phase microscope. The numbers of cell spheroids were counted and the diameters of these spheroids were measured in 6 fields in each well plate. Data analysis was performed using SPSS 19.0. [SPSS Inc., USA]. Data was considered statistically significant when p value ≤ 0.05.

3.3 Results:

3.3.1 Efficiency of spheroid formation*:*

3.3.1.1 96 round -bottom plates:

As shown in figure [3.3] after 24hr, 48hr and 7 days of culture cells attached to the surface of the well under both normal and osteogenic conditions. However, it was noticed that few cells were de-attached at low density [figure 3.4].

At day 14, 21, and 28 cells were still attached to the well surface at high cellular densities, whereas at low densities some cells still remained unattached. Interestingly, white precipitate was noticed under osteogenic conditions which started at day 14 in high cell density [figure 3.5] while the precipitate started to appear at day 21at low cell density [figure 3.6].

3.3.1.2 Serum free media:

As shown in figure [3.7] some cells grown after 24hr, and 48hr attached while others remained suspended in the media. After 7 days cellular accumulation was noticed at high density [figure 3.8]. And at day 14, 21 and 28 most cells grown in osteogenic media were suspended, though some cells are still attached at low density [figure 3.9].

Overall, removing the serum from the media didn't induce cell aggregation at either short or long term time points either in normal or osteogenic media.

3.3.1.3 Hanging drop method:

As it can be seen in figure [3.10], after 24hr cells were rounded in shape and after 48hrs spheres were formed, although some cells managed to attach to the lid surface

[figure 3.11]. After 7, 14, 21, and 28 days spheres grown under osteogenic conditions started to disintegrate [figure 3.12].

3.3.1.4 Methylcellulose cell entrapment

This method was used to form a semisolid media for cell entrapment. As seen in figure [3.13] most cells attached to the plastic surface while some cells were rounded at all methylcellulose concentrations and very few spheres were seen at high densities after 24hr. After 48hr, 7, 14, 21, and 28 days cells were still attached with very few rounded cells. Moreover, it was noted that after 21, and 28 days some cells grown under osteogenic media de-attached and formed irregular cellular clusters compared to cells grown under normal conditions [figure 3.14]. Additionally, precipitates were noted at high methylcellulose concentrations.

3.3.1.5 PolyHEMA coated dish

PolyHEMA was used as anti-adherent coating on tissue culture plastic. Preliminary data showed that the quality of the coating played a role in spheroid formation. When the plate was placed in the laminar flow hood for alcohol evaporation during surface preparation, subsequently some cells adhered to the well surface while others formed spheres [figure 3.2]. Therefore, to get a good coating the plates were left on the bench for a slower more even evaporation.

Figure [3.15] shows that rounded spheroids were formed after 24hr. Also, it was noted that at high cell density the quality of the spheres were better compared to low density, where sphere margins were irregular. In addition, after 14 days spheroids grown in osteogenic media started to dissociate [figure 3.16]. Furthermore, the size of the spheres was larger and the numbers were less in long term culture.

Comparing different concentrations of PolyHEMA shows that at higher concentration [40mg/ml] specifically after 14d the polyHEMA surfaces were broken [figure 3.17].

3.3.1.6 Liquid overlay technique

Agar can be used either to form a semi solid media for cells entrapment as in the case of methylcellulose, or to coat the surface of the culture plate as a way to prevent cells from adhering. In figure [3.18] it can be seen that after 24, and 48hr cells aggregated and formed irregular spheres at higher cell density, and in 1% and 2% agar compared to 0.5% there were a few cells that were attached but most of them were rounded in shape [figure 3.19]. After 7, 14, 21, and 28 days cells formed a large cluster with a high starting cell density [figure 3.20] compared to low seeding densities where some cells were suspended but most of the cells attached to the well plate surface [figure 3.21].

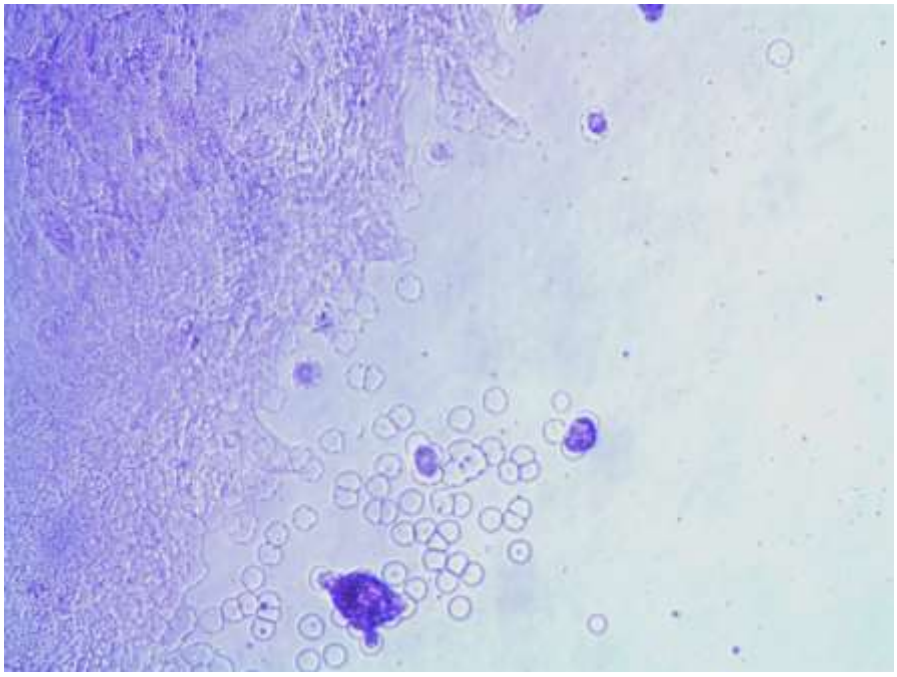

Figure 3.2 *Shows an uneven polyHEMA coating that led to cells attaching in some areas, while some cells aggregate and formed spheres.*

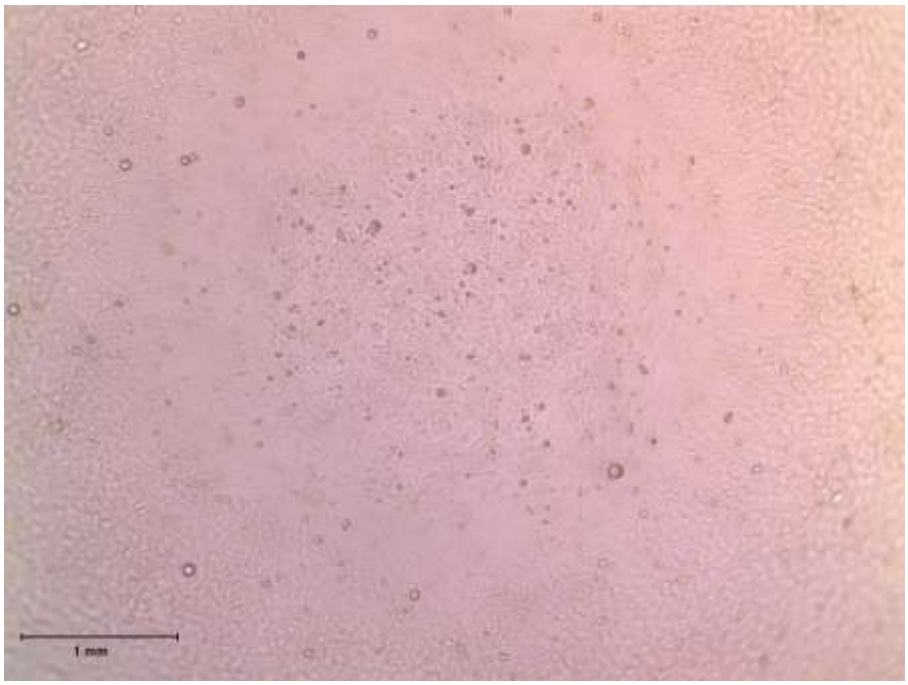

Figure 3.3: *Calvarial cells grown on the surface of a 96u rounded bottom plate where cells adhered to the surface after 24hr.*

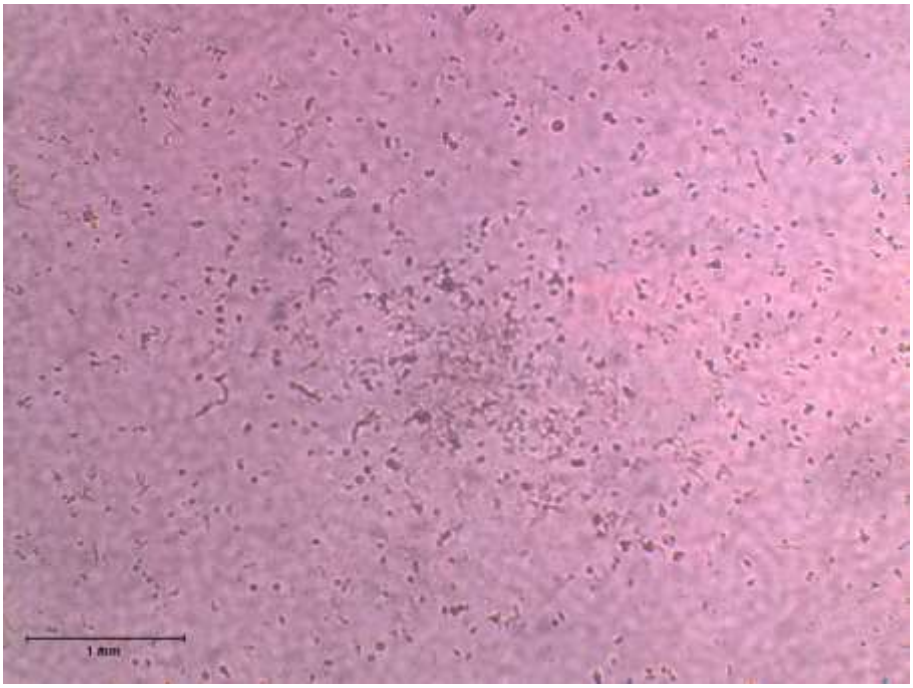

Figure 3.4: *Low density of calvarial cells grown on the surface of a 96u rounded bottom plate at 7days cells adhered to the surface with few cells floating in the medium.*

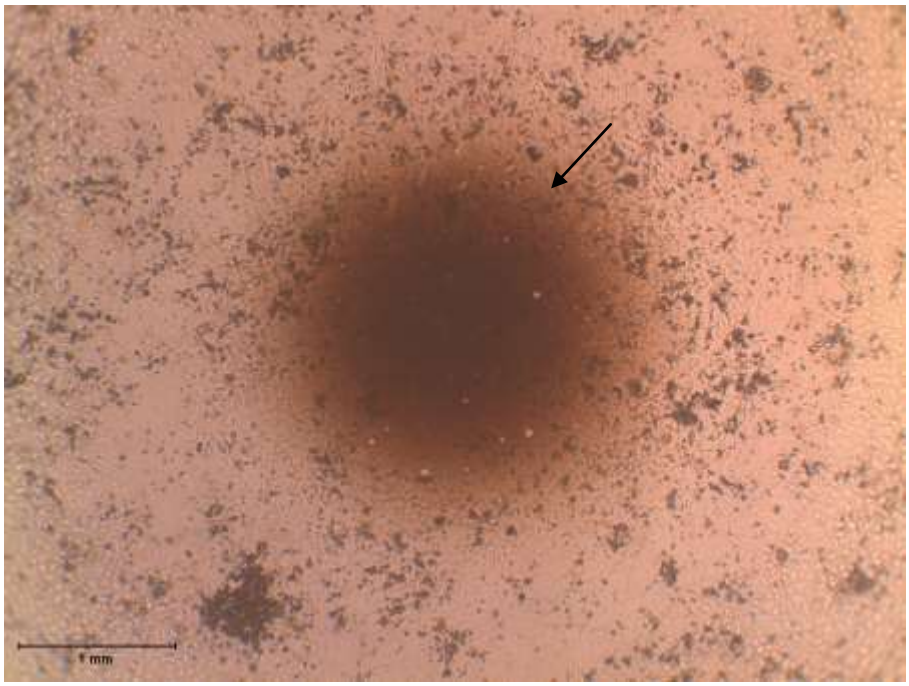

Figure 3.5: *Calvarial cells grown under osteogenic conditions on the surface of a 96u rounded bottom plate, precipitate appeared [arrow] at day 14 at high cell density*

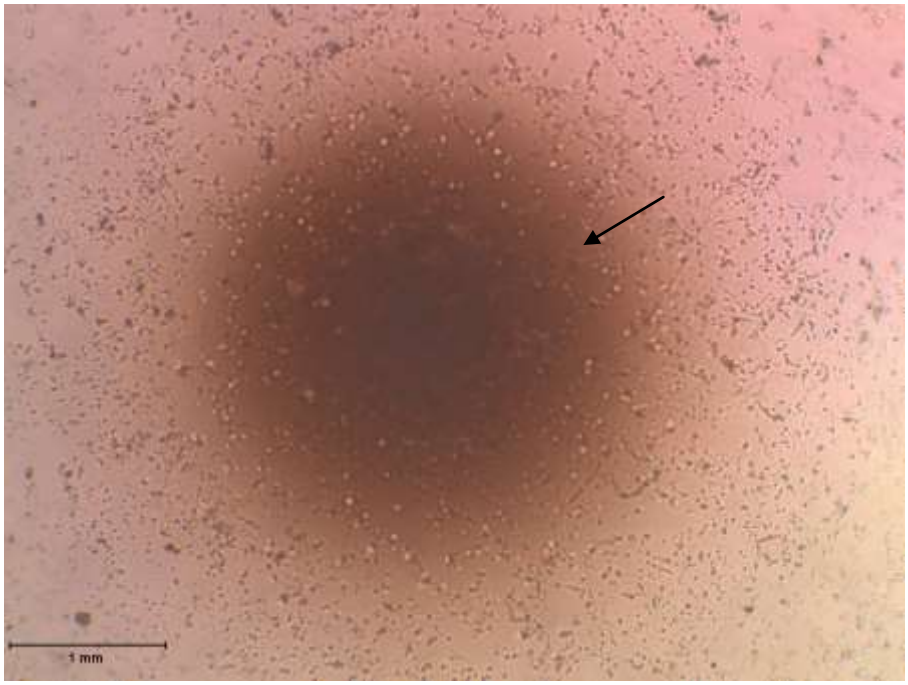

Figure 3.6 *Calvarial cells grown under osteogenic conditions on the surface of a 96u rounded bottom plate, precipitate appeared [arrow] at day 21 at low cell density*

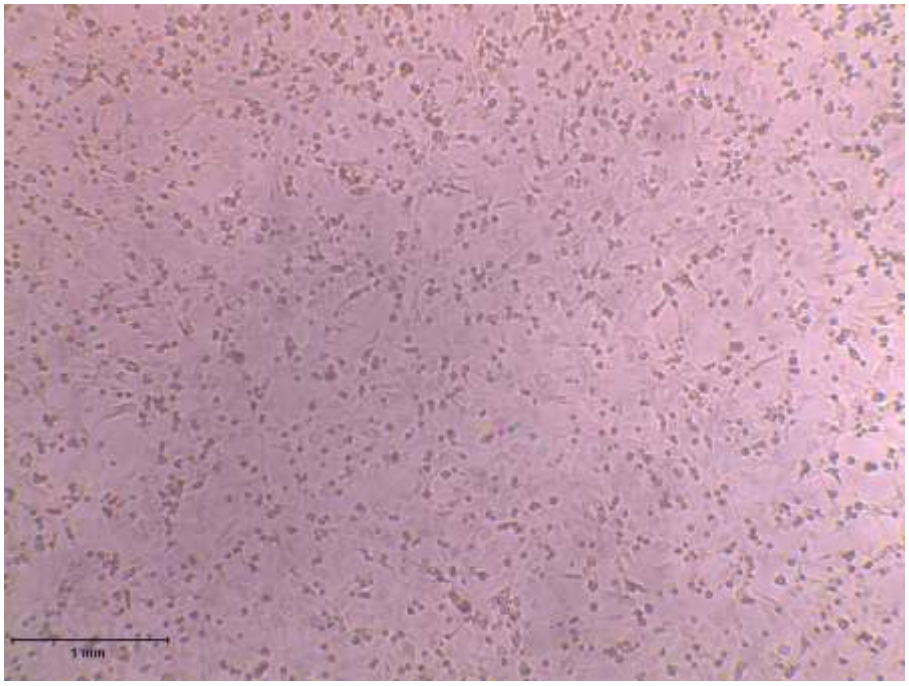

Figure 3.7 *Calvarial cells grown on the surface of a 24 well in a serum free media some cells attached to the surface while other cells were suspended in the media after 24hr.*

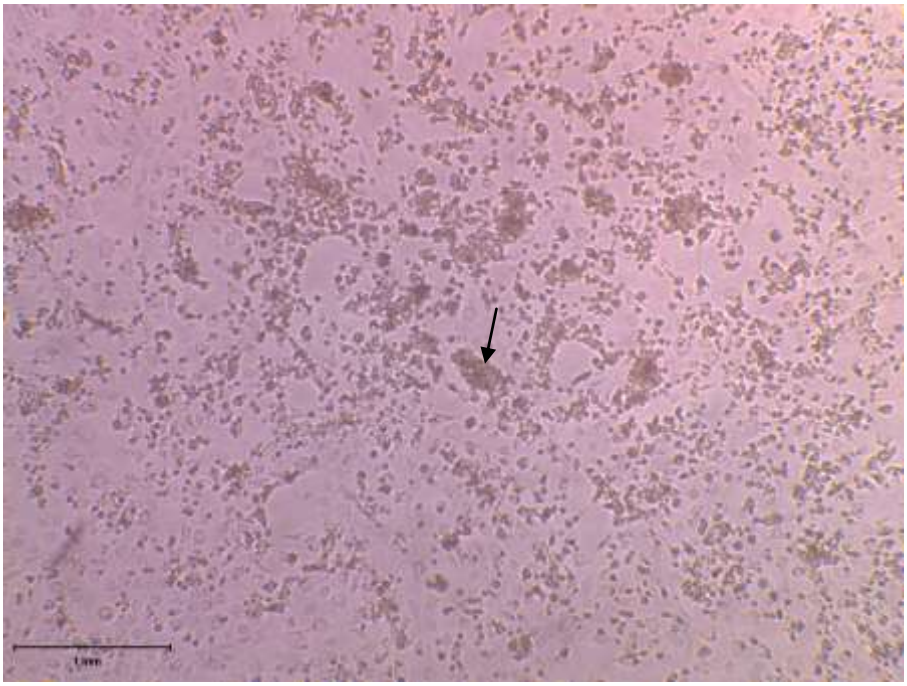

Figure 3.8 *High densities of calvarial cells grown on the surface of a 24 well in a serum free media at 7days where cells started to aggregate [arrow]*

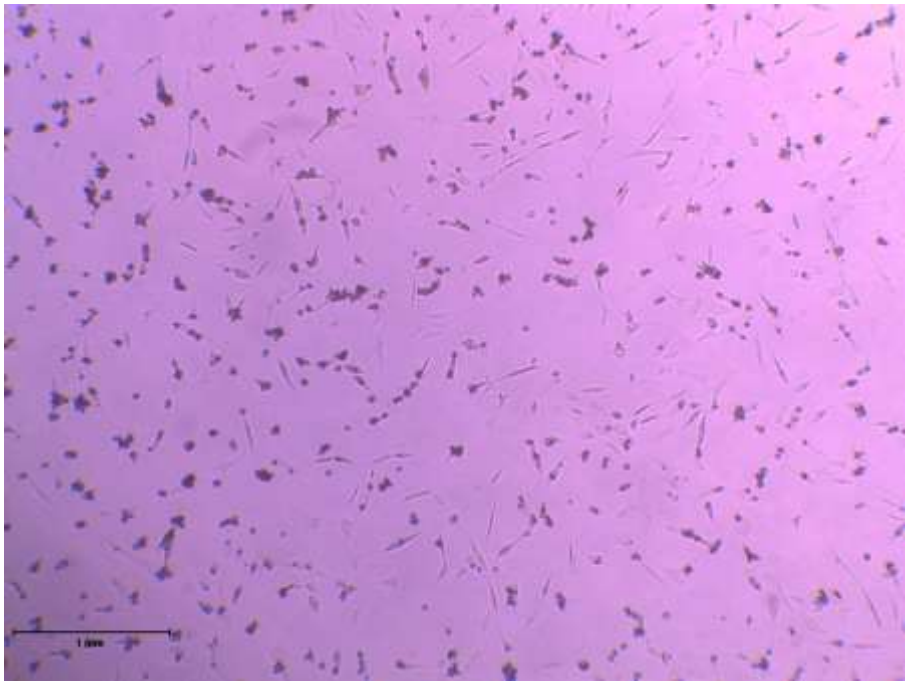

Figure 3.9 *Calvarial cells grown on the surface of a 24 well in a serum free media at 14days under osteogenic conditions where most cells are suspended though few cells are still attached*

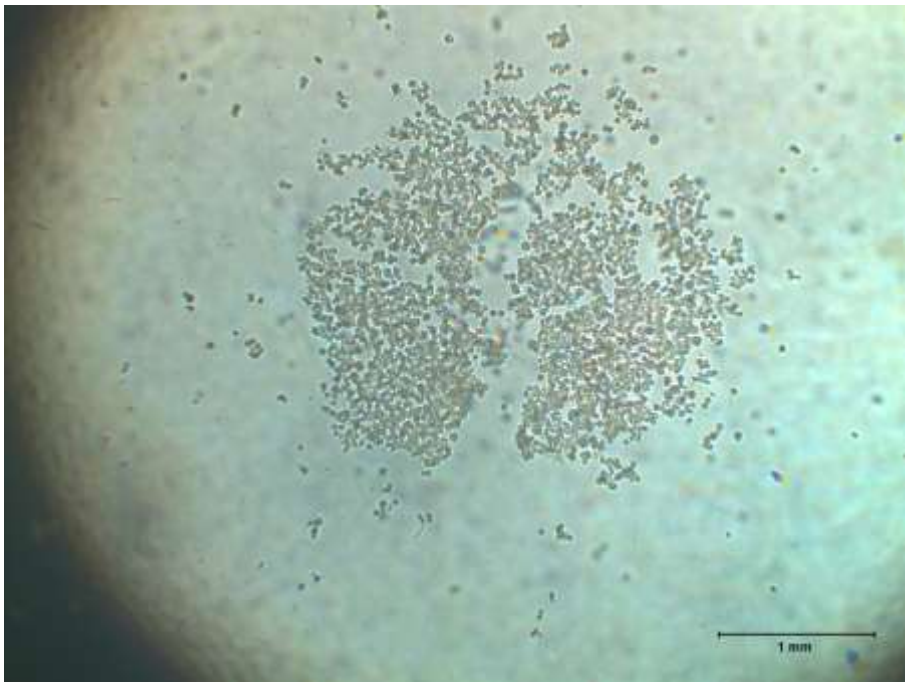

Figure 3.10 *Calvarial cells grown using hanging drop technique cells were rounded and didn't attach after 24hr*

Figure 3.11 *Calvarial cells grown after 48hr using hanging drop technique where some cells attached to the surface of the lid [black arrow] while other cells formed sphere [red arrow].*

Figure 3.12 *Calvarial cells grown at 21days using hanging drop technique where cells that aggregated and formed spheres started to disintegrate [black arrow]*

Figure 3.13 *Calvarial cells grown after 24hrin normal media mixed with methylcellulose where some cells attached to the plate surface [black arrow] while other cells aggregated [red arrow].*

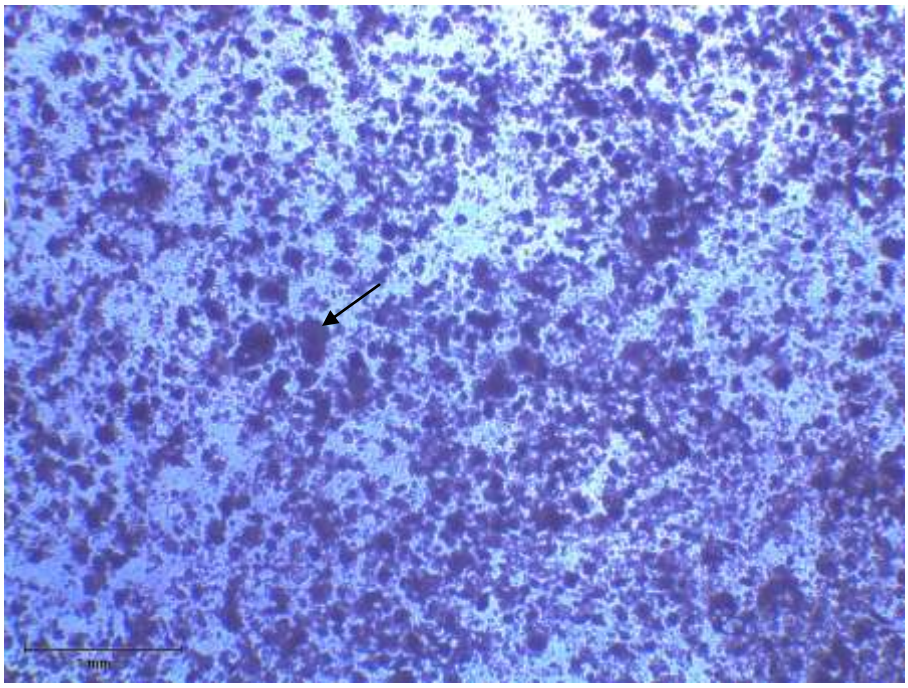

Figure 3.14 *Calvarial cells at 21days grown in osteogenic media mixed with methylcellulose where cells formed irregular accumulation [black arrow]*

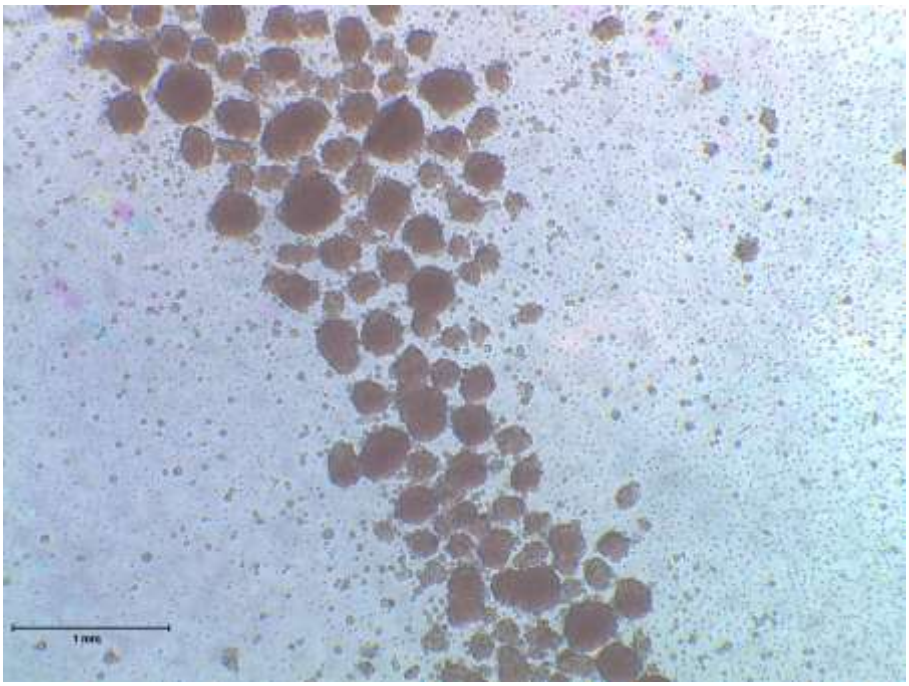

Figure 3.15 *Calvarial cells grown after 48hr on the surface of 24 well plate coated with polyHEMA to prevent cells from attachment, as a result cells aggregated and form spheroids*

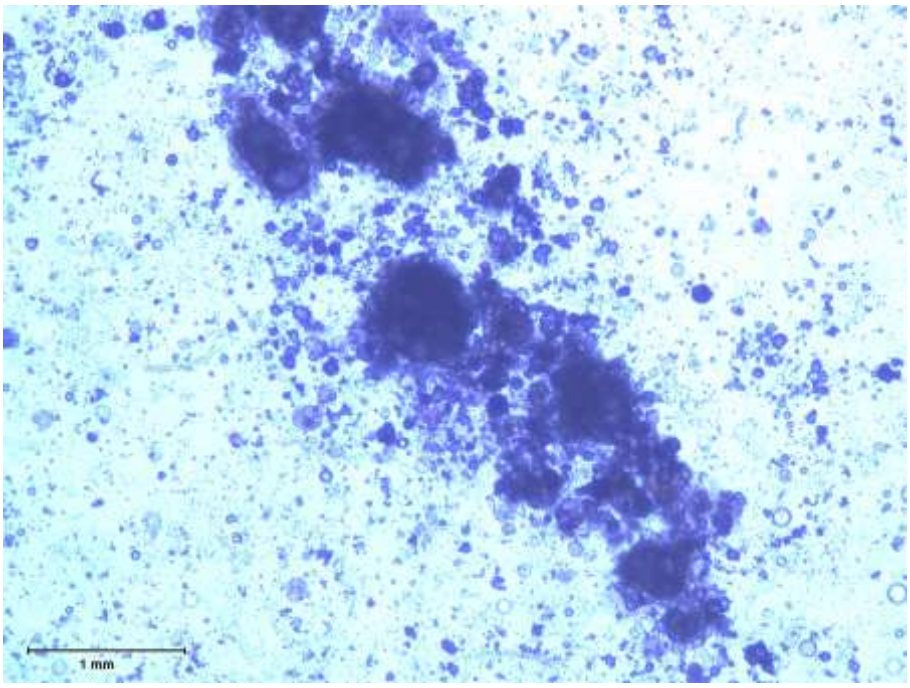

Figure 3.16 *Calvarial cells grown on the surface of a 24 well plate coated with polyHEMA shows spheroids disintegration after 14days of culture*

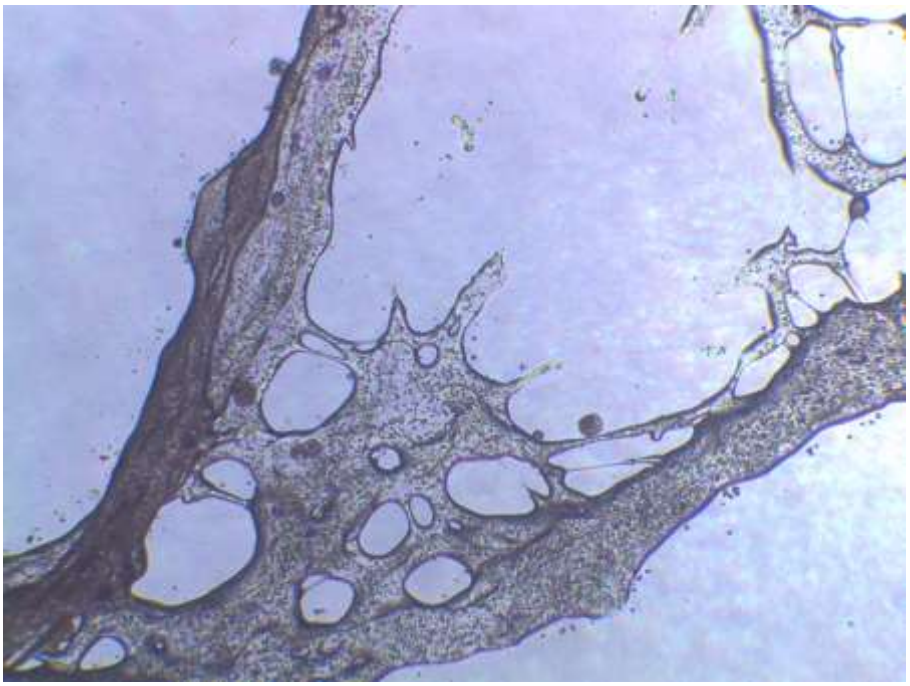

Figure 3.17 *Shows the surface of high concentration [40mg/ml] polyHEMA coating which was broken after 14 days*

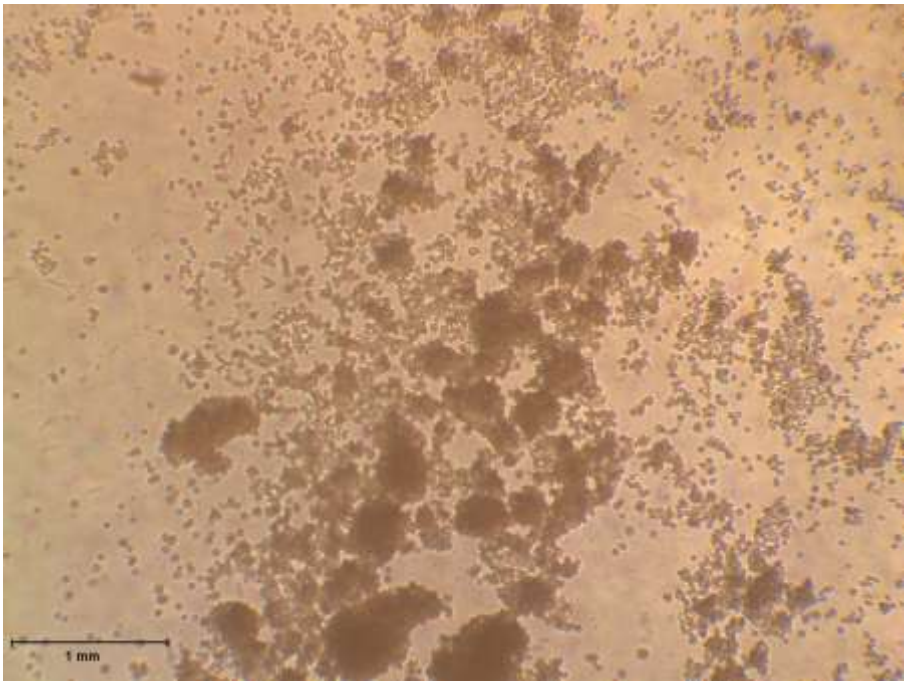

Figure 3.18 *Calvarial cells grown after 24hr on the surface of 24 well plate coated with 2% agar shows the accumulation of cells in irregular shape*

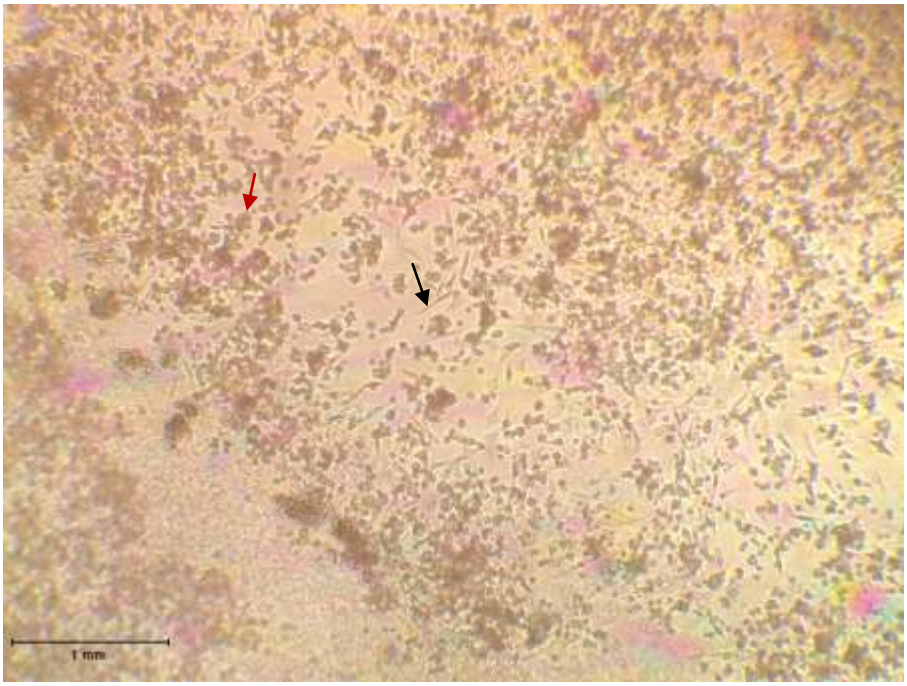

Figure 3.19 *Calvarial cells grown after 24hr on the surface of 24 well plate coated with 0.5% agar shows cells adhered to the surface [black arrow] while most of the cells were suspended in the media [red arrow].*

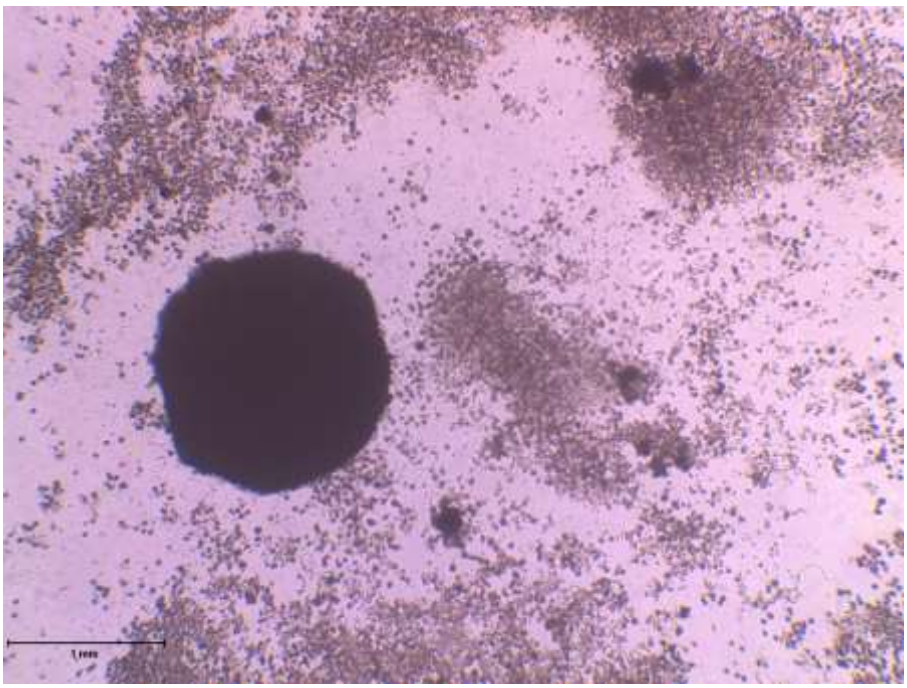

Figure 3.20: *Calvarial cells grown after 14 days shows the formation of large spheroid by time at high cells density*

Figure 3.21 *Calvarial cells grown after 14 days shows cells suspended in the media while most of the cells attached to the surface of the well.*

3.3.2 Cell viability and number*:*

Calvarial cell viability and number were assessed using MTT, a colorimetric assay where the compound is taken up by the cells and converted in the mitochondria to an insoluble coloured product. Therefore, low absorbance indicates a reduction in the number of viable cells and a higher absorbance indicates an increased number of cells.

3.3.2.1 96 U plate:

As shown in figures 3.22, 3.23, 3.24, 3.25, 3.26, 3.27, 3.28, and 3.29 the viability of the cells seeded at high density decreased at 48hr but increased afterwards, while it remained steady at 21 day with a slight increase at 28 days. In contrast, cell numbers grown under osteogenic conditions increased slightly at day 7 but decreased gradually at 14, 21, and 28 days.

In the case of low cell seeding density, cell viability increased after 48hr and reached a peak at day 14. While cell number, grown in osteogenic media, increased after 48hr and decreased after 14d.

At a very low density cell viability increased after 24hr then started to decline after 48hr, 7d, 14d, and 28d with a slight increase at 21d in both normal and osteogenic conditions.

3.3.2.2 Serum free media:

As shown in figures 3.22, 3.23, 3.24, 3.25, 3.26, 3.27, 3.28, and 3.29cell viability at a high seeding density decreased at 48hr but increased afterwards at 7, and 14 days, and declined after 21d, however, the viability of cells grown in osteogenic media declined after 7d and plateaued at 21, and 28 days.

In the second experiment with a high cell density and the first experiment with a low density the viability of cells grown in normal condition increased gradually after 24hr and continue rising over time. While in osteogenic media it raised and reached a peak at 7 days but declined at 14, and 21 days, surprisingly increasing again at 28days.

In contrast, in the second experiment [seeded at low density] the viability of cells decreased after 48hr under both normal and osteogenic conditions, but almost remains steady after 7d in normal media and surprisingly increased after 21 days in osteogenic media.

3.3.2.3 Methylcellulose cells entrapment

Cell viability grown in normal media increased after 24hr and 48hr and continued increasing over time in both high and low density cell density cultures. On the one hand, high cell density cultures under osteogenic conditions showed increased viability after 48hr and at 28 days. On the other hand, in the first experiment low density the viability of cells increased after 48hr and at 28 days with a slight decrease at 21 days, while in the second experiment low density seeding led to increased cell numbers after 48hr that continued rising over time in 0.01% of methylcellulose. But with high concentrations of methylcellulose (1%w/v and 3%w/v) cell number remains approximately constant after 14 days.

3.3.2.4 PolyHEMA coated dish

The data shows that cell number under normal media conditions and at high density declined after 24hr and at 21d, but increased afterwards. In contrast, cell viability grown under osteogenic conditions remains steady in plates coated with 30, 40, and 20 mg/ml but a decrease in cell number was noted at 7d in wells coated with 10 mg/ml polyHEMA.

At low density the viability of cells grown in normal and osteogenic media increased after 48hr, decreased at 21 days but increased again afterwards at 28 days.

3.3.2.5 Liquid overlay technique

The MTT assay revealed that cell viability increased considerably after 24hr under these culture conditions and reached a peak at 7d and declined after, but increased after 21 days in cells grown on wells coated with 1% and 2% agar while it remained stable in 0.5%.

Under osteogenic conditions cell viability increased after 48hr and at 28 days at high cell density and decreased after 7 days. While in low density it increased at 7 and 21 days and decreased at 14 and 28 days.

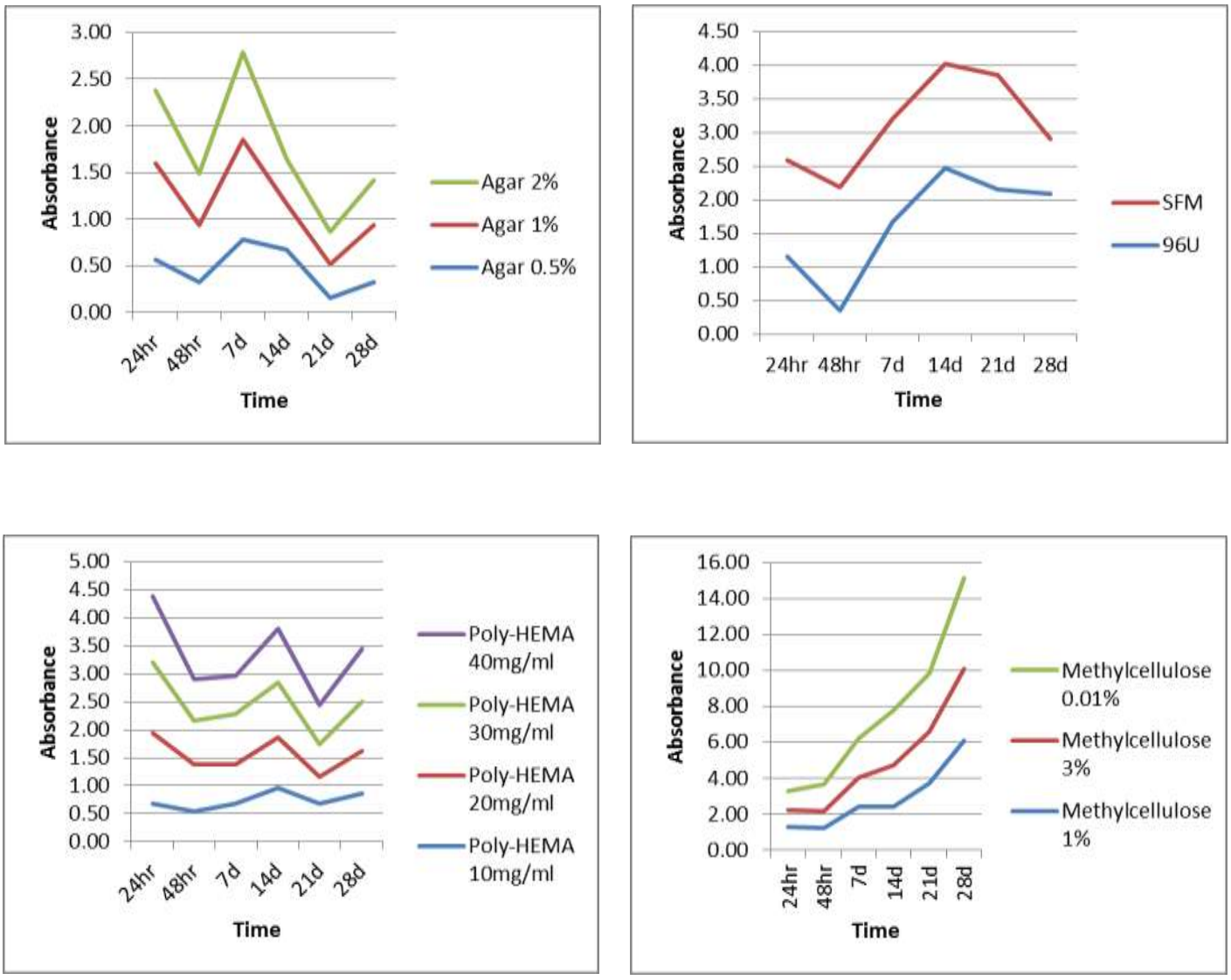

Figure 3.22: *shows MTT Viability assay results for cells grown in normal media (n=1) with cell density approximately 14 x10^5, .the vertical axis represents absorbance while horizontal axis represents time.*

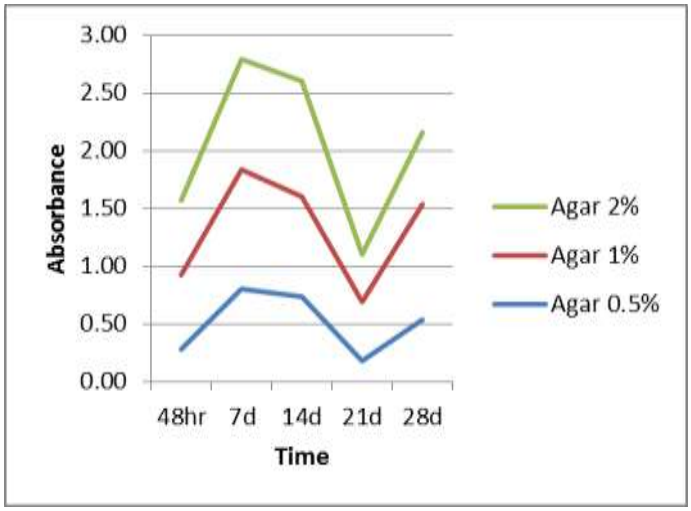

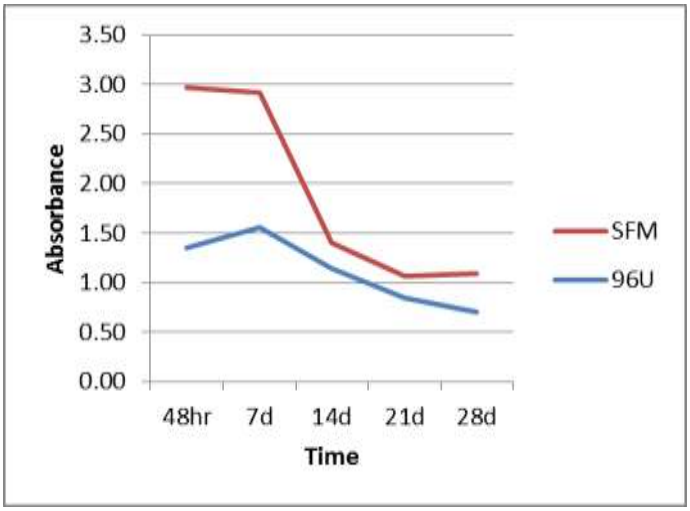

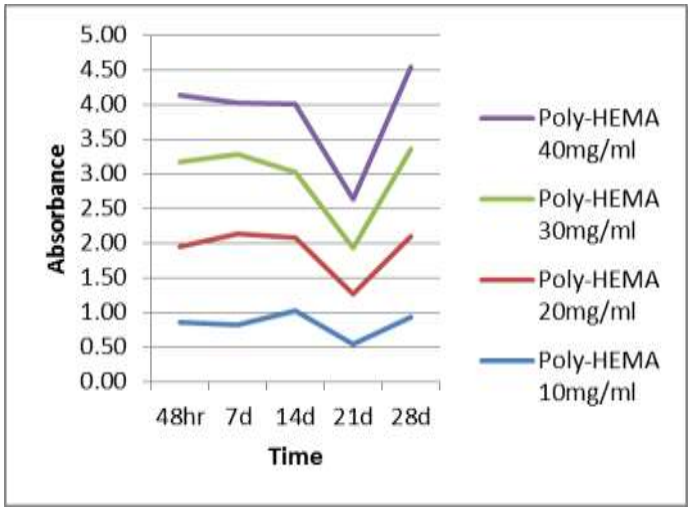

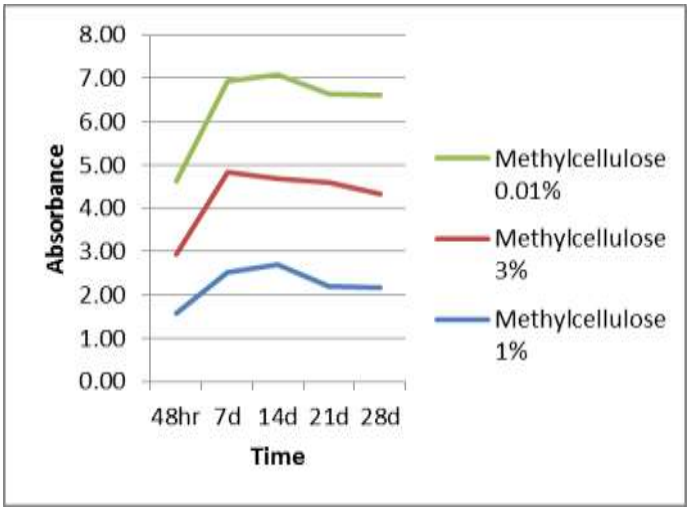

Figure 3.23: *shows MTT Viability assay results for cells grown in osteogenic media (n=1) with cell density approximately 14 x10^5*

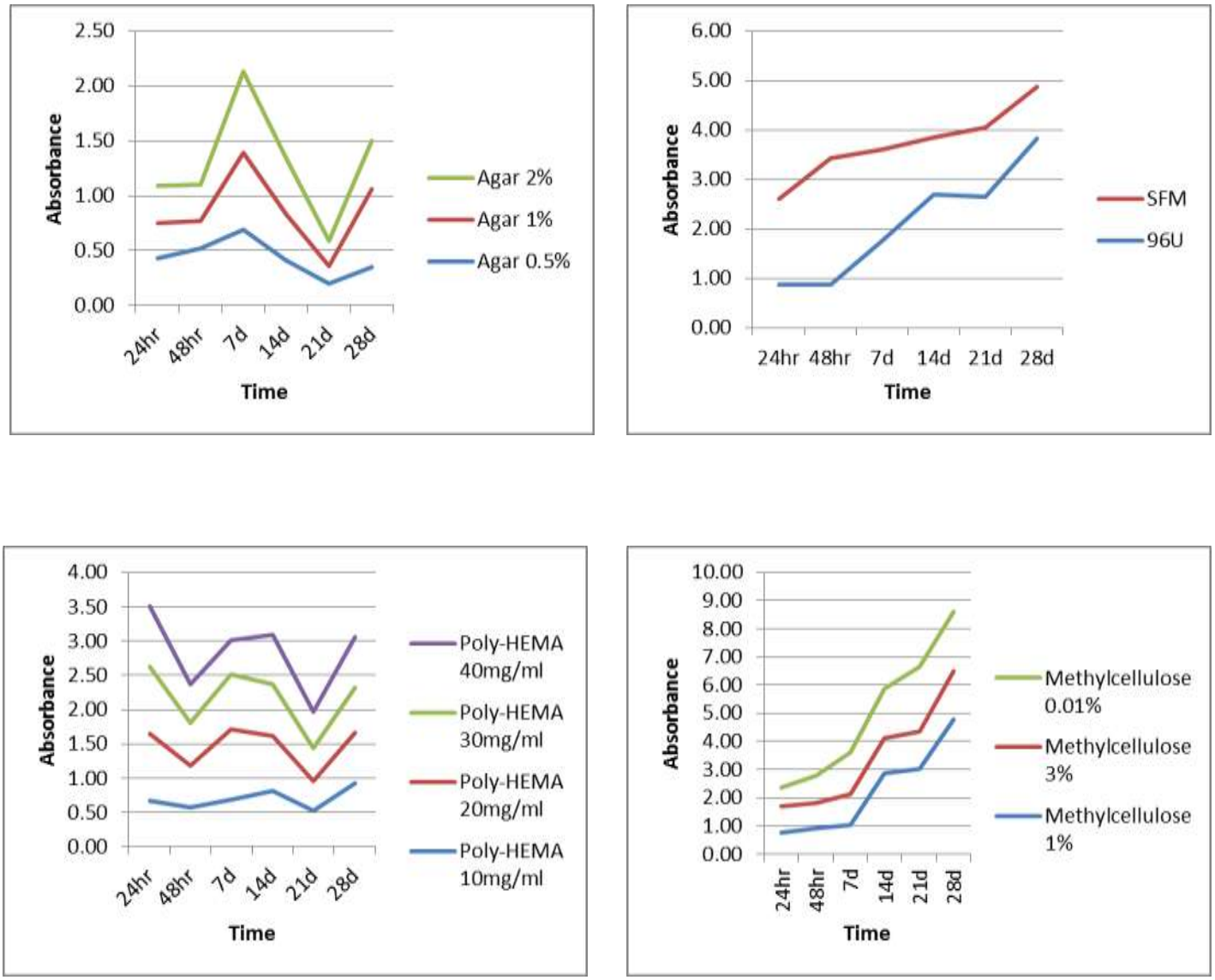

Figure 3.24: *shows MTT Viability assay results for cells grown in normal media (n=1) with cell density approximately 6 x10^5*

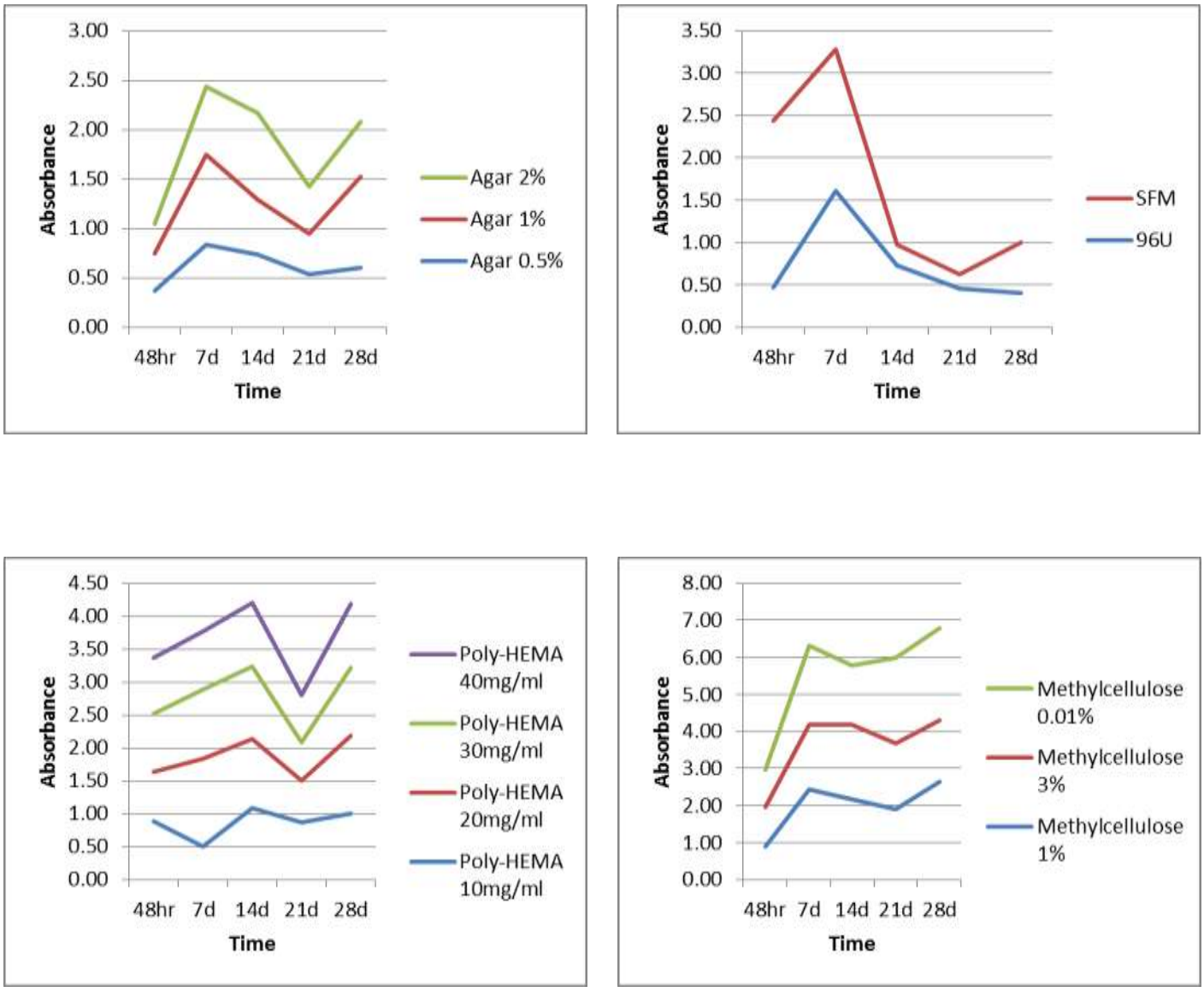

Figure 3.25: *is a graph that represents MTT Viability assay results for cells grown in osteogenic media (n=1) with cell density approximately 6 x10^5*

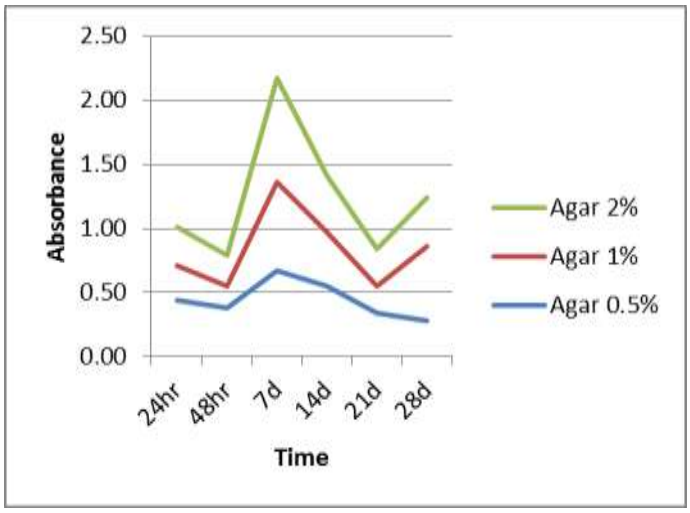

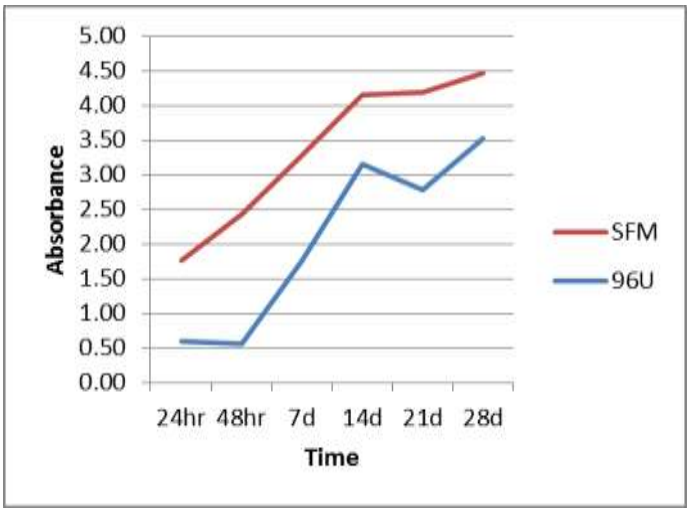

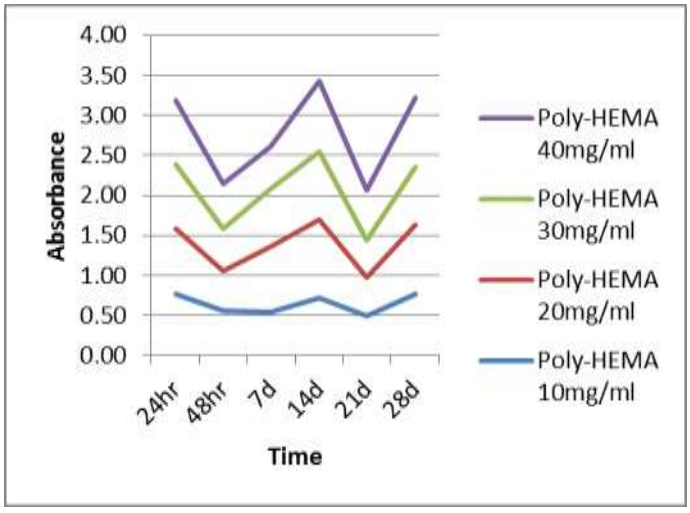

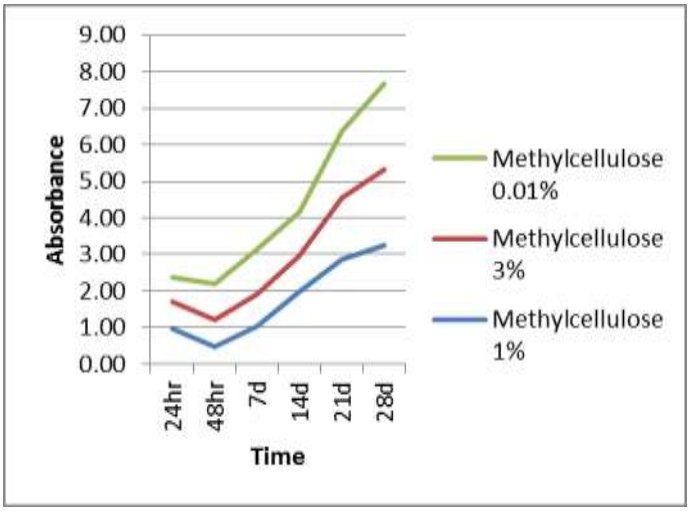

Figure 3.26: *shows MTT Viability assay results for cells grown in normal media (n=1) with cell density approximately 3.5 x10^5*

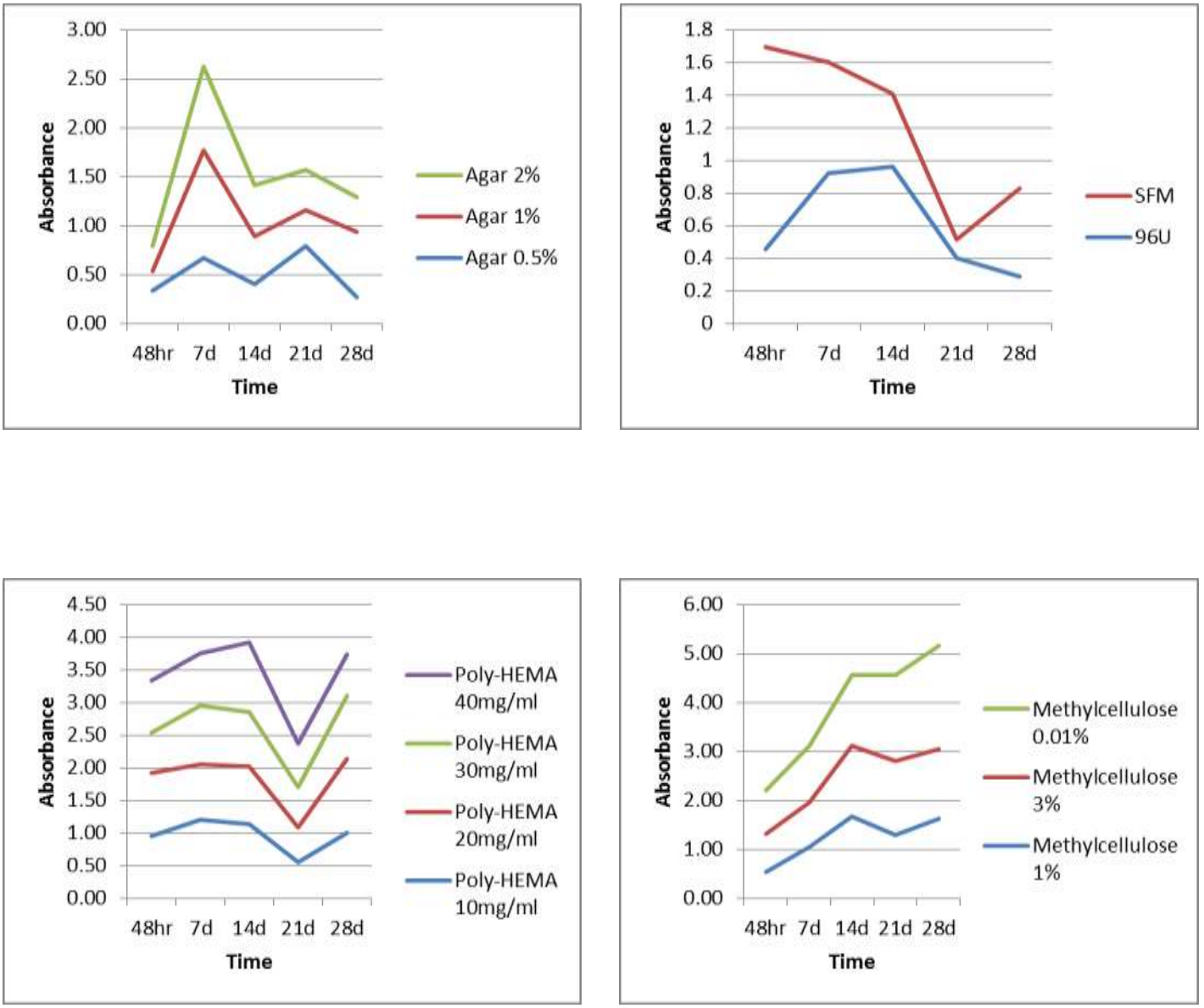

Figure 3.27: *shows MTT Viability assay results for cells grown in osteogenic media (n=1) with cell density approximately 3.5 x10^5*

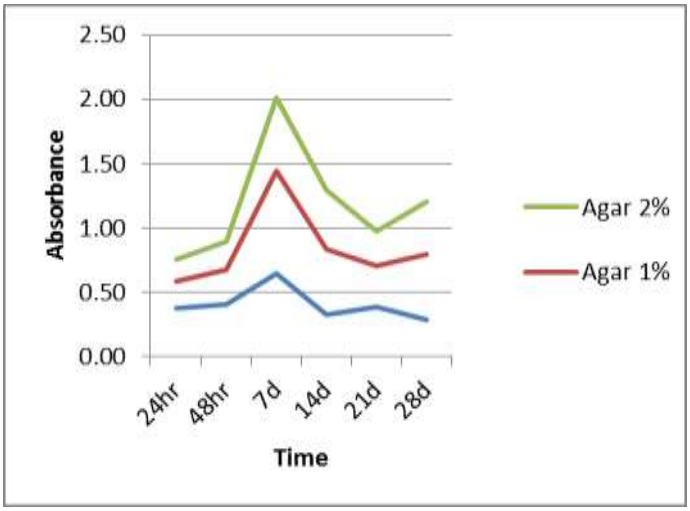

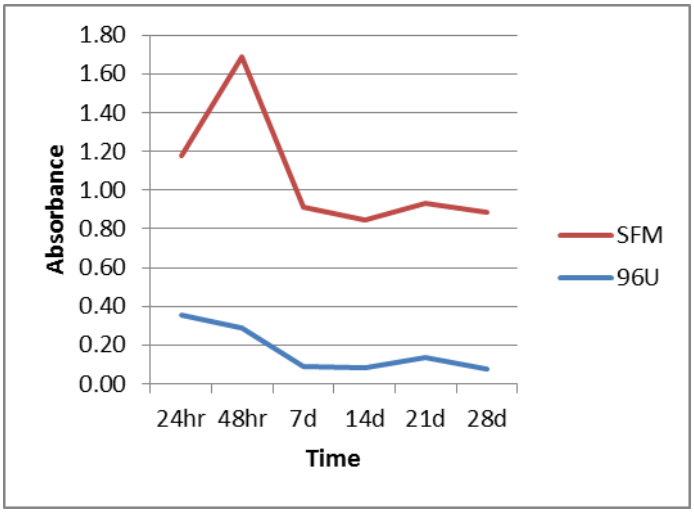

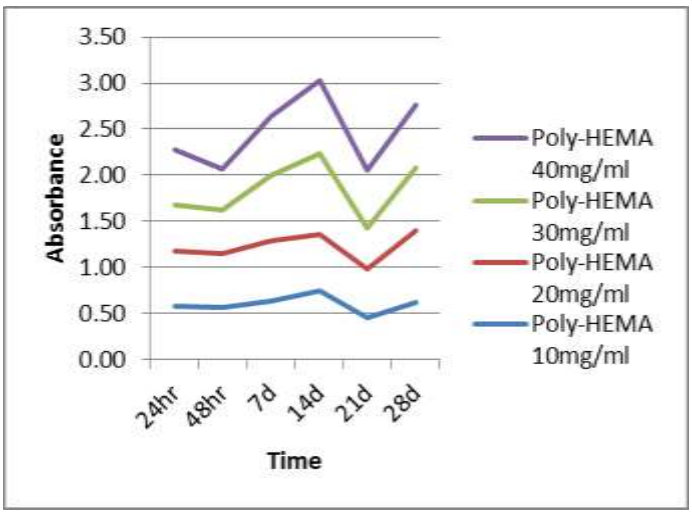

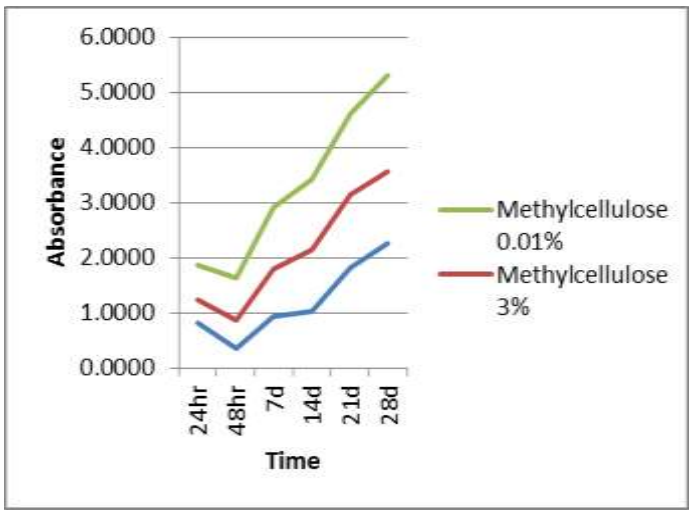

Figure 3.28: *shows MTT Viability assay results for cells grown in normal media (n=1) with cell density approximately 0.5 x10^5*

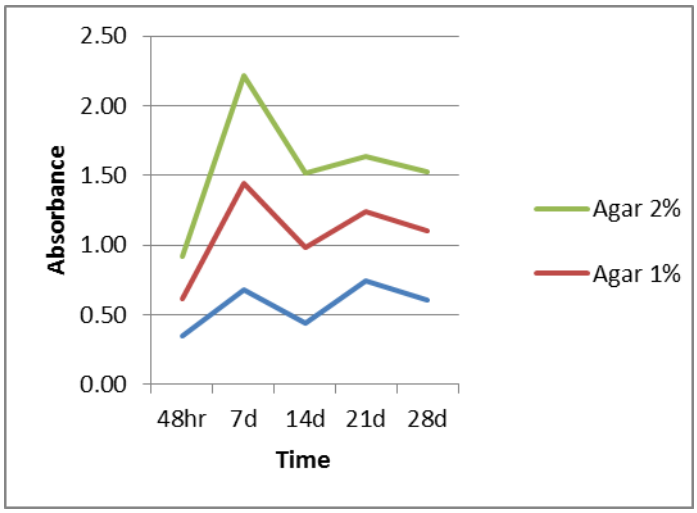

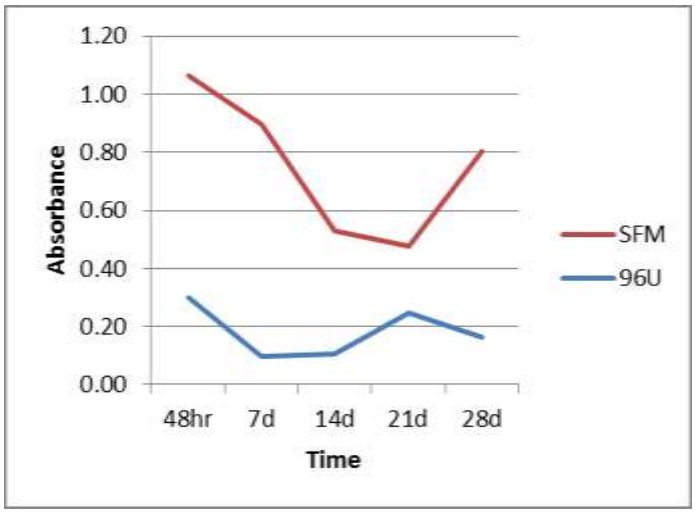

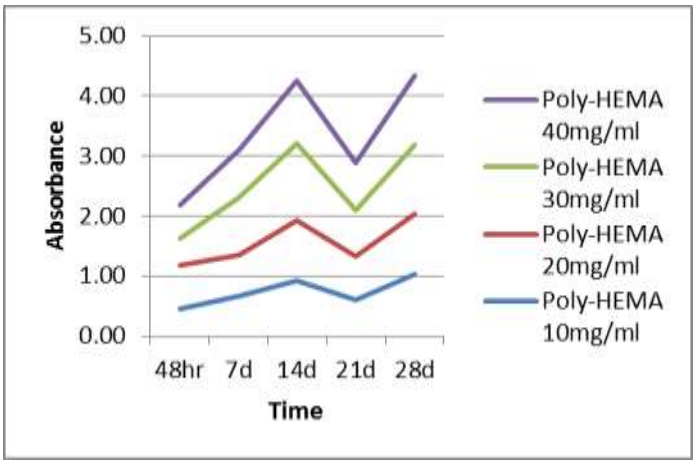

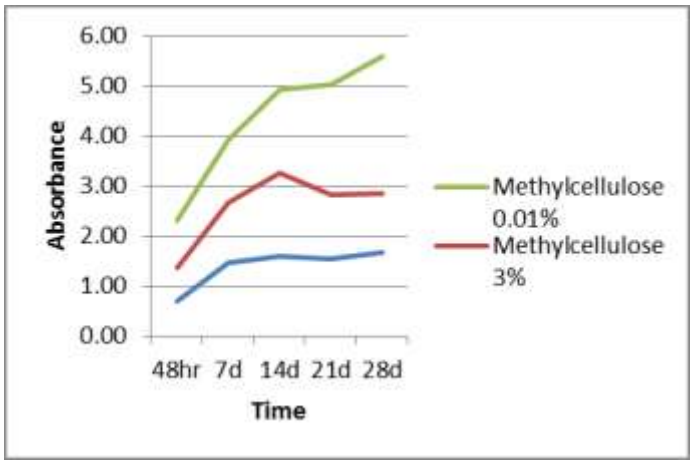

Figure 3.29: *shows MTT Viability assay results for cells grown in osteogenic media (n=1) with cell density approximately 0.5 x10^5*

3.3.3 Analysis of spheroid size and number in different culture environments

Images were taken using an inverted phase microscope where both spheroid diameter and the number of spheroids in six fields and three replicates were measured using SPOT imaging software (Diagnostic Instruments, Sterling Heights, MI) [see figure 3.30]. To compare the diameter of the spheroids and number of spheroids formed in both normal and osteogenic media over time the data was first tested checked for normal distribution. Since the data was not normally distributed a non-parametric Kruskal-Wallis test was used, and the test results revealed that there were significant differences between groups with a p value less than 0.05. Afterwards, a multiple comparison Boneferroni test was run to determine which means differ.

As seen in figure 3.31 there was a significant difference in spheroid number between cells grown in normal and osteogenic media after 24hr, 48hr and 7days. Also, between spheroids grown in normal and osteogenic media after 48hr, but there was no significant change in spheroid number in normal and osteogenic media after 7 days. On the other hand, spheroids diameter was significantly altered between cells in normal media after 24hr and cells in normal media after 48hr and 7 days. There was an also significant difference between spheroids grown in normal media after 24hr and spheroids grown in osteogenic media after 24hr and 48hr.

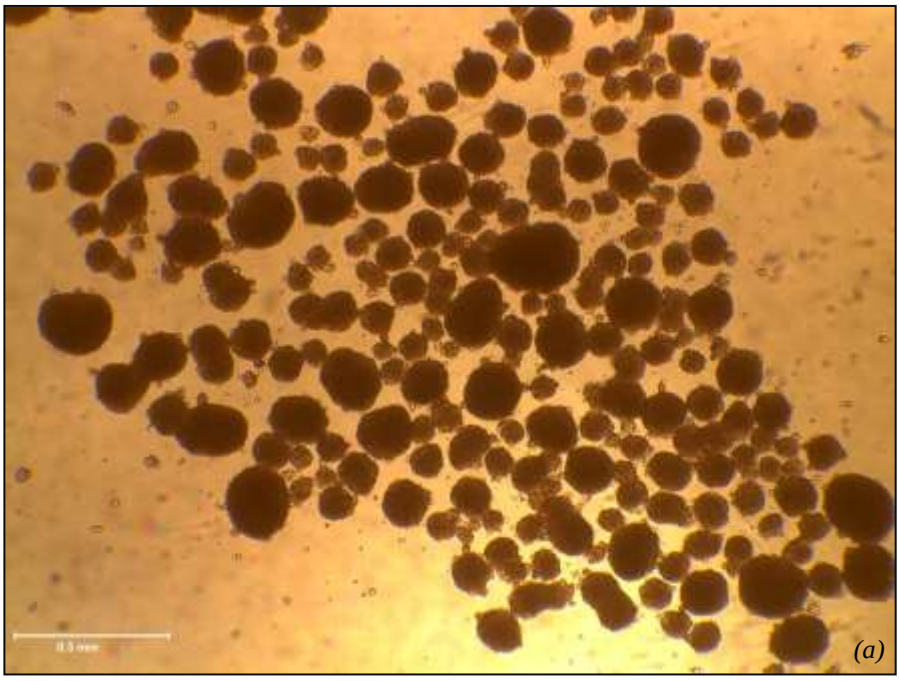

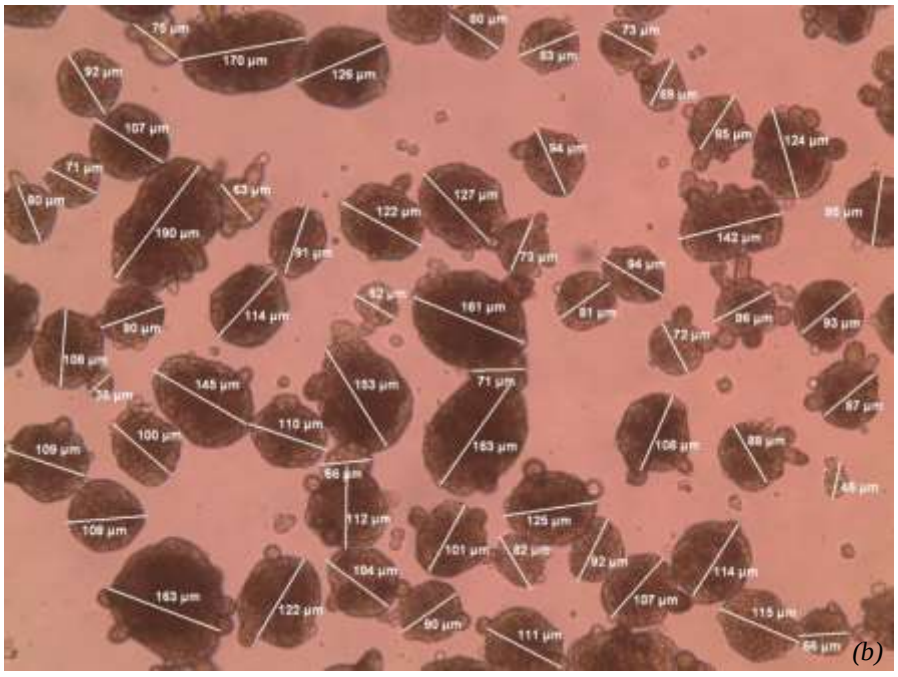

Figure 3.30 *shows spheroids number were counted and their diameter were measured using SPOT software (a) spheroids generation on plates coated with poly-HEMA (b) Spheroids diameter measurement note the different size of the spheroid*

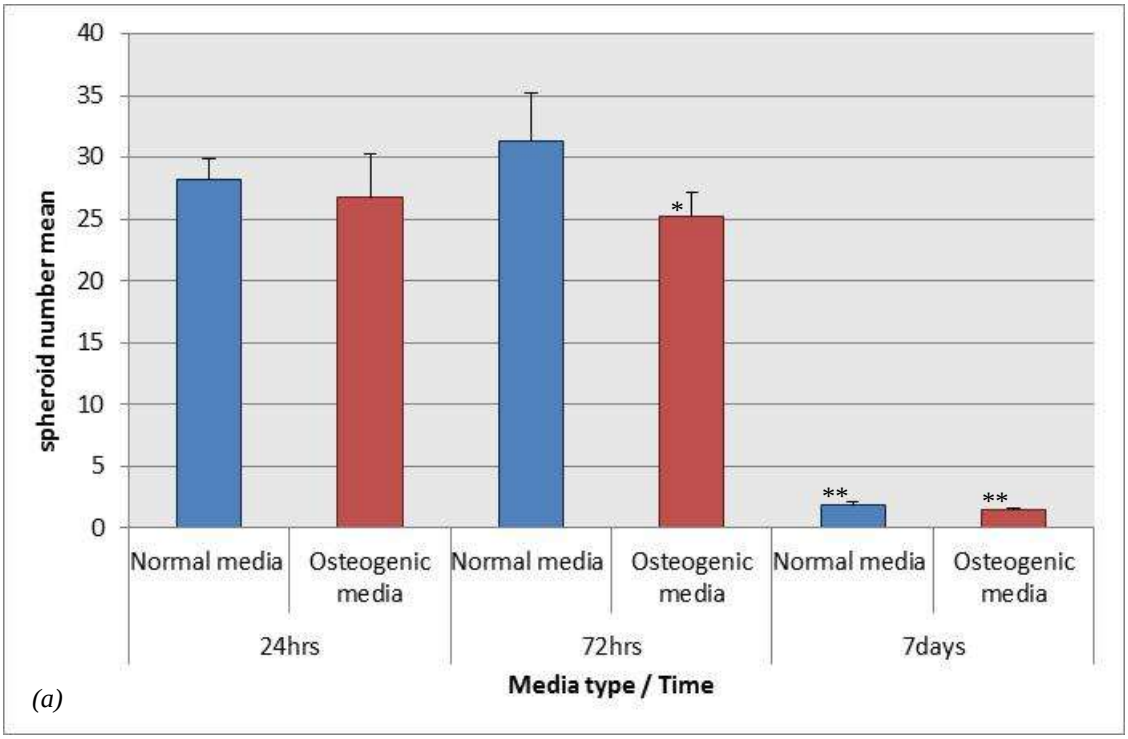

(a)

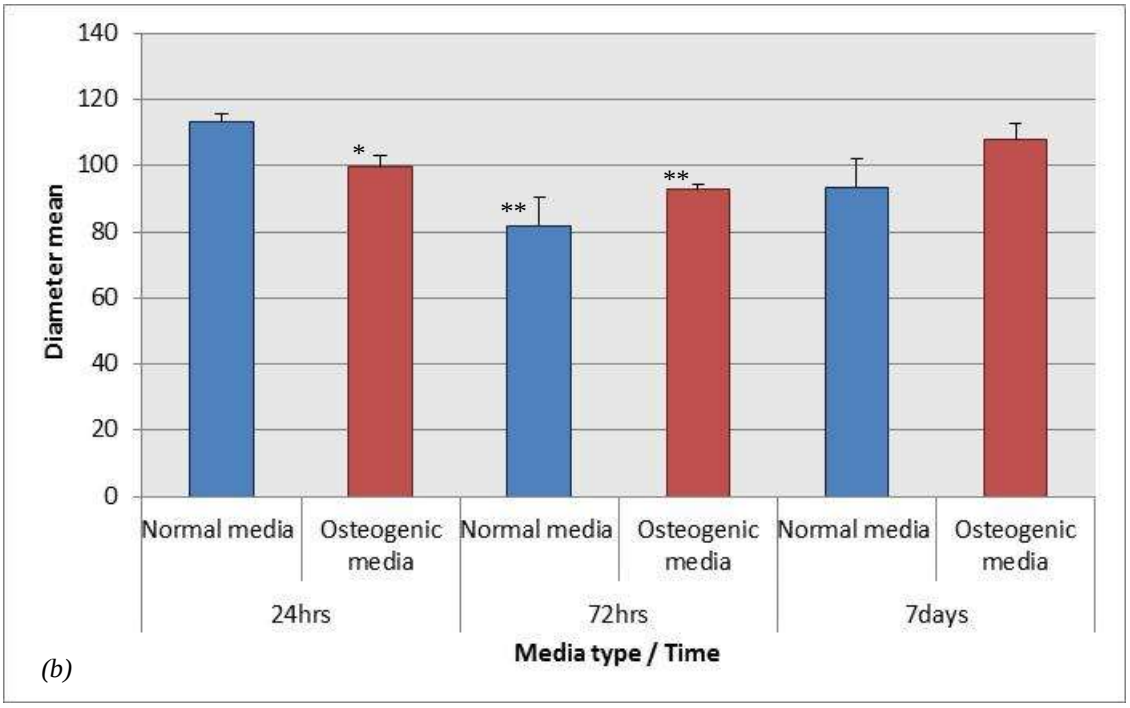

(b)

Figure 3.31 *Data represents the mean ± standard error of the mean statistical significant determined using Kruskal-Wallis test n=18, p value ≤ 0.05 was considered significant where (*) indicates significance compared to normal media while (**) compared to 24hr (a) number of spheroids. (b) Spheroids diameter measurements*

3.4 Discussion:

Cells are usually grown as a monolayer in 2 dimensional cultures; however, previous studies have noted the relevance and importance of growing cells in 3 dimensions. For example, in evaluating drugs for cancer research, it was found that 3D cultures not only mimic the in vivo environment but also that cells grown in a 3D culture environment were more resistant to chemotherapeutic agents compared to those grown in 2D (Phung, Barbone et al. 2011). It was also reported that cells grown in monolayer differ physiologically compared to those grown in 3D culture (Khoei, Goliaei et al. 2004). In light of this 3D spheroid culture is a useful tool in modelling cell (patho) physiology. In addition cell therapies for regenerative medicine will rely on the administration of cell suspensions and understanding how these cells aggregate both with each other and the host tissue will be fundamental for their long term success.

The present study aim was to test and compare different simple methods that will induce the formation of spheroids. Both the characteristics and the viability the cells under different culture conditions were evaluated.

It was reported before that spheroids formation is affected by various factors that include spheroid culture method choice, culture media, and cell viability (Atala and Lanza 2001). The results of the work presented here reinforces the view that choosing the appropriate method for a specific study or cell type(s) will influence the successful formation of spheroids. For example, previous studies have reported that serum is necessary at the beginning of culture (Atala and Lanza 2001) . However, it has been suggested that serum should be eliminated after spheroids formation for optimal genes expression (Atala and Lanza 2001). For the reason that serum could return cells back to monolayer growth (Ghosh 2006). Moreover, studies showed that melanocyte spheroid formation decreased when serum concentration increased and the growth is reduced when

serum is completely removed (Lin, Hsiao et al. 2006). In contrast to previous findings where eliminating serum led to spheroid formation, the results of the present study showed that removing serum did not induce spheroids. This could be due to the cell type used in this study. Previous studies that have shown successful spheroid formation using different cell lines include dental pulp cells, (Xiao and Tsutsui 2013), human gall bladder carcinoma cells (Shi, Gao et al. 2011), mouse corneal keratocytes (Yoshida, Shimmura et al. 2005). While other researchers combined eliminating the serum factor with other methods such as using a gyratory shaker to shake the plates continuously preventing cells from adhering (Bao, Fisher et al. 2013). Also, seeding cells in an ultra-low attachment 96 well plate (Liu, Ma et al. 2013) or low adhesion culture plates (Pease, Brewer et al. 2012) in a serum free media. This may suggest that eliminating serum alone may not be a good method for some cell types. In addition, the results of the work presented here does not support the findings of (Li, Pan et al. 1999) who demonstrated the importance of eliminating serum from the media in a non-adherent environment for spheroids generation. The cells used in our studies were able to aggregate and form spheroids in polyHEMA coated plates with the presence of serum in the media. Furthermore, it was reported that a high percentage of serum will permit the formation of a larger spheres (Raptis 2001).

On the other hand, our results show that using 96 rounded bottom plates failed to generate spheroids. Prior studies used this approach combined with other protocols such as coating the wells with agar (Ho, Yeap et al. 2012), or polyHEMA (Phung, Barbone et al. 2011) (Kurioka, Takagi et al. 2011), or mixing cells with agar (Ke, Albers et al. 2004) or methylcellulose (Rudisch, Kuip et al. 2012) then seeding them in the 96 u plate. While others used spinning force to collect cells and help them form spheroids in 96 u bottom well plate (Kawai, Hayashi et al. 2001).

The other method used in this study that failed to produce spheroids was methylcellulose which was used as a semi solid media for cells entrapment at three concentrations. Previous studies have used low concentration of methylcellulose 0.12% (Baum, Hlushchuk et al. 2007; Haycock 2011), 0.8% (Kubota, Preisler et al. 1981), and 12mg/ml (Rudisch, Kuip et al. 2012). Also, this approach has been combined with other methods, (Baum, Hlushchuk et al. 2007) for example induction of cell aggregation using the hanging drop as well as methylcellulose where cells were mixed with 0.12% methylcellulose then pipette drops of the mixture into the petri dish cover. Spheroid formation failure with this method could be due to cell type since it was reported that this method is usually used for hematopoietic cells (Liu, Ma et al. 2013).

By contrast, the hanging drop technique has been widely used by many researchers (Yusuf, Gopurappilly et al. 2013) (Tsukada, Kouki et al. 2013) . The results in this study found that using this method will induce cell aggregates, however, this method is technically challenging where gravity limits the volume of the droplet of cells suspension used ranging between 20-50µl and therefore changing media is an obstacle (Lee, Ortmann et al. 2010) (Breslin and O'Driscoll 2013). In addition, using this method it is not suitable for the production of spheroids at a large scale (Rungarunlert, Techakumphu et al. 2009). These obstacles may be overcome using a commercial 384 well plate developed by 3DBiomatrix, or the InSphero hanging drop plate that allows the generation of spheroids at a larger scale (Hsiao, Tung et al. 2012). Additionally these plates are designed so it would be easy to replace old media with fresh media (Breslin and O'Driscoll 2013).

In contrast, coating plates with polyHEMA enhanced spheroid generation at all concentrations. In accordance with the present results, previous studies have demonstrated that coating plates with a non-adhesive polymer such as polyHEMA

enhances cellular spheroids formation (Schwartz, Lechene et al. 1991) (Le Beyec, Xu R Fau - Lee et al. 2007). This led companies such as Greiner Bio-One to manufacture CELLSTAR® cell repellent surface plates which are coated with a polymer to induce spheroids formation (Taylor 2013). The way polyHEMA works in preventing cells adherence may be due to negative electrostatic reduction of the polystyrene surface (Folkman and Moscona 1978).

Although using polyHEMA coated plates enhances spheroid generation as well as being cost effective, this method has some limitations where it is difficult to control the size of the spheres, and it is important to insure a homogenous coating of polyHEMA (Ke, Albers et al. 2004). Where uneven coating occurs, this may result in poor ethanol evaporation and/or impurities in the PolyHEMA will affect the formation of the spheroids (Atala and Lanza 2001).

In the present study the viability and hence proliferation was assessed using the MTT assay that measures viable cells through their mitochondrial enzyme activity (Cree 2011). Cell growth in vitro is dictated by three main factors including cell type, cytokine/growth factor environment, and material related factors (Stachowiak 2010). Therefore cell growth and behaviour is affected since they are placed outside their natural environment into an artificial medium which usually comprises nutrients that helps cell growth and survival (Haycock 2011; Arora 2013). For that reason, replacing old media with new media effects cell viability and hence MTT levels will increase. Additionally, cell competition for nutrients and their interaction with each other plays a role, therefore viable cell numbers could decrease at a very high and low cell density over time. Overall, this explains the results in this study where MTT levels decreased after 7 days in some cases and by 21 days in most cases studied. However at 28 days the viability of cells in most cases increases.

On the other hand, β-glycerophospate, ascorbic acid, and dexamethasone were added to the media to induce osteogenesis (Martinez, Donato et al. 2012). β -glycerophosphate works as a source of inorganic phosphate for the mineralization process (Kaveh, Ibrahim et al. 2011). Whereas ascorbic acid is added as a cofactor for the enzyme that hydroxylates the proline residues in proteins [collagen], ensuring it folds correctly (Kaveh, Ibrahim et al. 2011). Dexamethasone is a synthetic glucocorticoid that enhances osteogenic, chondrogenic and adipogenic differentiation of MSC, upregulating alkaline phosphatase an early marker for bone (Wang, Pang et al. 2012). In this chapter both the efficiency of spheroids generation and cell viability under osteogenic conditions were investigated. The results of this study showed that spheroids start to disintegrate in long term culture in osteogenic media. Dissociation of spheroids may be due to mechanical or shear fluid force that are caused when changing the culture media (Debruyne, Mareel et al. 2009). However, this shouldn't be the case since spheroids grown under normal conditions were compact and rigid indicating that it might be related to changing activity of the cells in response to the osteogenic media supplements. Previous studies showed that dexamethasone supplementation decreased cell proliferation and increased apoptosis (Kim, Kim et al. 2013). In contrast, other studies suggested that dexamethasone increases osteoprogenitor cell proliferation (Bellows, Heersche et al. 1990). Moreover, previous results on dexamethasone effects on apoptosis are contradictory where it depends on cell type, for example, adding it to lymphocytes, thymocytes and some tumour cells induced apoptosis, whilst in neutrophils and hepatocytes it was reduced (Song, Caplan et al. 2009). However, it was also reported that the presence of dexamethasone in long term culture may have a toxic effect on cells and may cause cell lysis (Kaveh, Ibrahim et al. 2011). Also it was reported that cells apoptosis increases at a higher cell density but the effect is diminished in a medium that contains 100nM of dexamethasone (Song, Caplan et

al. 2009). So, overall the type of cell line, the concentration of dexamethasone, and period of cell culture play a role on cell viability and spheroid dissociation due to cell death. Interestingly, the MTT assay shows that the viability of cells increased after 21 days. The reason for this is not clear but it may have something to do with cell line used in this study and/or changing old with new media.

We also measured the diameter and counted the number of spheroids formed. The findings observed in this study support those of the previous studies which showed an increase in the size of spheroids over time (Jing and Jian-Xiong 2011). A possible explanation for this might be due to spheroids gathering together increasing the size and decreasing the number of spheroids at the same time. This gathering may be caused by the movements of the spheres when observing and/or changing media. Changing media also may cause the loss of spheroids which may explain the reduction of spheroid number.

In conclusion, although some previous studies showed success in generating spheroids diverse cell lines behave differently the work presented here suggests that coating the surface of the well plate with Poly-HEMA is considered as the most reproducible way to develop spheroids in culture that can be studied over several weeks. In this chapter only the efficiency of spheroids and viability were examined, although it may be worth investigating alkaline phosphatase levels as well in the future.

Chapter 4: Investigating cell gene expression and communication in 2D and 3D cultures

4.1 Introduction:

Bone homeostasis and structural maintenance is controlled by cellular communication (Edwards and Mundy 2008). Whilst soluble mediators and immobilised growth factors and cytokines play a hugely significant role in coordinating cell activity, direct cell-cell interactions such as those formed by gap junctions are equally important. Connexin 43 [Cx43] is a gap junction protein that is expressed abundantly by bone cells including osteocytes, osteoblasts, and osteoclasts, where it plays an important role in cell-cell communication (Plotkin and Bellido 2013). Previous studies reported an up-regulation of Cx43 during fracture healing supporting its role in bone formation (Loiselle, Paul et al. 2013). Gap junctions also interact with other cell-cell structures including Eph/ephrin signalling in cells (Arvanitis and Davy 2008). Bone cells express ephrin B1, ephrin B2, Eph B2, Eph B3, Eph B4, Eph B6, and Eph A4 (Xing, Kim et al. 2010). Ephrin B2 is reported to be upregulated at sites of bone injury (Benson, Opperman et al. 2012). In addition, treating cells in vitro with ephrin B2 increases osteoblastic genes such as ALP, and osterix (Zhao, Irie et al. 2006).

The objective of this part of the study was to evaluate the expression of genes that are associated with cell-cell interaction in bone namely ALP, Runx2, osterix, ephrin B1, ephrin B2, ephrin B4, and Cx43; and furthermore identify how cell growth in 2D and 3D under normal and osteogenic conditions influences the regulation of these genes.

4.2 Materials and methods:

All materials and reagents were purchased from Sigma-Aldrich company, Ltd Ayrshire, UK unless otherwise specified.

4.2.1 Cell culture

Tissue culture was carried out in an aseptic environment using a class II laminar flow hood. Cells were grown as monolayer [2D] and as suspension [3D] using plates coated with polyHEMA.

4.2.1.1Poly-HEMA stock solution:

PolyHEMA stock solution was prepared as previously described in section 3.2.1.2.

4.2.1.2 Preparation of Poly-HEMA Coated Plates:

The plate wells were coated with PolyHEMA following the method in section 3.2.2.2.

4.2.1.3 Rat calvarial cell culture:

Rat cells culture was carried out following sections 2.1.1., 3.2.2.1.

4.2.1.4 Human mesenchymal stem cells cell culture:

Human mesenchymal stem cells were purchased from Lonza and cultured as described previously in sections 2.1.1 but using Dulbecco's Modified Eagle's Medium - low glucose.

4.2.2 Histology and immunoflourescent studies:

4.2.2.1 Hematoxylin and eosin staining:

Samples were prepared and stained with standard Hematoxylin and eosin stain as described previously in section 2.1.8.1.

4.2.2.2 Immunofluorescent staining:

Immunolocalization of CX43 was performed as described previously in section 2.1.8.2. Samples that had been embedded in wax were deparaffinised using xylene for 3m, rehydrated in 100% then 98% ethanol for 3min each, then underwent antigen retrieval as described in section 2.1.8.2. (Mayer, Walker et al. 1988).

4.2.3 Scanning electron microscopy [SEM]:

To examine spheroid structure and morphology samples were prepared as described previously section 2.1.7.

4.2.4 Evaluation of cell viability and proliferation using MTT assay:

Cells viability was performed as described in sections 2.1.3 and 3.2.2.3.

4.2.5 Alkaline phosphatase assay:

Osteoblastic differentiation of both cell lines was assessed by measuring alkaline phosphatase activity following the method outlined in section 2.1.4.

4.2.6 RNA isolation and quantitative real time polymerase chain reaction:

The expression of mRNA levels for genes associated with osteogenesis, including Runx2, ALP, osterix and osteocalcin were determined using a quantitative real time polymerase chain reaction [qPCR]. Methodology was followed as previously described

in section 2.1.6. The cycle threshold [Ct] values were normalized against the house keeping gene GAPDH.

4.2.7 Statistical analysis:

Data management and analysis was performed using SPSS 19.0. [SPSS Inc., USA]. Data were first explored to verify if they were normally distributed with a *p* value above 0.05 using Shapiro-Wilk's test to indicate a normally distributed data (Shapiro and Wilk 1964; Razali and Wah 2011). The data histograms, normal Q-Q plots which determine if two data sets come from a population with a common distribution, and box plots to identify outliners and compare distributions were also inspected visually. Since the analysis showed that some of the data were normally distributed while others were not normally distributed parametric and non- parametric methods were used respectively. In the former case a one way analysis of variance [ANOVA] was conducted to determine if there are any significant differences between the means, the variance was then subjected to a Post-hoc analysis with Bonferroni to determine which means differ. In case of non-Gaussian distributed data, a Kruskal-Wallis analysis of variance was conducted. The variance was then subjected to a multi-comparison analysis Mann – Whitney U test with Bonferroni correction to determine the significance. Data were considered statistically significant when p value ≤ 0.05.

4.3 Results:

4.3.1 Connexin 43 localisation in 2D and 3D culture:

To visualize Cx43 gap junctions, samples were stained with anti-Cx43 antibody. As shown in Figure 4.1, Cx43 was localized around the nucleus and the membrane in cells grown in normal media on tissue culture plastic. While those grown in osteogenic media showed more Cx43 at cell-cell contact regions [figure 4.2]. However using conventional epifluorescence microscopy, in 3D cell culture it was hard to visualize Cx43 compared to 2D culture [figure 4.3 and 4.4] although Cx43 was seen in the centre of some spheroids [figure 4.3]. Therefore, confocal microscopy was used where an x,y,z series of images could be obtained throughout the thickness of the sample. This approach allowed Cx43 to be localised in each layer of the spheroid. In early attempts we used a normal microscope slide, but this caused flattening of the cell aggregates. So, a concave slide was used in order to retain the original spherical shape of the spheroids. As seen in Figure 4.7 and 4.8 I was able to maintain the spherical structure, however, I was unable to localize Cx43 as observed in 2D. Subsequently, collodion bags were used and the spheroids were sectioned and stained first with a routine H & E stain [figure 4.9]. Some sections were then de-waxed and stained with antiCx43 antibody to check if it was possible to localize Cx43 and it was difficult to do so.

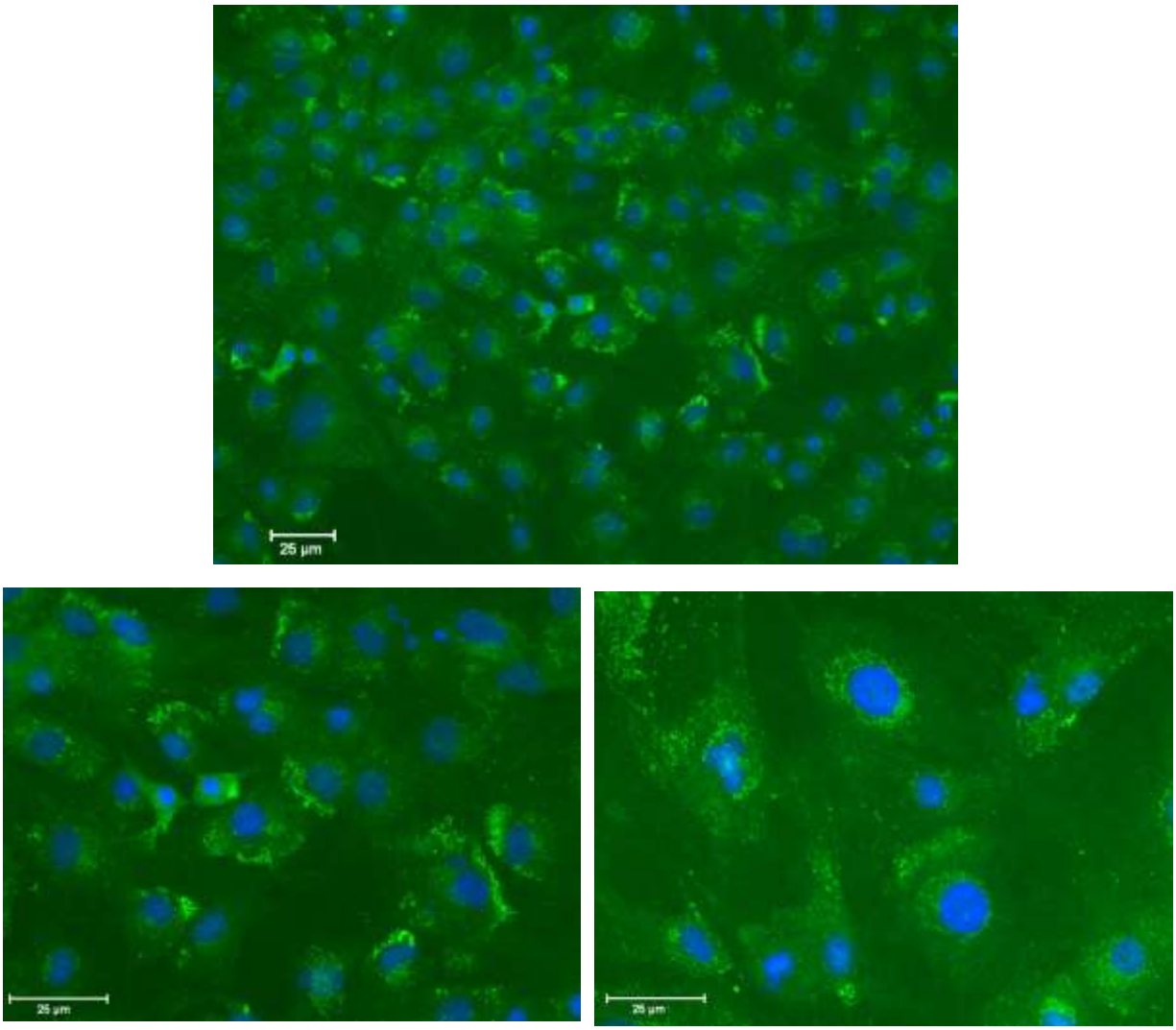

Figure 4.1: *Immunofluroescent staining of Cx43 in rat calvarial cells monolayers grown for 7 days under normal conditions. Cx43 [green] localize around the nucleus [blue] and at the cell membrane*

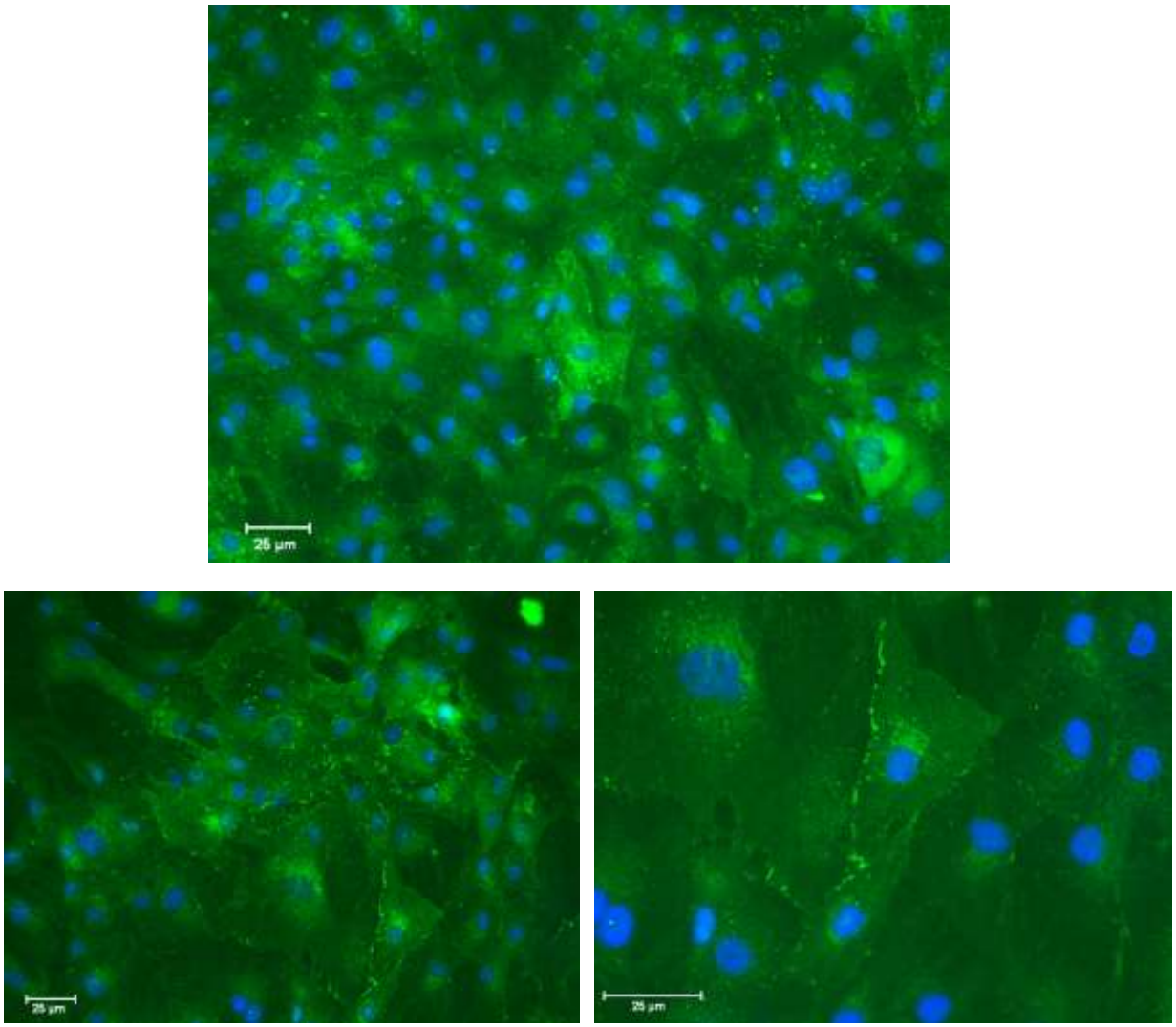

Figure 4.2: *Immunofluorescent staining of Cx43 in rat calvarial cells monolayers grown for 7 days under osteogenic conditions. Cx43 [green] localize at the cell membrane*

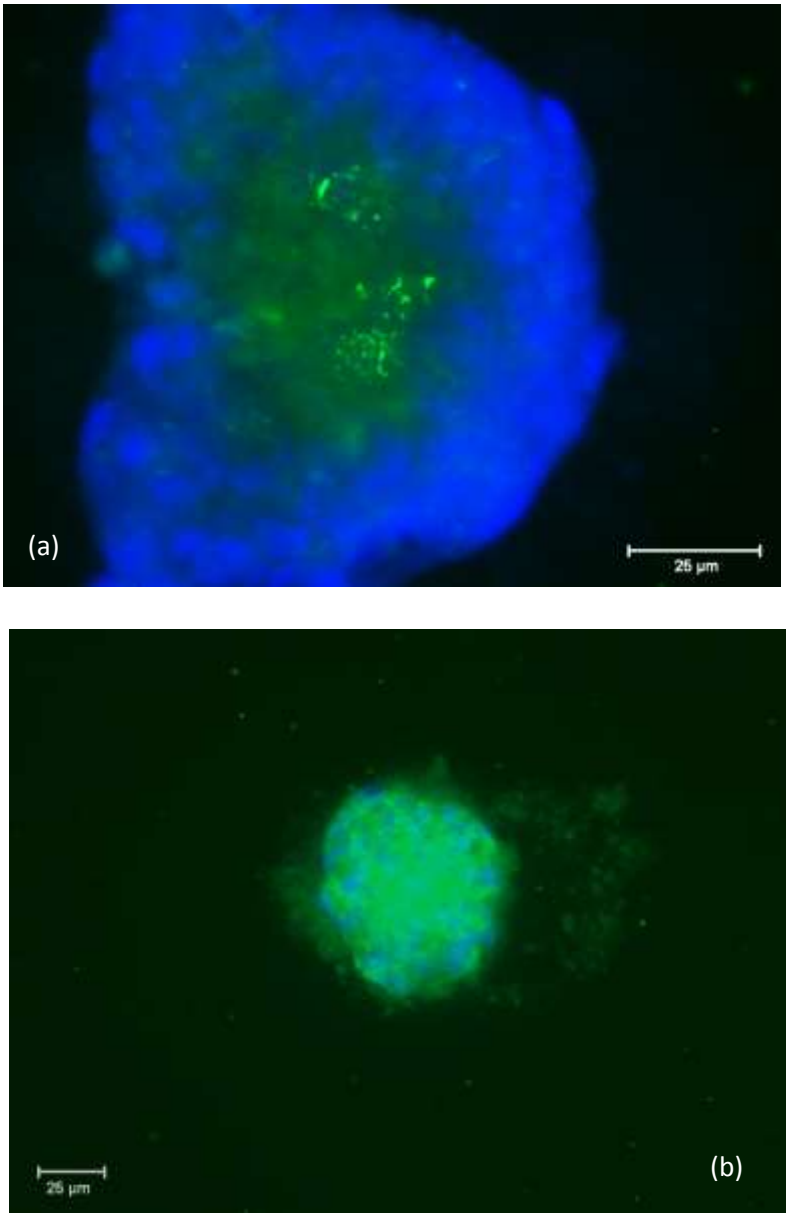

Figure 4.3: *Immunofluorescent staining of Cx43 in rat calvarial cells 3D grown for 7 days (a) Normal media (b) osteogenic media. Cx43 [green] while nucleus is stained with DAPI [blue]*

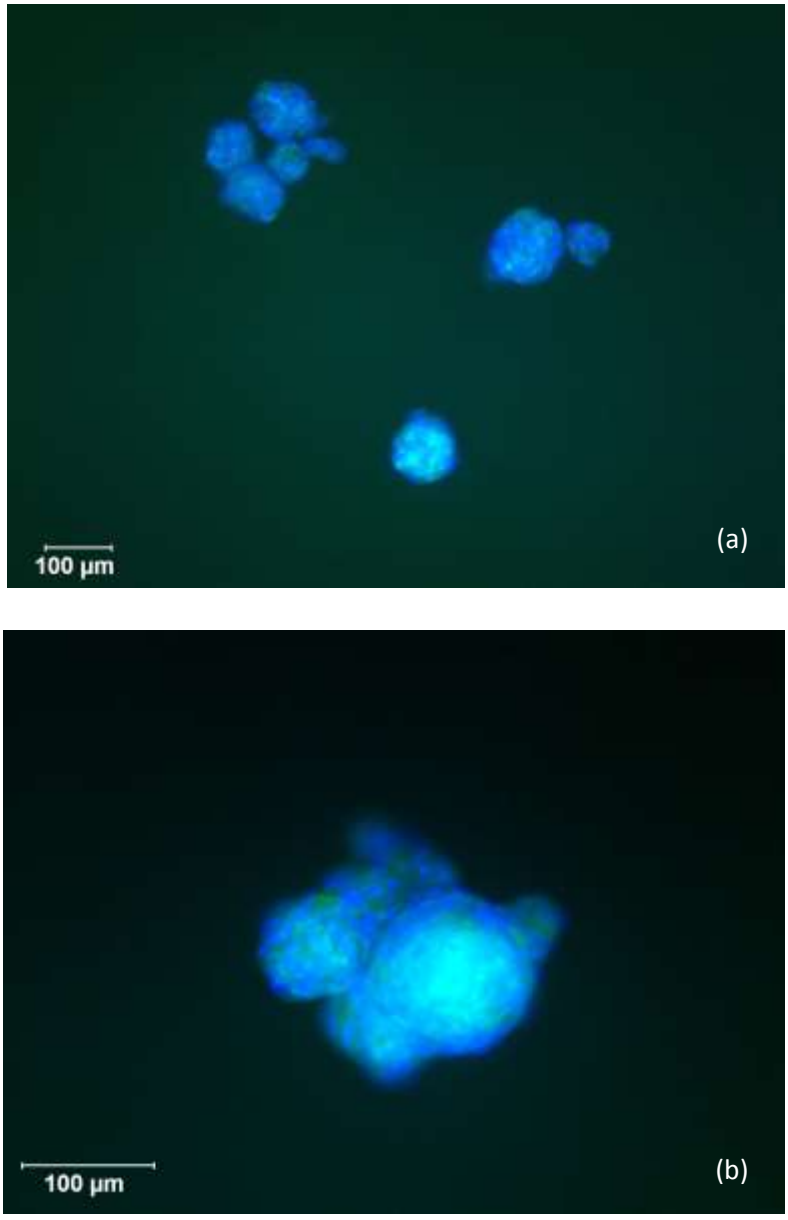

Figure 4.4: *Immunofluorescent staining of Cx43 in human mesenchymal stem cells 3D grown for 7 days (a) Normal media (b) osteogenic media. Cx43 [green] while nucleus is stained with DAPI [blue]*

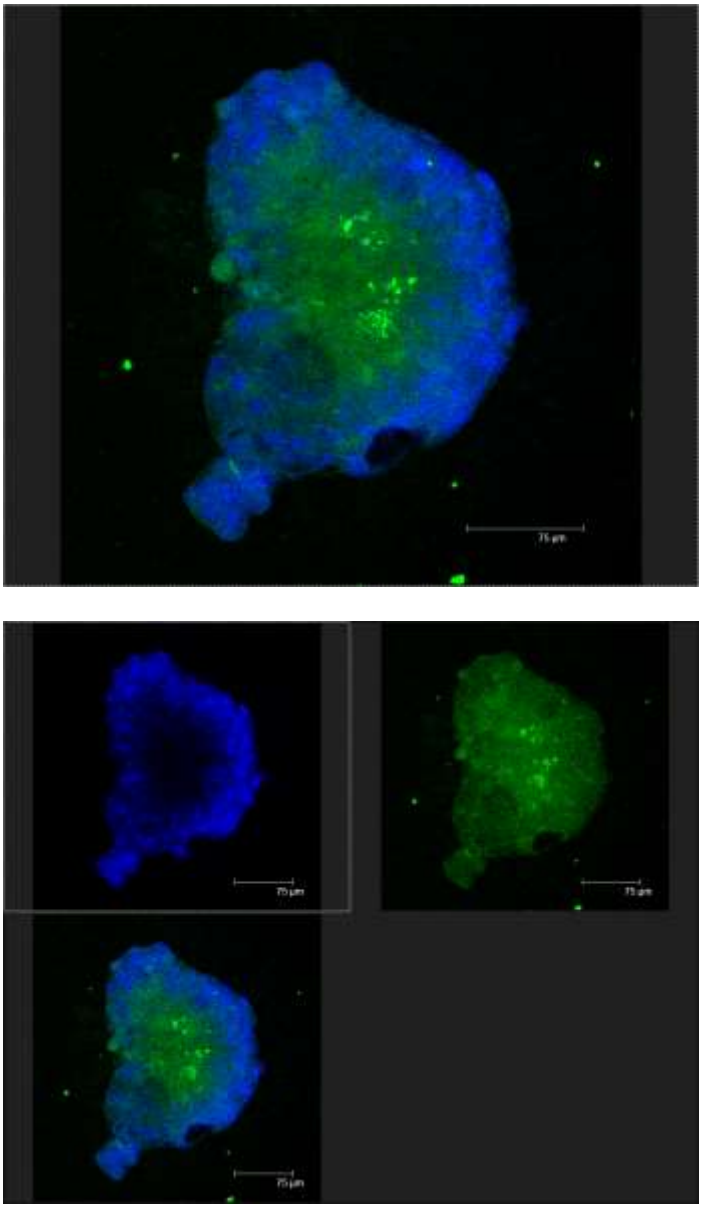

Figure 4.5: *laser confocal images of Cx43 in rat calvarial cells 3D grown for 7 days (a) Normal media (b) osteogenic media. Cx43 [green] while nucleus is stained with DAPI [blue]*

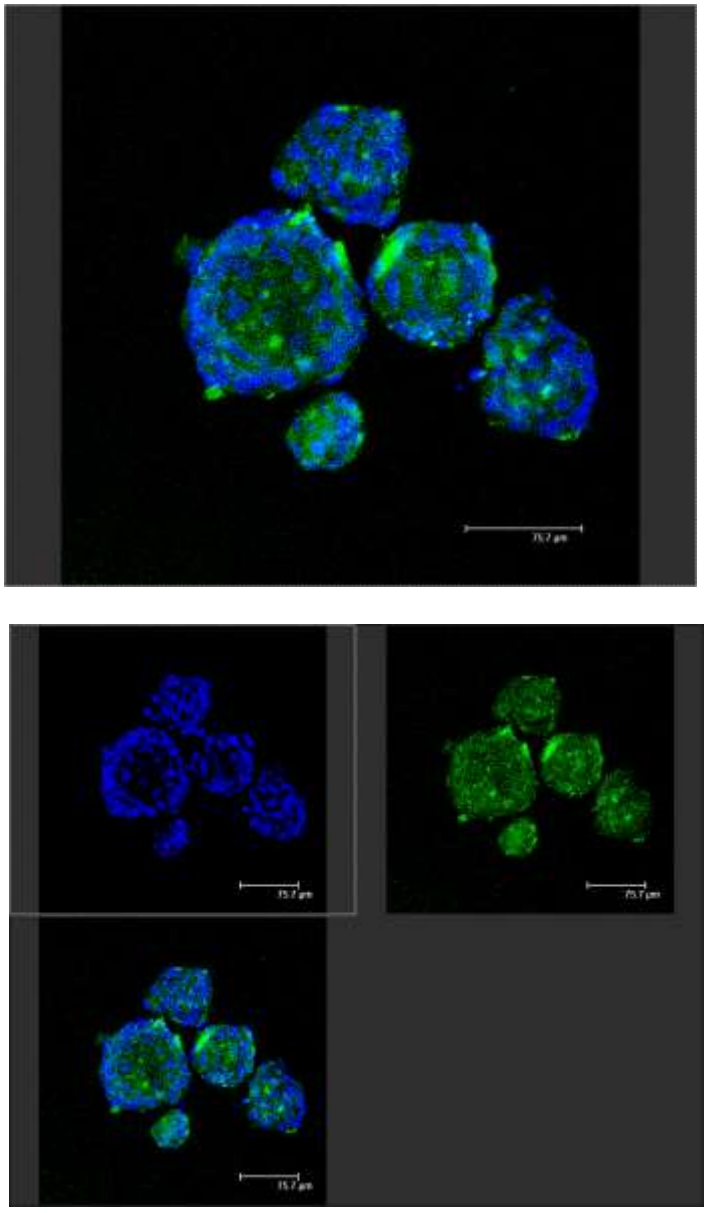

Figure 4.6: *laser confocal images of Cx43 in human mesenchymal stem cells 3D grown for 7 days (a) Normal media (b) osteogenic media. Cx43 [green] while nucleus is stained with DAPI [blue]*

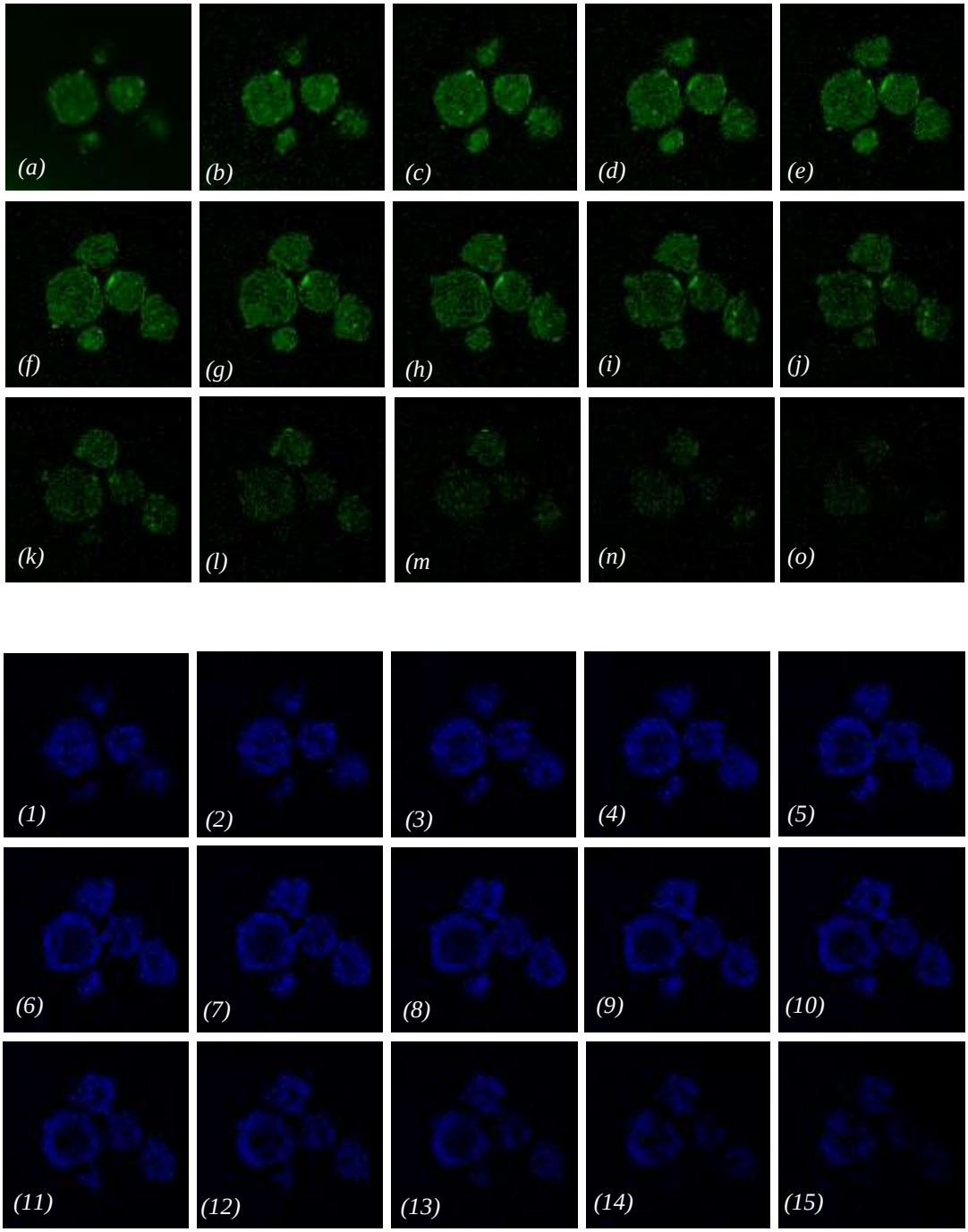

Figure 4.7: *Laser confocal microscopy series of images of a spheroid. [a-o] images of Cx43 localization [green] while [1-15] are images of the cell nuclei stained with DAPI [blue]*

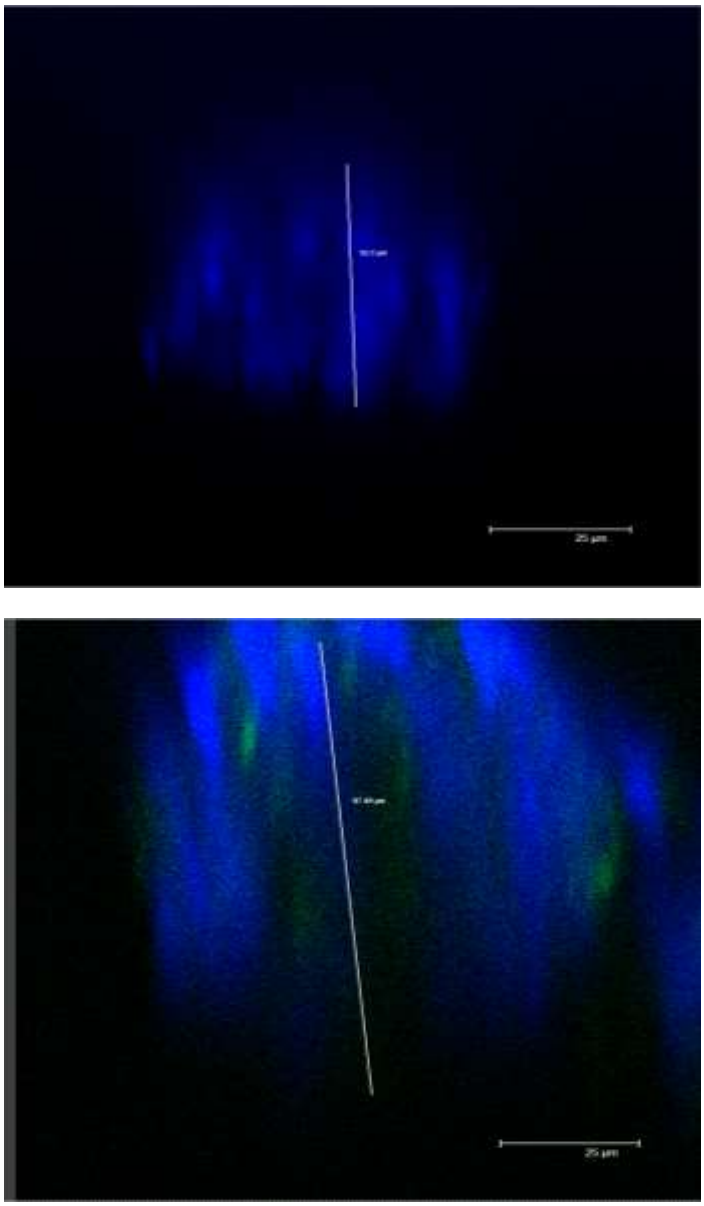

Figure 4.8: *A Z -section confocal microscope image of spheroids placed on a concave slide in order to maintain the spherical shape of the sphere, spheroid thickness in (a) 52.2µm and (b) 97.49µm*

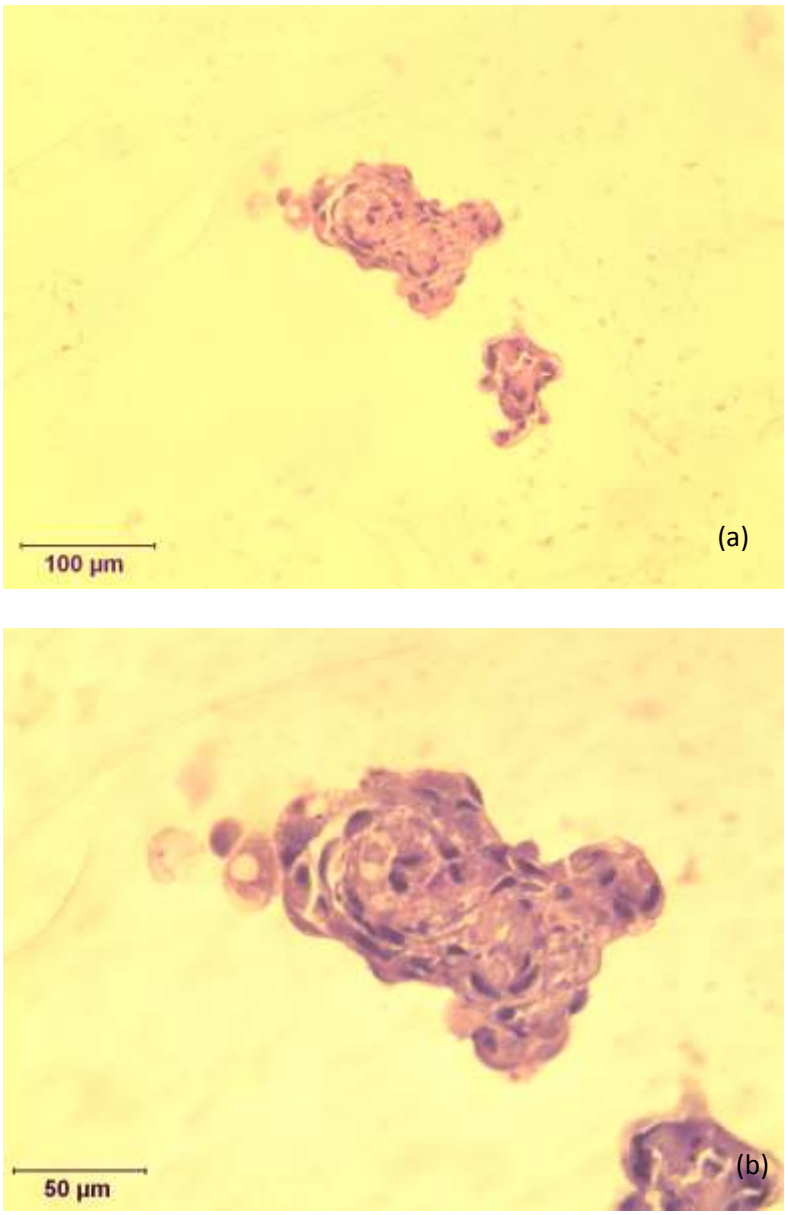

Figure 4.9: *Hematoxylin and Eosin [H&E] stain of a spheroid section cultured for 7 days; nucleus [dark purple] and cytoplasm [light purple] (a) lower and (b) higher magnification*

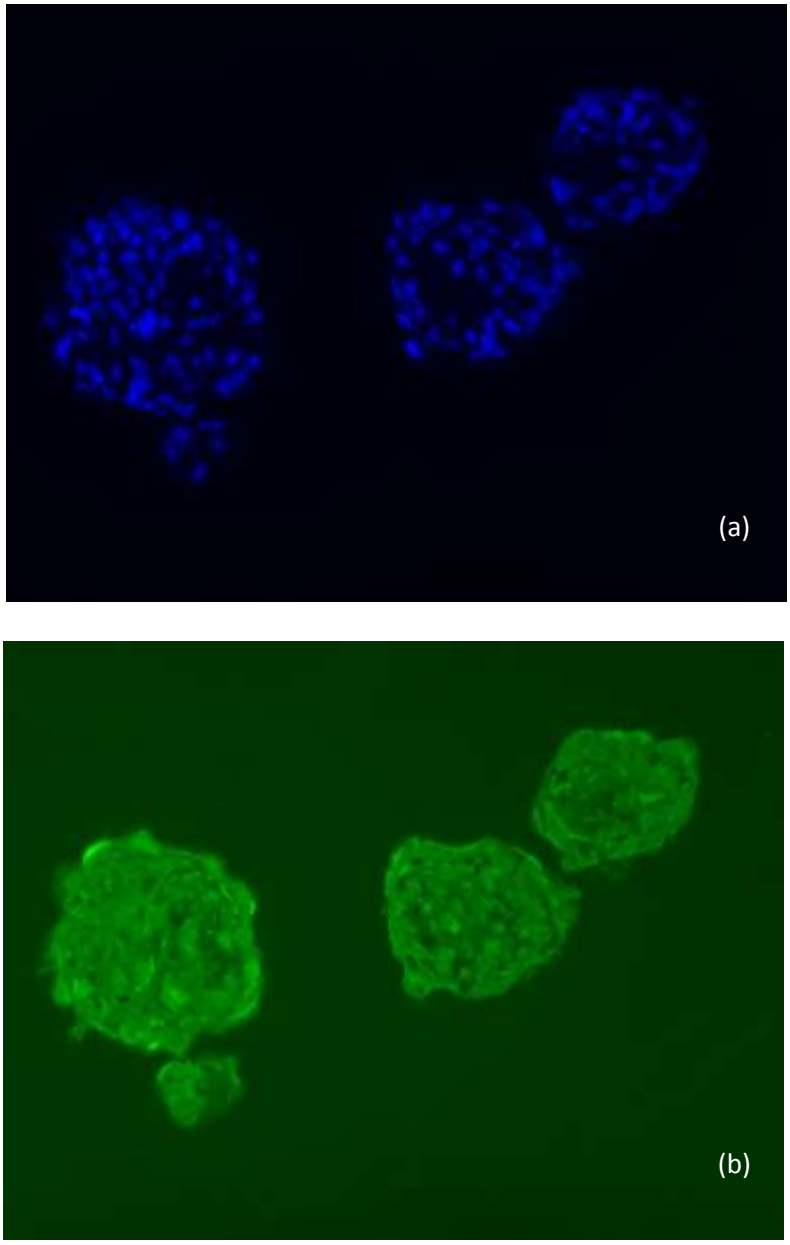

Figure 4.10: *Immunofluorescent analysis of Cx43 [green], the spheroid section stained with antiCx43 antibody (a) nucleus stained [blue] using DAPI (b) Cx43*

4.3.2 Morphological analysis of spheroids:

Scanning electron microscopy (SEM) was used to obtain high resolution structural images of spheroids. Two technical approaches were investigated to prepare the samples, first, spinning the spheroids at a low speed to from a pellet. The second was to collect the spheroids gently using a pipette tip.

In Figure 4.11 it can be seen that using the centrifugation approach the sphere shape was deformed as collected by pellet method, unlike the collection method where they maintained their spherical shape. After 24hrs the spheroids begin to form more irregular shapes which may be caused by small spheres merging to larger ones under both normal and osteogenic culture conditions [Figures 4.12 and 4.13]. Also, communication between spheroids was noted [see Figure 4.12]. After 7days of culture the spheres appeared compact and solid when grown under normal conditions [Figure 4.14]. While those maintained under osteogenic conditions formed spheroids that were much looser and in fact started to dissociate [Figure 4.15]. On the other hand, SEM images of human mesenchymal stem cells spheroids revealed that they were more compact compared to calvaria cells, for those grown after 24hr and 7days and in both normal and osteogenic media [see figures 4.16 and 4.17]

It is worth mentioning here that spheroids must be placed in another well plate before starting the processing for SEM. If not, this will cause the formation of amorphous substance at the surface of the spheres caused by polyHEMA dissolved from the well surface [Figure 4.18].

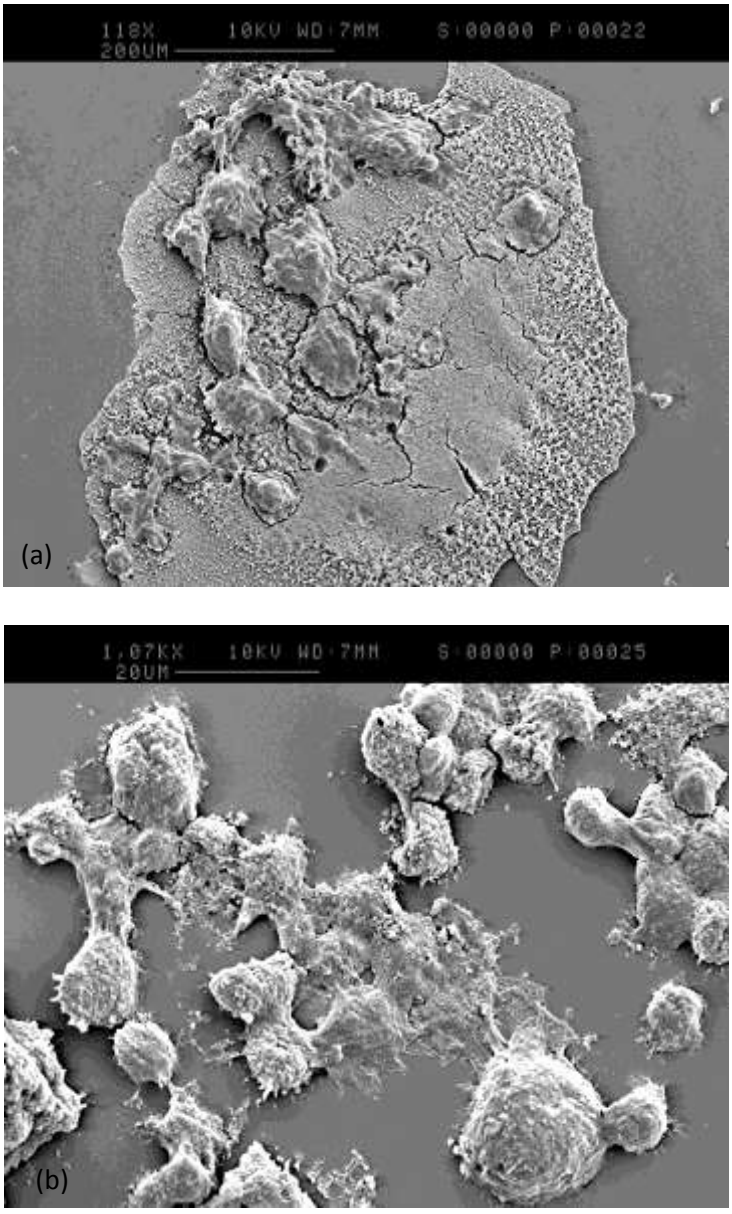

Figure 4.11: *SEM image of rat calvarial cell spheroids where they lose their spherical shape with no differences between both those grown in normal and osteogenic media (a) normal media (b) osteogenic media*

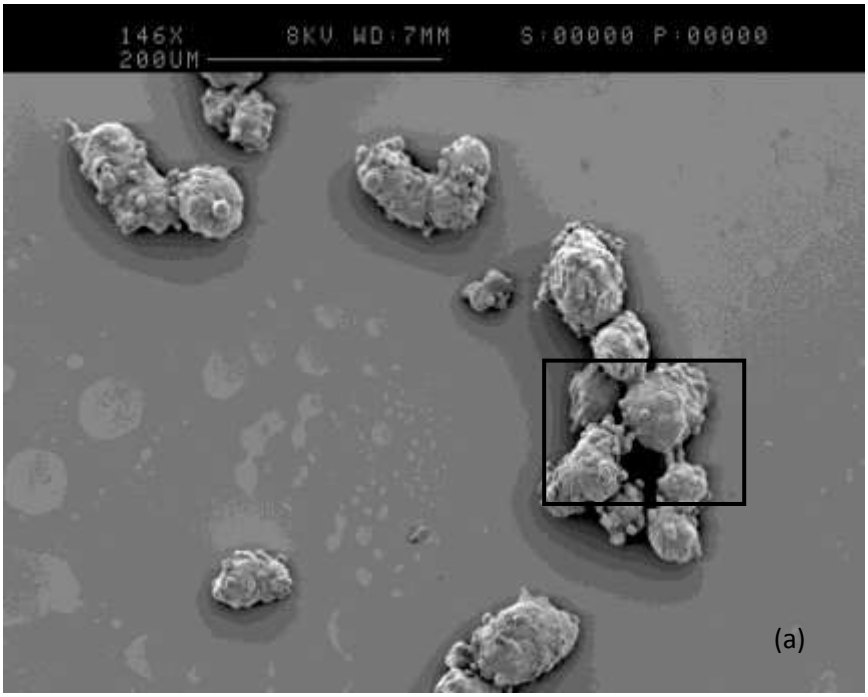

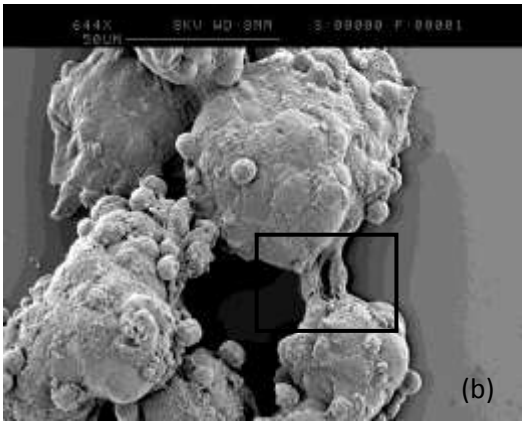

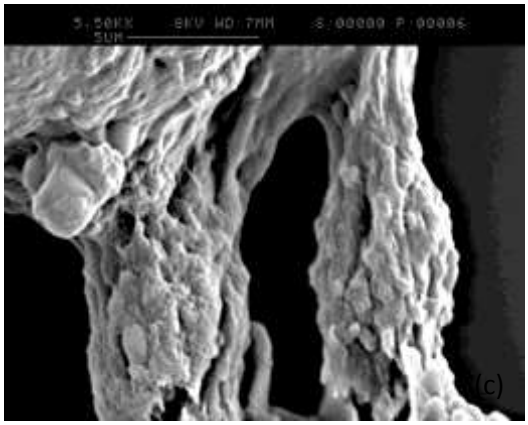

Figure 4.12: *SEM image of rat calvarial cells spheroids after 24hr grown in normal media (a) lower magnification (b) and (c) higher magnification illustrates communication [intracellular filopedia] between spheroids*

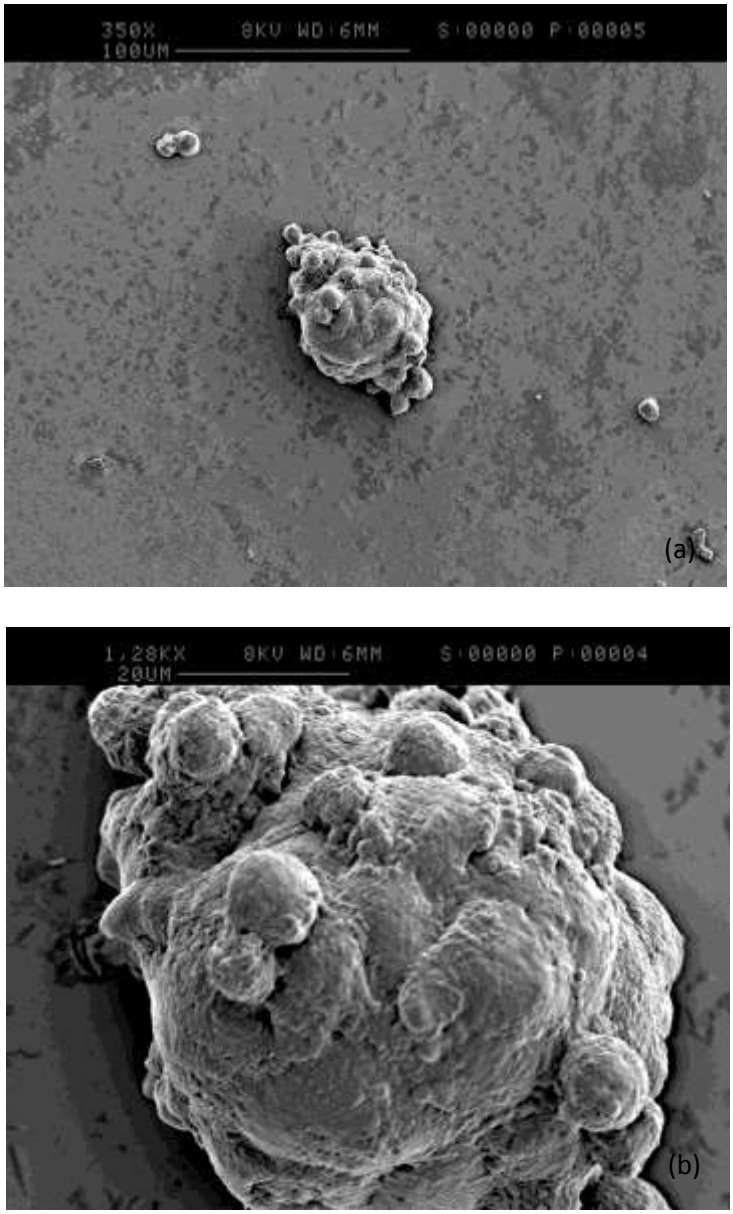

Figure 4.13: *SEM image of rat calvarial cells spheroids after 24hr grown in osteogenic media (a) lower and (b) higher magnification illustrates small spheres in contact with a larger sphere*

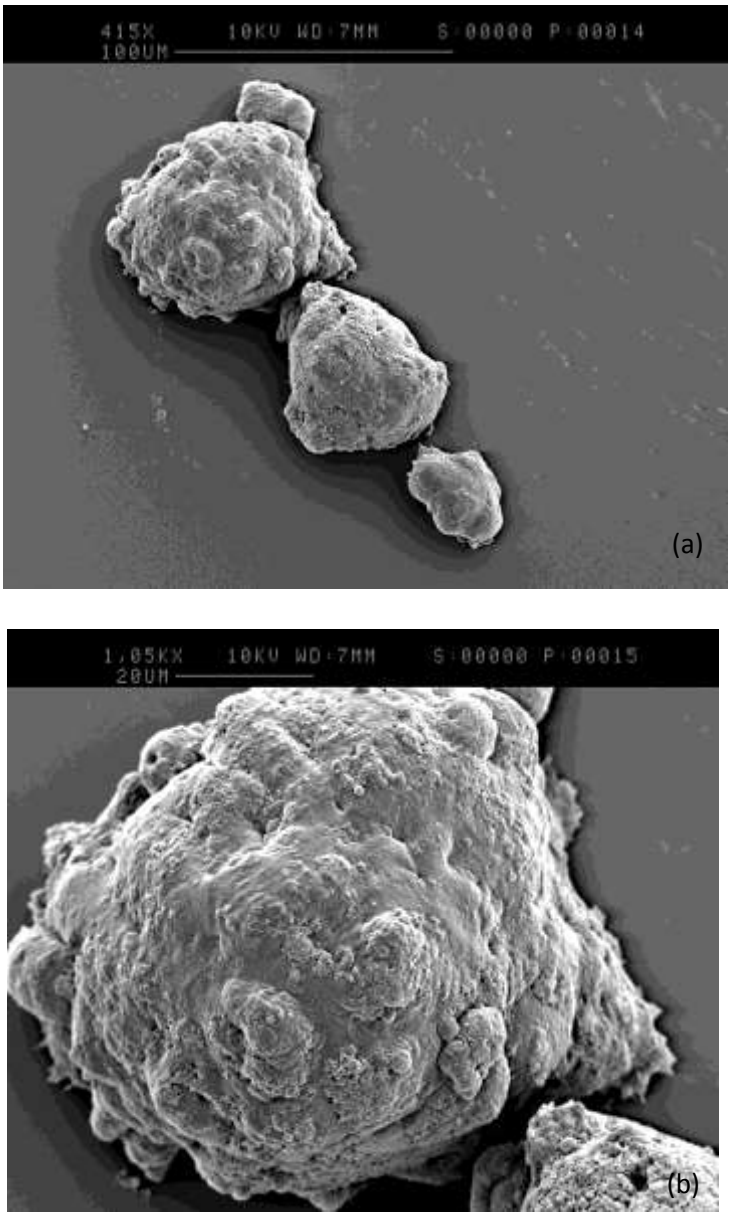

Figure 4.14: *SEM image of rat calvarial cells spheroids at 7days grown in normal media (a) lower and (b) higher magnification illustrates a compact sphere*

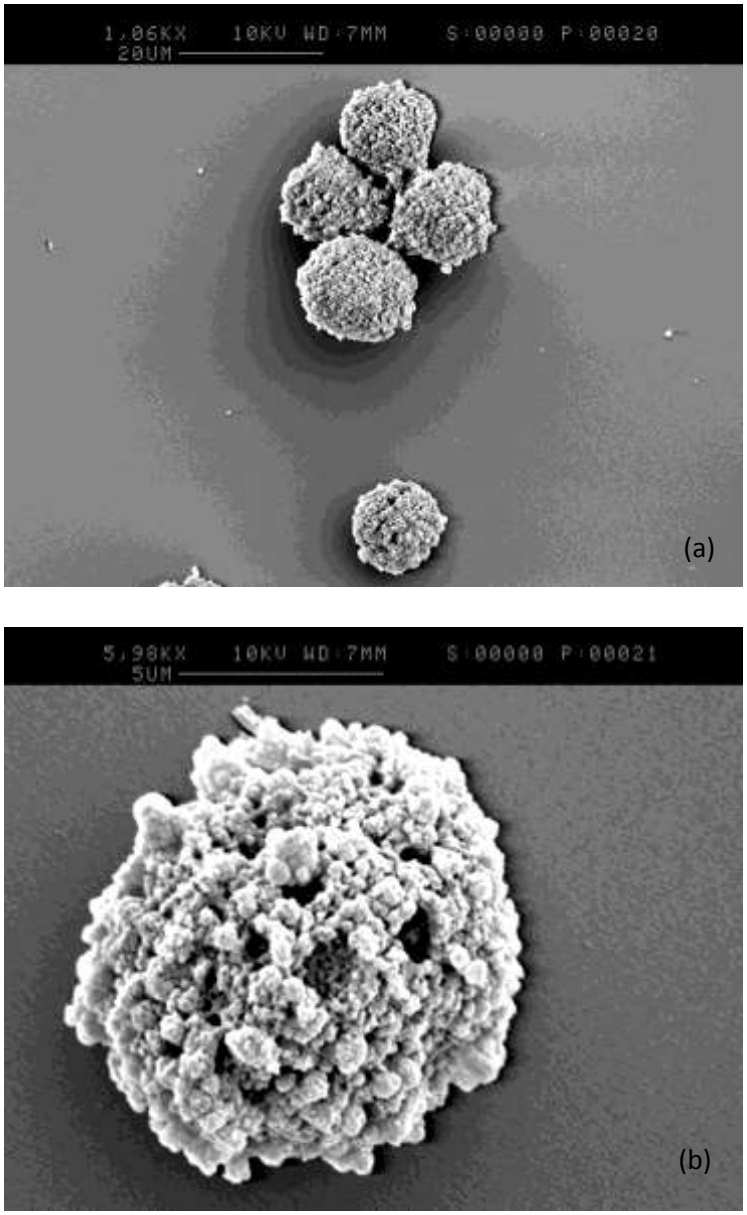

Figure 4.15: *SEM image of rat calvarial cells spheroids at 7days grown in osteogenic media (a) lower and (b) higher magnification illustrates spheres that dissociate*

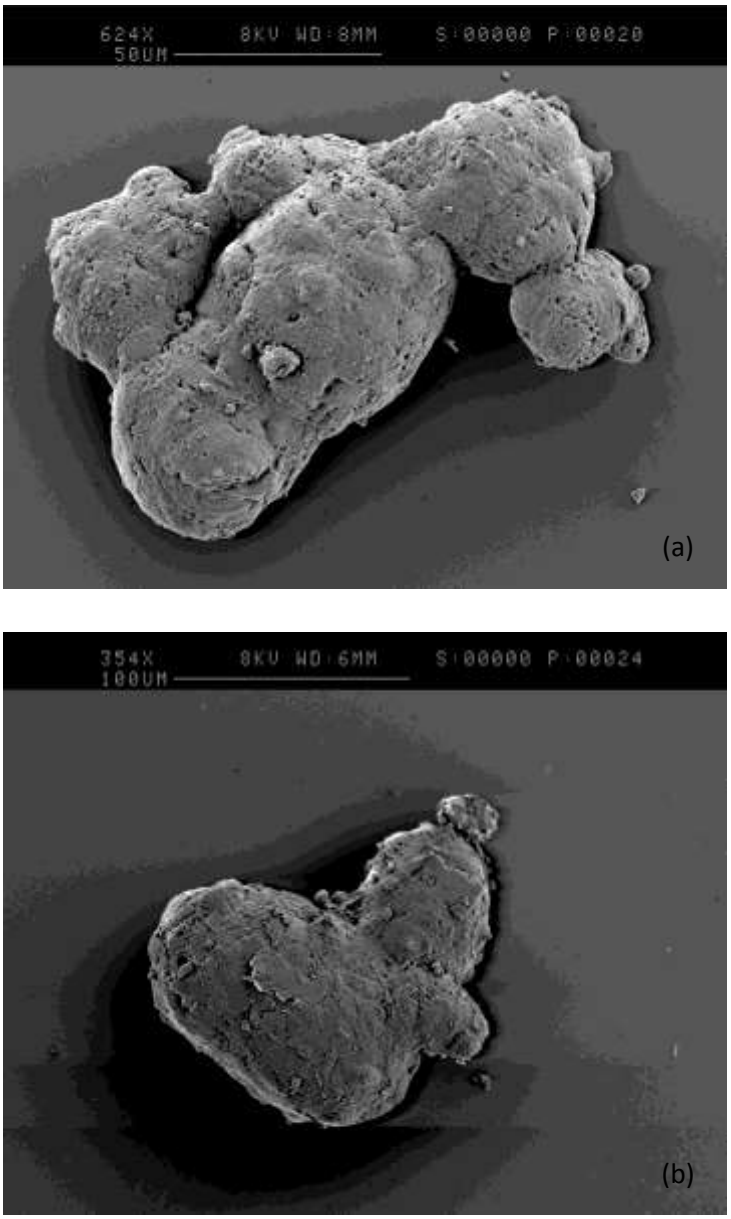

Figure 4.16: *SEM image of human mesenchymal stem cells spheroids after 24hr grown in (a) normal media and (b) osteogenic media*

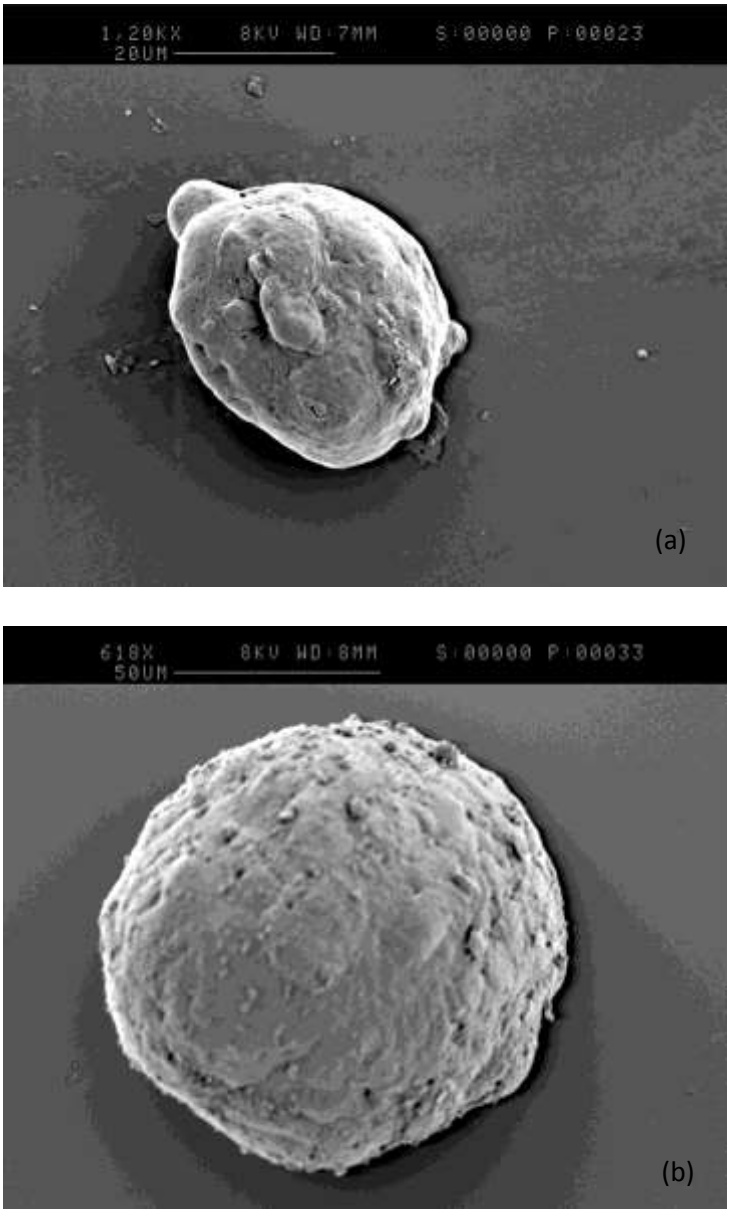

Figure 4.17: *SEM image of human mesenchymal stem cells spheroids at 7days grown in (a) normal media and (b) osteogenic media*

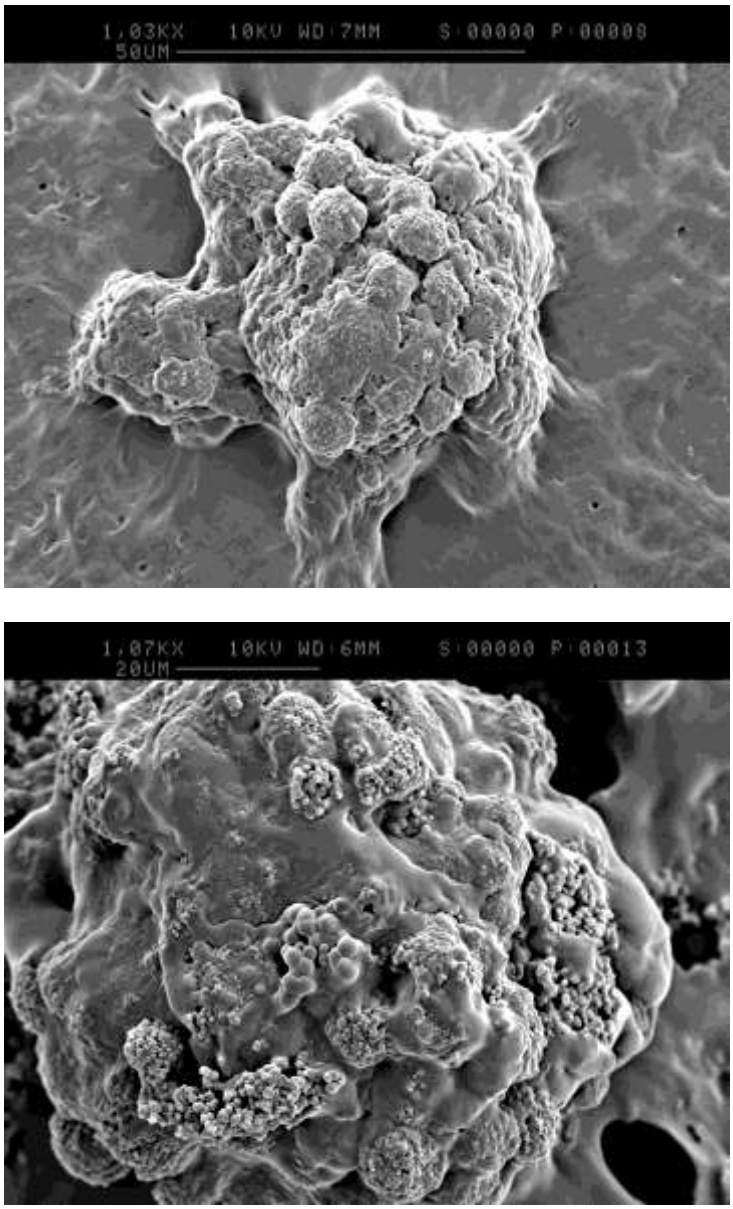

Figure 4.18: *SEM image of spheroids with amorphous coating believed to be polyHEMA from the surface of the culture plates*

4.3.3 Cell Viability in 2D and 3D*:*

Cell viability and proliferation was assessed using an MTT colorimetric assay. The MTT assay showed that cell number grown as monolayer are higher than those grown as 3D culture in both cell lines. After 24hr cells grown in 2D with normal culture media were more abundant than those grown under osteogenic conditions [Figure 4.19 and 4.20]. However, the viability of the cells grown in 3D under routine and osteogenic conditions was almost equal [Figures 4.19 and 4.20].

At 72hrs the viability of cells grown in 3D culture decreased, while the viability of those grown in 2D increased [figure 4.21 and 4.22]. The cell number at 7 days in cells grown in normal media in 2D remained elevated compared to those grown in osteogenic media [Figure 4.23 and 4.24]. In contrast, the viability of cells in 3D decreased with a slight reduction between cells in normal and osteogenic media [Figure 4.23 and 4.24].

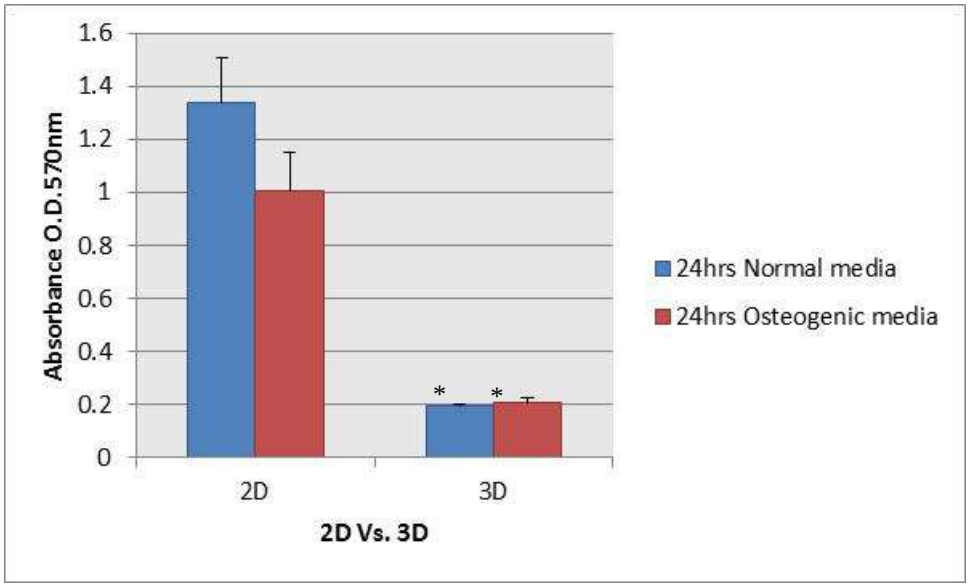

Figure 4.19 *Graph shows the viability of calvarial rat cells after 24hr, the data represents the mean ± standard error of the mean n=9, a statistical significant was considered when P value ≤ 0.05 where (*) indicates significance compared to 2D normal media.*

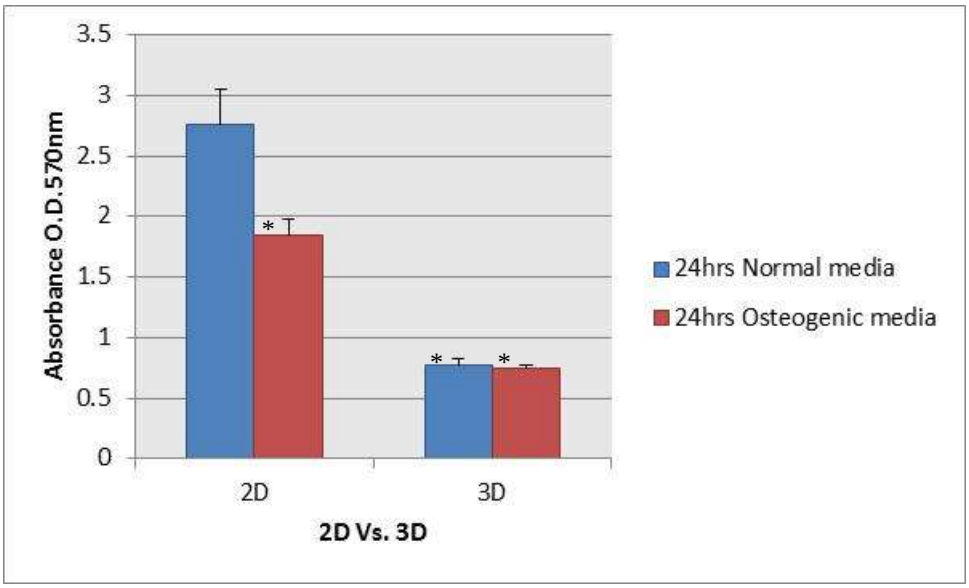

Figure 4.20 *Graph shows the viability of human MSCs after 24hr, the data represents the mean ± standard error of the mean n=9, a statistical significant was considered when P value ≤ 0.05 where (*) indicates significance compared to 2D normal media.*

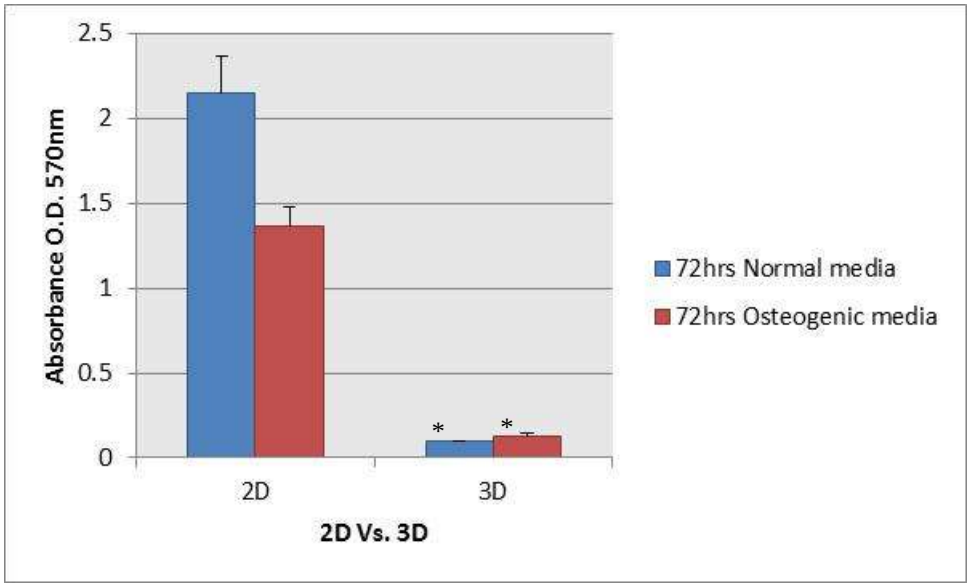

Figure 4.21 *Graph shows the viability of rat calvarial cells at 72hr, the data represents the mean ± standard error of the mean n=9, a statistical significant was considered when P value ≤ 0.05 where (*) indicates significance compared to 2D normal media.*

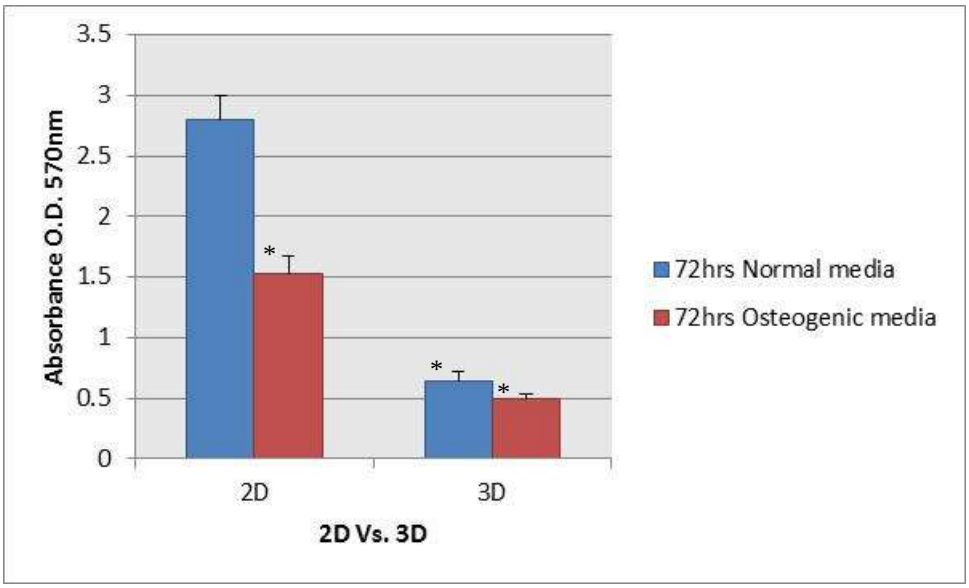

Figure 4.22 *Graph shows the viability of human MSCs at 72hr, the data represents the mean ± standard error of the mean n=9, a statistical significant was considered when P value ≤ 0.05 where (*) indicates significance compared to 2D normal media.*

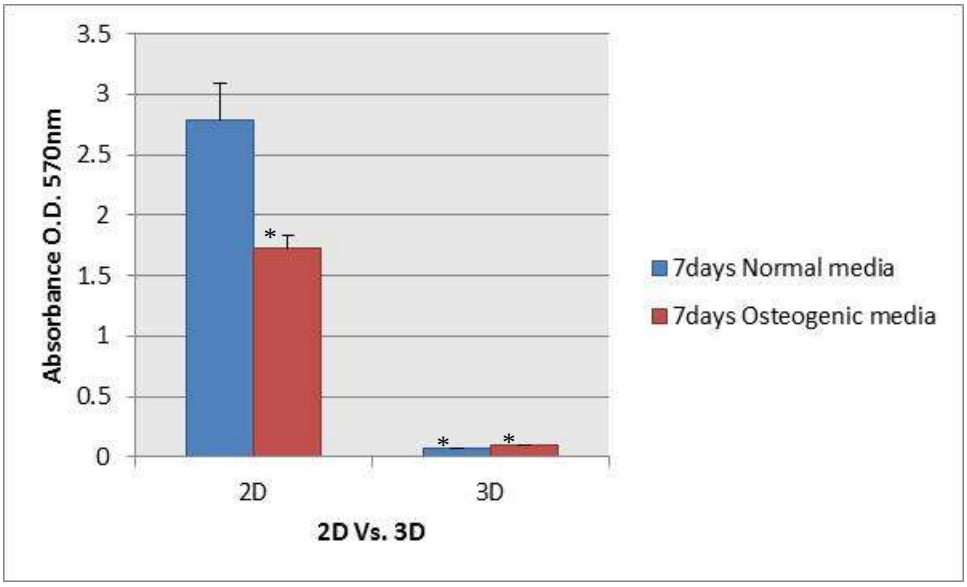

Figure 4.23 *Graph shows the viability of rat calvarial cells at 7days, the data represents the mean ± standard error of the mean n=9, a statistical significant was considered when P value ≤ 0.05 where (*) indicates significance compared to 2D normal media.*

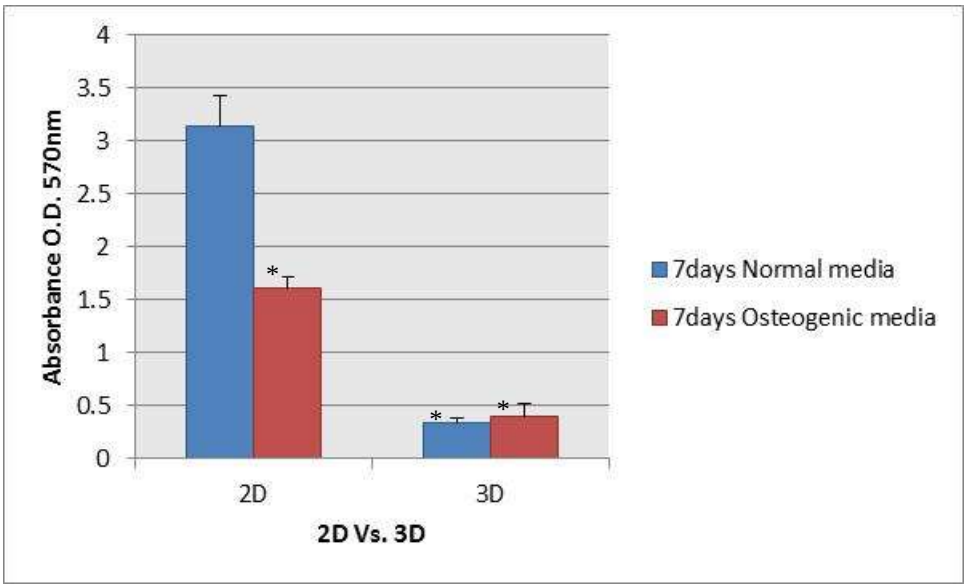

Figure 4.24 *Graph shows the viability of human MSCs at 7days, the data represents the mean ± standard error of the mean n=9, a statistical significant was considered when P value ≤ 0.05 where (*) indicates significance compared to 2D normal media.*

4.3.4 Alkaline phosphatase assay:

The alkaline phosphatase assay was performed to assess osteogenic differentiation of rat and human cells in both 2D and 3D culture.

Data showed that after 24hr there was no significant difference in the ALP activity in rat cells grown in 2D compared to those in 3D [Figure 4.25]. Though, the expression of the ALP enzyme differs significantly in human MSCs between both grown under normal and osteogenic conditions [Figure4.26]. At 72hr the enzyme expression increased in cells grown in 2D and under osteogenic conditions compared to those in normal media in rat cells but with no significant differences. While in MSCs the expression of the enzyme increased in osteogenic media in 2D, but remains almost the same in normal media [Figure 4.26]. In contrast, MSCs in a 3D culture enzyme activity was almost the same in osteogenic media with a slight decrease in normal media [Figure 4.26].

In comparison, at 7 days the ALP enzyme activity of calvarial cells interestingly increased slightly in normal media rather than osteogenic media [Figure 4.29]. However, in 2D MSCs the ALP level decreased in cells grown in normal media with a slight decrease in 3D, while it increased slightly in those grown in osteogenic media [Figure 4.30].

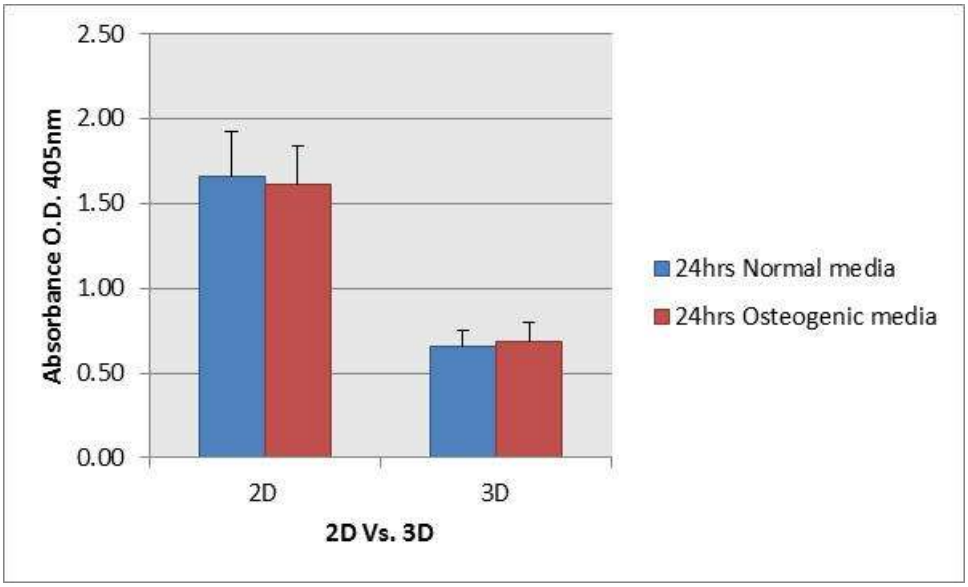

Figure 4.25 *Graph shows the alkaline phosphatase activity level of rat calvarial cells after 24hr, the Data represents the mean ± standard error of the mean n=9, a statistical significant was considered when P value ≤ 0.05, no significant were seen after 24 hr*

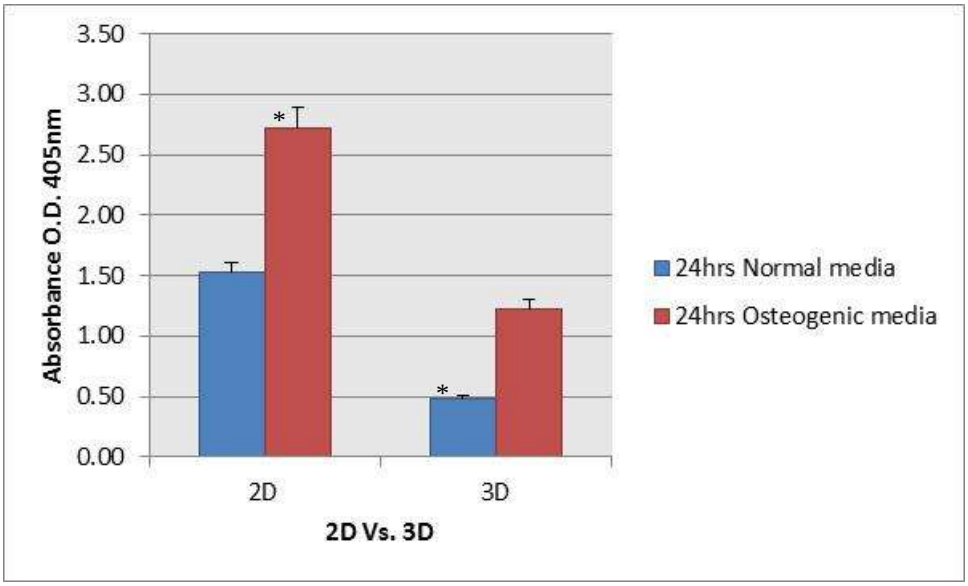

Figure 4.26 *Graph shows the alkaline phosphatase activity level of human MSCs after 24hr, the Data represents the mean ± standard error of the mean n=9, a statistical significant was considered when P value ≤ 0.05 where (*) indicates significance compared to 2D normal media*

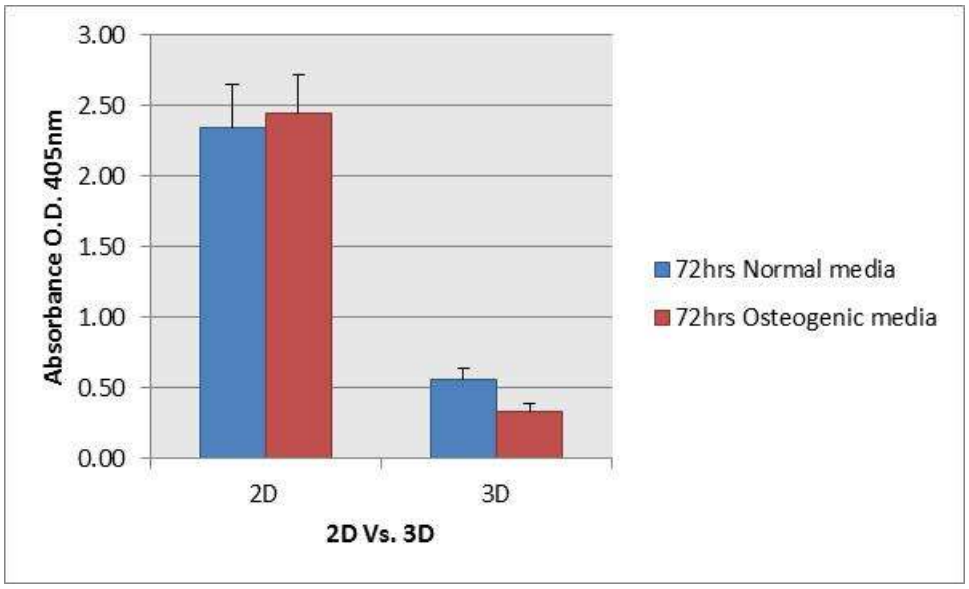

Figure 4.27 *Graph shows the alkaline phosphatase activity level of rat calvarial cells at 72hr, the Data represents the mean ± standard error of the mean n=9, a statistical significant was considered when P value ≤ 0.05, as 24hr no significant were seen here as well*

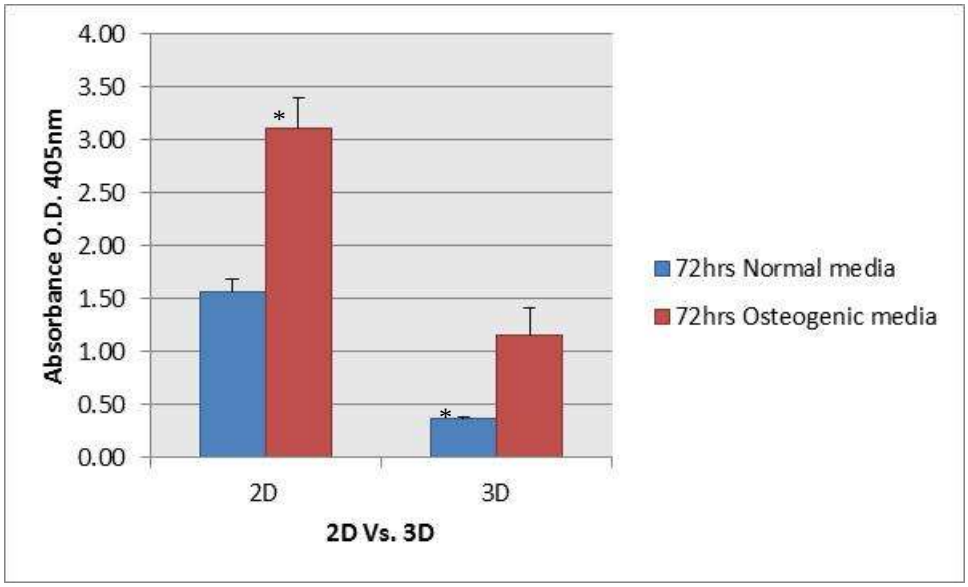

Figure 4.28 *Graph shows the alkaline phosphatase activity level of human MSCs at 72hr, the Data represents the mean ± standard error of the mean n=9, a statistical significant was considered when P value ≤ 0.05 05 where (*) indicates significance compared to 2D normal media*

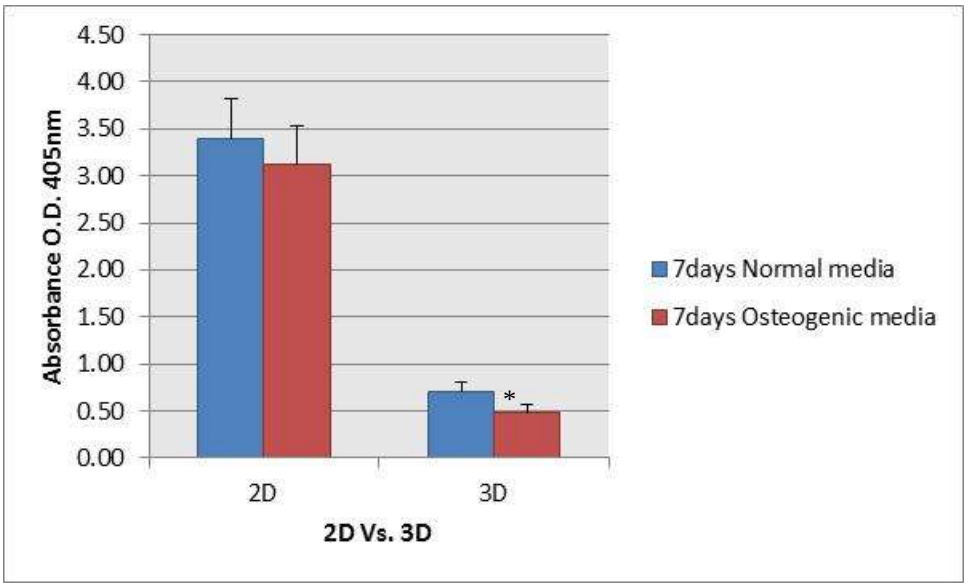

Figure 4.29 *Graph shows the alkaline phosphatase activity level of rat calvarial cells at 7days, the Data represents the mean ± standard error of the mean n=9, a statistical significant was considered when P value ≤ 0.05 where (*) indicates significance compared to 2D normal media*

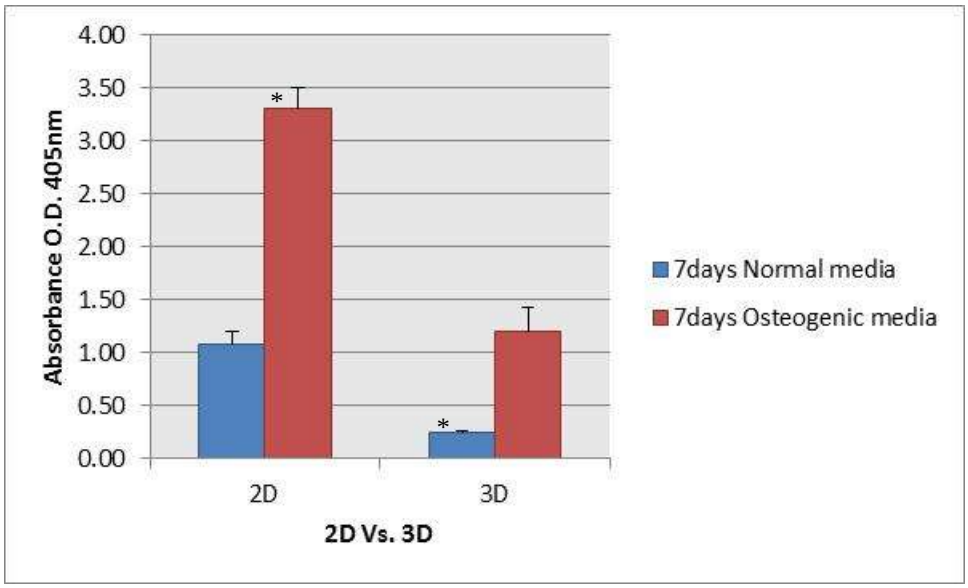

Figure 4.30 *Graph shows the alkaline phosphatase activity level of human MSCs at 7days, the Data represents the mean ± standard error of the mean n=9, a statistical significant was considered when P value ≤ 0.05 where (*) indicates significance compared to 2D normal media*

4.3.5 Changes in gene expression between 2D and 3D culture:

Quantitative real-time reverse transcription polymerase chain reaction (qRT-PCR) analysis was conducted to compare the relative expression of osteogenic genes in cells grown in 2D and 3D culture under different media conditions. The mRNA transcripts investigated in this study included ALP, Runx2, SP7, Cx43, EphrinB1, Ephrin B2, and Ephrin B4.

After 24hr calvarial cells grown on tissue culture plastic in normal media demonstrated a significantly higher expression of ALP compared to those grown in osteogenic media and 3D culture cells in normal and osteogenic media [Figure 4.31]. Similarly, MSCs in 2D culture osteogenic media showed a higher ALP expression compared to 2D normal and 3D normal and osteogenic media [Figure 4.32]. In addition, ALP expression showed no significant difference between 2D culture of cells grown in normal media and 3D cells grown in normal and osteogenic media [Figure 4.32].

However at 72hr ALP expression increased significantly in cells grown in osteogenic media as monolayers for both rat calvarial and human MSCs [Figure 4.33 and 4.34].

Interestingly, at 7days the ALP level decreased in calvarial cells grown in osteogenic media while it increased in cells grown in normal media [Figure 4.35]. In comparison, ALP increased significantly in MSCs grown in osteogenic media as monolayers compared to cells in 2D normal media and 3D normal and osteogenic media [Figure 4.36].

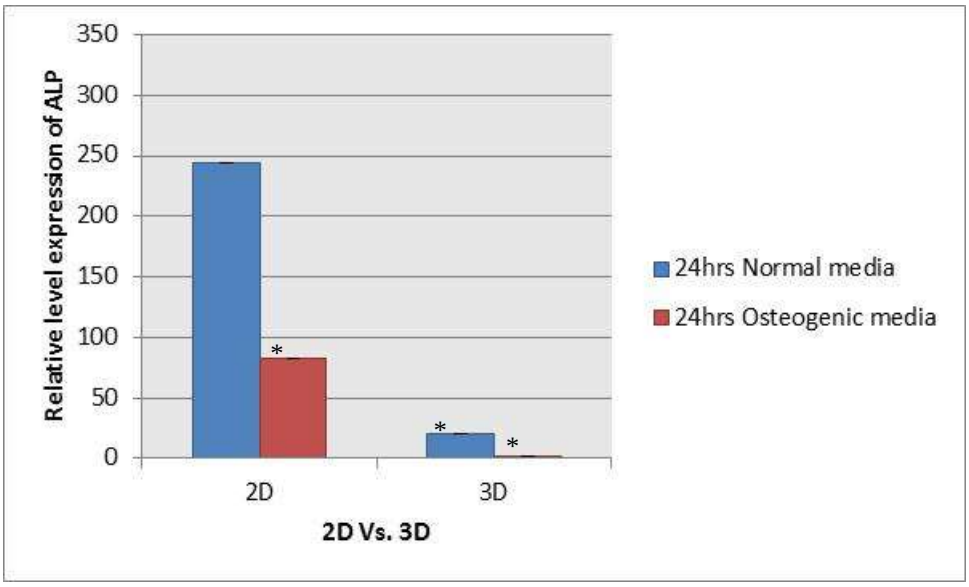

Figure 4.31 *ALP relative level expression in rat calvarial cells after 24hr, the data represents the mean ± standard error of the mean n=9, a statistical significant was considered when P value ≤ 0.05 where (*) indicates significance compared to 2D normal media*

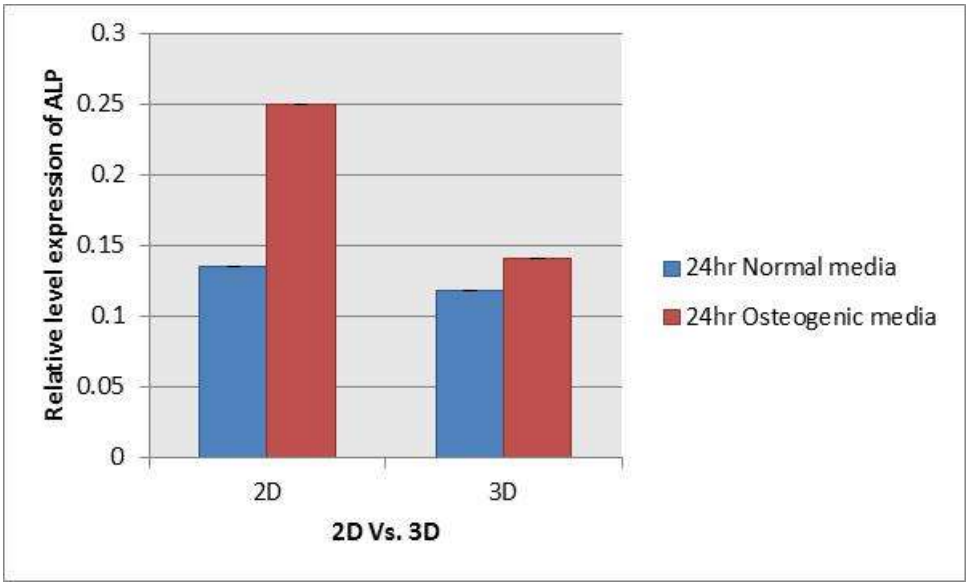

Figure 4.32 *ALP relative level expression in MSCs after 24hr, the data represents the mean ± standard error of the mean n=9, a statistical significant was considered when P value ≤ 0.05, as shown in the graph no significance were seen.*

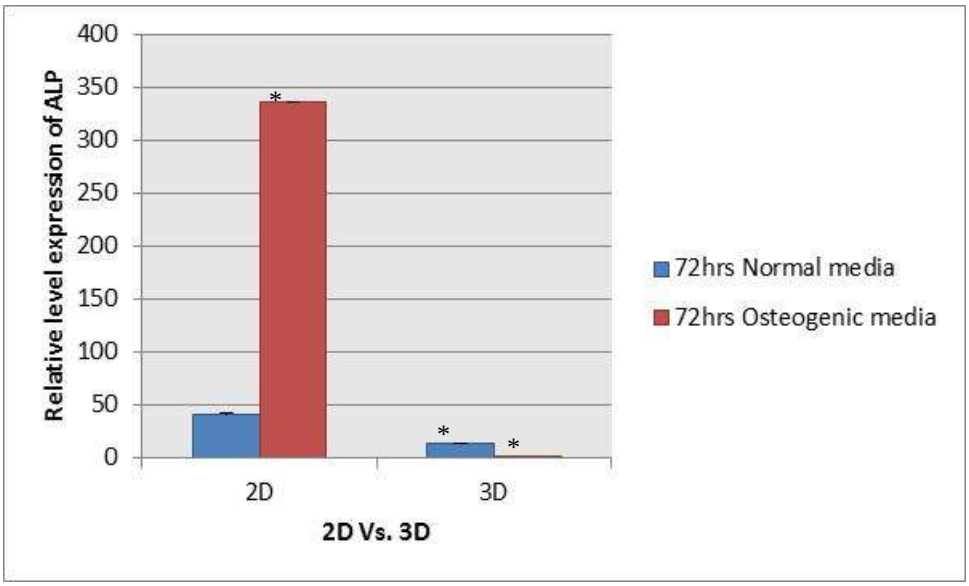

Figure 4.33 *ALP relative level expression in rat calvarial cells at 72hr, the data represents the mean ± standard error of the mean n=9, a statistical significant was considered when P value ≤ 0.05 where (*) indicates significance compared to 2D normal media*

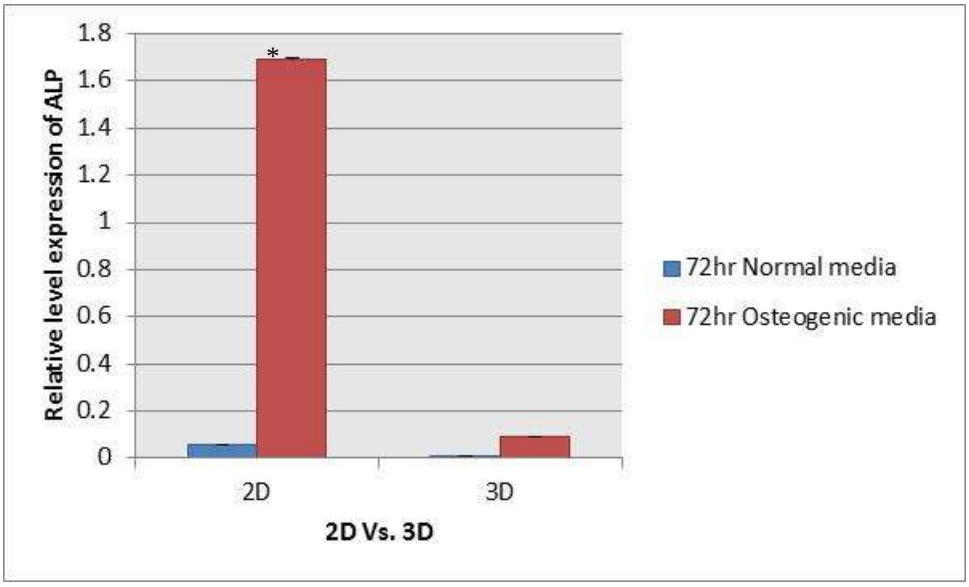

Figure 4.34 *ALP relative level MSCs at 72hr, the data represents the mean ± standard error of the mean n=9, a statistical significant was considered when P value ≤ 0.05 where (*) indicates significance compared to 2D normal media*

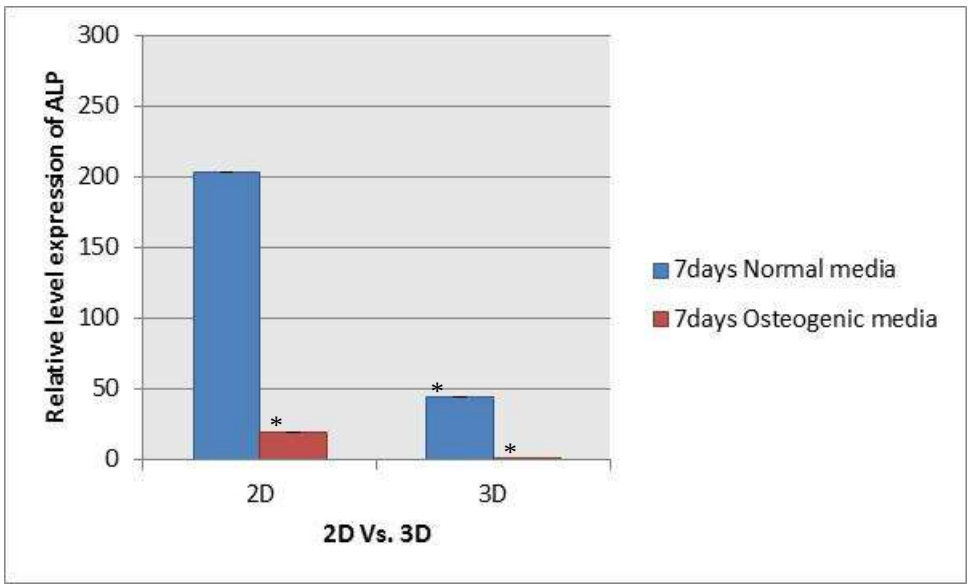

Figure 4.35 *ALP relative level Rat cells at 7days, the Data represents the mean ± standard error of the mean n=9, a statistical significant was considered when P value ≤ 0.05 where (*) indicates significance compared to 2D normal media*

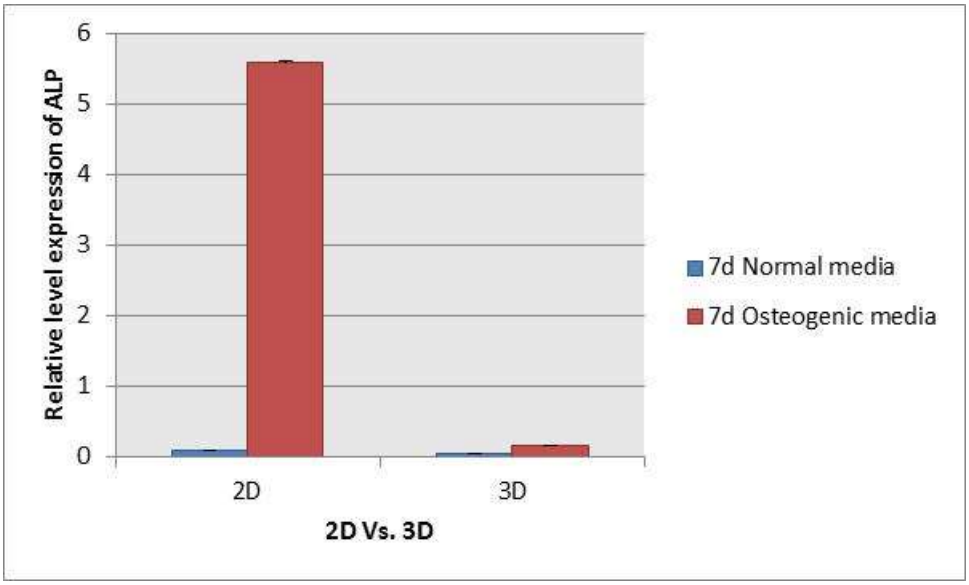

Figure 4.36 *ALP relative level MSCs cells at 7days, the Data represents the mean ± standard error of the mean n=9, a statistical significant was considered when P value ≤ 0.05 where (*) indicates significance compared to 2D normal media*

After 24hrs rat cells grown in 2D normal media showed a significantly higher Runx2 expression compared to cells grown in osteogenic media. In contrast, those grown in 3D culture showed a significantly higher expression when grown in osteogenic media [Figure 4.37]. MSCs grown on tissue culture plastic in osteogenic media showed a higher Runx2 expression with significant difference compared to 2D normal media and 3D normal and osteogenic media [Figure 4.38]

At 72hrs Runx2 expression was significantly increased in both cell types for those grown in osteogenic media as a monolayer compared to 2D normal media and 3D normal and osteogenic media [Figure 4.39] and [Figure 4.40].

At 7days Runx2 expression in rat cells decreased in both cells grown in normal and osteogenic media, while the expression increased significantly in cells grown in 3D normal media compared to osteogenic media [Figure 4.41]. MSCs Runx2 expression remained almost the same in 2D and 3D osteogenic and normal media respectively, though it decreased in 2D and 3D normal and osteogenic media respectively [Figure 4.42].

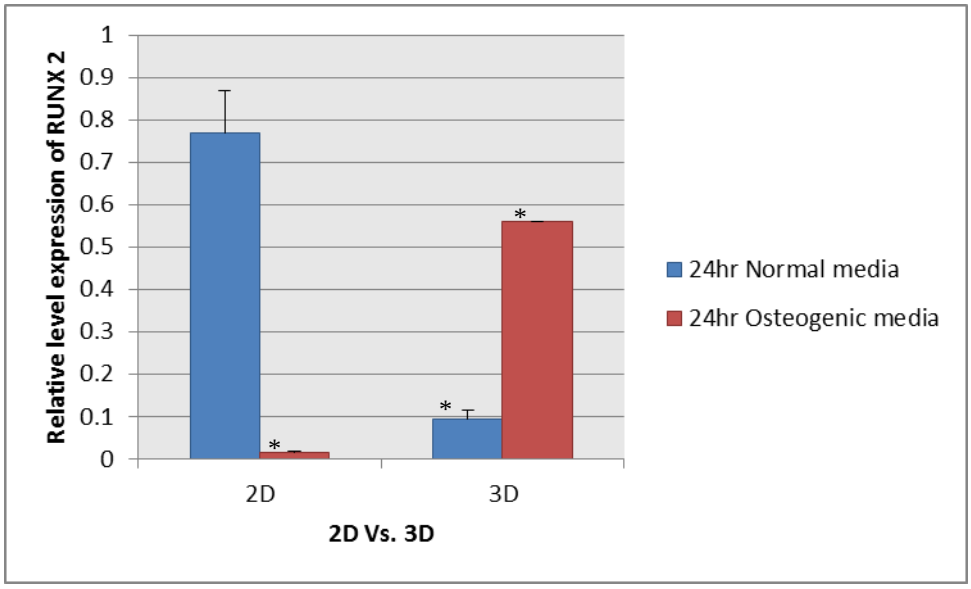

Figure 4.37 *RUNX 2 relative level expression in rat cells after 24hr, the data represents the mean ± standard error of the mean n=9, a statistical significant was considered when P value ≤ 0.05 where (*) indicates significance compared to 2D normal media*

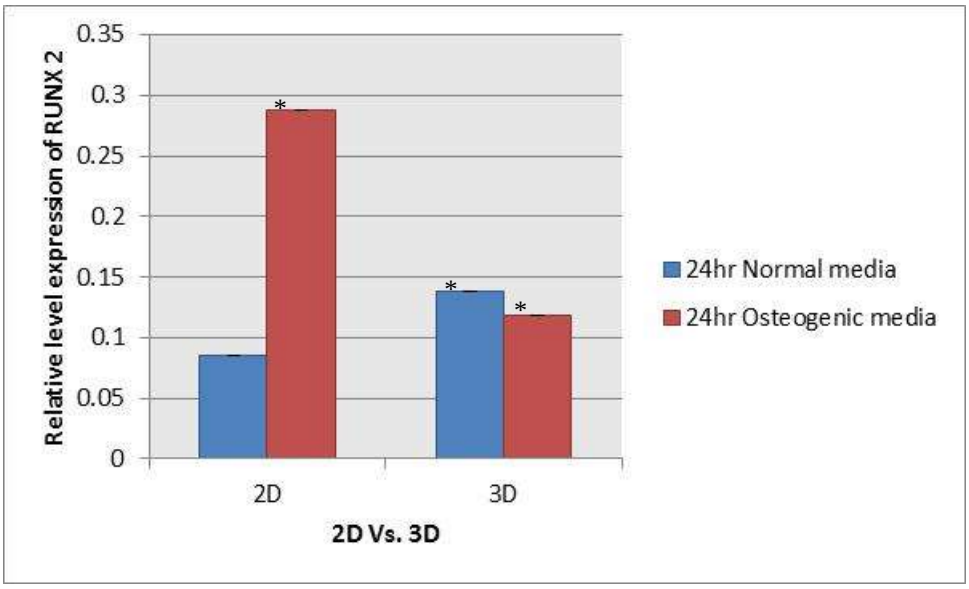

Figure 4.38 *RUNX 2 relative level expression in MSCs after 24hr, the data represents the mean ± standard error of the mean n=9, a statistical significant was considered when P value ≤ 0.05 where (*) indicates significance compared to 2D normal media*

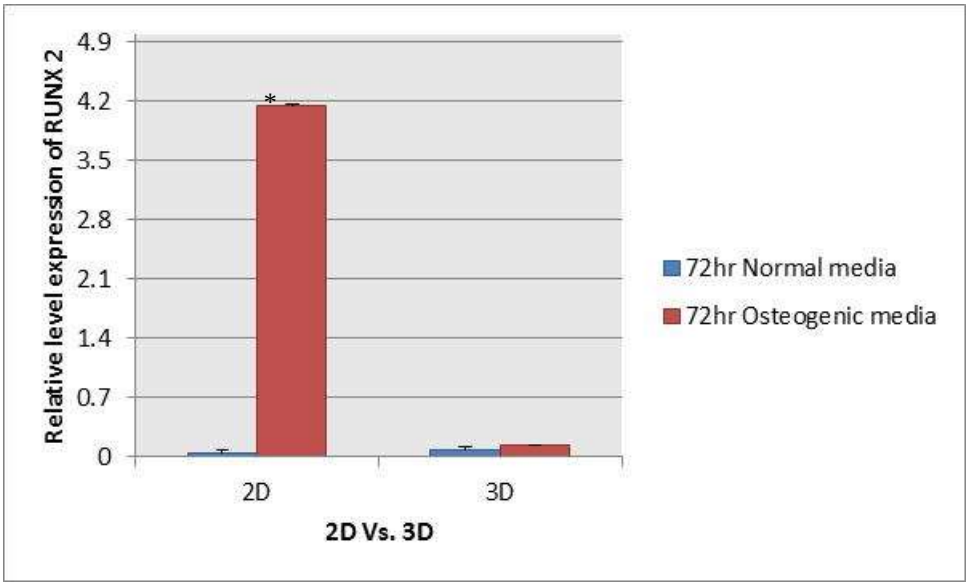

Figure 4.39 *RUNX 2 relative level expression in rat cells at 72hr, the data represents the mean ± standard error of the mean n=9, a statistical significant was considered when P value ≤ 0.05 where (*) indicates significance compared to 2D normal media*

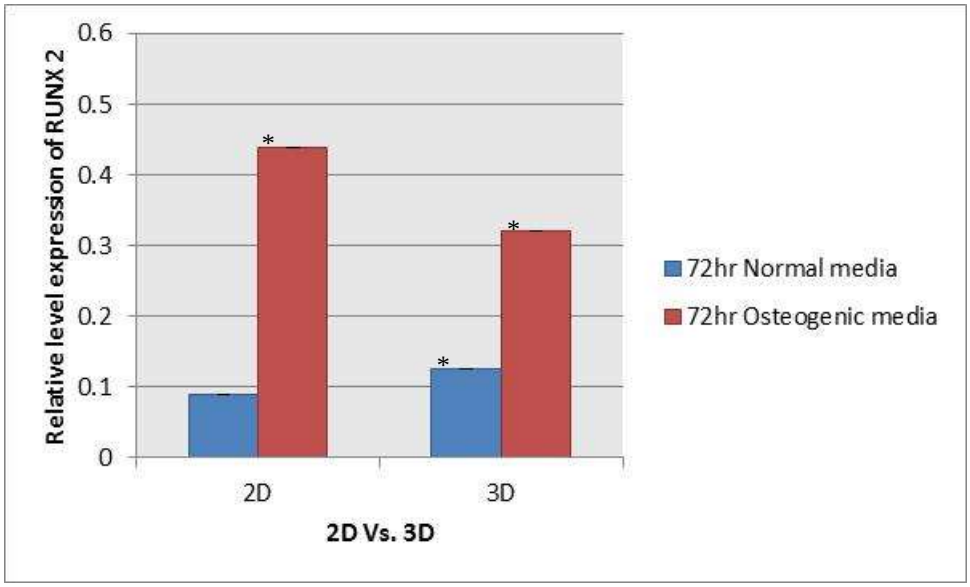

Figure 4.40 *RUNX 2 relative level expression in MSCs at 72hr, the data represents the mean ± standard error of the mean n=9, a statistical significant was considered when P value ≤ 0.05 where (*) indicates significance compared to 2D normal media*

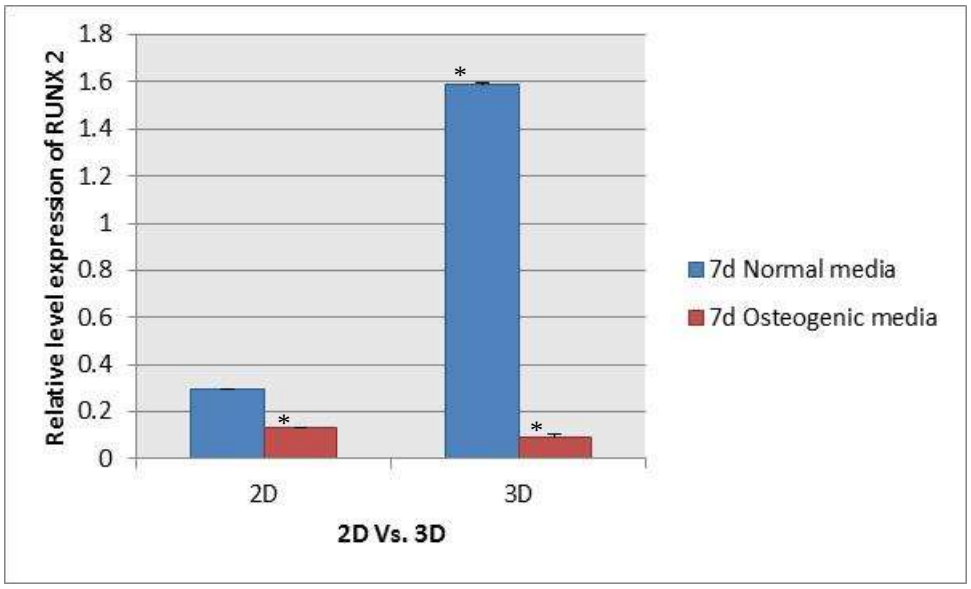

Figure 4.41 *RUNX 2 relative level expression in rat cells at 7days, the data represents the mean ± standard error of the mean n=9, a statistical significant was considered when P value ≤ 0.05 where (*) indicates significance compared to 2D normal media*

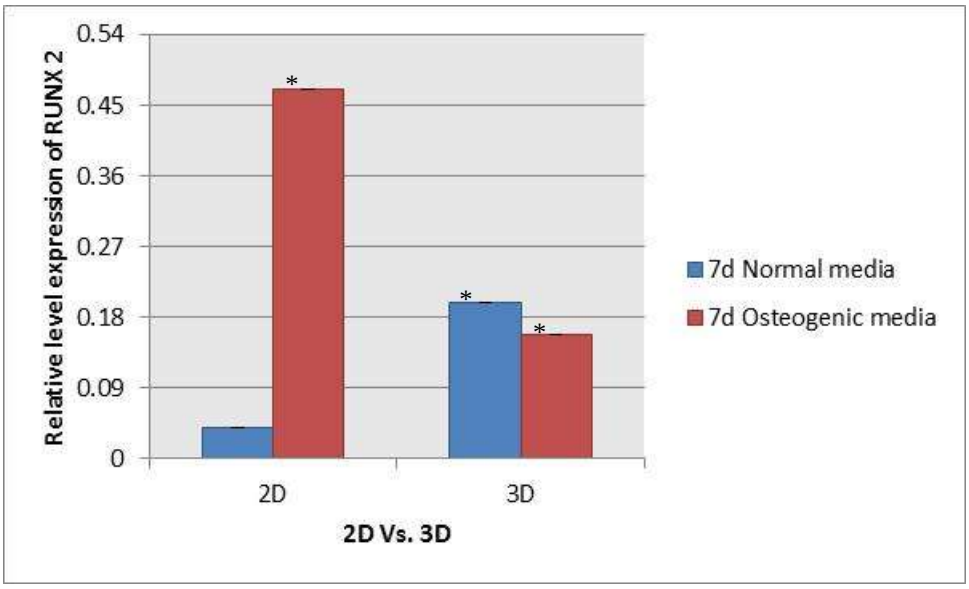

Figure 4.42 *RUNX 2 relative level expression in MSCs at 7days, the data represents the mean ± standard error of the mean n=9, a statistical significant was considered when P value ≤ 0.05 where (*) indicates significance compared to 2D normal media*

Osterix or SP7 gene expression was high after 24hr in 2D and 3D calvarial cells grown in normal media compared to those under osteogenic conditions [Figure 4.43]. Osterix expression decreased significantly at 72 hrs in 2D normal media with a significant increase in 2D osteogenic media. There was a slight increase in cells grown in 3D under normal and osteogenic media [Figure 4.45]. At 7days the SP7 gene expression continues to decrease in both cells grown in 2D and 3D and in both media conditions compared to 24hr and 72hr [Figure 4.47].

On the other hand human MSCs SP7 gene expression levels were very low compared to calvarial cells. After 24hr of cells seeding the expression level of the gene was significantly higher in monolayer cells grown in osteogenic media compared to 2D normal and 3D normal and osteogenic media [Figure 4.44]. Nonetheless, SP7 expression increased significantly in all cells grown in 2D and 3D culture and under both normal and osteogenic media at 72hr. Surprisingly at 7 days the level of the gene in cells grown in 3D under osteogenic media increased significantly with a slight increase in 2D normal and osteogenic media and in 3D normal media [Figure 4.48].

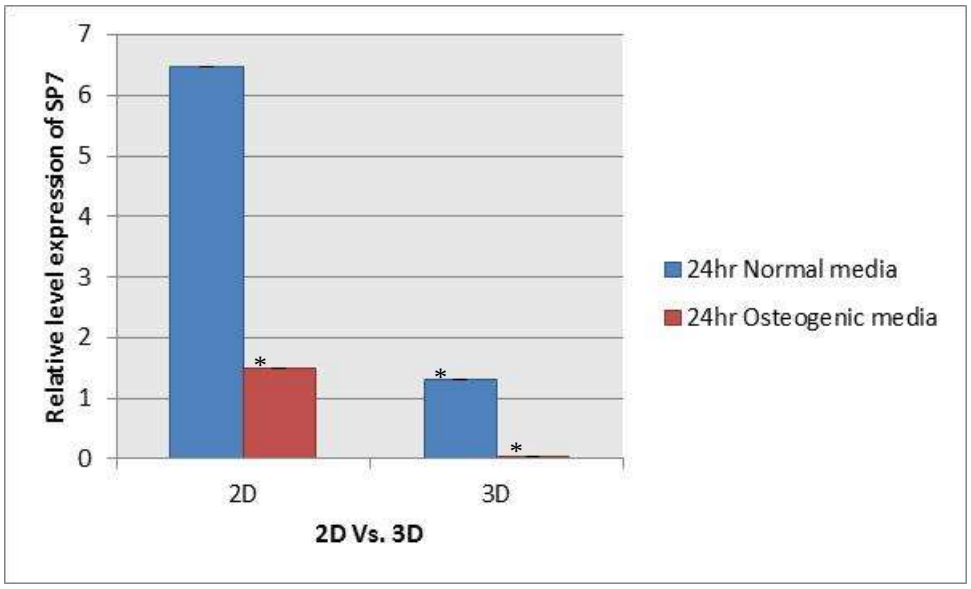

Figure 4.43 *SP7 relative level expression in rat cells after 24hr, the data represents the mean ± standard error of the mean n=9, a statistical significant was considered when P value ≤ 0.05 where (*) indicates significance compared to 2D normal media*

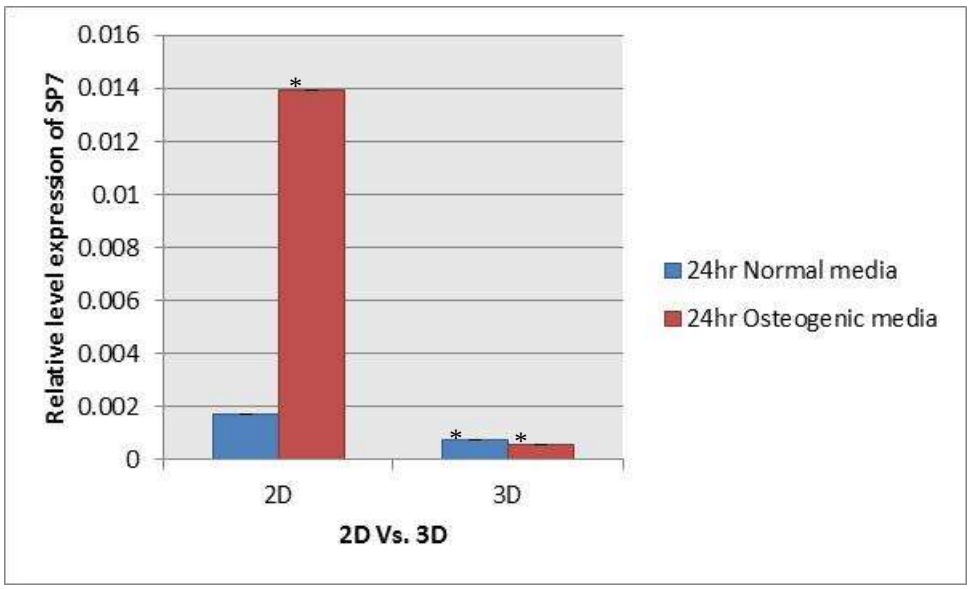

Figure 4.44 *SP7 relative level expression in MSCs after 24hr, the data represents the mean ± standard error of the mean n=9, a statistical significant was considered when P value ≤ 0.05 where (*) indicates significance compared to 2D normal media*

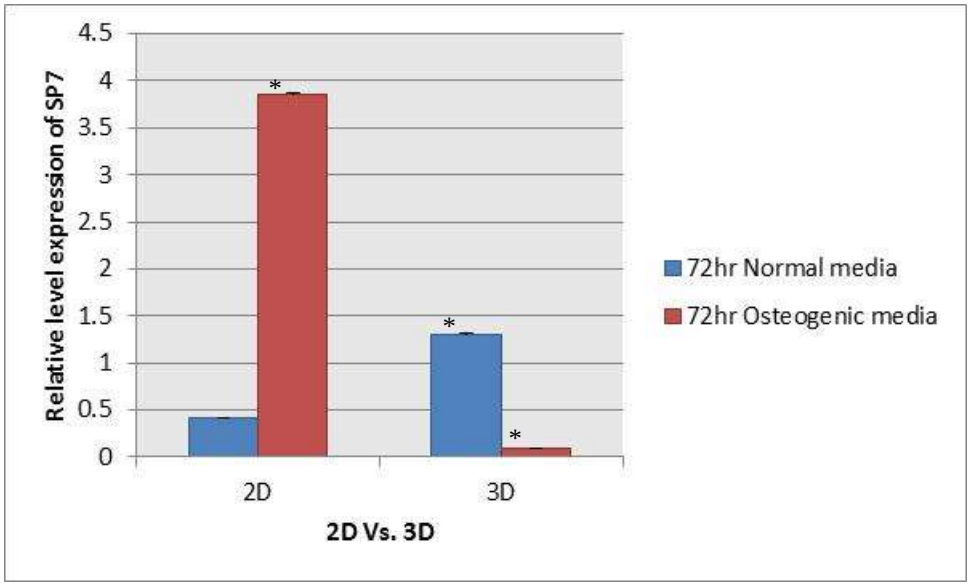

Figure 4.45 *SP7 relative level expression in rat cells at 72hr, the data represents the mean ± standard error of the mean n=9, a statistical significant was considered when P value ≤ 0.05 where (*) indicates significance compared to 2D normal media*

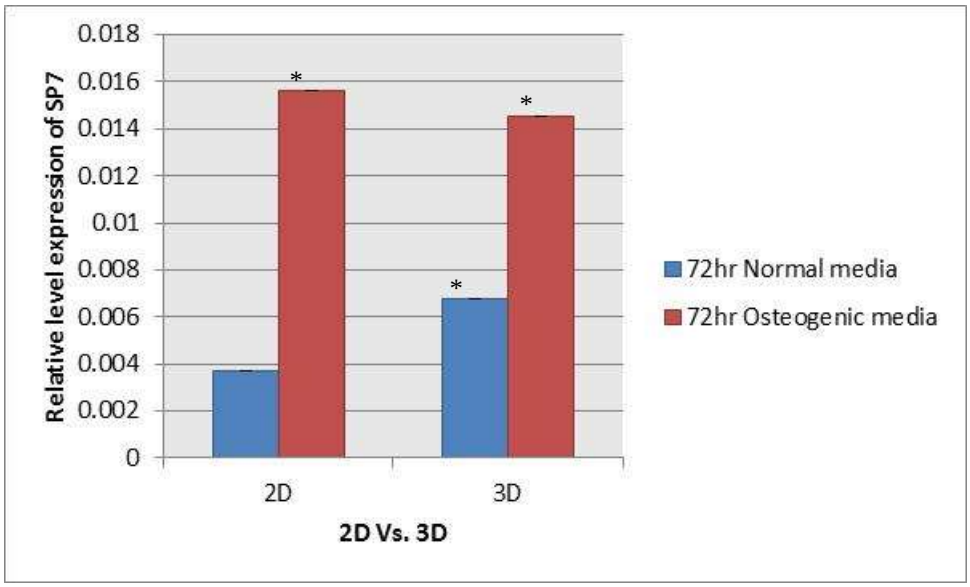

Figure 4.46 *SP7 relative level expression in MSCs at 72hr, the data represents the mean ± standard error of the mean n=9, a statistical significant was considered when P value ≤ 0.05 where (*) indicates significance compared to 2D normal media*

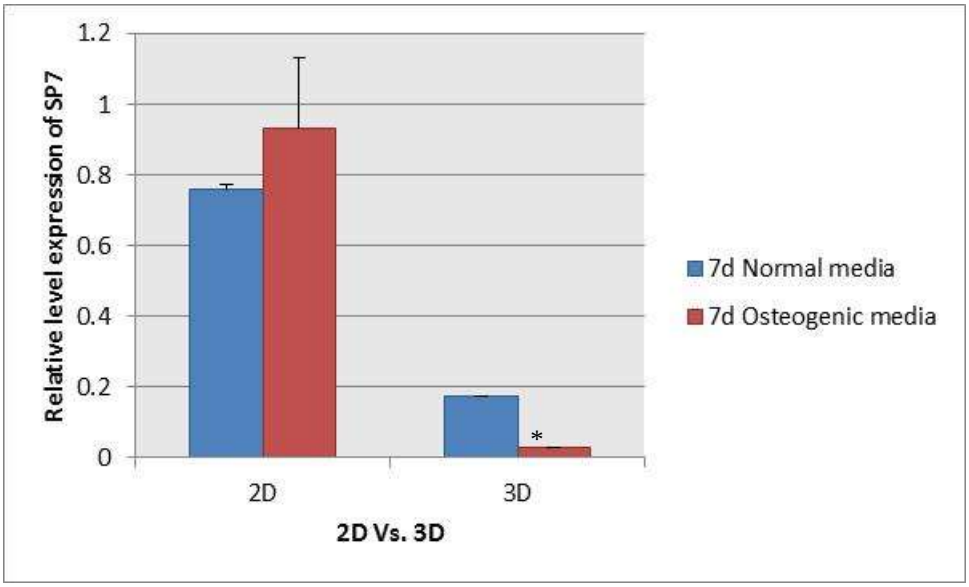

Figure 4.47 *SP7 relative level expression in Rat cells at 7days, the data represents the mean ± standard error of the mean n=9, a statistical significant was considered when P value ≤ 0.05 where (*) indicates significance compared to 2D normal media*

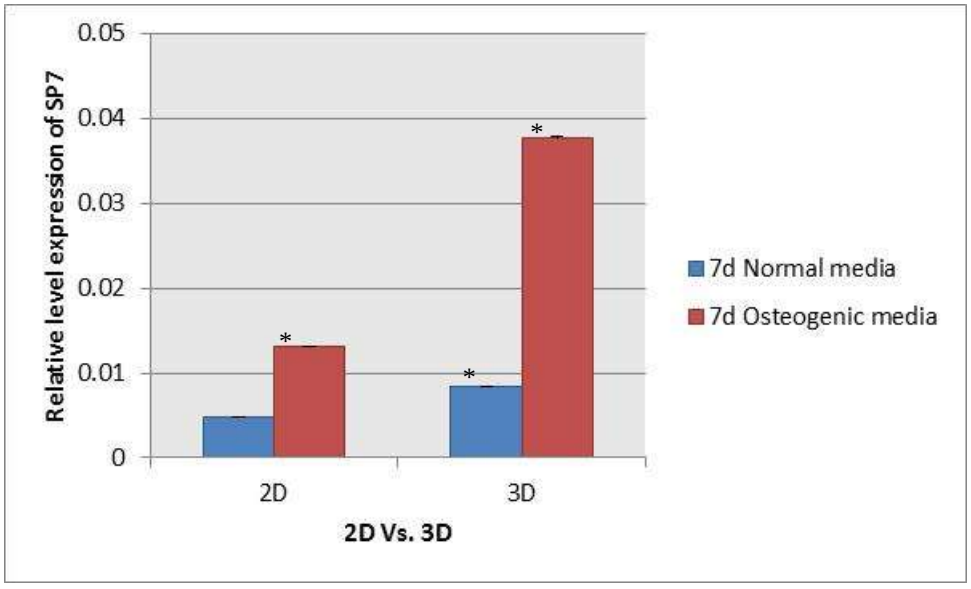

Figure 4.48 *SP7 relative level expression in MSCs at 7days, the data represents the mean ± standard error of the mean n=9, a statistical significant was considered when P value ≤ 0.05 where (*) indicates significance compared to 2D normal media*

After 24hrs a significantly higher level of Cx43 gene expression was detected in calvarial cells grown in normal media as monolayers [Figure 4.49]. Whereas no significant different was detected in Cx43 expression in MSCs grown under normal and osteogenic media in both 2D and 3D culture [Figure 4.50].

Conversely at 72hr, Cx43 expression raised in monolayers grown in osteogenic media and decreased in normal media [Figure 4.51]. Nevertheless, Cx43 levels decreased in cells grown in normal and osteogenic media in 3D culture [Figure 4.51]. In contrast, MSCs showed a significant increase in Cx43 expression in cells grown under osteogenic conditions in both 2D and 3D culture [Figure 4.52]. Also, a significant increase in the Cx43 transcript abundance was observed in 3D culture grown in normal media compared to 2D [figure 4.52].

Interestingly, Cx43 expression at 7 days increased again in 2D cultured cells in normal media and decreased in cells grown in osteogenic media [Figure 4.53]. This was accompanied by an approximately similar level of gene expression in 3D culture [Figure 4.53]. Cx43 expression continued to rise in MSC monolayers grown in osteogenic media and strikingly rise in 3D cells grown in normal media where the gene expression approximately at the same level as 2D osteogenic media [figure 4.54]. Though, a significant decrease in Cx43 level in 3D cells grown in osteogenic media was observed with a slight decrease in 2D cells grown in normal media [Figure 4.54].

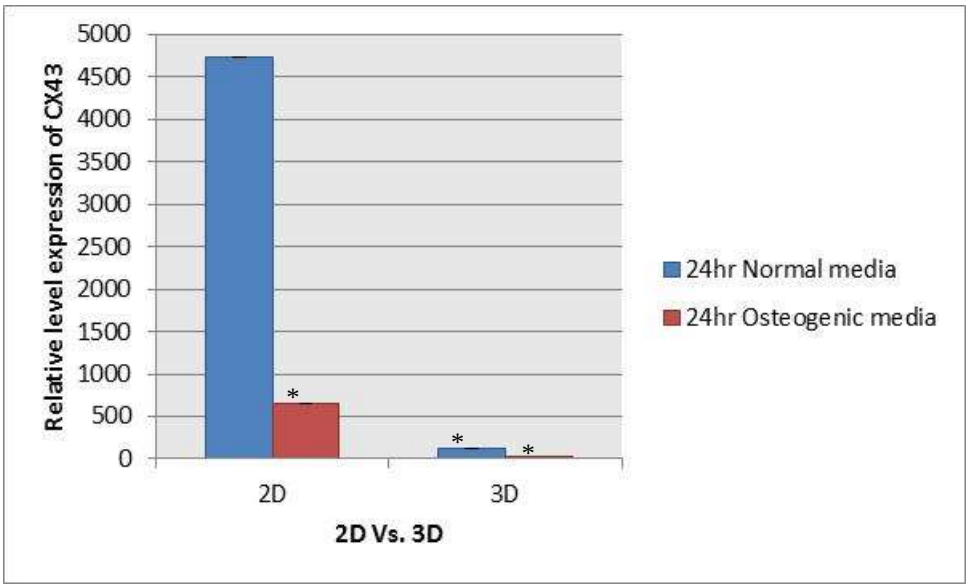

Figure 4.49 *CX43 relative level expression in rat cells after 24hr, the data represents the mean ± standard error of the mean n=9, a statistical significant was considered when P value ≤ 0.05 where (*) indicates significance compared to 2D normal media*

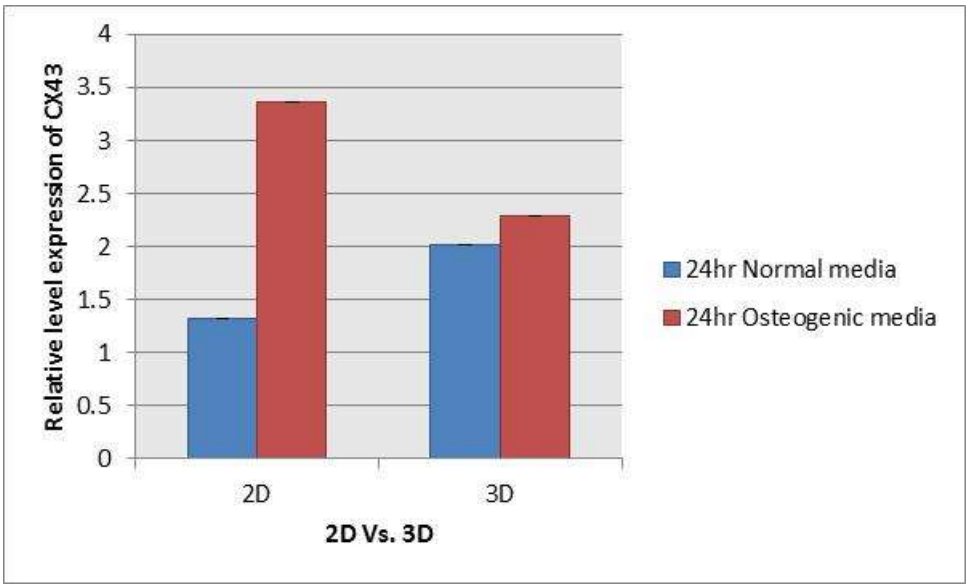

Figure 4.50 *CX43 relative level expression in MSCs after 24hr, the data represents the mean ± standard error of the mean n=9, a statistical significant was considered when P value ≤ 0.05. No significant were seen here.*

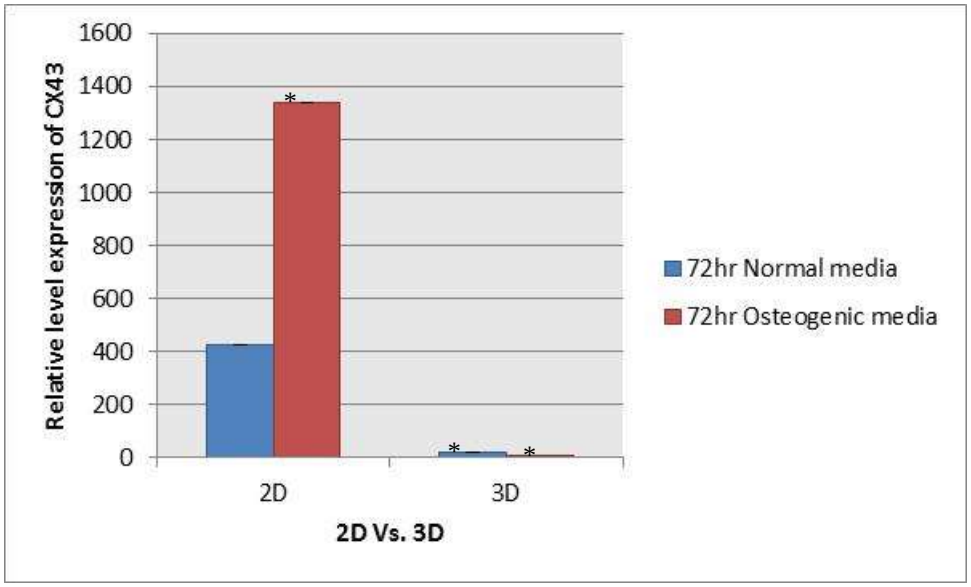

Figure 4.51 *CX43 relative level expression in rat cells at 72hr, the data represents the mean ± standard error of the mean n=9, a statistical significant was considered when P value ≤ 0.05 where (*) indicates significance compared to 2D normal media*

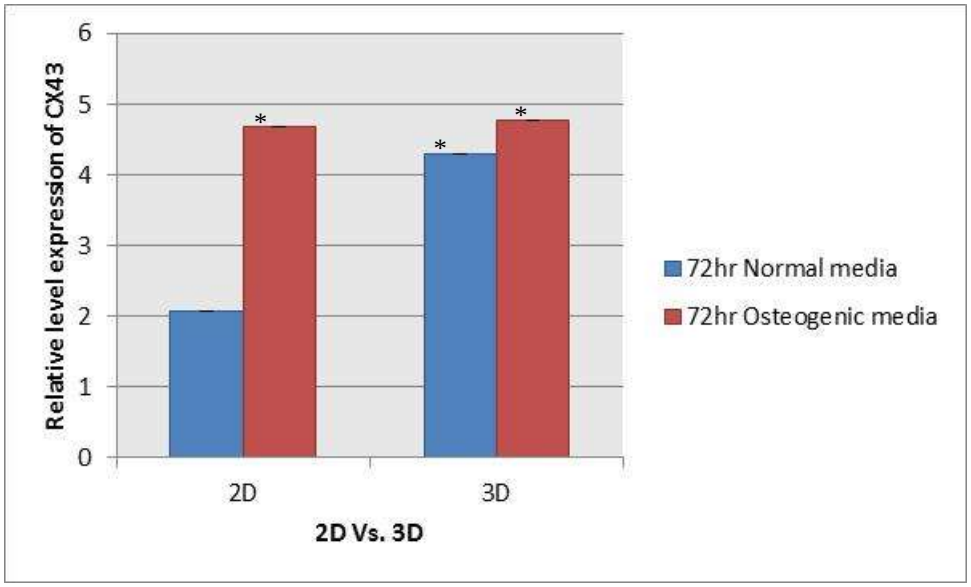

Figure 4.52 *CX43 relative level expression in MSCs at 72hr, the data represents the mean ± standard error of the mean n=9, a statistical significant was considered when P value ≤ 0.05 where (*) indicates significance compared to 2D normal media*

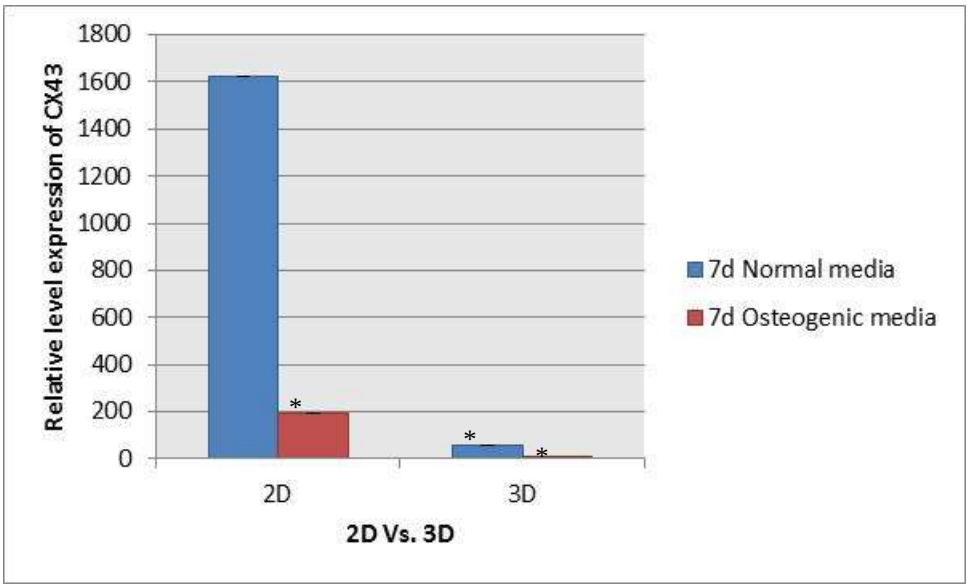

Figure 4.53 *CX43 relative level expression in rat calvarial cells at 7days, the data represents the mean ± standard error of the mean n=9, a statistical significant was considered when P value ≤ 0.05 where (*) indicates significance compared to 2D normal media*

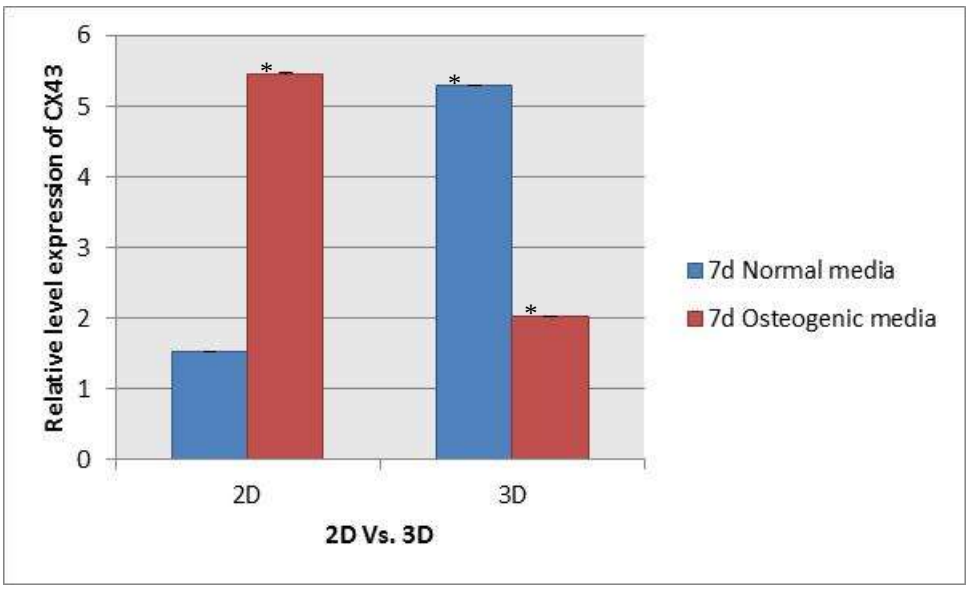

Figure 4.54 *CX43 relative level expression in MSCs at 7days, the data represents the mean ± standard error of the mean n=9, a statistical significant was considered when P value ≤ 0.05 where (*) indicates significance compared to 2D normal media*

After 24hrs ephrin B1 expression was significantly higher in 2D rat cells grown in normal media compared to 2D grown in osteogenic media and 3D culture [Figure 4.55]. Whereas the level of the transcript abundance in MSCs was significantly higher in 2D and 3D cells under osteogenic and normal conditions respectively [Figure 4.56].

At 72hrs, a significant increase in ephrin B1 expression in 2D rat cells under osteogenic conditions was observed with a significant decrease in those grown under normal conditions [Figure 4.57]. There was a decrease in ephrin B1 expression in 3D cells grown in normal media [Figure 4.57]. After 72 hrs the gene expression in MSCs increased significantly in 2D and 3D cells grown in normal and osteogenic media compared to cells grown after 24hr. There was a significant increase in the gene expression in 2D cells grown in osteogenic media compared to normal media [Figure 4.58]. There was a high level of the gene detected in 3D culture with a similar level in both grown in normal and osteogenic media [Figure 4.58].

At day 7 the transcript abundance decreased significantly in cells grown in 2D and 3D in normal and osteogenic media compared to 24hr and 72hr [Figure 4.59]. Whereas, MSCs 2D gene level grown in osteogenic media continued significantly to rise [Figure 4.60].

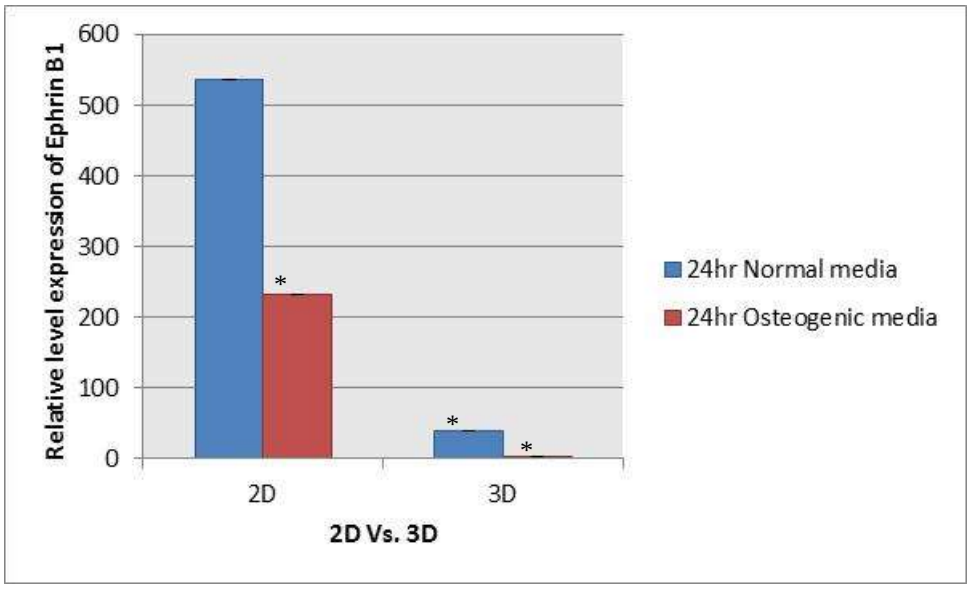

Figure 4.55 *Ephrin B1 relative level expression in rat calvarial cells after 24hr, the data represents the mean ± standard error of the mean n=9, a statistical significant was considered when P value ≤ 0.05 where (*) indicates significance compared to 2D normal media*

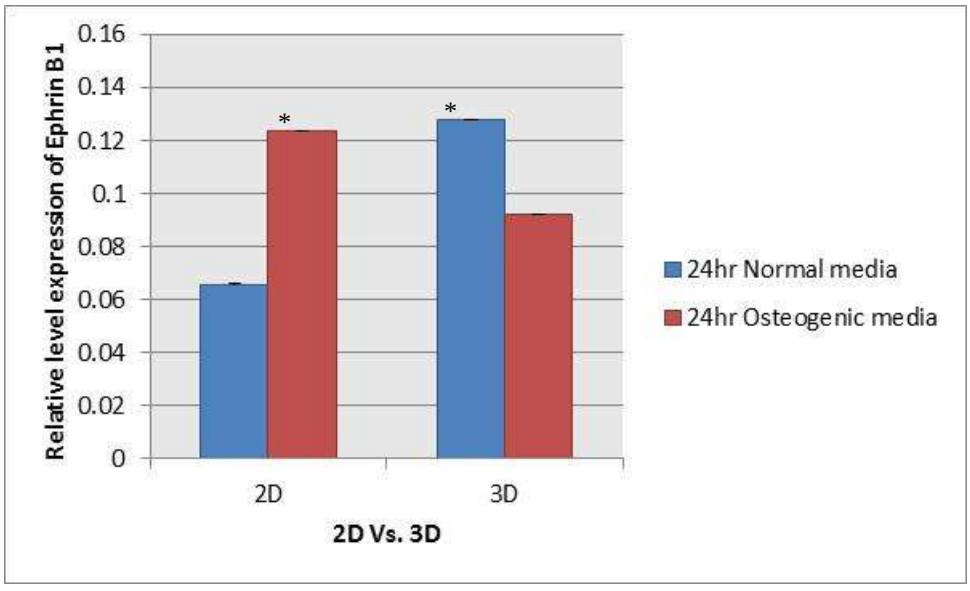

Figure 4.56 *Ephrin B1 relative level expression in MSCs after 24hr, the data represents the mean ± standard error of the mean n=9, a statistical significant was considered when P value ≤ 0.05 where (*) indicates significance compared to 2D normal media*

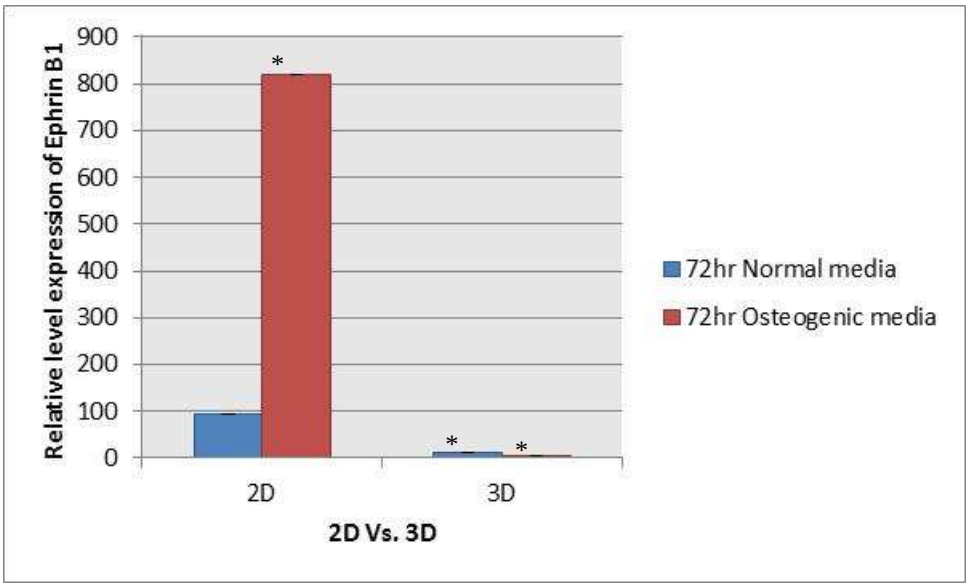

Figure 4.57 *Ephrin B1 relative level expression in rat cells at 72hr, the data represents the mean ± standard error of the mean n=9, a statistical significant was considered when P value ≤ 0.05 where (*) indicates significance compared to 2D normal media*

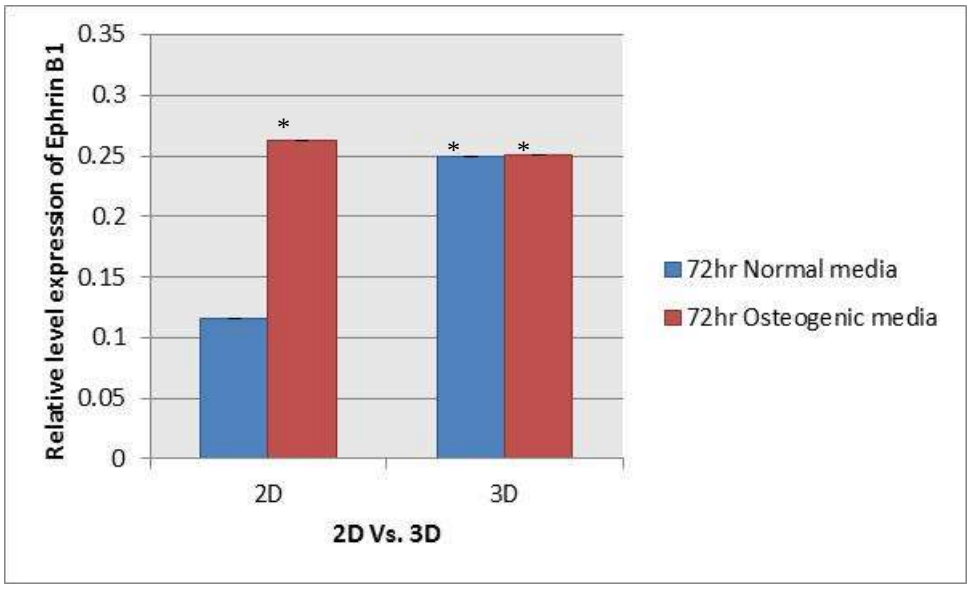

Figure 4.58 *Ephrin B1 relative level expression in MSCs at 72hr, the data represents the mean ± standard error of the mean n=9, a statistical significant was considered when P value ≤ 0.05 where (*) indicates significance compared to 2D normal media*

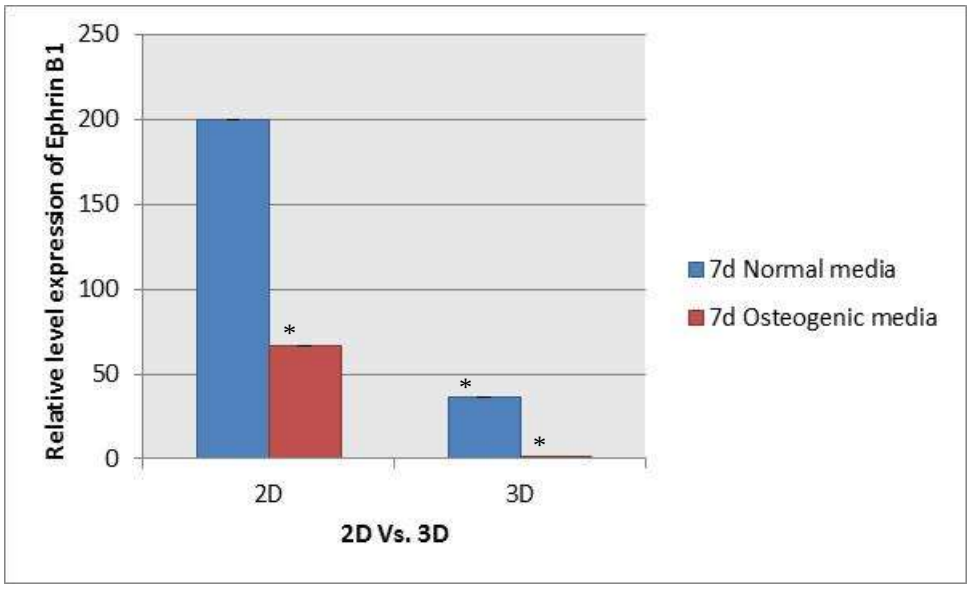

Figure 4.59 *Ephrin B1 relative level expression in rat cells at 7days, the data represents the mean ± standard error of the mean n=9, a statistical significant was considered when P value ≤ 0.05 where (*) indicates significance compared to 2D normal media*

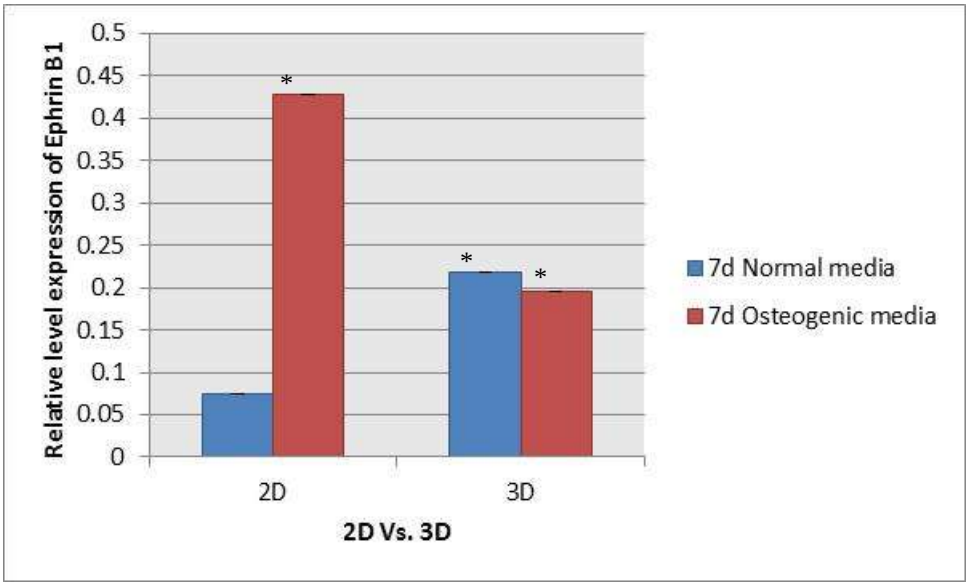

Figure 4.60 *Ephrin B1 relative level expression in MSCs at 7days, the data represents the mean ± standard error of the mean n=9, a statistical significant was considered when P value ≤ 0.05 where (*) indicates significance compared to 2D normal media*

After 24hrs a significantly high level of ephrin B2 gene expression was observed in 2D cells grown in normal media in comparison with those grown in osteogenic media and 3D cells grown in both normal and osteogenic media [Figure 4.61]. While in MSCs both 2D and 3D cells grown in normal media showed an approximately similar level of gene expression [Figure 4.62]. In addition, approximately equivalent expression was detected in 2D and 3D cells grown in osteogenic media [figure 4.62].

A significant decrease in gene level was detected in 2D rat cells grown in normal media; conversely, a significant increase was identified cells grown in 2D in osteogenic media for 72hr [Figure4.63]. While MSCs showed a significantly higher expression in 2D under both media conditions [Figure 4.64] there was a decrease in 3D culture under both media conditions [Figure 4.64].

At 7 days, a significantly lower level of ephrinB2 transcripts was observed in 2D rat cells with increase in cells grown in normal media and approximately similar expression in 3D cells grown at 24 and 72hrs [Figure 4.65]. Under osteogenic conditions, the gene expression levels continued to increase significantly in 2D and 3D conditions in MSCs [Figure 4.66].

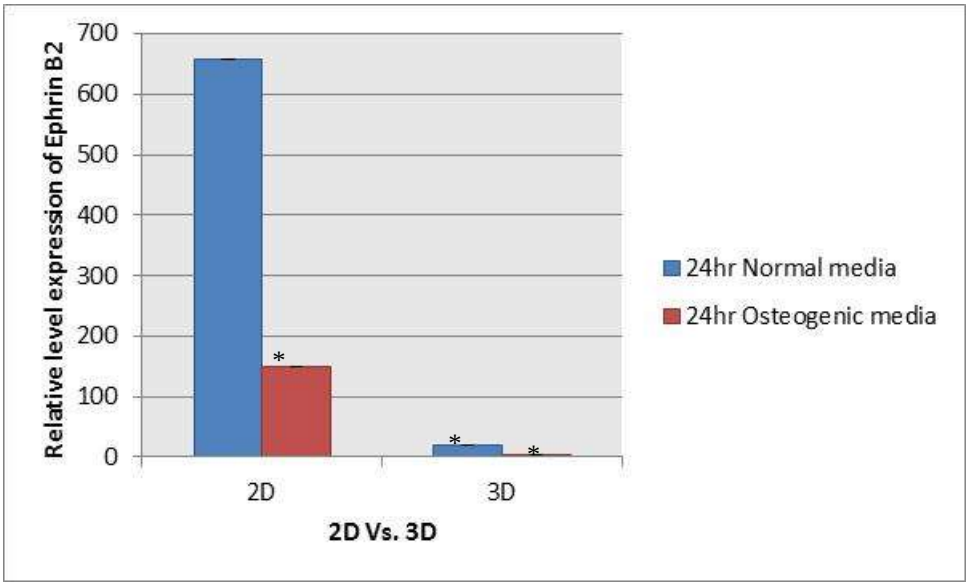

Figure 4.61 *Ephrin B2 relative level expression in rat cells after 24hr, the Data represents the mean ± standard error of the mean n=9, a statistical significant was considered when P value ≤ 0.05 where (*) indicates significance compared to 2D normal media*

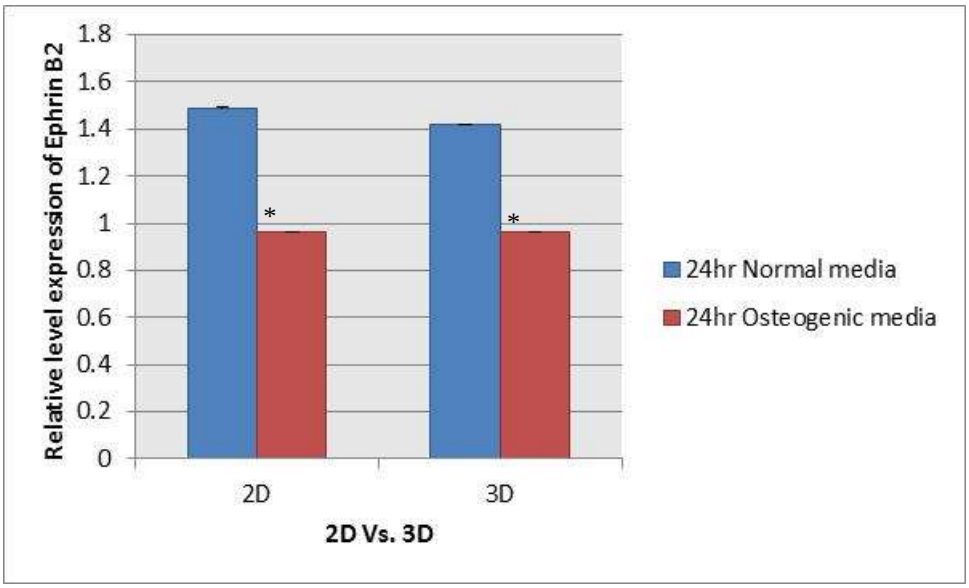

Figure 4.62 *Ephrin B2 relative level expression in MSCs after 24hr, the Data represents the mean ± standard error of the mean n=9, a statistical significant was considered when P value ≤ 0.05 where (*) indicates significance compared to 2D normal media*

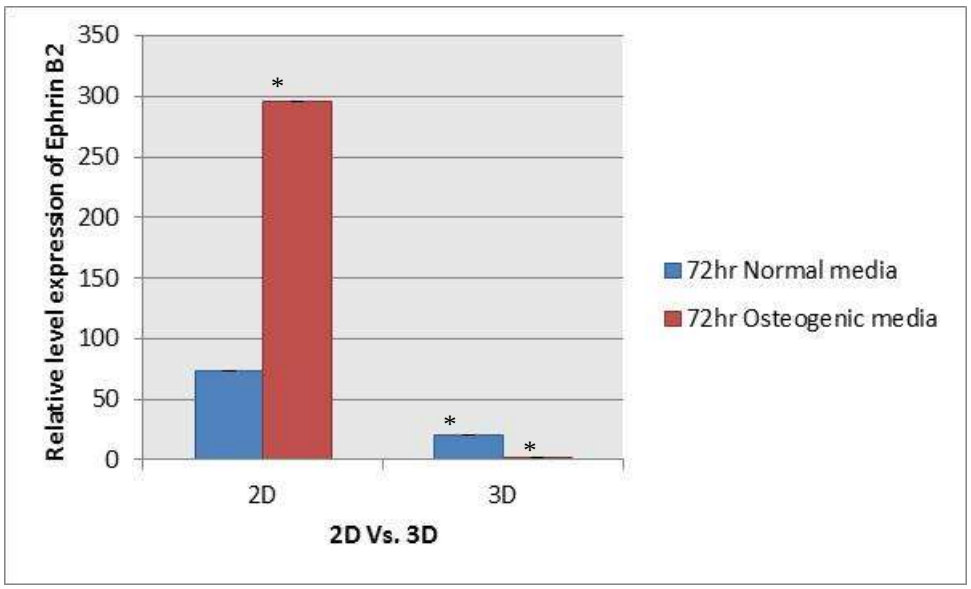

Figure 4.63 *Ephrin B2 relative level expression in rat cells at 72hr, the data represents the mean ± standard error of the mean n=9, a statistical significant was considered when P value ≤ 0.05 where (*) indicates significance compared to 2D normal media*

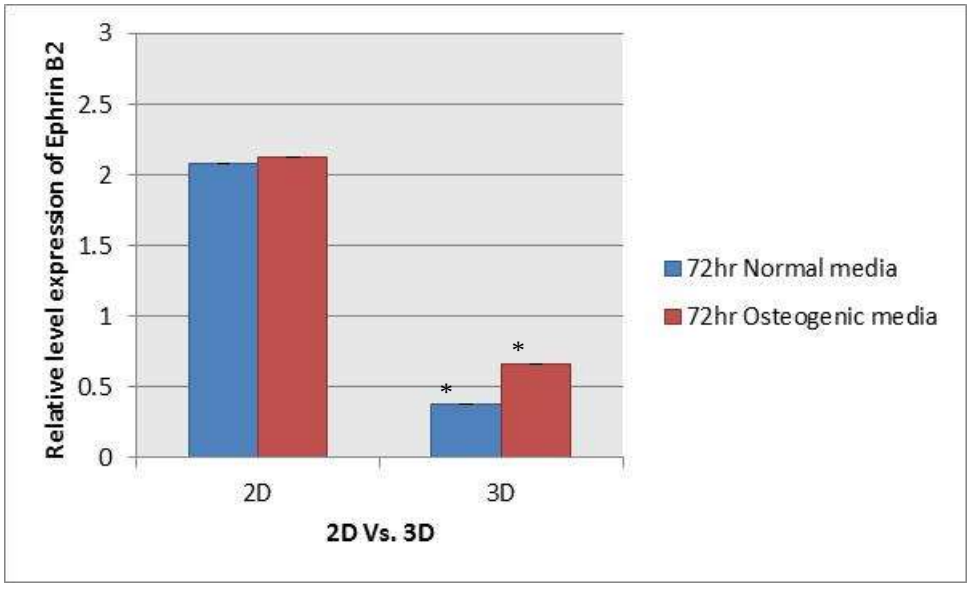

Figure 4.64 *Ephrin B2 relative level expression in MSCs at 72hr, the data represents the mean ± standard error of the mean n=9, a statistical significant was considered when P value ≤ 0.05 where (*) indicates significance compared to 2D normal media*

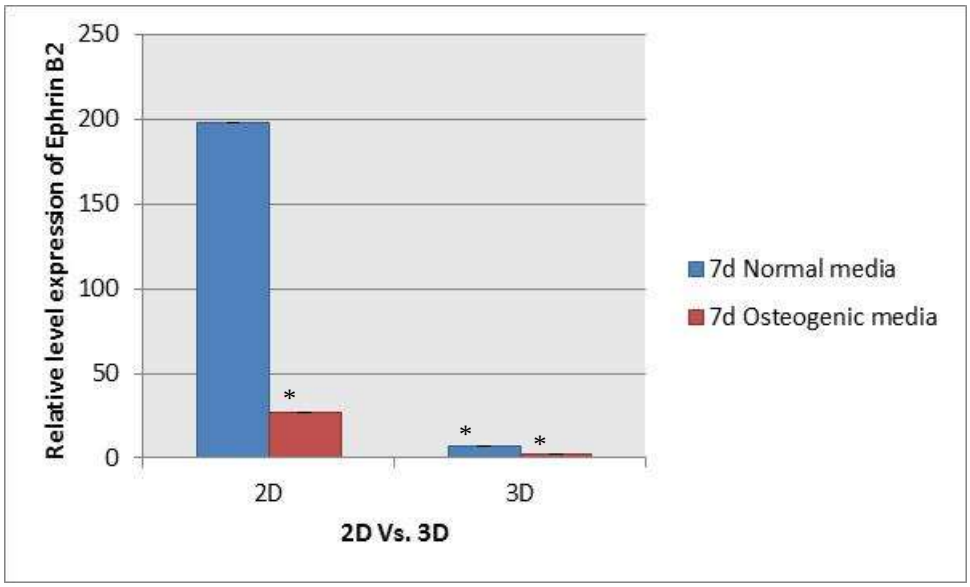

Figure 4.65 *Ephrin B2 relative level expression in rat cells at 7days, the data represents the mean ± standard error of the mean n=9, a statistical significant was considered when P value ≤ 0.05 where (*) indicates significance compared to 2D normal media*

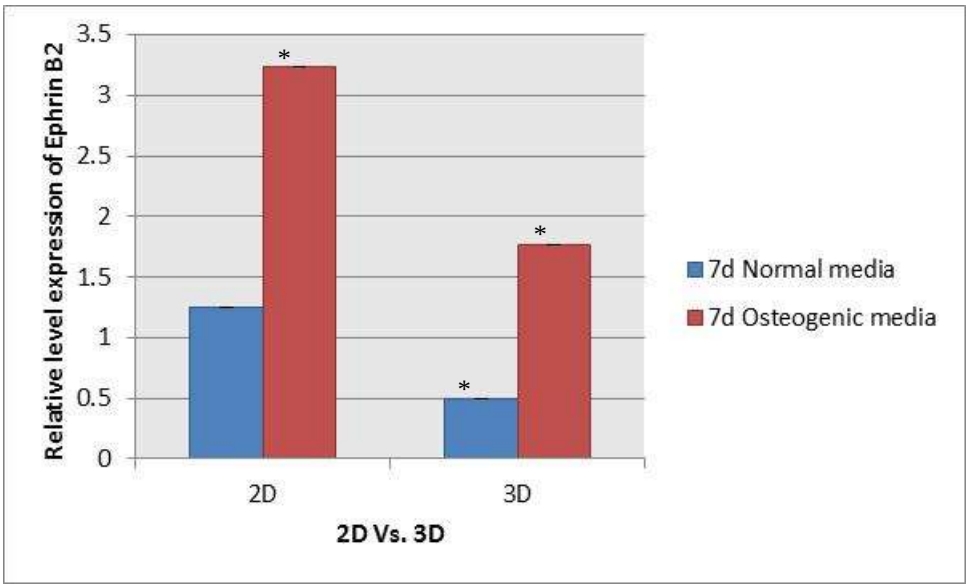

Figure 4.66 *Ephrin B2 relative level expression in MSCs at 7days, the data represents the mean ± standard error of the mean n=9, a statistical significant was considered when P value ≤ 0.05 where (*) indicates significance compared to 2D normal media*

After 24hrs a significantly higher level of ephrin B4 gene expression was detected in 2D rat cells grown in normal media compared to those grown in osteogenic media and those 3D cultures grown in normal and osteogenic media [Figure 4.67]. While MSCs showed a significantly high level gene expression in 2D cells grown under osteogenic conditions [Figure 4.68].

Unlike cells grown for 24hr, at 72hrs higher ephrin B4 expression was detected in 2D cells grown in osteogenic media with a significant low level in 2D cells grown in normal media [Figure 4.69]. A decrease in gene expression was also detected in 3D cultures grown in normal media [Figure 4.69]. Whereas a significant increase in ephrin B4 transcript levels was detected in 2D and 3D cultures under both media conditions, it was also noted that both 2D and 3D culture under osteogenic conditions scored similarly [Figure 4.70].

At 7days, strikingly the level of the gene decreased significantly in 2D cells grown under osteogenic media, and significantly increased in 2D cells in normal media while approximately no noticeable change to the level of the gene was observed in 3D cultures [Figure 4.71]. MSCs showed a slight decrease in ephrin B4 expression in 2D and 3D cultures in both media compared to those grown at 72hr [Figure 4.72].

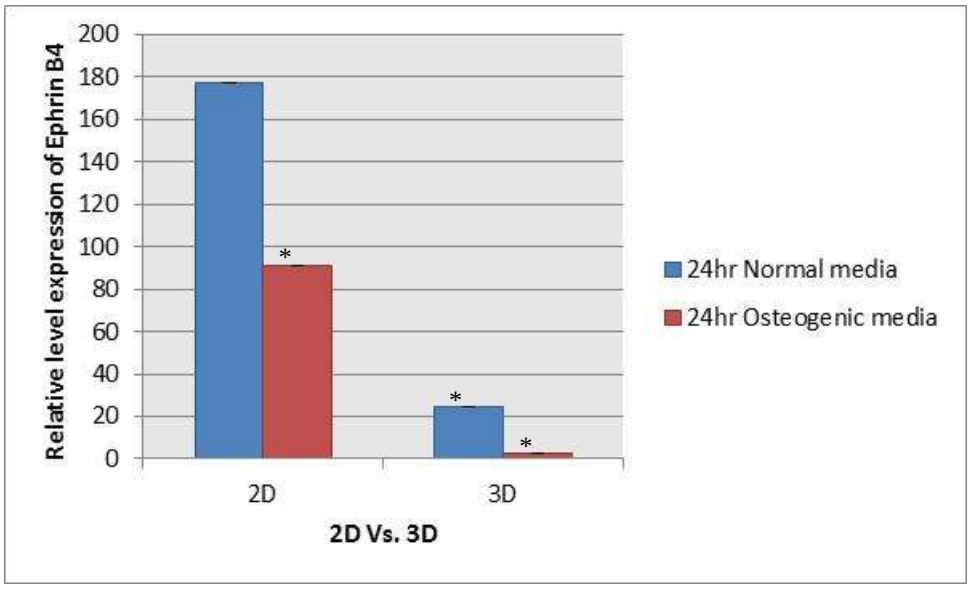

Figure 4.67 *Ephrin B4 relative level expression in rat cells after 24hr, the Data represents the mean ± standard error of the mean n=9, a statistical significant was considered when P value ≤ 0.05 where (*) indicates significance compared to 2D normal media*

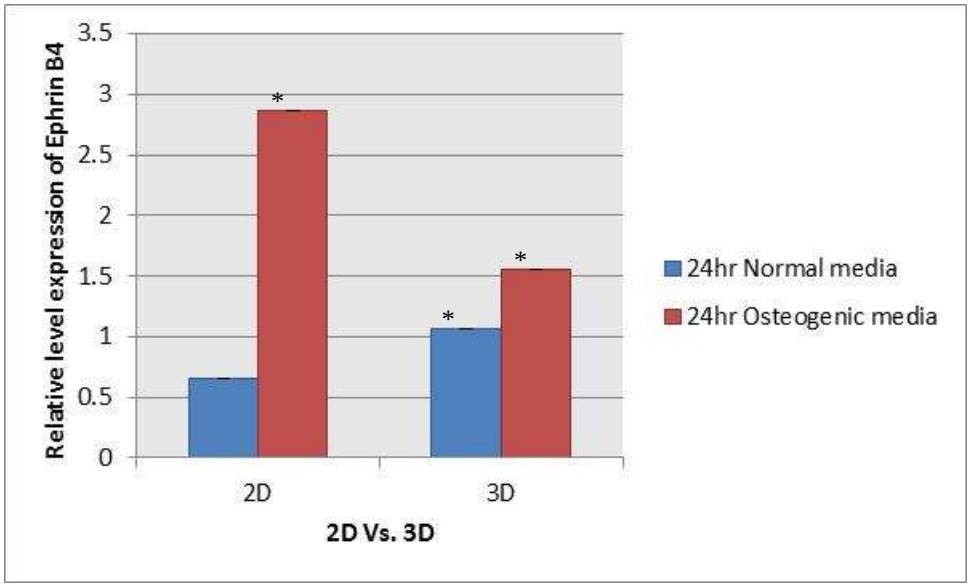

Figure 4.68 *Ephrin B4 relative level expression in MSCs after 24hr, the Data represents the mean ± standard error of the mean n=9, a statistical significant was considered when P value ≤ 0.05 where (*) indicates significance compared to 2D normal media*

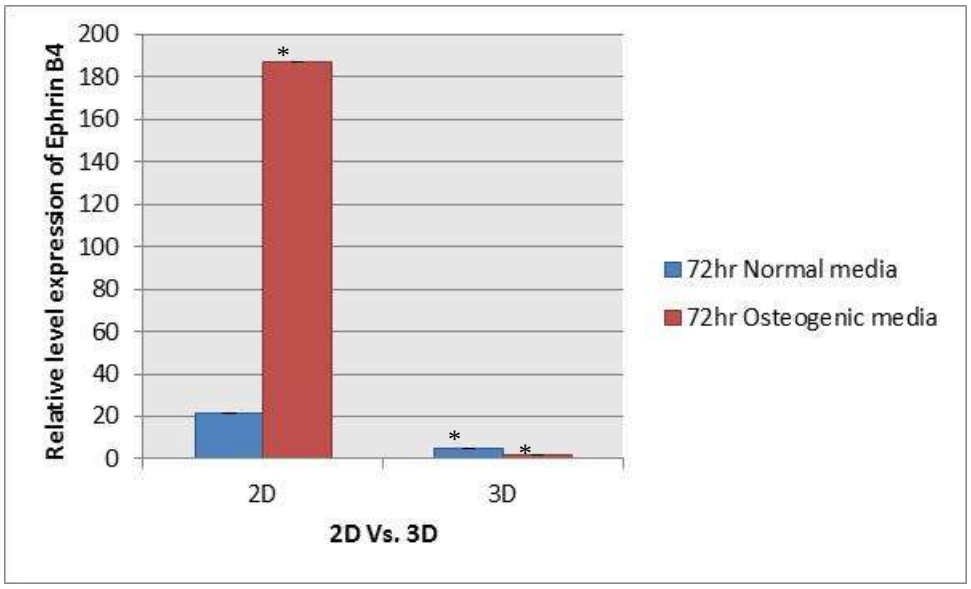

Figure 4.69 *Ephrin B4 relative level expression in rat cells at 72hr, the data represents the mean ± standard error of the mean n=9, a statistical significant was considered when P value ≤ 0.05 where (*) indicates significance compared to 2D normal media*

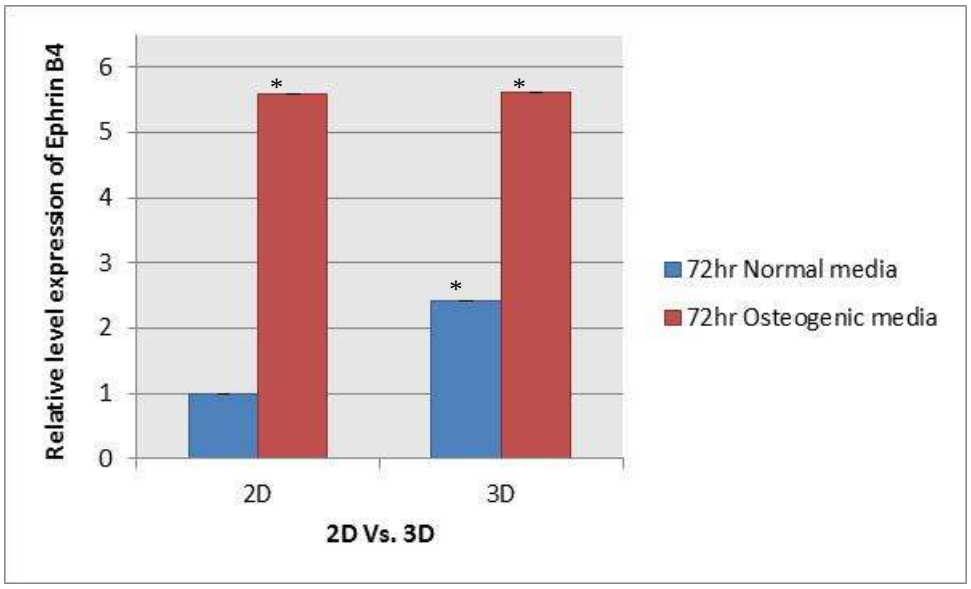

Figure 4.70 *Ephrin B4 relative level expression in MSCs at 72hr, the data represents the mean ± standard error of the mean n=9, a statistical significant was considered when P value ≤ 0.05 where (*) indicates significance compared to 2D normal media*

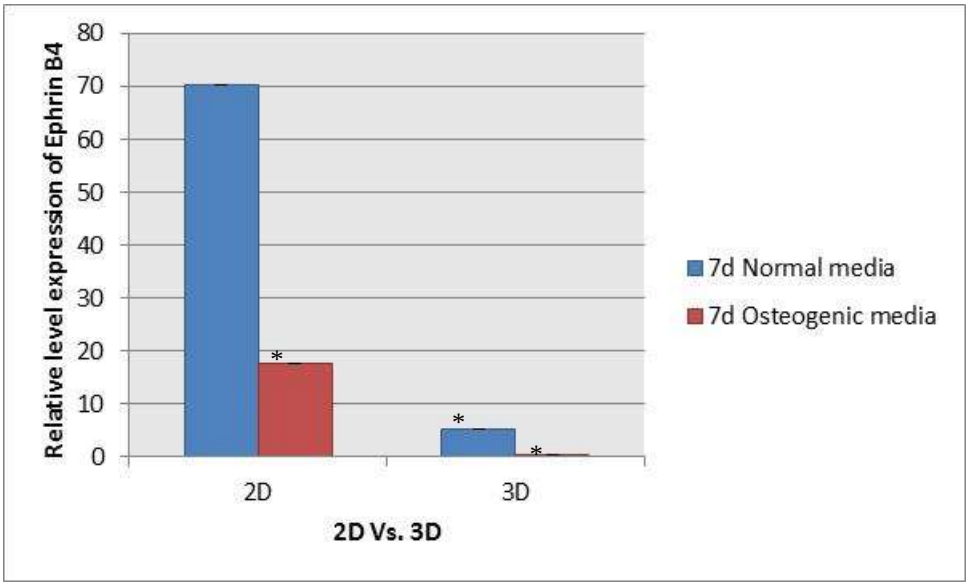

Figure 4.71 *Ephrin B4 relative level expression in rat cells at 7days, the data represents the mean ± standard error of the mean n=9, a statistical significant was considered when P value ≤ 0.05 where (*) indicates significance compared to 2D normal media*

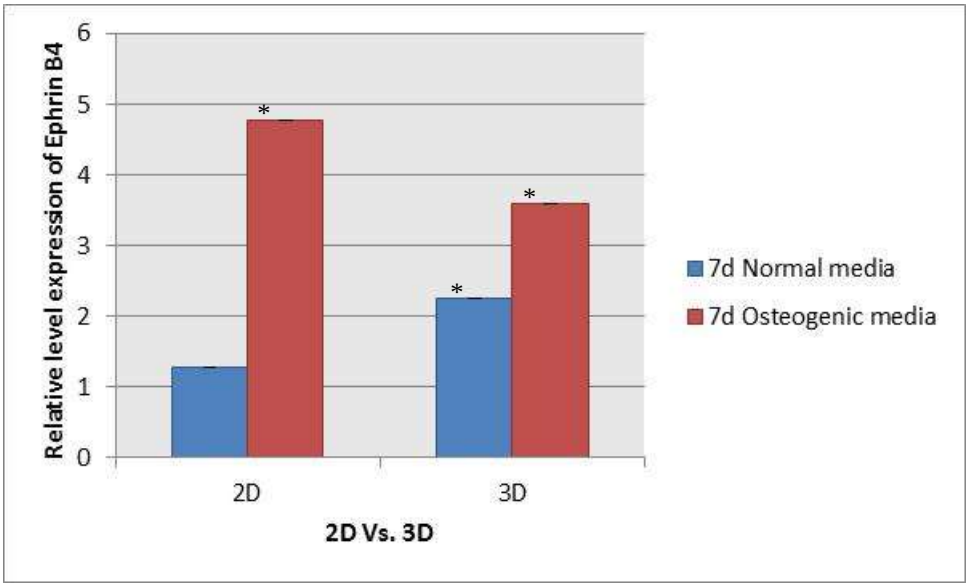

Figure 4.72 *Ephrin B4 relative level expression in MSCs at 7days, the data represents the mean ± standard error of the mean n=9, a statistical significant was considered when P value ≤ 0.05 where (*) indicates significance compared to 2D normal media*

4.4 Discussion:

Cx43 is a key component in bone cells signalling where it plays a vital role in bone cells proliferation, differentiation, and survival (Loiselle, Paul et al. 2013). In previous studies, Cx43 expression level and localization was found to correlate with the gap junction protein phosphorylation where Cx43 hyperphosphorylation indicates an increase of Cx43 in the cell membrane while a reduction of Cx43 localization in the membrane was coupled with Cx43 hypophosphorylation (de Feijter, Matesic et al. 1996). Moreover, it was found that Eph/ephrin signalling inhibits gap junction (Arvanitis and Davy 2008). Where ephrin B1 was reported to disrupt the distribution of Cx43 preventing it from forming a functional gap junction at the cell membrane and thus affecting cells communication (Gross 2006).

In this study the expression and localization of Cx43 were examined. Results showed that in cells grown in monolayer at 7days; in most of the cells Cx43 localized around the nucleus under normal conditions indicating an increase of Cx43 hypophosphorylation. While in osteogenic media, Cx43 was localized at the cell surface in contact with other cells indicating an increase of Cx43 hyperphosphorylation. A high expression of Cx43 over time is expected as the SEM images of the results showed more compact spheres at 7days.

In 3D culture the fluorescent microscopy images were not clear although Cx43 was spotted, but even with the use of confocal microscopy it was hard to identify Cx43 junctions. Previously it was noted the challenges of obtaining a high resolution images in 3D culture systems (Pampaloni, Reynaud et al. 2007; Mueller-Reichert 2010).

On the other hand, both Cx43 and ephrin B1 transcript levels were high in cells grown in normal media at 7days. A high level of ephrin B1 may explain the reason for Cx43 perinuclear localization ephrin B1 inhibits Cx43 gap formation in the cell membrane. The

mechanism by which ephrins signalling inhibits Cx43 gap junction is still unclear (Arvanitis and Davy 2008).

Another key component in bone cells is Runx2 which has been identified as the master gene that controls osteoblasts differentiation (Shui, Spelsberg et al. 2003). Runx2 expression is higher at the early stages of osteogenesis and in particular by pre-osteoblasts/immature osteoblasts and the expression is down regulated in mature osteoblasts (Choi 2012). Runx2 regulates both osteoblast proliferation and differentiation and promotes osteoblast maturation (Pratap, Galindo et al. 2003). Furthermore, the expression of bone matrix protein genes, mineralization, and alkaline phosphatase activity is induced by Runx2 in both immature MSCs and osteoblastic cells in vitro (Fujita, Azuma et al. 2004). Another factor that directs the fate of mesenchymal cells towards osteogenesis is SP7 which is known also as osterix (Choi 2012). Osterix function during osteoblasts differentiation is not fully understood but it is induced by Runx2 overexpression (Matsubara, Kida et al. 2008; Haycock 2011). However, previous studies have reported an osteogenic activity by osterix in Runx2 deficient MSCs suggesting that either osterix functions distinct from Runx2 or it works downstream of Runx2 (Matsubara, Kida et al. 2008). Moreover, osterix expression increases when cells are treated with ephrin B2 and a rise in other osteoblastic genes including ephrin B1, alkaline phosphatase, osteocalcin, and collagen type1 (Benson, Opperman et al. 2012; Shaohong, Chandrasekhar et al. 2013).

The qRT-PCR results of this study demonstrated an up-regulation of Runx2 in both 2D calvarial cells and 3D MSCs grown under normal and osteogenic conditions respectively. The findings of the current study are consistent with those of (Fujita, Azuma et al. 2004) who found that Runx2 induces ALP activity. Additionally, Runx2 upregulation was accompanied by an increase in osterix, ephrin B1, ephrin B2, and ephrin

B4. In accordance with the present results, previous studies have demonstrated an increase in osterix expression via Runx2 (Matsubara, Kida et al. 2008). Osterix also is regulated by ephrin B1 thus increases the level of both gene expressions (Xing, Kim et al. 2010). Also, previous research reported that ephrin B4 receptor is activated by ephrin B2 gene expression (Kwan Tat, Pelletier et al. 2008).

Interestingly a high level of transcripts for genes that play a role in osteogenesis was observed in MSCs grown under osteogenic media, whereas in calvarial cells the expression was higher when grown in normal media. These results may be explained by the fact that calvarial cells contain a subpopulation of osteoprogenitors also known as preosteoblasts (Kadono, Kido et al. 1999). While MSCs are a multipotent stromal cells that can give rise to different cell lineages (Abdi, Fiorina et al. 2008).

Overall, the results suggest that growing MSCs under osteogenic media directs towards osteogenic differentiation regardless if they were grown in 2D or 3D culture. While rat calvarial cells are directed towards osteogenic differentiation under normal media regardless of if they were grown in 2D or 3D culture.

Chapter 5: In vitro osteogenic differentiation of cells encapsulated within a nanofiberous environment

5.1 Introduction

Three dimensional biomaterials represent a promising tool in tissue engineering (Dvir-Ginzberg, Gamlieli-Bonshtein et al. 2003). Hydrogels are one class of biomaterials that have been explored as scaffolds for tissue engineering applications (Drury and Mooney 2003). These hydrogel scaffolds can be modified physically and chemically to adapt to the specific application, by altering parameters including surface morphology, shape, stiffness and porosity (El-Sherbiny and Yacoub 2013). Recently, the emergence of nanotechnology as a new efficient tool in tissue engineering has identified nano-materials for biomedical applications (Zhang, Li et al. 2011). In particular a new type of biomaterial, the ionic self-complementary oligopeptides have been introduced (Zhao and Zhang 2006).

RAD-16 also known commercially as Puramatrix is a self-assembly peptide which forms a hydrogel scaffold and designed by Zhang et al (Ozeki, Kuroda et al. 2011). Previous studies showed that using Puramatrix allows cells to proliferate and differentiate within a 3D environment (Zhang, Zhao et al. 2005).

The aim of the work presented here was to examine the effects of different hydrogel scaffolds (including Puramatrix) either presented on a surface or encasing the cells, on the cells viability and differentiation towards the osteoblast lineage.

5.2 Materials and methods:

All materials and reagents were purchased from Sigma-Aldrich company, Ltd Ayrshire, UK unless otherwise specified.

5.2.1 Cell culture

Tissue culture was carried out in aseptic environment using class II laminar flow hood. Cells were plated on the surface of the hydrogel and encapsulated within the hydrogel.

5.2.1.1. Rat calvaria cell culture:

Rat cells culture was carried out following methods represented in sections 2.1.1., 3.2.2.1.

5.2.1.2 Human mesenchymal stem cells cell culture:

Human mesenchymal stem cells were purchased from Lonza and cultured as described previously in sections 2.1.1 but using Dulbecco's Modified Eagle's Medium - low glucose.

5.2.2 Hydrogel scaffold preparation:

5.2.2.1 Self-assembling peptide nanofibres:

Puramatrix peptide was purchased from BD Bioscience, the vial contained 5 ml of 1% [w/v] solution of purified peptide. The hydrogel scaffold was prepared following the manufacturers protocol. Briefly, the viscosity of the stock solution was decreased by vortexing or using a sonicator bath, and then to eliminate air bubbles - if present - centrifugation was performed. Three different concentrations [0.1%, 0.25%, and 0.5%] of the peptide were prepared by diluting the stock solution with sterile water. For surface plating, 250µl of each concentration was plated on 24 well plate surfaces; 500µl of DMEM was then added slowly to promote gelation. The plates were then placed in the

incubator for 30-60 minutes depending on the peptide concentration, a higher concentration taking less time to form gel. The cell suspension was then added slowly and very carefully on top of the hydrogel. To achieve cell encapsulation a drop technique was used to resemble the formation of 3D spheroids. In this approach after decreasing the viscosity of the solution the concentrations were diluted with sterile 20% sucrose to generate 2x of the final desired concentration [figure 5.1]. After cell trypsinization the cells were collected by centrifugation and washed with sterile 10%(w/v) sucrose. Then, an equal volume of cell/sucrose mixture was combined with each concentration of Puramatrix/sucrose mixture. Then, multiple drops of 15µl of the cell/hydrogel mixture were placed alongside of the well plate containing media to initiate peptide self-assembling. The plates were then placed in the incubator for 24hr, 72hr, and 7 days.

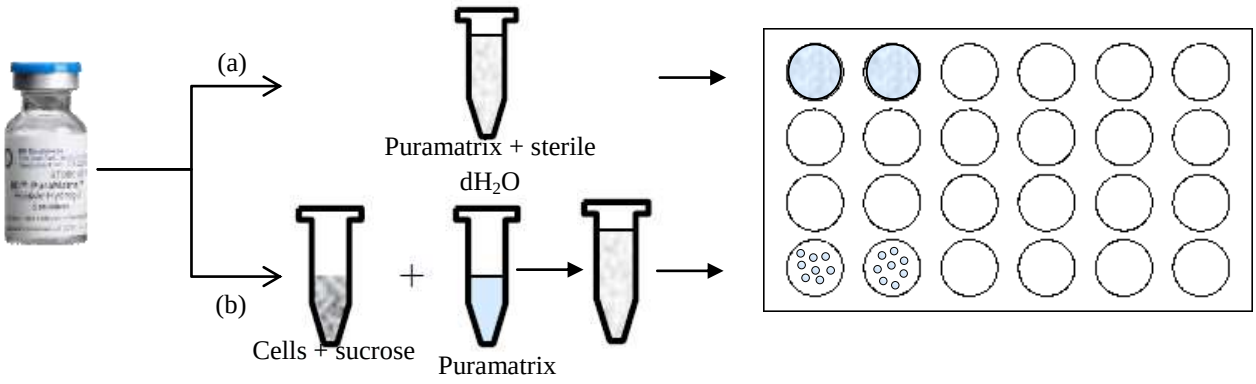

Figure 5.1: *Flowchart of puramatrix hydrogel scaffold preparation (a) cells plating on the surface of the puramatrix (b) cells encapsulation using drop technique method*

5.2.2.2 Mussel adhesive protein:

MAPTrix HyGel containing mussel adhesive protein coupled with collagen type1 peptide was purchased from Kollodis Bioscience. The hydrogel scaffold was prepared following the manufacturers protocol. In brief, the lyophilized protein [5mg/ml] was diluted with

PBS to a final concentration of 2.0 wt% [w/v] solution. After that the MAPTrix linker [50mg/ml] [Kollodis Bioscience] was prepared by diluting with PBS to a final concentration of 3.0 wt% [w/v] solution. Then, an equal volume – 0.24ml for a 24 well plate – of both MAPTrix protein and MAPTrix linker were mixed and placed immediately on the well plate surface and once the hydrogel are formed cells were plated on top of the scaffold.

5.2.3 Scanning electron microscopy [SEM]:

To examine the hydrogel surface with and without cells the samples were prepared as described previously in section 2.1.7.

5.2.4 Evaluation of cell viability using the MTT assay:

To assess the viability of the encapsulated cells the MTT assay was performed. In brief, the cell/Puramatrix drops were mechanically disrupted by pipetting up and down in the well then transferred to a conical tube, the well was further washed with PBS and collected in the tube. After spinning for 5 minutes at low speed the supernatant was discarded and the pellet containing cells/Puramatrix was re-suspended in PBS. After centrifugation the pellet was collected for MTT assay as described in sections 2.1.3 and 3.2.2.3.

5.2.5 Alkaline phosphatase assay:

To assess osteoblastic differentiation cells were recovered as previously described in section 5.2.4. Then alkaline phosphatase activity was measured following the method in section 2.1.4.

5.2.6 RNA isolation and quantitative real time polymerase chain reaction:

The expression of mRNA levels of genes associated with osteogenesis including Runx2, ALP, osterix and osteocalcin were determined using a quantitative real time polymerase chain reaction [qPCR]. After recovering cells as previously described in section 5.2.4, RNA isolation and qRTPCR were carried out following method previously described in section 2.1.6. The cycle threshold [Ct] values were normalized against the house keeping gene GAPDH.

5.2.7 Statistical analysis:

Statistical analysis was performed using SPSS 19.0. [SPSS Inc., USA]. Data were analysed as previously described in section 4.2.7.

5.3 Results:

5.3.1 Morphological observations:

At first, cell interactions with the surface of the hydrogel scaffolds were assessed to understand the relationship between scaffold and cell morphology. Puramatrix scaffold was mechanically weak and fragile even at high concentrations and often failed to form a continuous layer of the surface of the tissue culture plates. As seen in Figures 5.2, 5.3, 5.4, and 5.5 after 24hr and at 7days [Figures 5.6, 5.7, 5.8, and 5.9] due to the weak mechanical properties of Puramatrix hydrogel it broke away allowing cells to adhere to the surface of the well while others aggregated and formed clusters. Some of the cellular clusters can be seen communicating with each other's as seen in figure [5.4].

On the other hand, MAPTrix hydrogel scaffold was morphologically stiffer compared to Puramatrix. After seeding cells on the surface of the scaffold the cells adhered to the surface and proliferated [Figures 5.10, and 5.11].

Studies were then performed to encapsulate the cells within the hydrogel in an attempt to create a model system that would allow us to understand how the balance between cell-cell and cell-ECM signals can be used to influence cell fate and differentiation. A cell drop technique was used to create cell aggregates resembling the spheroids described in Chapter 4. As seen in Figure 5.12 the hydrogel drops at low concentration 0.1% were not firm compared to 0.2% and 0.5%. Under microscopic observation the 0.1% drops were homogenous in structural appearance unlike 0.2% and 0.5%, where at higher concentrations bubbles formed.

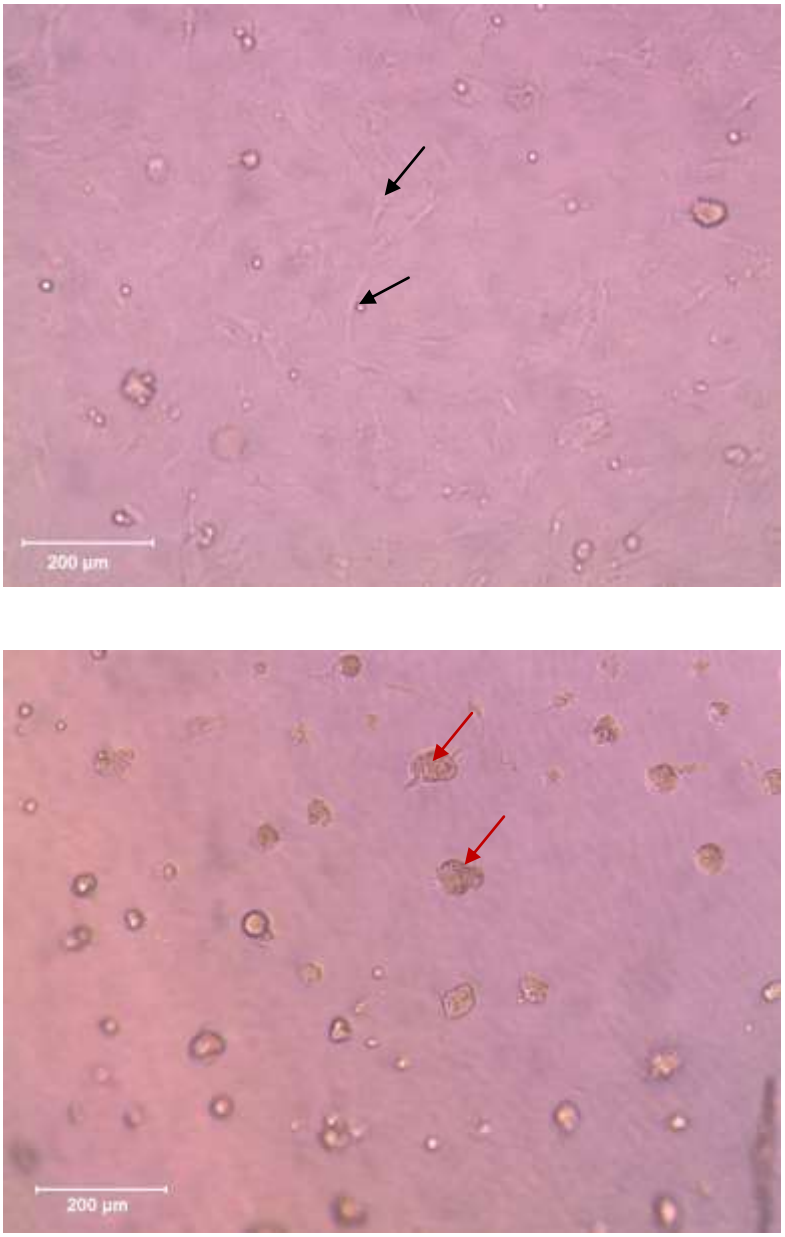

Figure 5.2: *Rat calvarial cells grown after 24hr on 0.1% Puramatrix in normal media, cells adhered [black arrows] while others formed clusters [red arrows] because of hydrogel breakage*

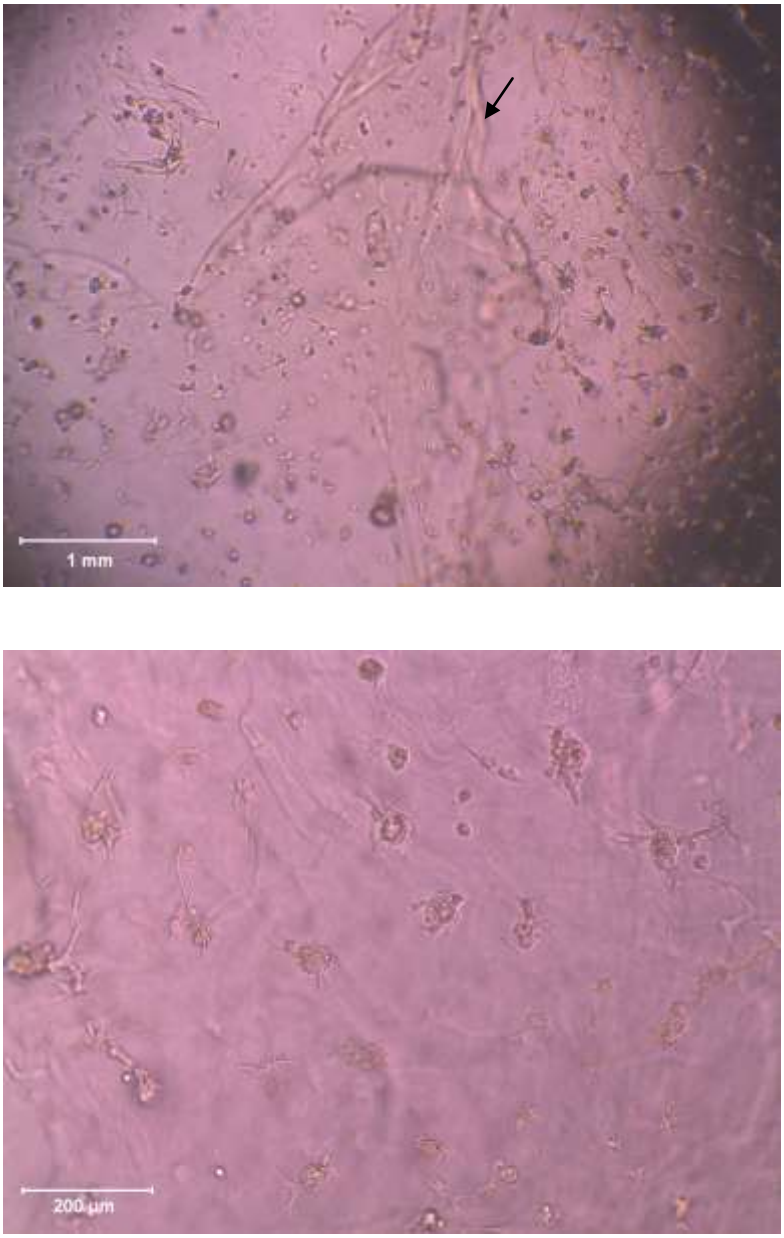

Figure 5.3: *Rat calvarial cells grown after 24hr on 0.25% Puramatrix in normal media, cells formed clusters note the hydrogel breakage [black arrow].*

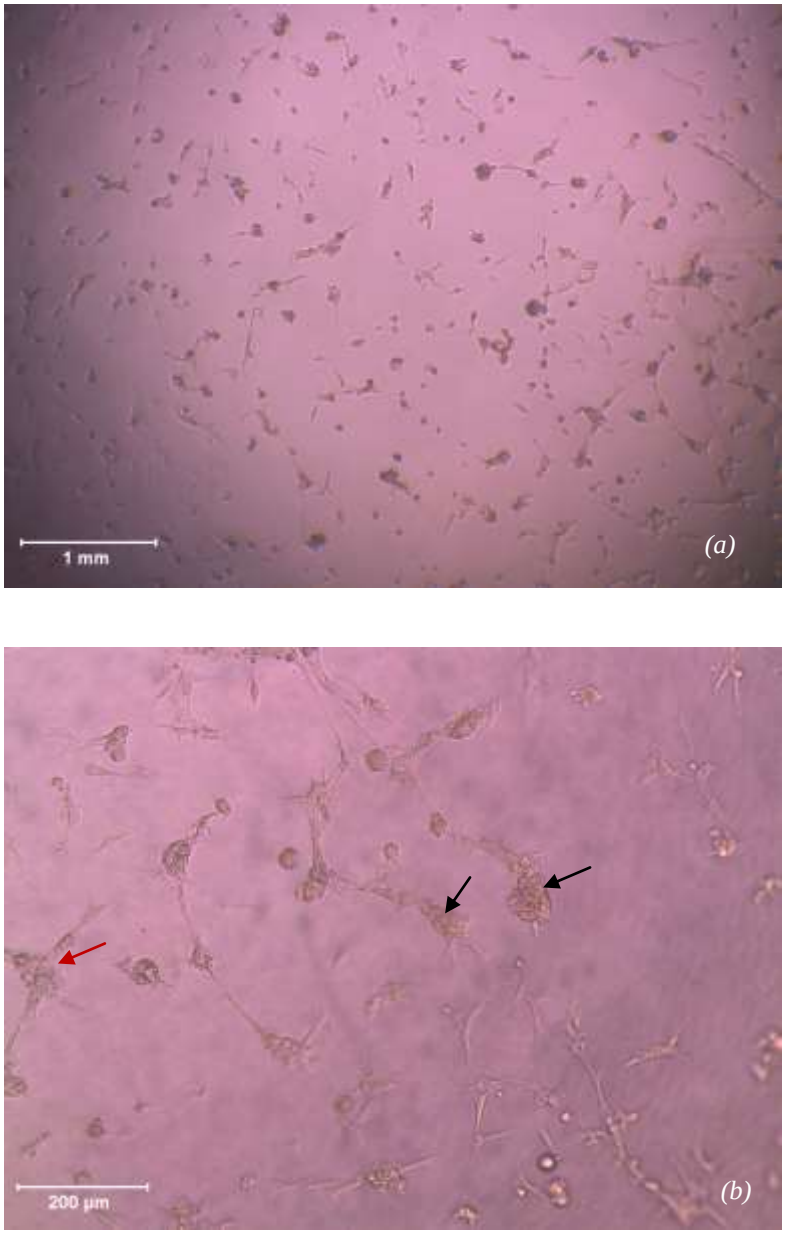

Figure 5.4: *Rat calvarial cells grown after 24hr on 0.5% Puramatrix in normal media, cells formed clusters [black arrow] and some communicated with each other [red arrow]*

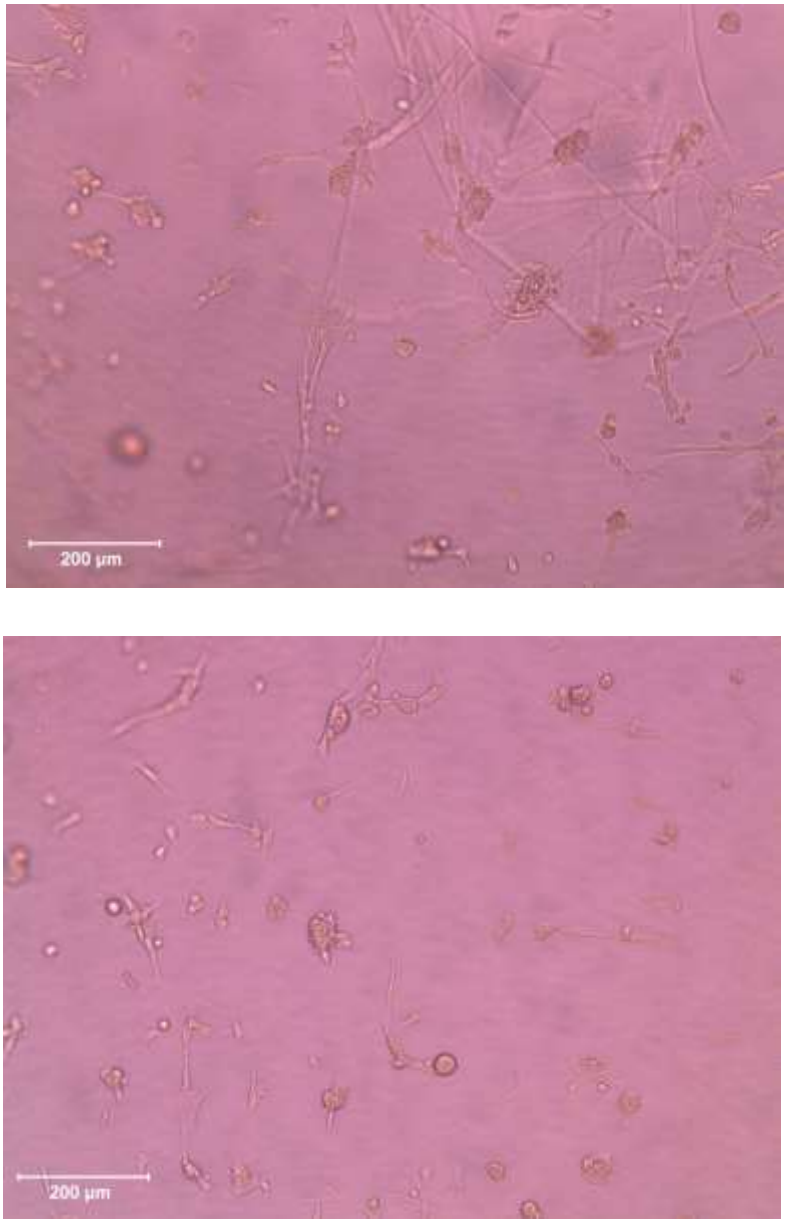

Figure 5.5: *Rat calvarial cells grown after 24hr on 1% Puramatrix in normal media, some cells formed clusters and some adhered to the hydrogel scaffold. The hydrogel is fragile though a high concentration was used.*

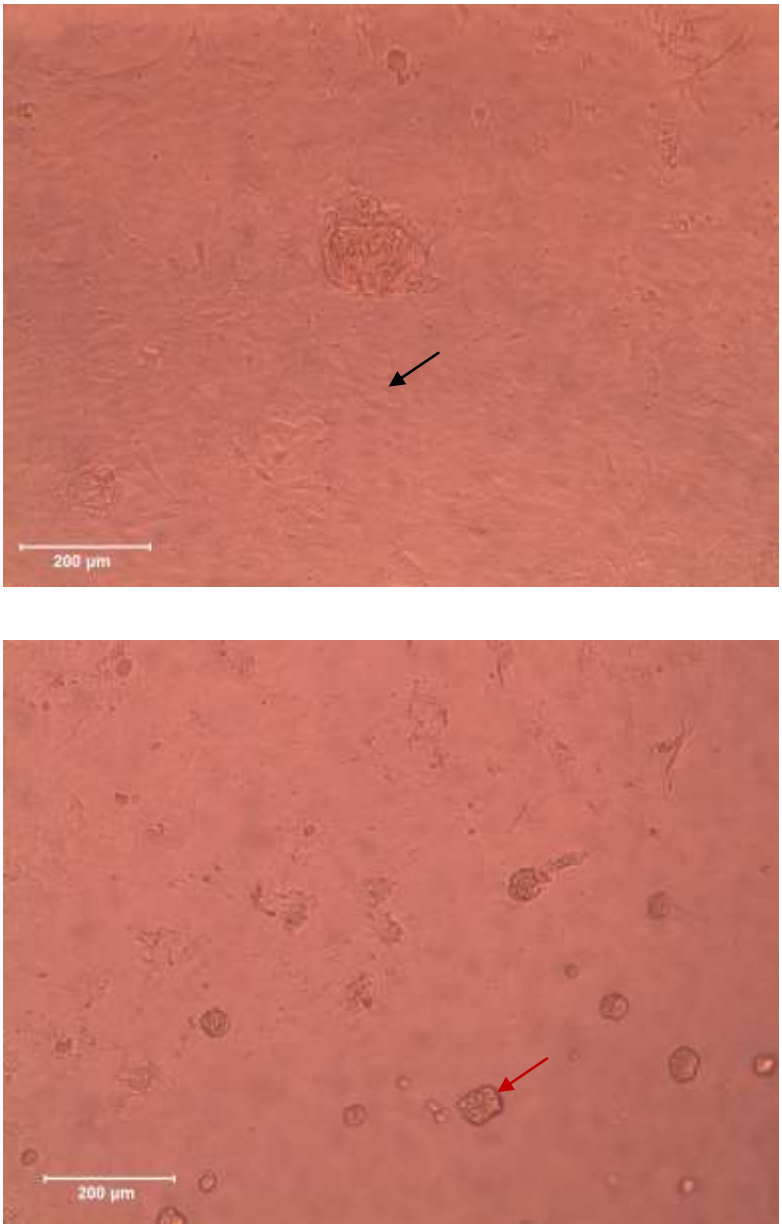

Figure 5.6: *Rat calvarial cells grown at 7days on 0.1% Puramatrix in normal media, most of the cells adhered to the plate surface [black arrow] with few clusters [red arrow]*

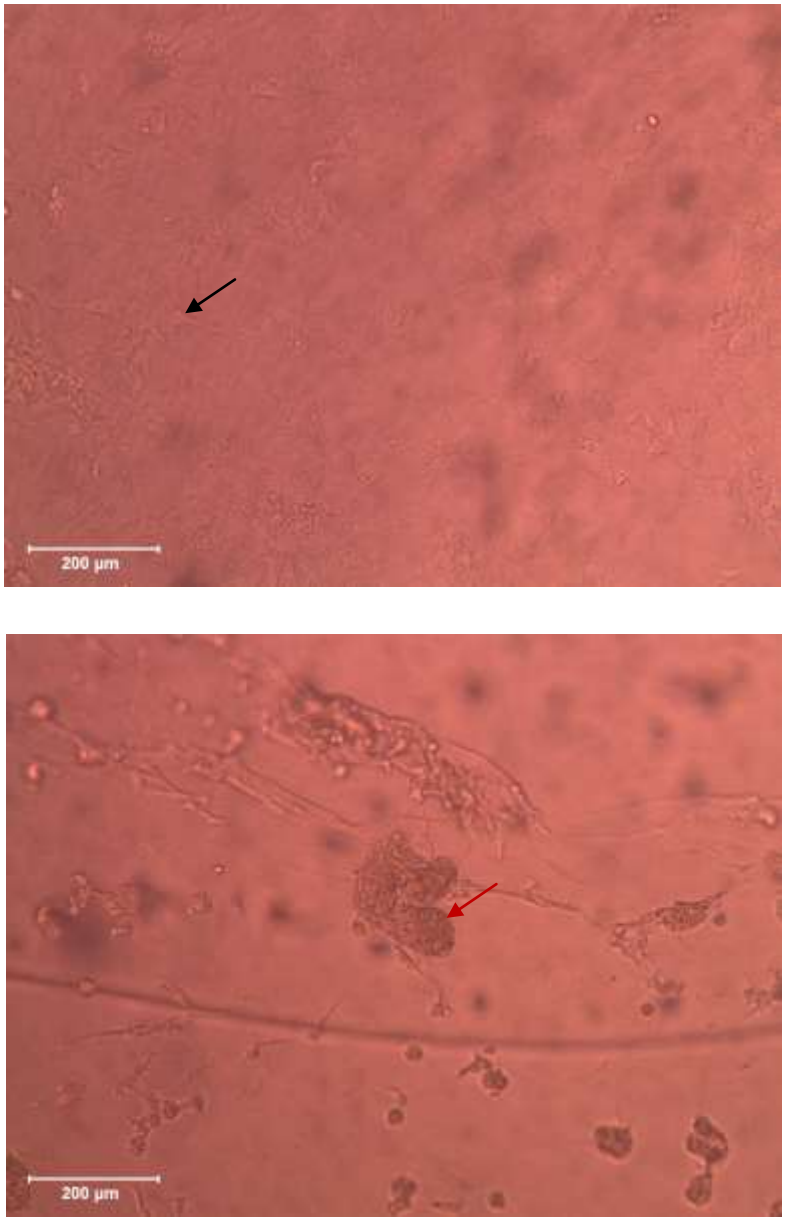

Figure 5.7: *Rat calvarial cells grown at 7days on 0.25% Puramatrix in normal media, most of the cells adhered to the plate surface [black surface] with few clusters [red arrow]*

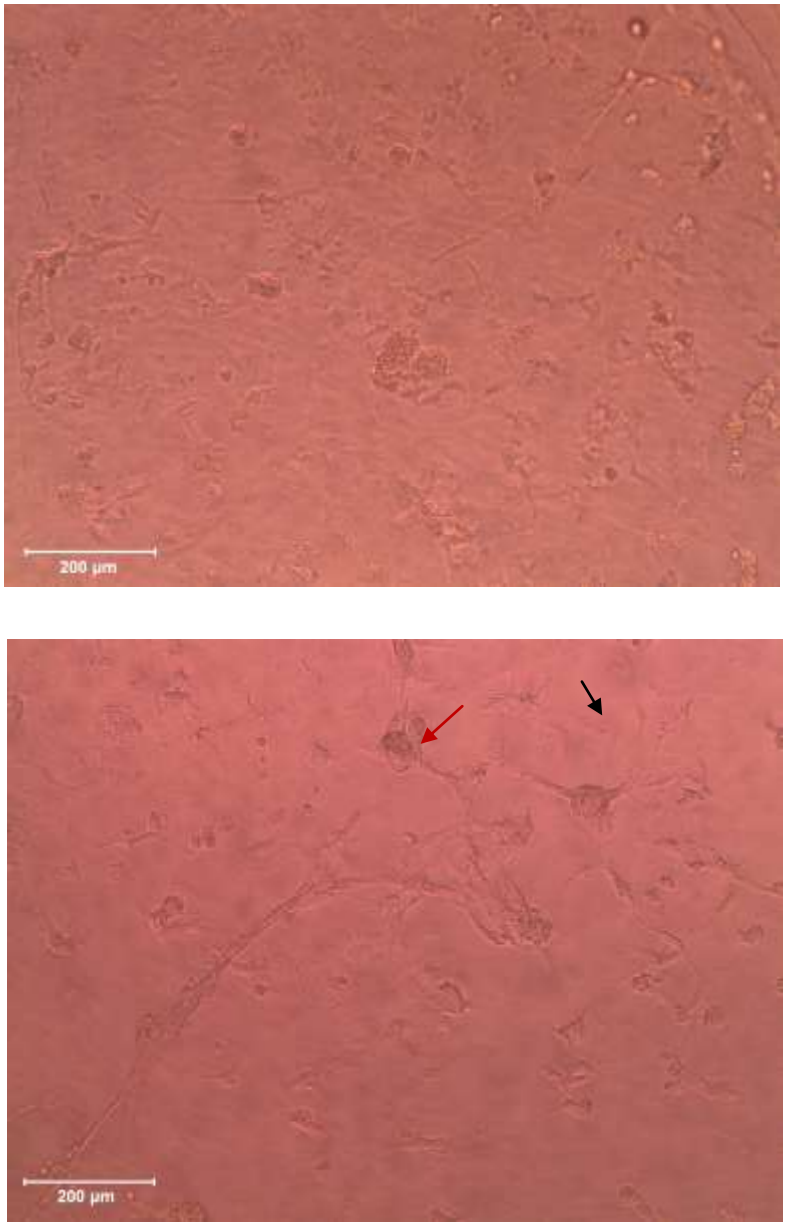

Figure 5.8: *Rat calvarial cells grown at 7days on 0.5% Puramatrix in normal media, most of the cells adhered to the plate surface [black arrow] with few cellular clusters contacting each other red arrow].*

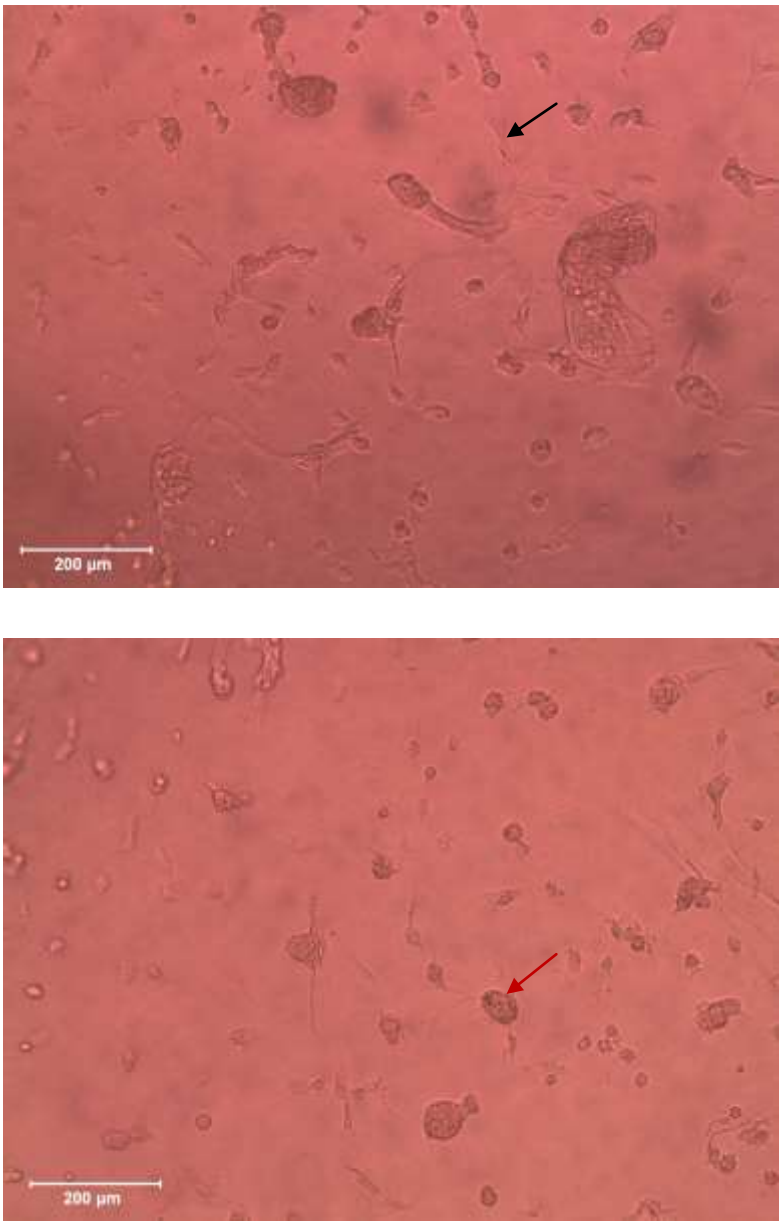

Figure 5.9: *Rat calvarial cells grown at 7days on 1 % Puramatrix in normal media, few cells adhering to the surface [black arrow] with cellular clusters [red arrow].*

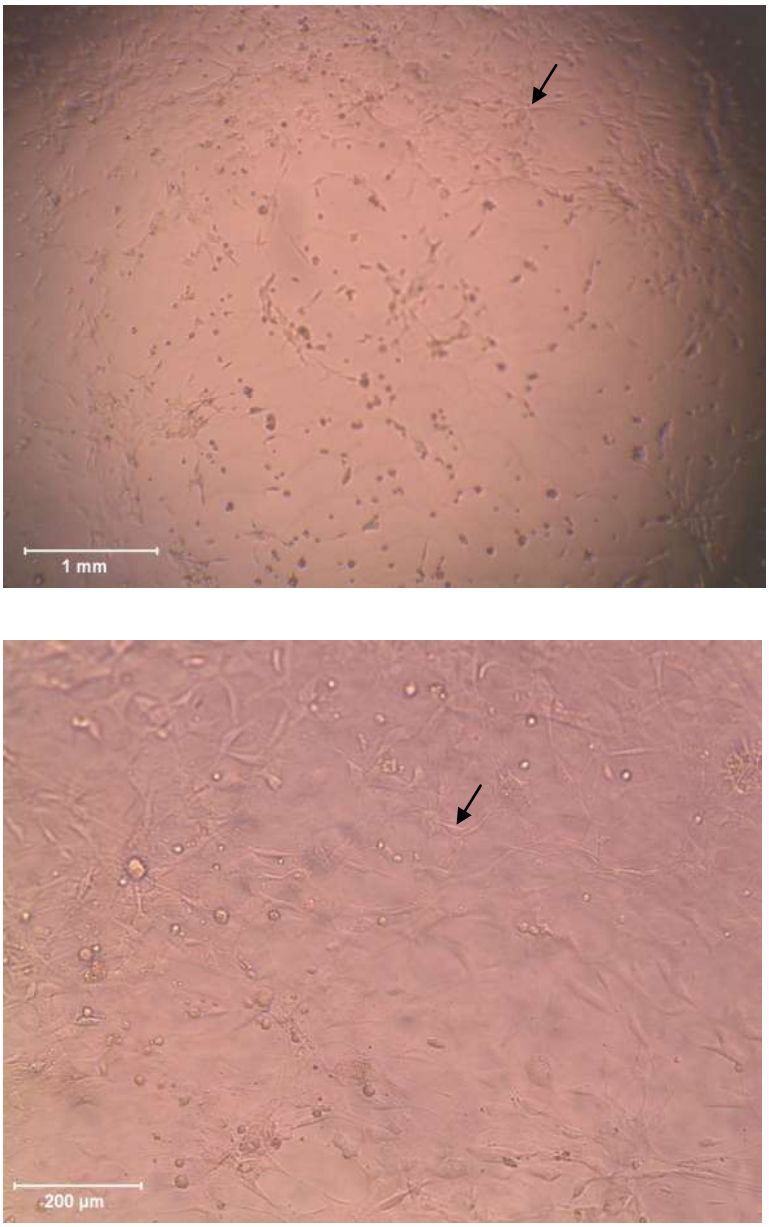

Figure 5.10: *Rat calvarial cells grown on MAPTrix hydrogel where cells adhered to the surface of the scaffold after 24hr [black arrow]*

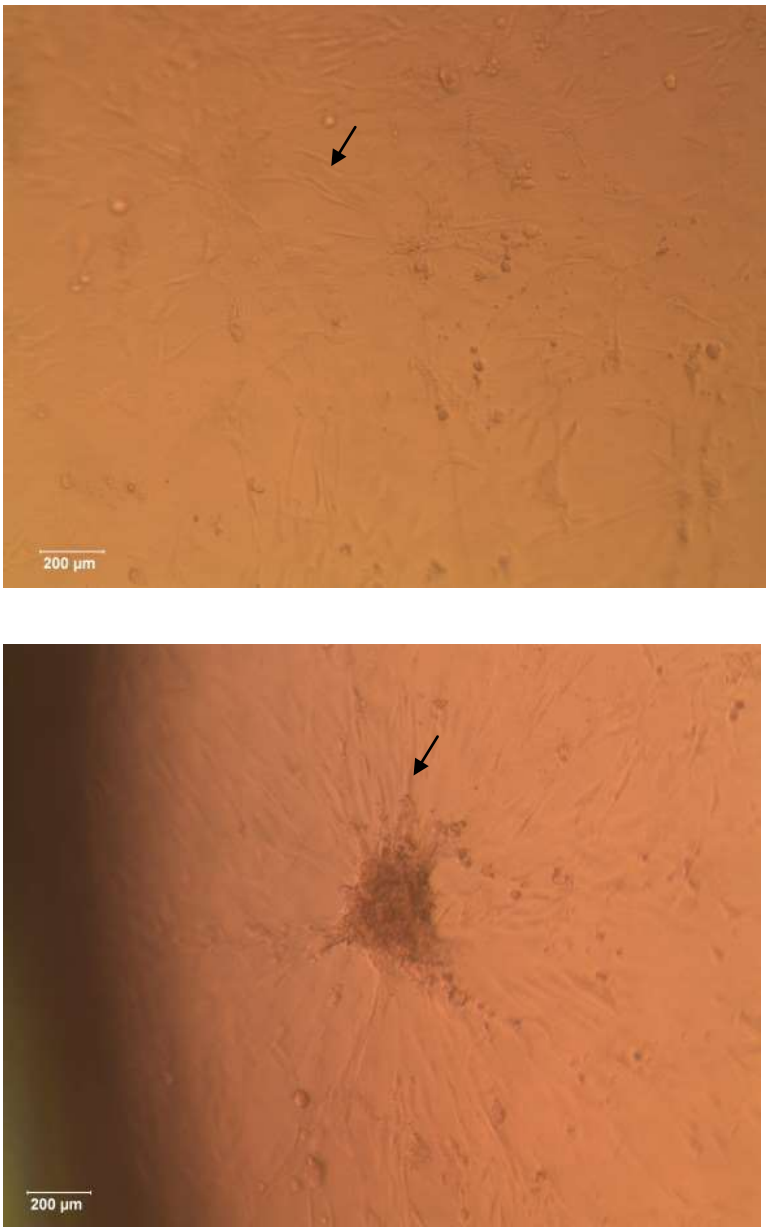

Figure 5.11: *Rat calvarial cells grown at 7days on MAPTrix hydrogel cells continue to grow on the surface of the scaffold [black arrow]*

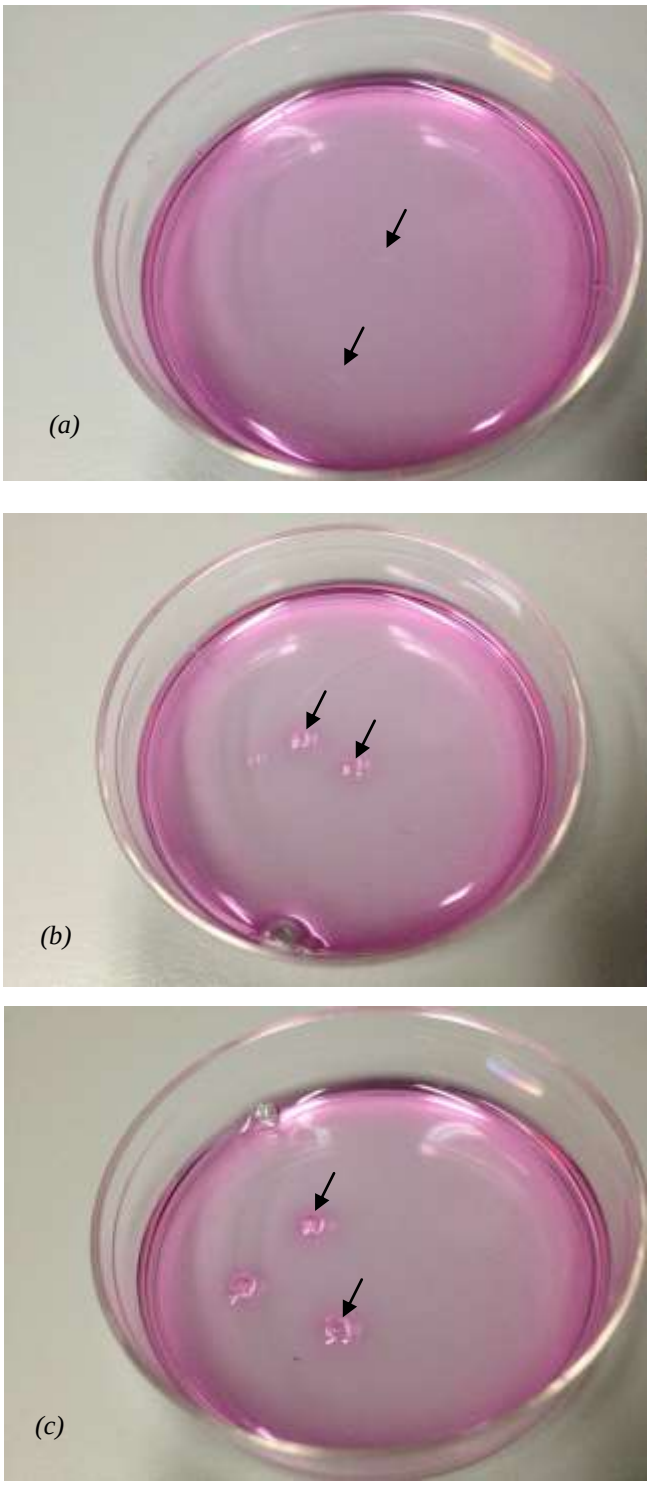

Figure 5.12: *Shows drops of cells encapsulated within Puramatrix hydrogel [black arrow] grown in media using the drop technique (a) 0.1% (b) 0.25% (c) 0.5%*

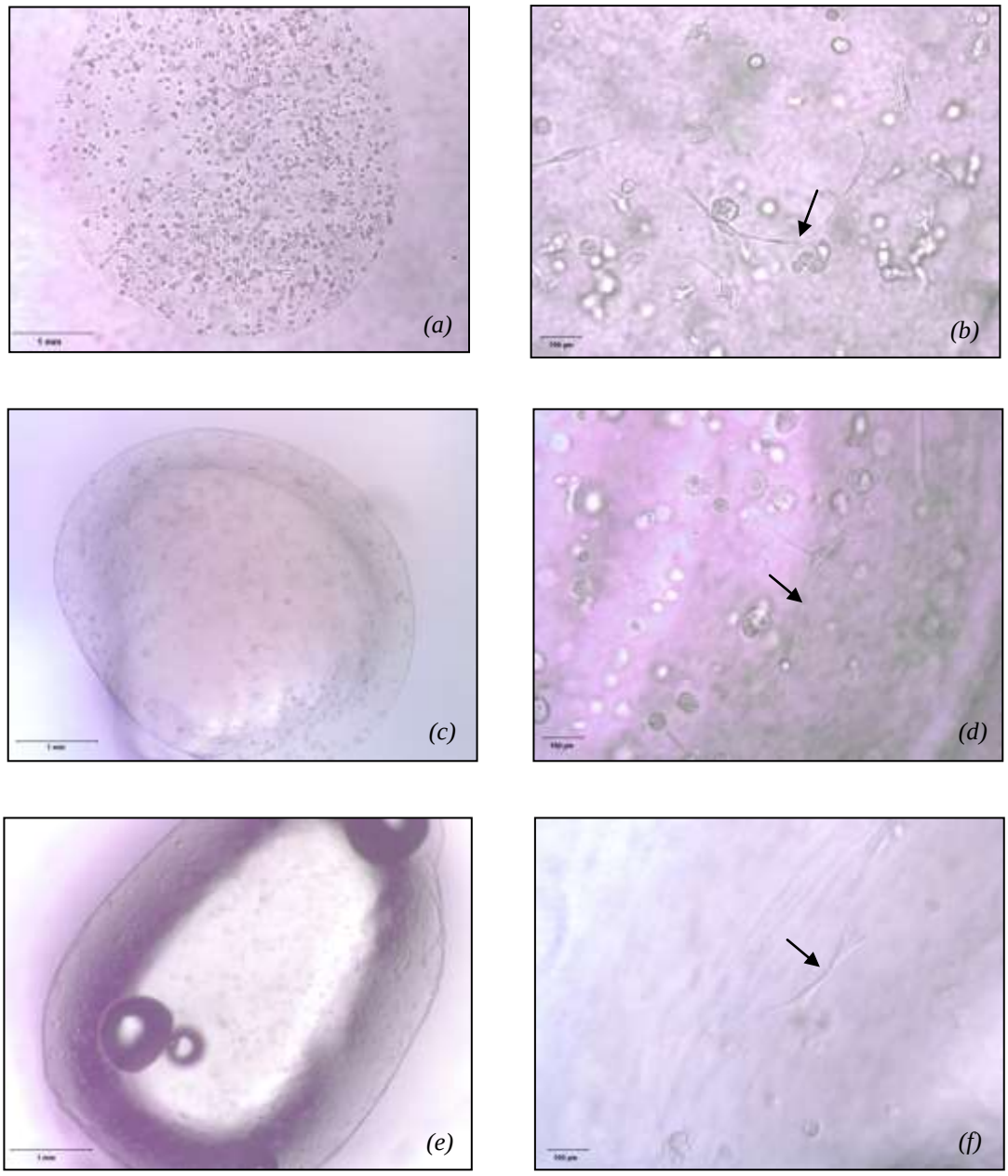

Figure 5.13: *Shows drops of cells encapsulated within different concentrations of Puramatrix hydrogel (a) 0.1% low magnification (b) 0.1% high magnification (c) 0.25% low magnification (d) high magnification (e) 0.5% low magnification (f) high magnification. Note the difference in homogeneity, where the spheres are more homogenously distributed at low Puramatrix concentration. Cells are communicating with the hydrogel matrix and with other cells [black arrow].*

5.3.2 SEM morphology study:

Scanning electron microscopy was used to confirm and examine the formation of the nanofiber scaffold after the peptide self-assembly process.

The SEM images of Puramatrix hydrogel revealed the formation of nanofibers network which was more dense at higher concentrations [figure 5.14]. On the other hand, examination of cell/scaffold interaction revealed of the formation of cellular clusters in all concentrations but this was apparently increased in 0.1% [Figure 5.15] and 0.25% [Figure 5.16]. Moreover, the SEM images revealed the formation of a thin layer of hydrogel that cells were interacting with and at a higher magnification; a cytoplasmic projections can be observed [Figure 5.15, and 5.18]

As seen in Figure 5.16 cellular spheroids were spotted on top of the nanofibers mesh while others managed to attach to the surface. In the case of 0.5% Puramatrix concentration few spheroids were noticed and they were interacting with a sheet of adhered cells [figure 5.17]. Few cell clusters were also noted in 0.1% Puramatrix with cells expanding across the surface of the tissue culture plastic [Figure 5.18].

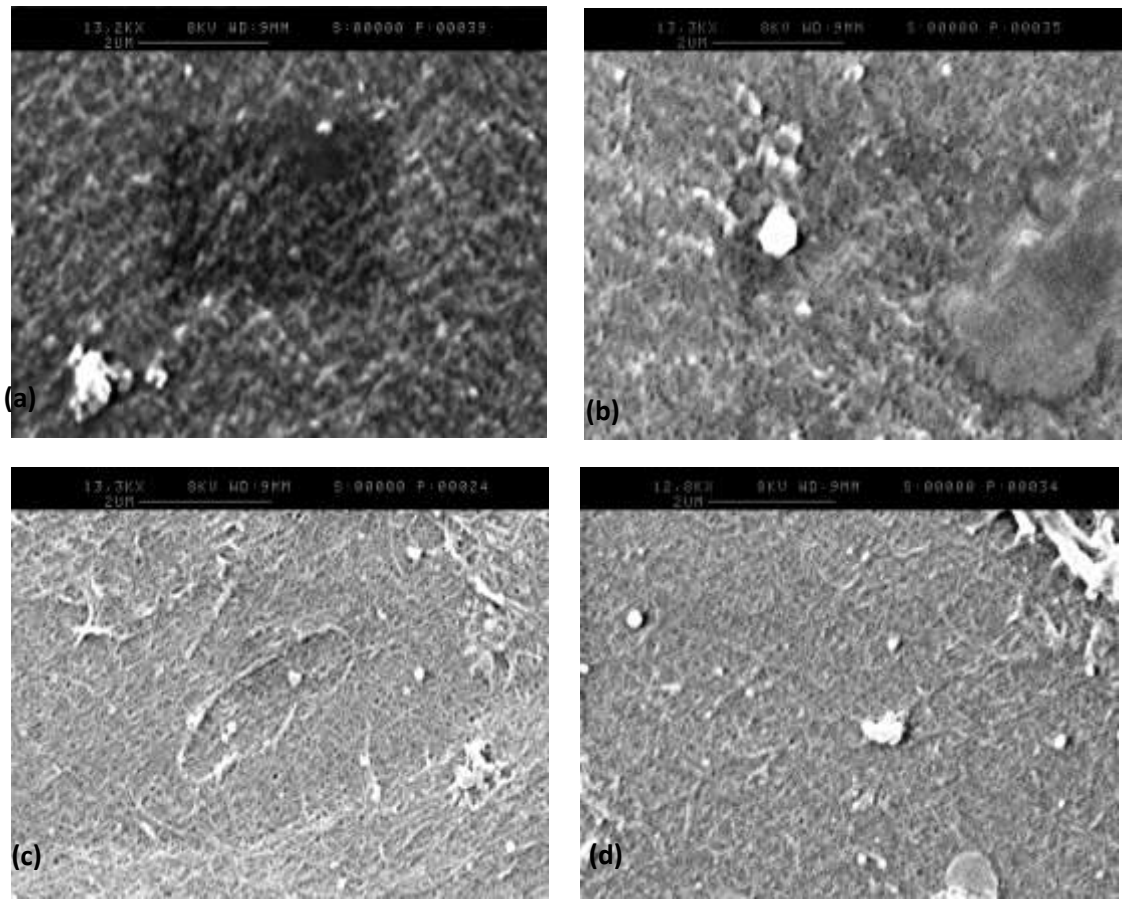

Figure 5.14: *Shows SEM images of nanofiber networks formed after adding media to Puramatrix peptide. Hydrogel nanofibers are more dense at higher peptide concentrations (a) 0.1% (b) 0.25% (c) 0.5% (d) 1%*

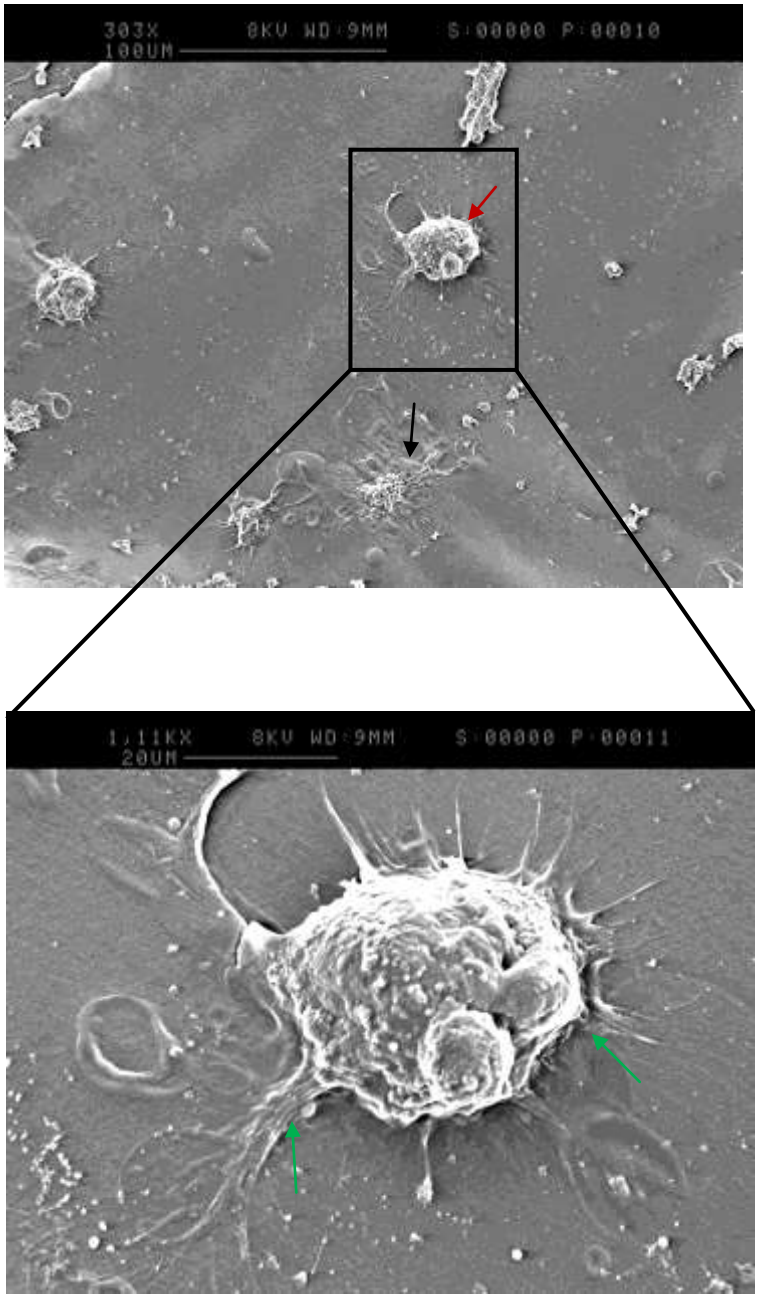

Figure 5.15: *Shows SEM images of rat calvarial cells grown on the surface of 0.1% Puramatrix hydrogel. Cells attached to the surface [black arrow] as well as cellular spheres [red arrow] can be seen, lamellipodia-like cell surface projections also are cleared [green arrow].*

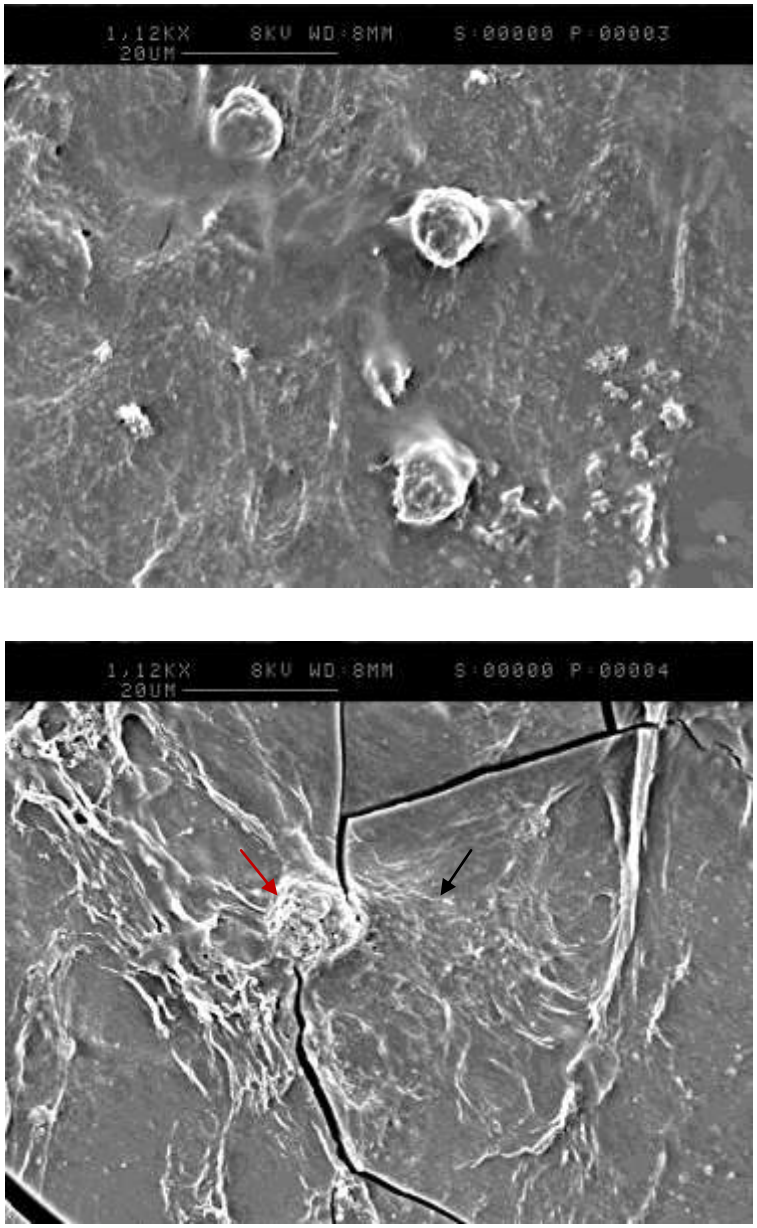

Figure 5.16: *Shows SEM images of rat calvarial cells grown on the surface of 0.25% Puramatrix hydrogel, cells attached to the surface of the hydrogel [black arrow] while others aggregated and formed spheres [red arrow]*

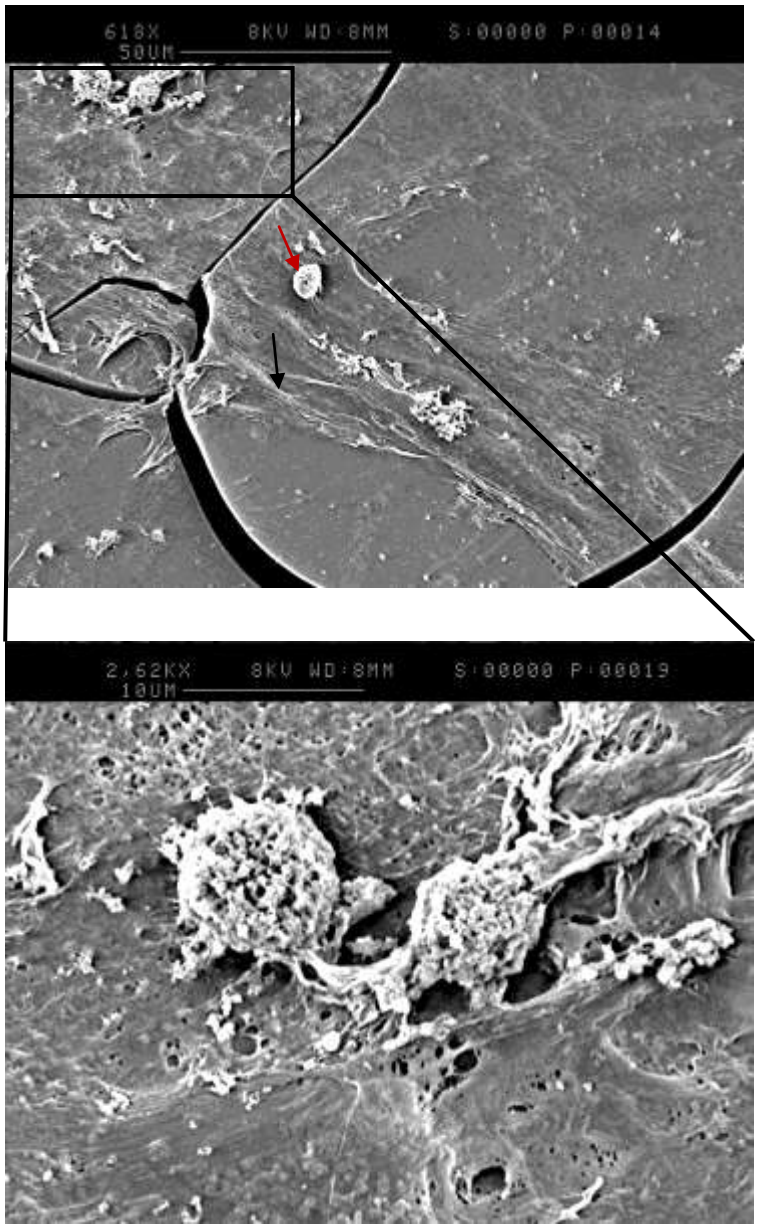

Figure 5.17: *Shows SEM images of rat calvarial cells grown on the surface of 0.5% Puramatrix hydrogel, most of the cells adhered to the surface [black arrow] forming monolayer with few clusters [red arrow]*

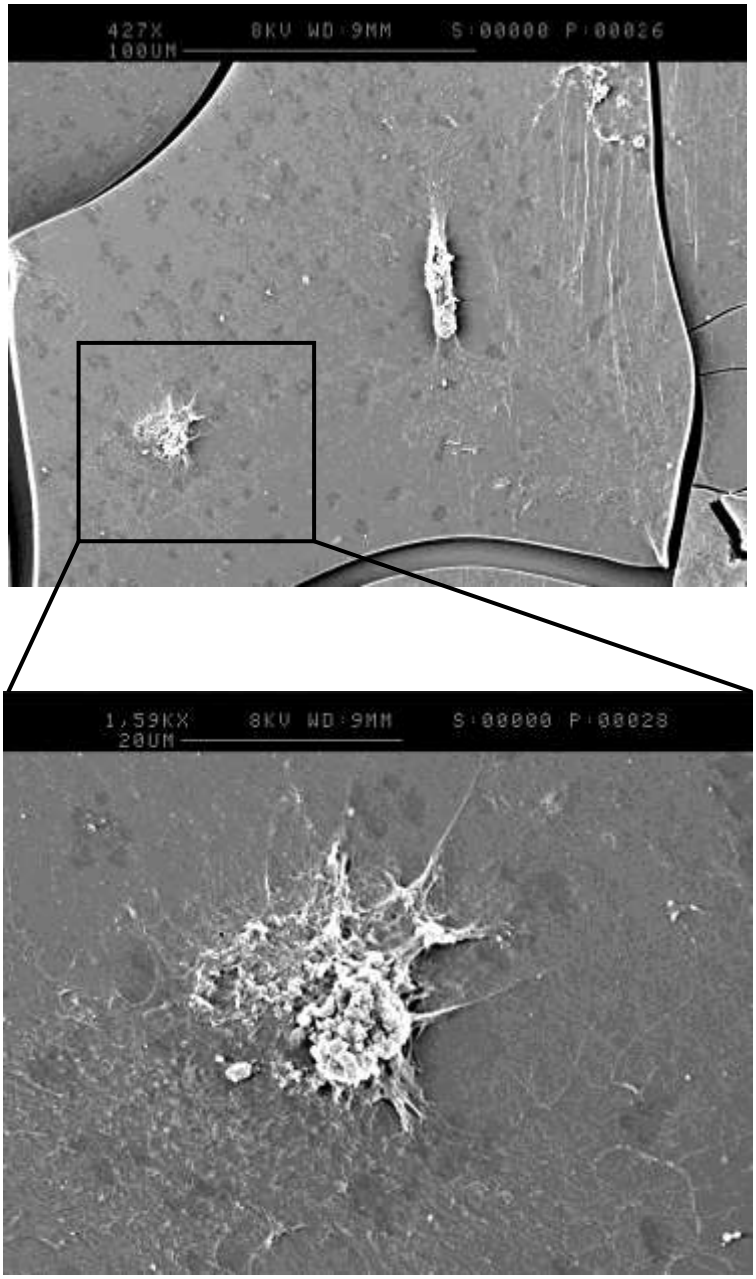

Figure 5.18: *Shows SEM images of rat calvarial cells grown on the surface of 1% Puramatrix hydrogel, few of the cells adhered to the surface of the scaffold [black arrow] and cellular clusters [red arrow] formed*

5.3.3 Cell viability in the hydrogel environment*:*

Cell viability was quantified using a standard MTT assay after 24hr, 72hr, and 7days of cell culture.

In Figure 5.19 the viability of calvarial cells and after 24hr of encapsulation with 0.25% of Puramatrix was significantly higher compared to 0.1% and 0.5%, with a significant increase in cells grown in normal media compared to osteogenic media. However, the viability was almost the same in both 0.1% and 0.5% with a non-significant small increase in cells grown under normal and osteogenic conditions, respectively. In contrast, the viability of encapsulated MSCs in both 0.25% and 0.5% grown in osteogenic and normal media respectively was significantly higher [Figure 5.20].

At 72hr the viability of the calvarial cells increased significantly in 0.1% and 0.5% while it decreased in 0.25% in both normal and osteogenic media [Figure 5.21]. While the viability of MSCs in 0.1% and 0.25%, with a slight decrease in 0.5%, was evident [Figure5.22]

At 7 days the viability of calvarial cells in all Puramatrix concentrations decreased compared to cells at 72hr, with significant differences between groups [Figure 5.23]. Whereas with MSCs the viability increased again in 0.1% and 0.5% in both normal and osteogenic media but decreased in 0.25% in cells grown under osteogenic media but there was a slight increase in the viability of cells in 0.25% under normal conditions [Figure 5.24].

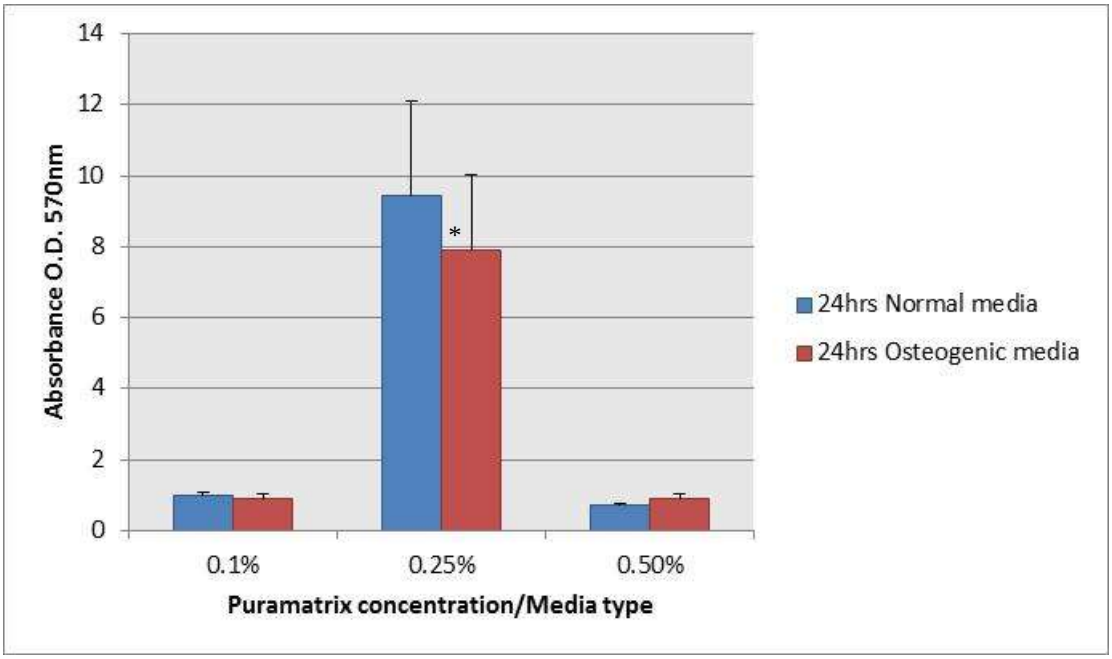

Figure 5.19 *Graph shows the viability of encapsulated calvarial rat cells after 24hr, the data represents the mean ± standard error of the mean n=9, a statistical significant was considered when P value ≤ 0.05 where (*) indicates significance compared to normal media.*

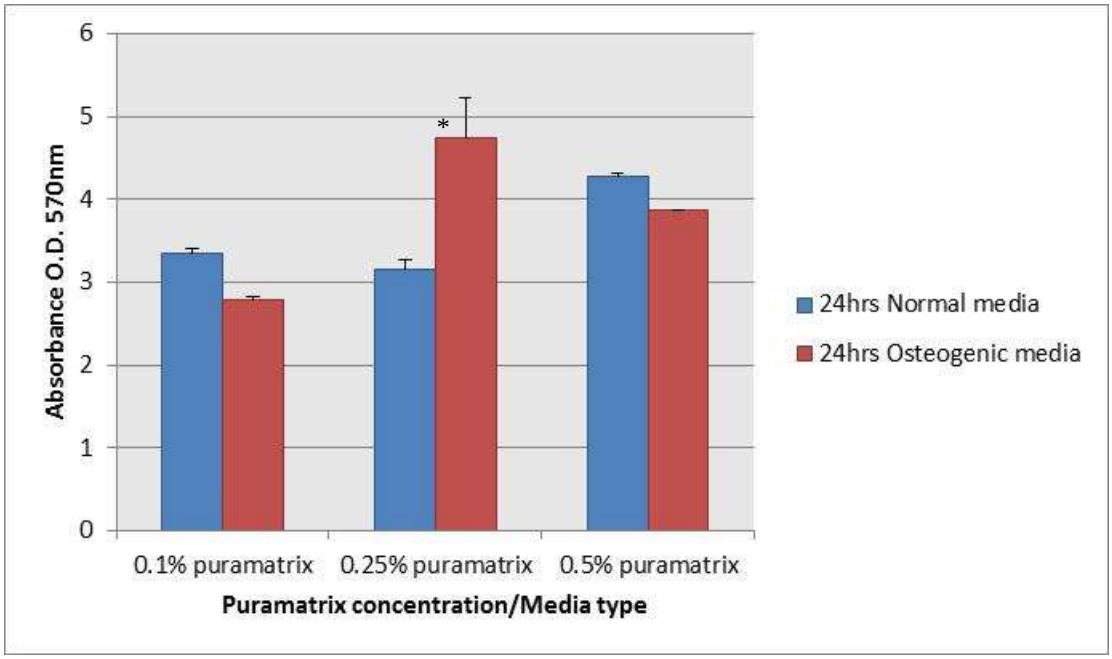

Figure 5.20 *Graph shows the viability of encapsulated human MSCs after 24hr, the data represents the mean ± standard error of the mean n=9, a statistical significant was considered when P value ≤ 0.05 where (*) indicates significance compared to normal media.*

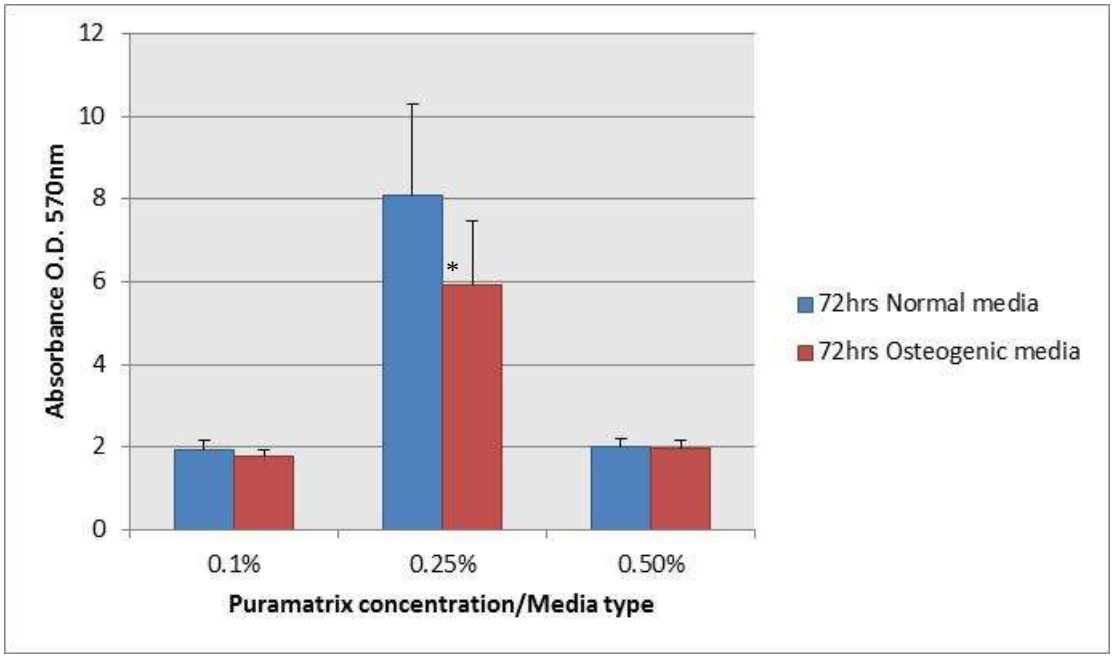

Figure 5.21 *Graph shows the viability of encapsulated calvaria rat cells at 72hr, the data represents the mean ± standard error of the mean n=9, a statistical significant was considered when P value ≤ 0.05 where (*) indicates significance compared to normal media.*

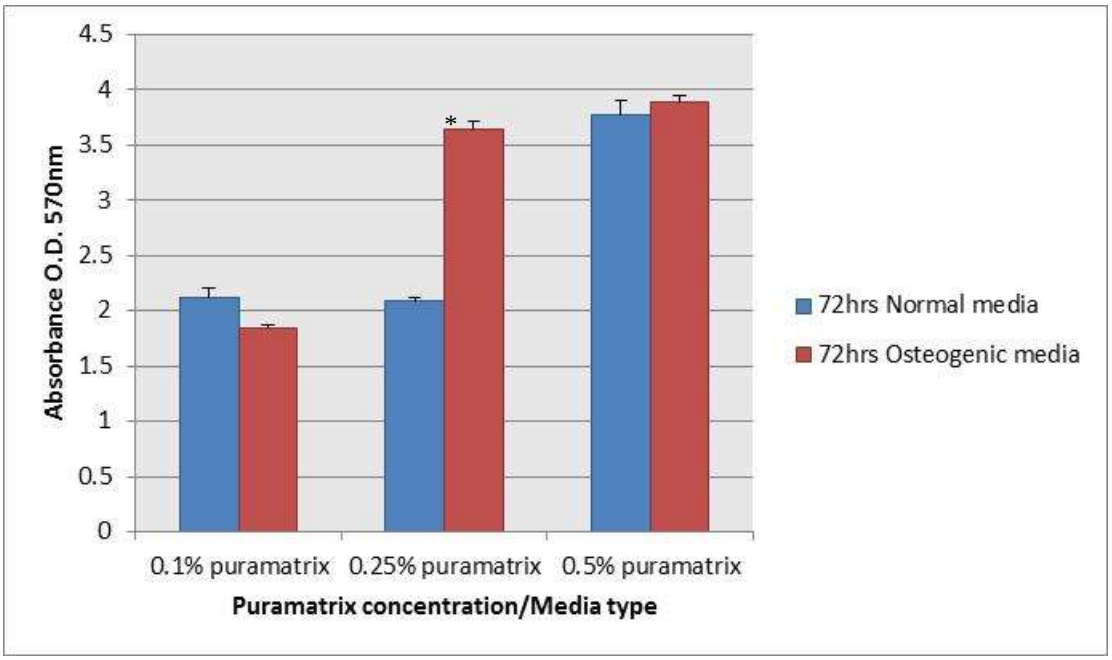

Figure 5.22 *Graph shows the viability of encapsulated human MSCs at 72hr, the data represents the mean ± standard error of the mean n=9, a statistical significant was considered when P value ≤ 0.05 where (*) indicates significance compared to normal media.*

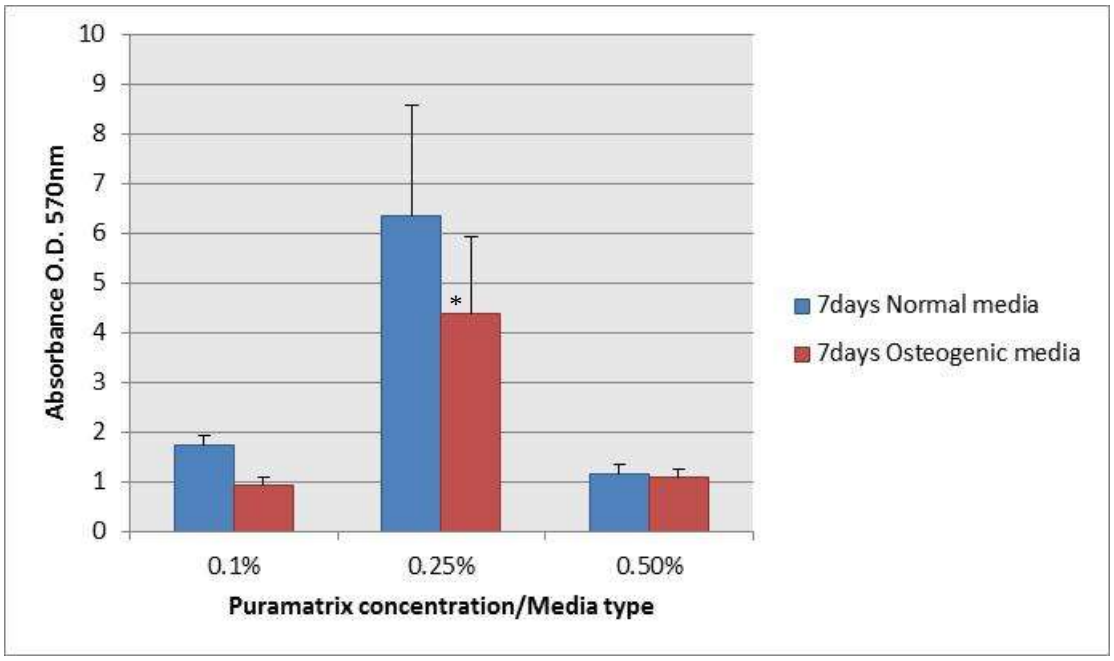

Figure 5.23 *Graph shows the viability of encapsulated calvarial rat cells at 7days, the data represents the mean ± standard error of the mean n=9, a statistical significant was considered when P value ≤ 0.05 where (*) indicates significance compared to normal media.*

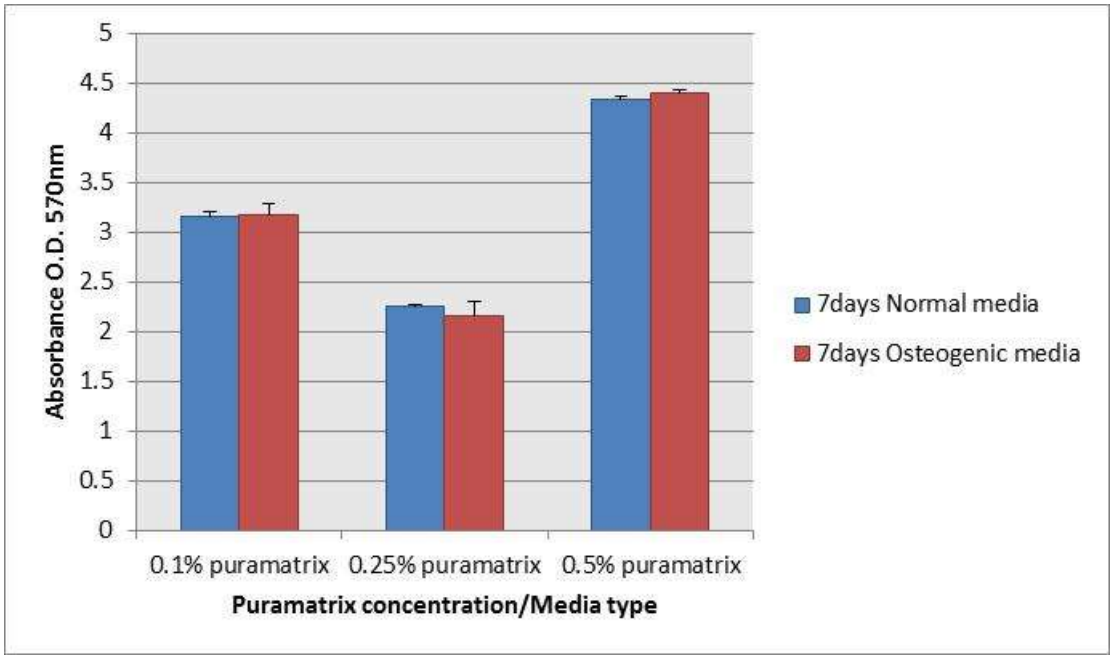

Figure 5.24 *Graph shows the viability of encapsulated human MSCs at 7days, the data represents the mean ± standard error of the mean n=9, a statistical significant was considered when P value ≤ 0.05. No significance were seen compared to normal media, though there were significance between groups*

5.3.4 Alkaline phosphatase activity assay:

Osteogenic differentiation was evaluated by measuring ALP enzyme activity. Figure 5.25 compares ALP activity between the three Puramatrix concentrations where a significant high level of ALP was recorded in calvarial cells encapsulated within 0.25% Puramatrix compared to 0.1% and 0.5% after 24 hr. Similarly, a significant high level of ALP was recorded in MSCs encapsulated within 0.25% Puramatrix but only under osteogenic conditions, whereas it was slightly higher in MSCs encapsulated within 0.5% compared to 0.1% and 0.25% [Figure 5.26]

At 72hr ALP activity decreased in calvarial cells within 0.25% Puramatrix, while the level remained almost the same in 0.1% Puramatrix in normal media with a slight decrease in osteogenic media. Interestingly, the activity of calvarial ALP within 0.5% Puramatrix increased in both normal and osteogenic media [Figure 5.27]. On the other hand, the activity of ALP enzyme in MSCs encapsulated in 0.1% Puramatrix decreased and reached almost the same level in both normal and osteogenic media. ALP activity also decreased in MSCs encapsulated with 0.25%, whereas in 0.5% the level of ALP increased under both normal and osteogenic conditions [Figure 5.28].

ALP activity at 7 days increased again in both calvarial cells grown in normal and osteogenic media in 0.1% Puramatrix. There was a slight increase in ALP activity in calvarial cells within 0.25% Puramatrix in normal media, but conversely, under osteogenic conditions, a slight decrease in ALP activity was noted. ALP activity decreased in calvarial cells encapsulated within 0.5% Puramatrix grown in normal media with a slight increase for those grown in osteogenic media [Figure 5.29]. However, ALP level in MSCs decreased slightly in MSCs encapsulated in 0.1% and 0.5% Puramatrix grown in normal media, while it increased under osteogenic conditions. In 0.25%

Puramatrix concentration the activity of the enzyme decreased in both normal and osteogenic media [figure 5.30].

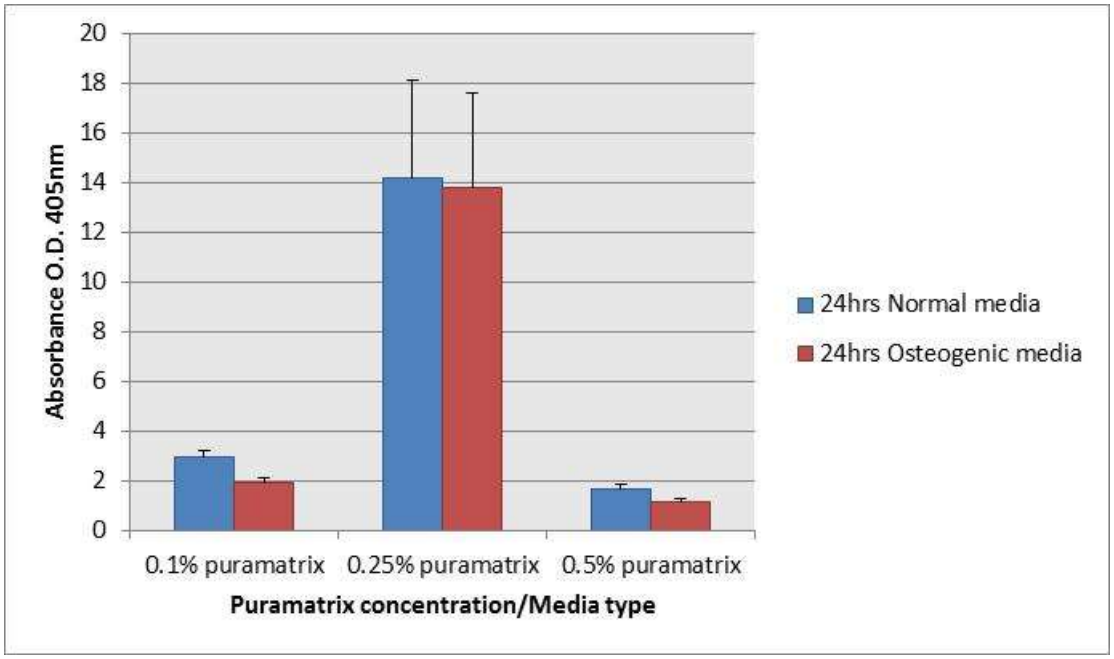

Figure 5.25 *Graph shows the alkaline phosphatase activity level of encapsulated calvarial cells after 24hr, the Data represents the mean ± standard error of the mean, n=9, a statistical significance was considered when P value ≤ 0.05. No significance detected compared to normal media, however there were between groups*

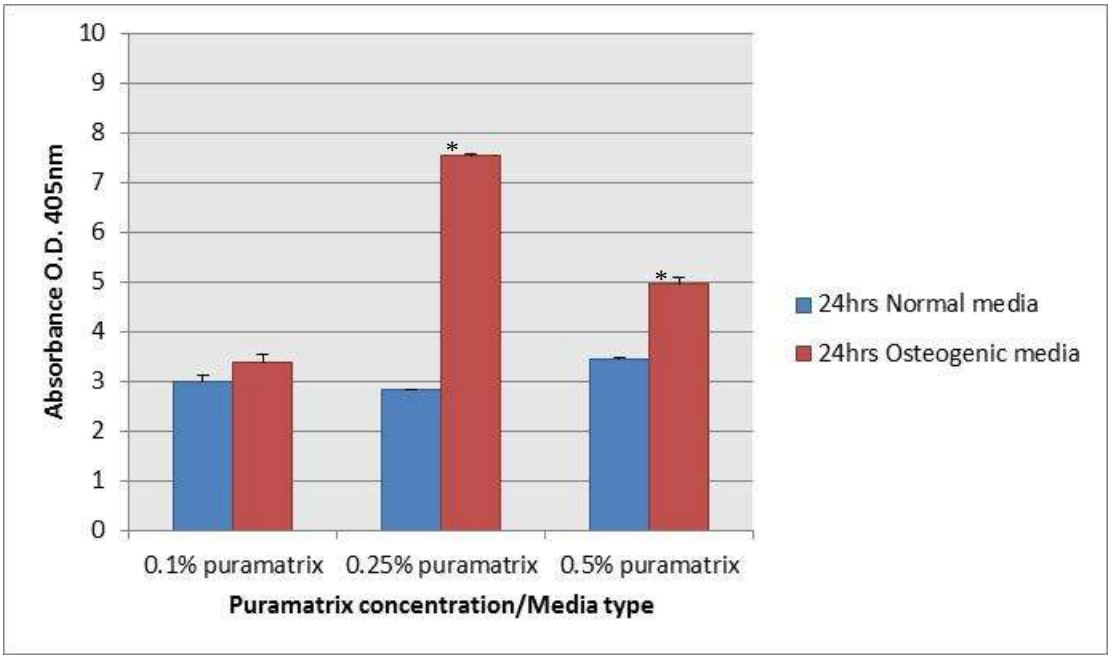

Figure 5.26 *Graph shows the alkaline phosphatase activity level of encapsulated human MSCs after 24hr, the Data represents the mean ± standard error of the mean n=9, a statistical significance was considered when P value ≤ 0.05 where (*) indicates significance compared to normal media.*

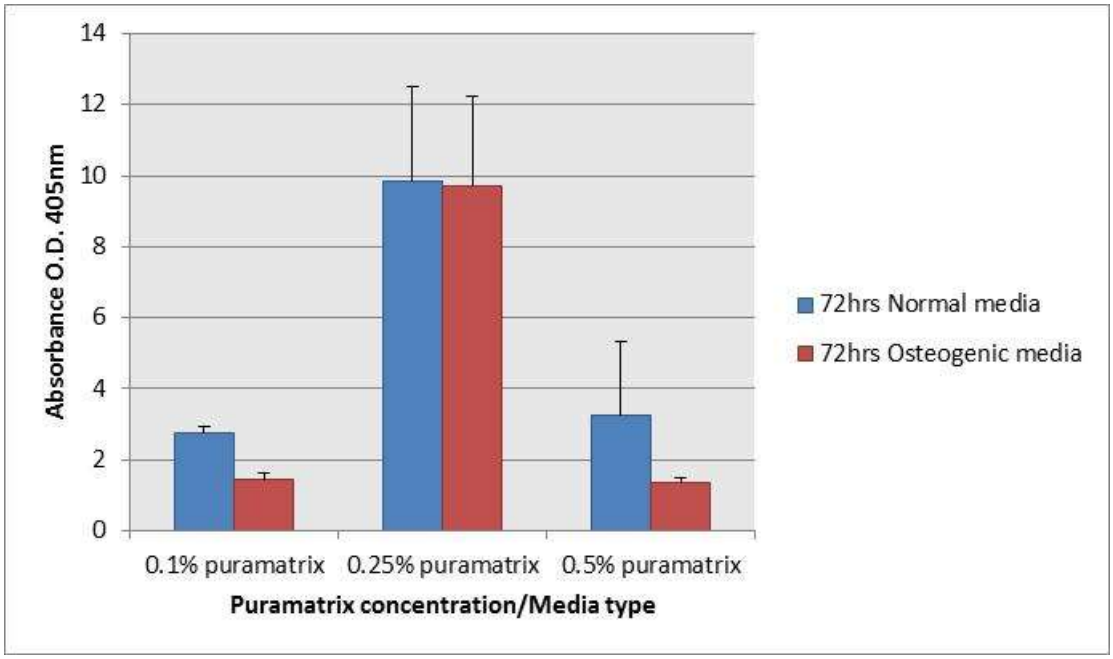

Figure 5.27 *Graph shows the alkaline phosphatase activity level of encapsulated calvarial cells at 72hr, the Data represents the mean ± standard error of the mean n=9, a statistical significance was considered when P value ≤ 0.05. No significance was detected compared to normal media, though significance was detected between groups.*

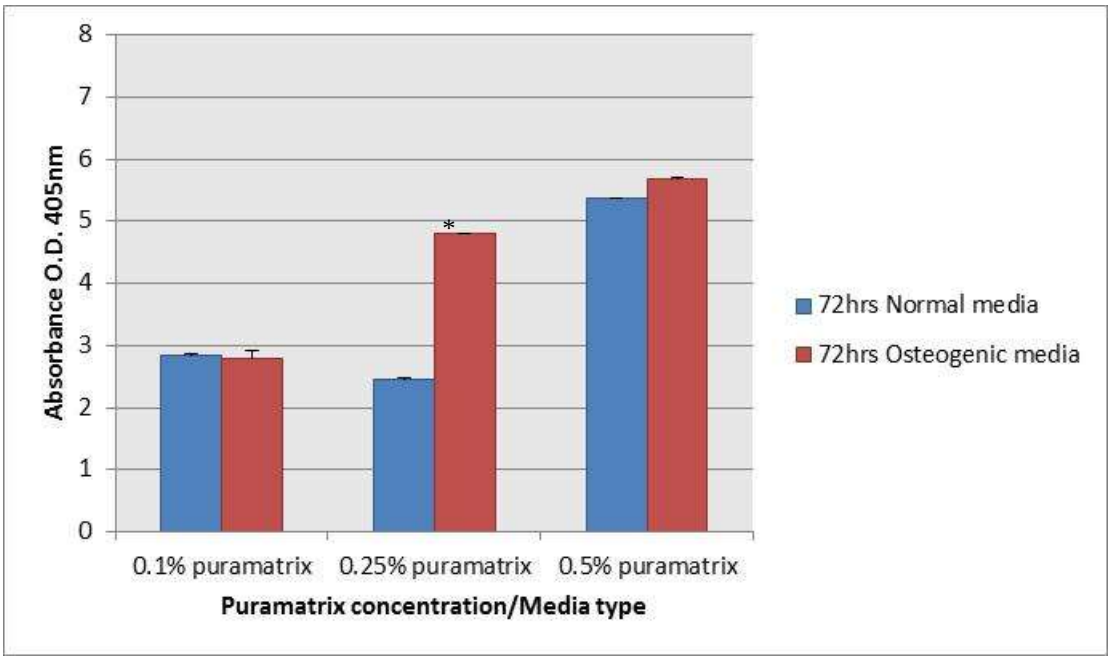

Figure 5.28 *Graph shows the alkaline phosphatase activity level of encapsulated human MSCs at 72hr, the Data represents the mean ± standard error of the mean n=9, a statistical significance was considered when P value ≤ 0.05 where (*) indicates significance compared to normal media.*

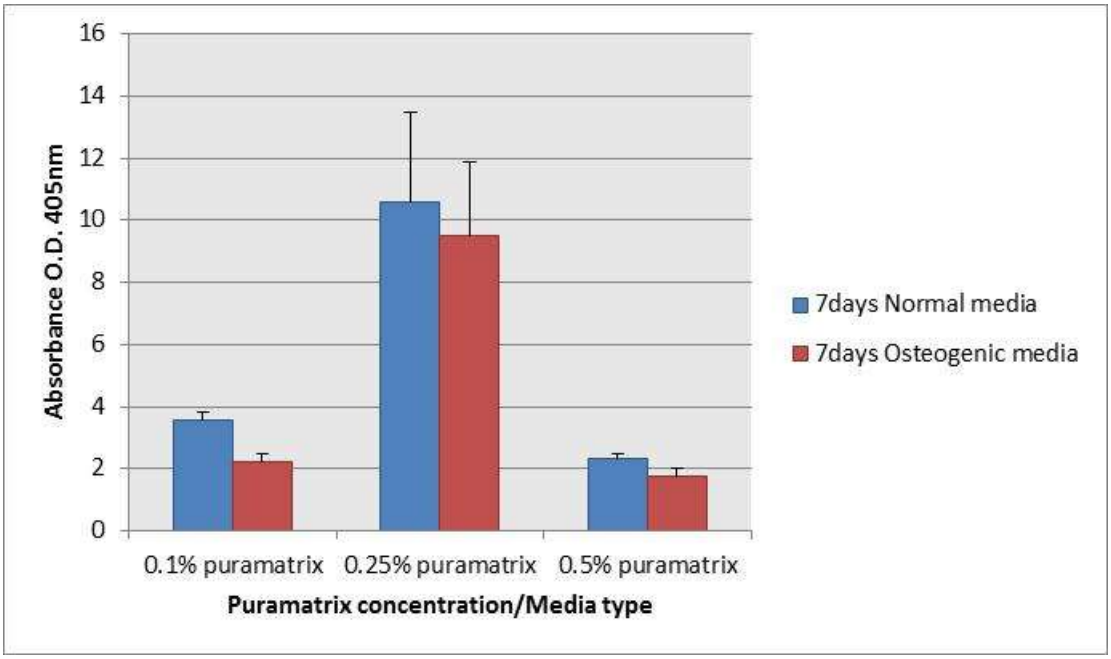

Figure 5.29 *Graph shows the alkaline phosphatase activity level of encapsulated calvarial cells at 7days, the data represents the mean ± standard error of the mean n=9, a statistical significance was considered when P value ≤ 0.05 No significance was detected compared to normal media, though significance was detected between groups.*

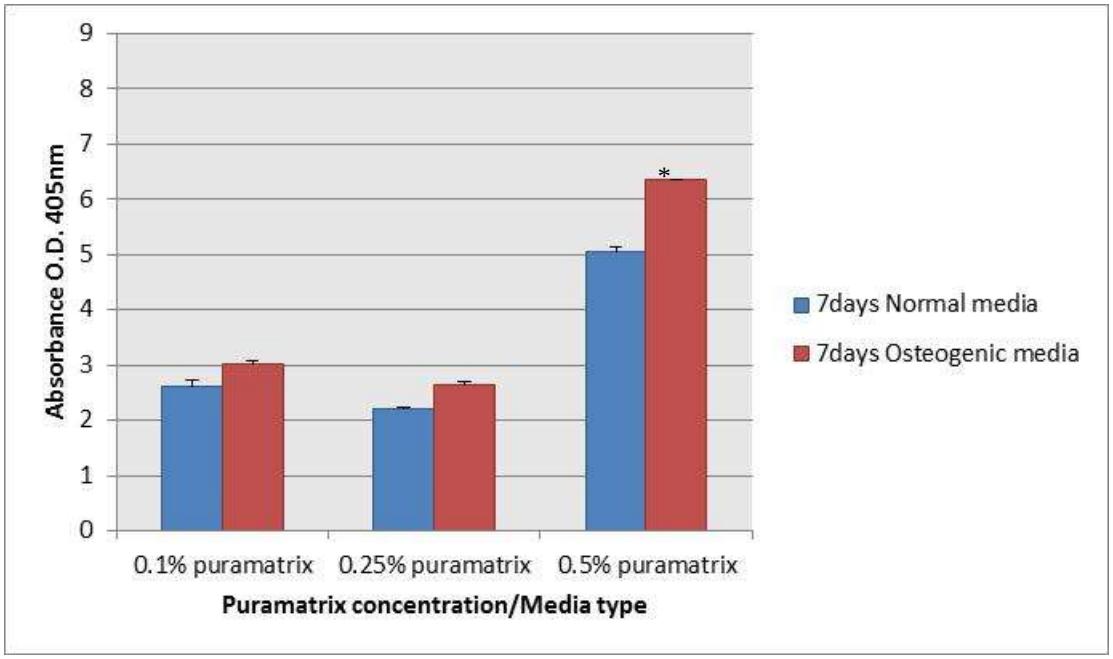

Figure 5.30 *Graph shows the alkaline phosphatase activity level of encapsulated human MSCs at 7days, the data represents the mean ± standard error of the mean, n=9, statistical significance was considered when P value ≤ 0.05 where (*) indicates significance compared to normal media.*

5.3.5 Modulation of gene expression by cells interacting with the hydrogel matrix:

The assessment of gene expression of osteogenic markers of cells encapsulated within the Puramatrix hydrogel was carried out using qRT-PCR.

After 24hr significant levels of ALP mRNA transcripts were detected in calvarial cells encapsulated within 0.5% and 0.25% grown in normal and osteogenic media respectively [Figure 31]. While a significant ALP expression was noted in MSCs encapsulated within 0.25% and 0.5% under osteogenic conditions [Figure 5.32].

The expression of the enzyme increased significantly at 72hr in calvarial cells in 0.1% in normal and osteogenic media and in 0.25% osteogenic media [Figure 5.33]. However, ALP mRNA levels reached a high level in MSCs under osteogenic conditions in 0.5% Puramatrix while it significantly decreased in 0.25% both under osteogenic condition [Figure 5.34].

Interestingly ALP expression in calvarial cells was higher in normal media compared to osteogenic media, where it was significant in 0.25% Puramatrix. However, the expression decreased in 0.1% normal compared to 72hr [Figure 5.35]. On the contrary, ALP gene expression was significantly high in MSCs encapsulated with 0.5% Puramatrix [Figure 5.36].

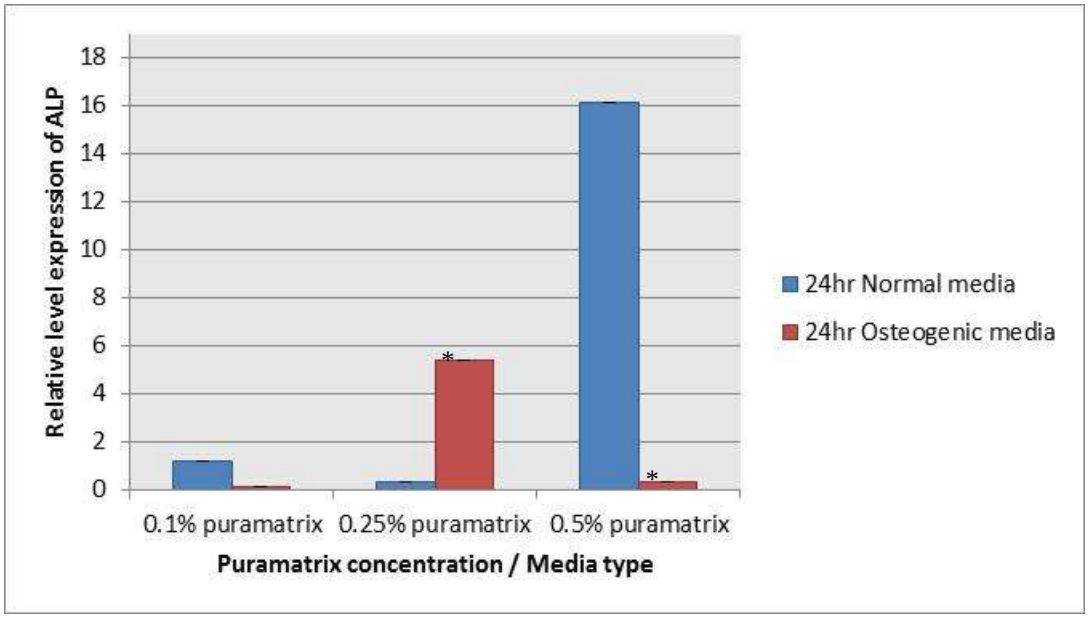

Figure 5.31 *ALP relative expression level in encapsulated calvarial cells after 24hr, the data represents the mean ± standard error of the mean n=9, a statistical significant was considered when P value ≤ 0.05 where (*) indicates significance compared to normal media.*

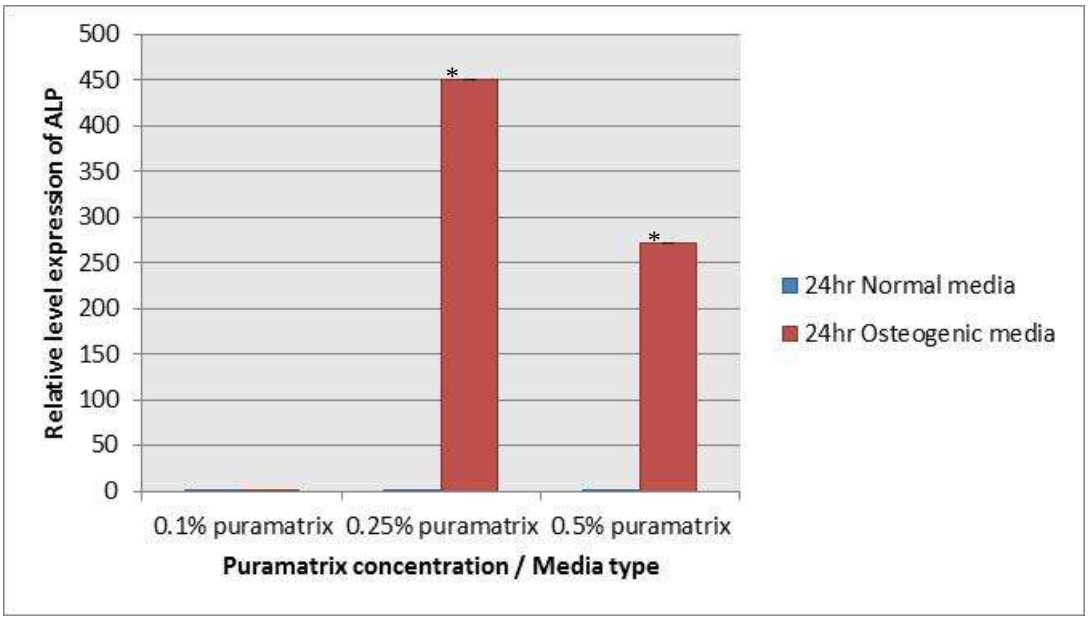

Figure 5.32 *ALP relative expression level in encapsulated MSCs after 24hr, the data represents the mean ± standard error of the mean n=9, a statistical significant was considered when P value ≤ 0.05 where (*) indicates significance compared to normal media.*

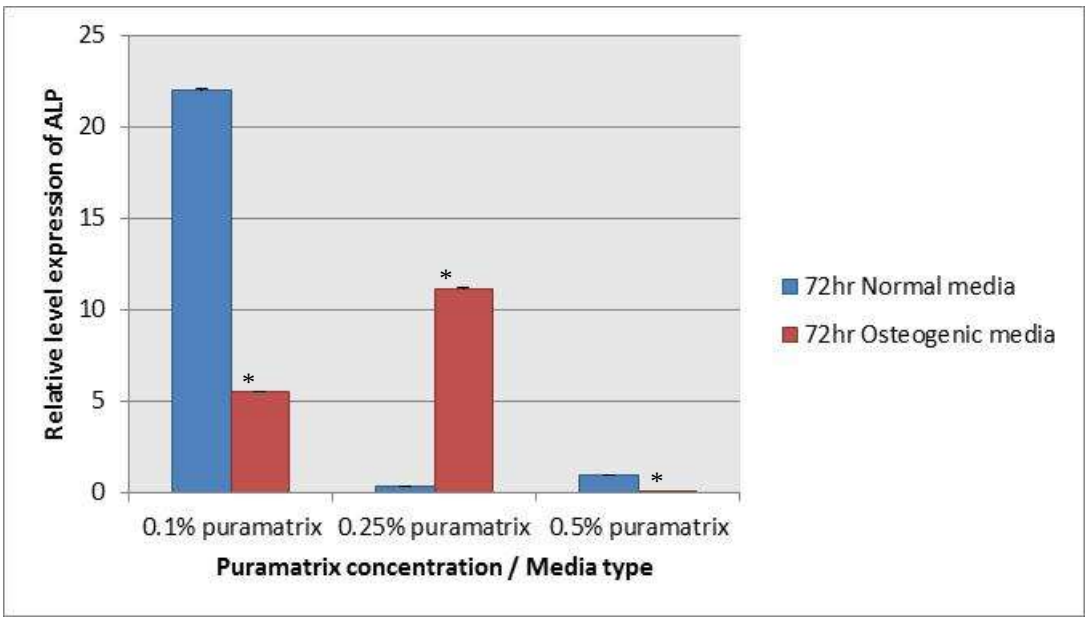

Figure 5.33 *ALP relative expression level in encapsulated calvarial cells at 72hr, the data represents the mean ± standard error of the mean n=9, a statistical significant was considered when P value ≤ 0.05 where (*) indicates significance compared to normal media.*

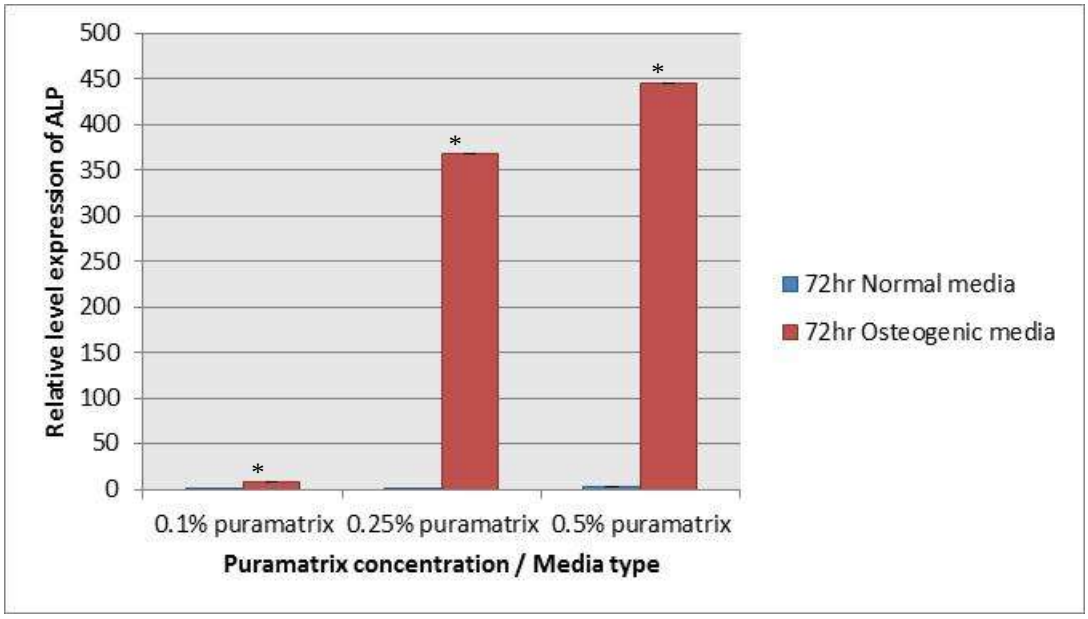

Figure 5.34 *relative expression level in encapsulated MSCs at 72hr, the data represents the mean ± standard error of the mean n=9, a statistical significant was considered when P value ≤ 0.05 where (*) indicates significance compared to normal media.*

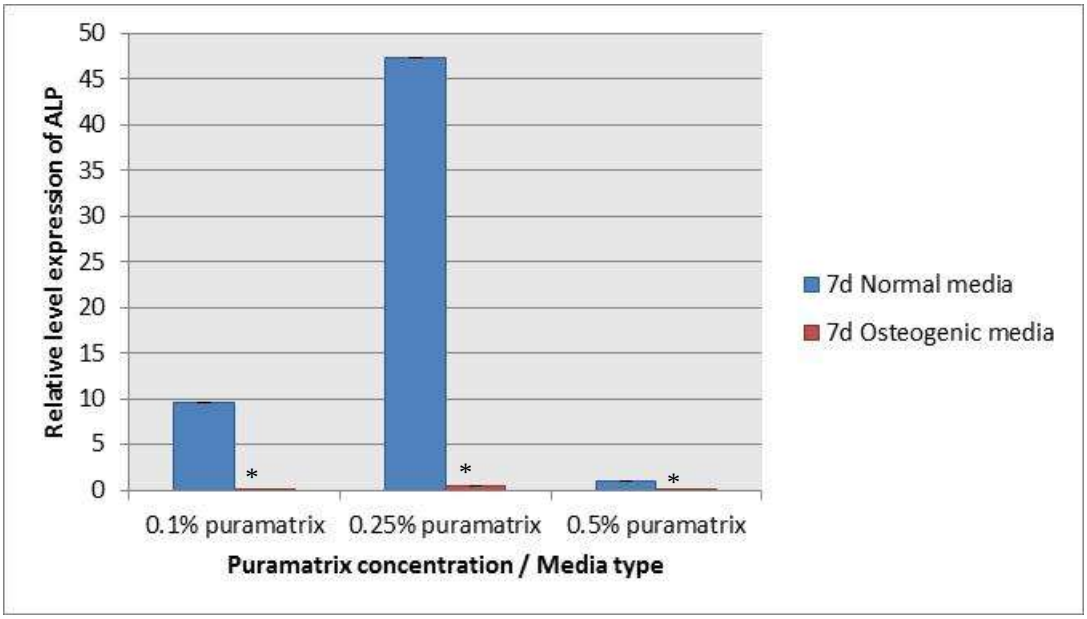

Figure 5.35 *ALP relative expression level in encapsulated calvarial cells at 7days, the Data represents the mean ± standard error of the mean n=9, a statistical significant was considered when P value ≤ 0.05 where (*) indicates significance compared to normal media.*

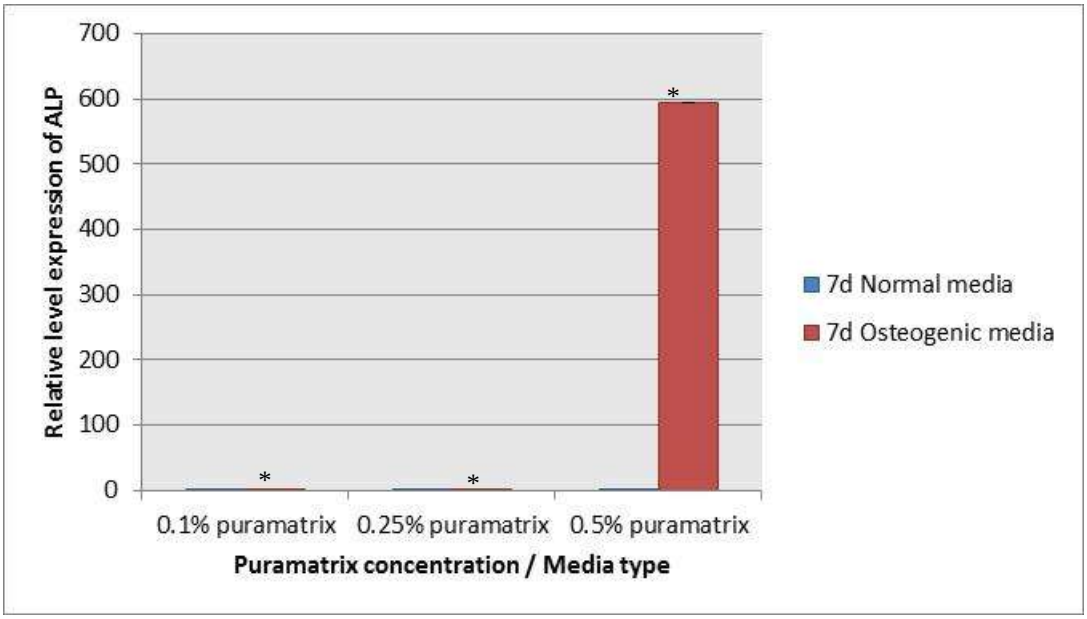

Figure 5.36 *ALP relative expression level in encapsulated MSCs at 7days, the Data represents the mean ± standard error of the mean n=9, a statistical significant was considered when P value ≤ 0.05 where (*) indicates significance compared to normal media.*

After 24hr the level of Runx2 gene expression was higher in 0.1% and 0.25% Puramatrix under osteogenic conditions compared to normal, interestingly expression was higher in normal media at the higher Puramatrix concentration (0.5%). Though, overall calvarial cells in 0.5% normal media scored a significant high level [Figure 5.37]. In contrast, Runx2 expression in MSCs encapsulated in 0.25% and 0.5% were higher in osteogenic media, whereas in 0.1% a slight increase in gene expression in normal media compared to osteogenic media was observed [Figure 5.38].

At 72hr Runx2 mRNA levels decreased in calvarial cells encapsulated in 0.5% Puramatrix while it increased in 0.1% and 0.25% in both normal and osteogenic media [Figure 5.39]. Whereas the expression increased significantly in MSCs encapsulated in 0.1%, 0.25% and 0.5% under osteogenic conditions, with a higher expression in 0.25% noted [Figure 5.40].

At 7 days the expression decreased in calvarial cells encapsulated in 0.1% Puramatrix, but increased in 0.25 and 0.5% under normal conditions [Figure 5.41]. In MSCs the expression of Runx2 decreased in 0.25% while it increased in 0.5% grown in osteogenic media compared to 72hr, but overall Runx2 expression was more under osteogenic not normal media [Figure 5.42].

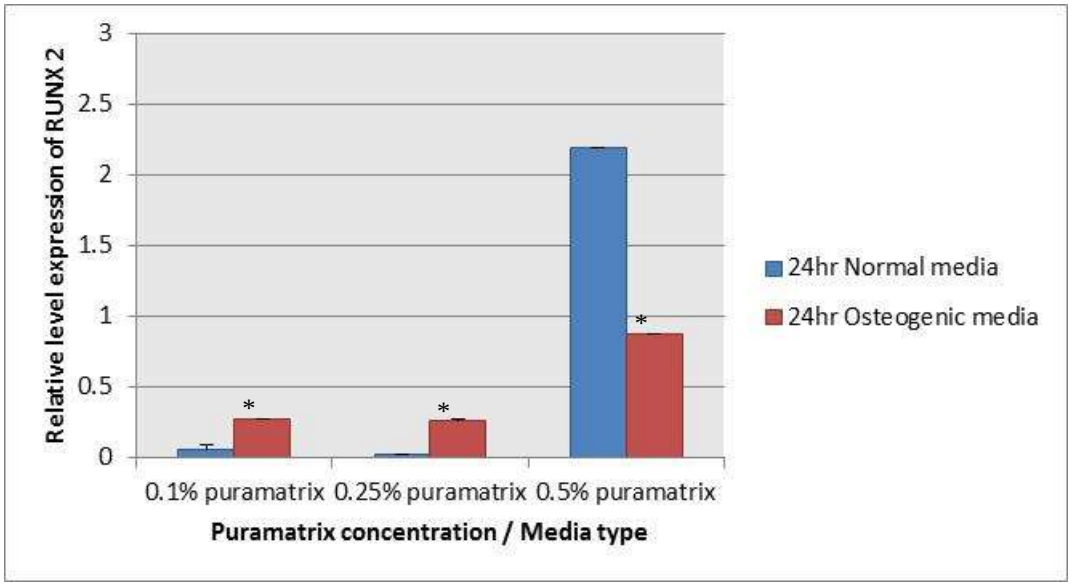

Figure 5.37 *RUNX 2 relative expression level in encapsulated calvarial cells after 24hr, the data represents the mean ± standard error of the mean n=9, a statistical significant was considered when P value ≤ 0.05 where (*) indicates significance compared to normal media.*

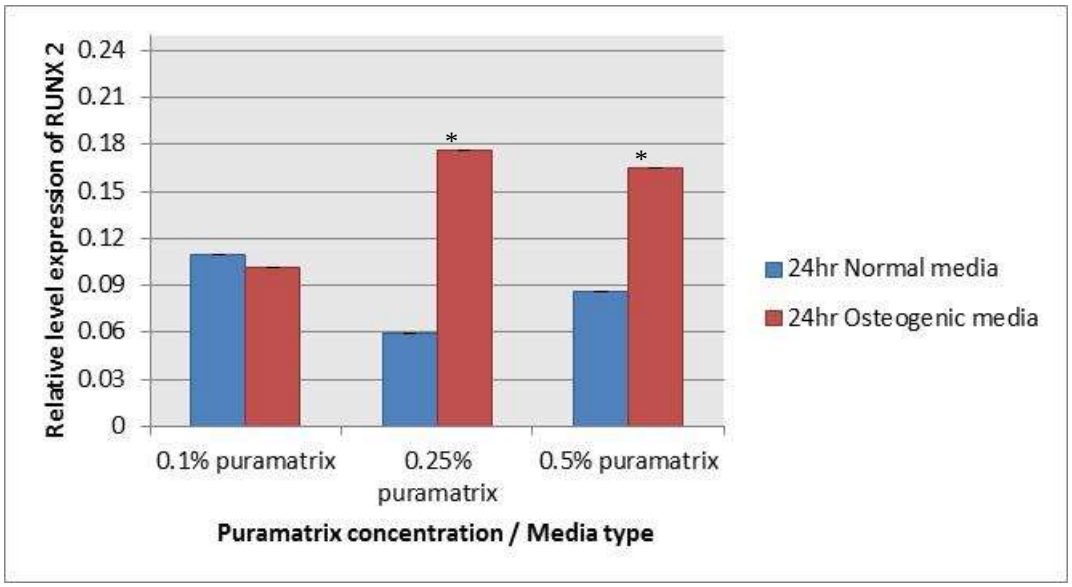

Figure 5.38 *RUNX 2 relative expression level in encapsulated MSCs after 24hr, the data represents the mean ± standard error of the mean n=9, a statistical significant was considered when P value ≤ 0.05 where (*) indicates significance compared to normal media.*

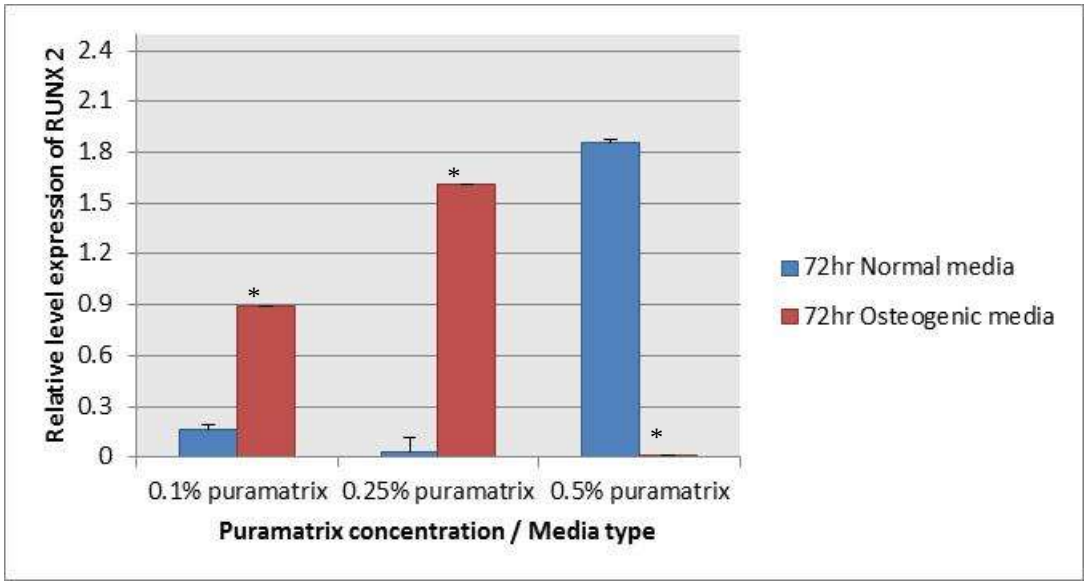

Figure 5.39 *RUNX 2 relative expression level in encapsulated calvarial cells at 72hr, the data represents the mean ± standard error of the mean n=9, a statistical significant was considered when P value ≤ 0.05 where (*) indicates significance compared to normal media.*

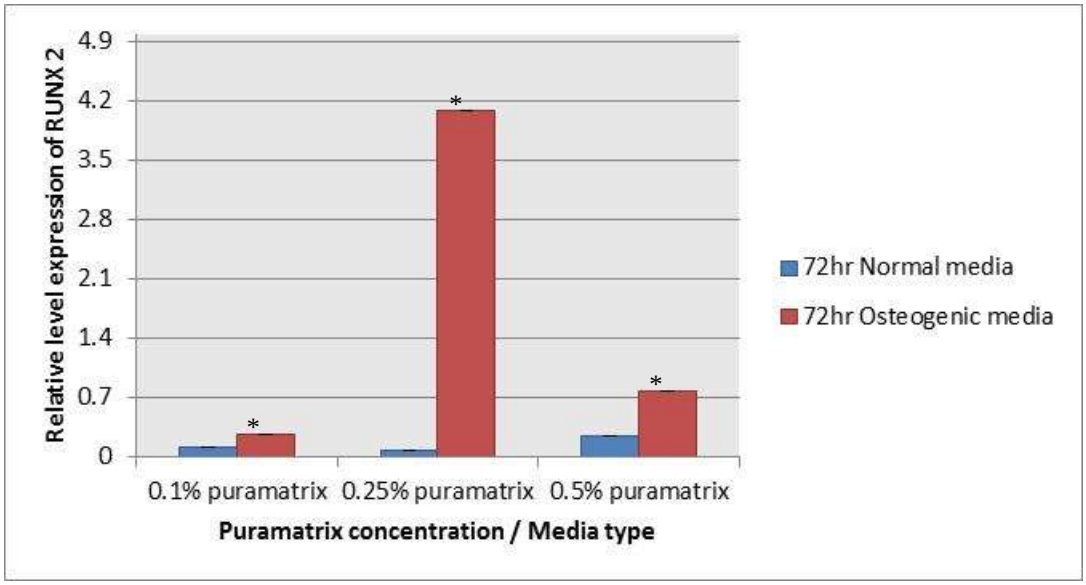

Figure 5.40 *RUNX 2 relative expression level in encapsulated MSCs at 72hr, the data represents the mean ± standard error of the mean n=9, a statistical significant was considered when P value ≤ 0.05 where (*) indicates significance compared to normal media.*

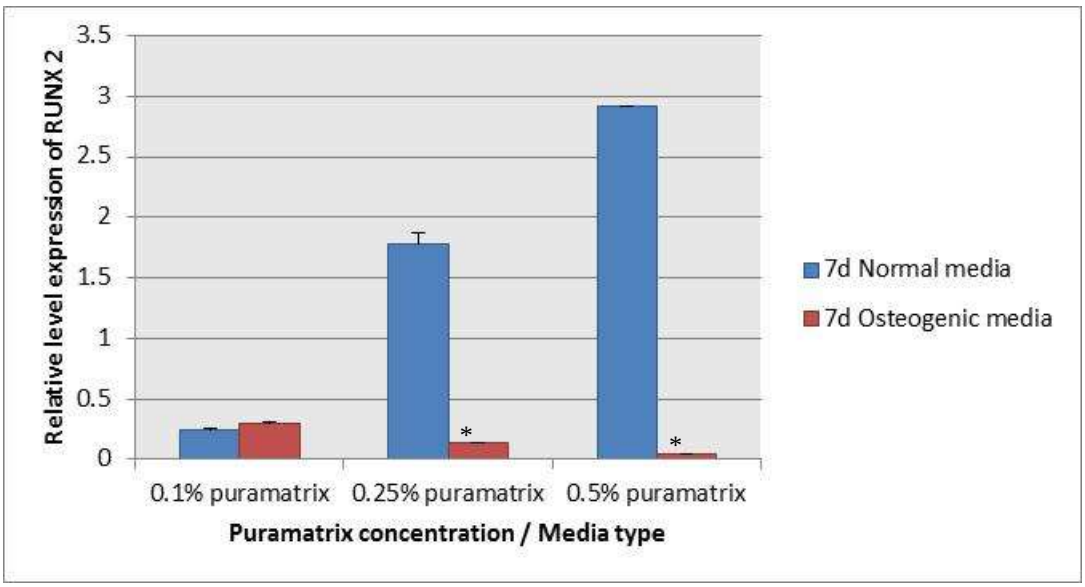

Figure 5.41 *RUNX 2 relative expression level in encapsulated calvaria cells at 7days, the data represents the mean ± standard error of the mean n=9, a statistical significant was considered when P value ≤ 0.05 where (*) indicates significance compared to normal media.*

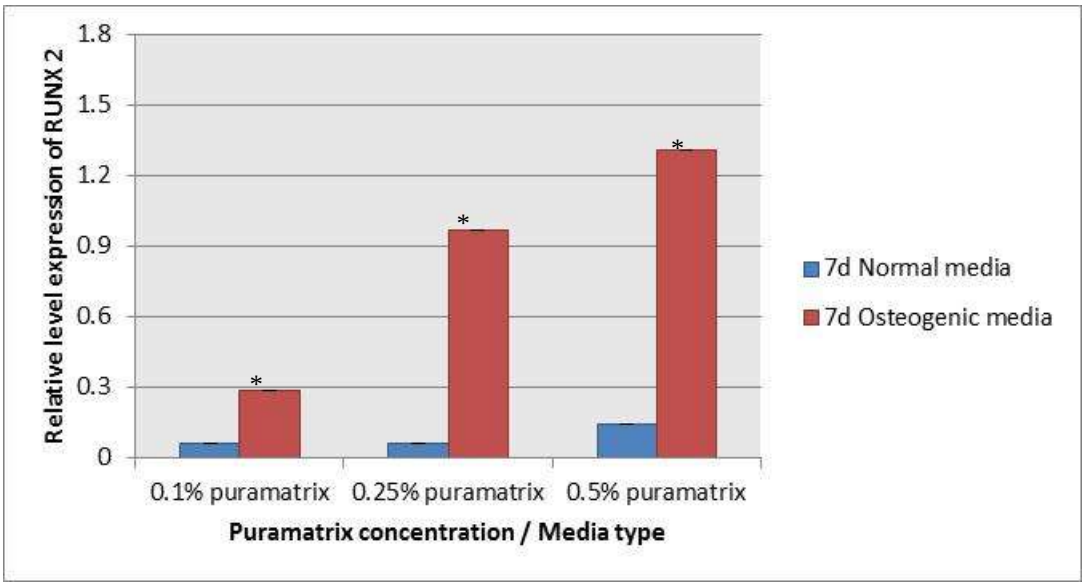

Figure 5.42 *RUNX 2 relative expression level in encapsulated MSCs at 7days, the data represents the mean ± standard error of the mean n=9, a statistical significant was considered when P value ≤ 0.05 where (*) indicates significance compared to normal media.*

SP7 gene expression was significantly elevated in calvarial cells in 0.5% Puramatrix and osteogenic media after 24hr; the expression was also high in 0.25% Puramatrix and osteogenic media unlike 0.1% Puramatrix where it was higher in normal media [Figure 5.43]. Similarly, in MSCs the expression was higher in 0.5% Puramatrix and osteogenic media [Figure 5.44].

At 72hr, the expression of SP7 increased significantly in calvaria cells encapsulated in all Puramatrix concentrations under osteogenic media conditions [Figure 5.45]. However, in MSCs the expression increased significantly in 0.1% and 0.25% in osteogenic media, increased in 0.5% in normal media only while it decreased in osteogenic media [figure 4.46].

At 7 days, the expression of the gene decreased significantly in all Puramatrix concentrations, though the expression was higher in osteogenic media [Figure 5.47]. In contrast, SP7 expression increased in MSCs encapsulated within 0.5% Puramatrix grown in osteogenic media and decreased when grown in normal media. Conversely, the expression decreased in MSCs encapsulated in 0.2% and 0.1% grown in osteogenic media with a slight increase in those grown in normal media [Figure 4.48].

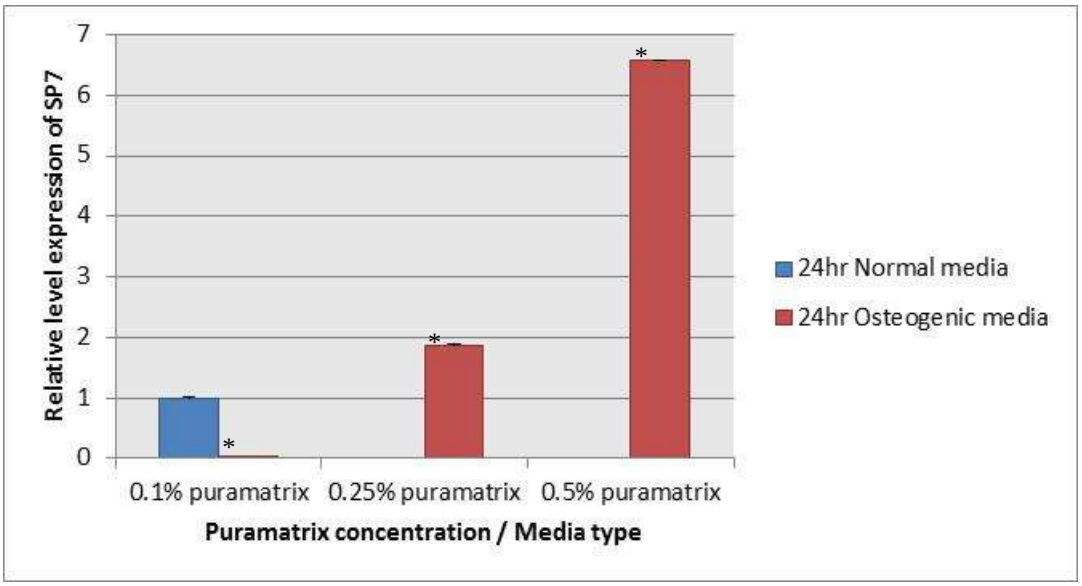

Figure 5.43 *SP7 relative expression level in encapsulated calvarial cells after 24hr, the data represents the mean ± standard error of the mean n=9, a statistical significant was considered when P value ≤ 0.05 where (*) indicates significance compared to normal media.*

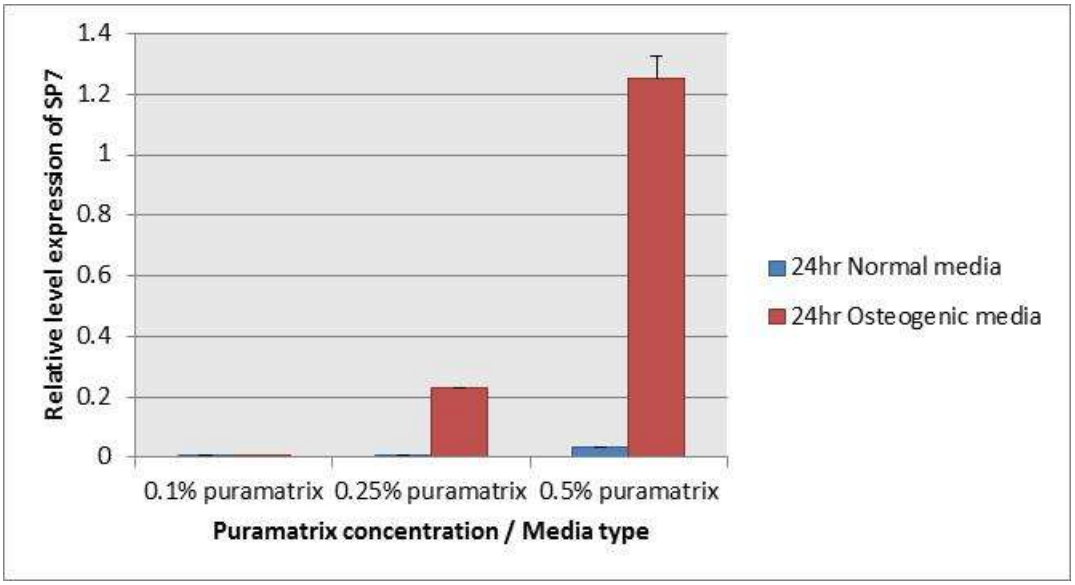

Figure 5.44 *SP7 relative expression level in encapsulated MSCs after 24hr, the data represents the mean ± standard error of the mean, n=9, No statistical significant was detected.*

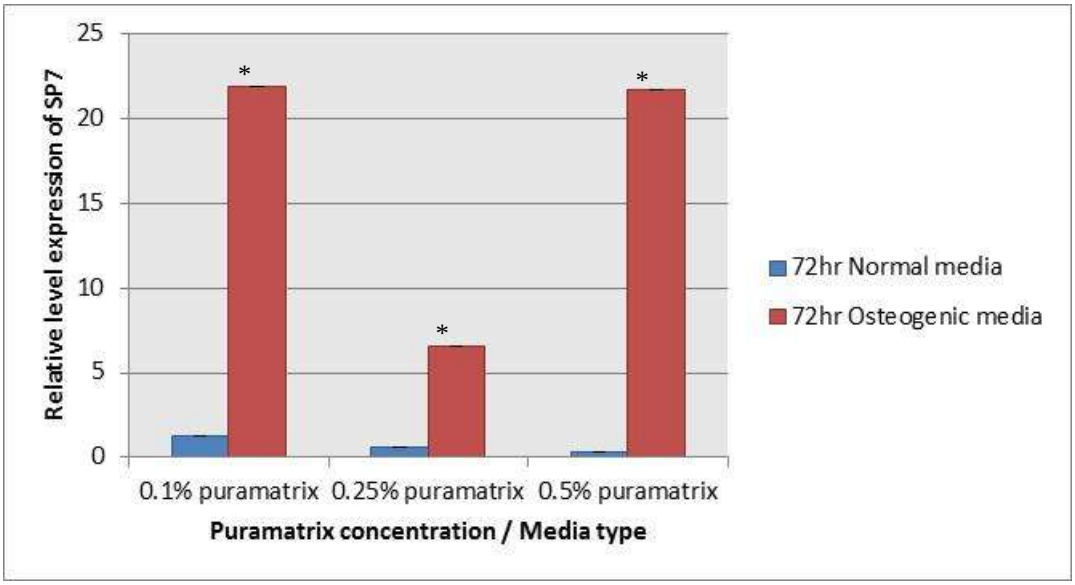

Figure 5.45 *SP7 relative expression level in encapsulated calvaria cells at 72hr, the data represents the mean ± standard error of the mean n=9, a statistical significant was considered when P value ≤ 0.05 where (*) indicates significance compared to normal media.*

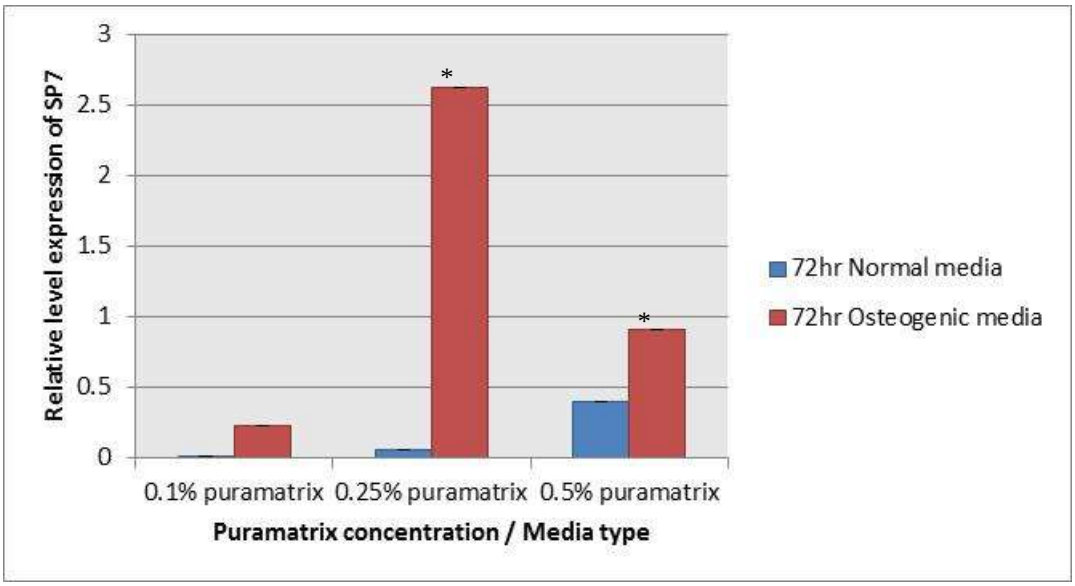

Figure 5.46 *SP7 relative expression level in encapsulated MSCs at 72hr, the data represents the mean ± standard error of the mean n=9, a statistical significant was considered when P value ≤ 0.05 where (*) indicates significance compared to normal media.*

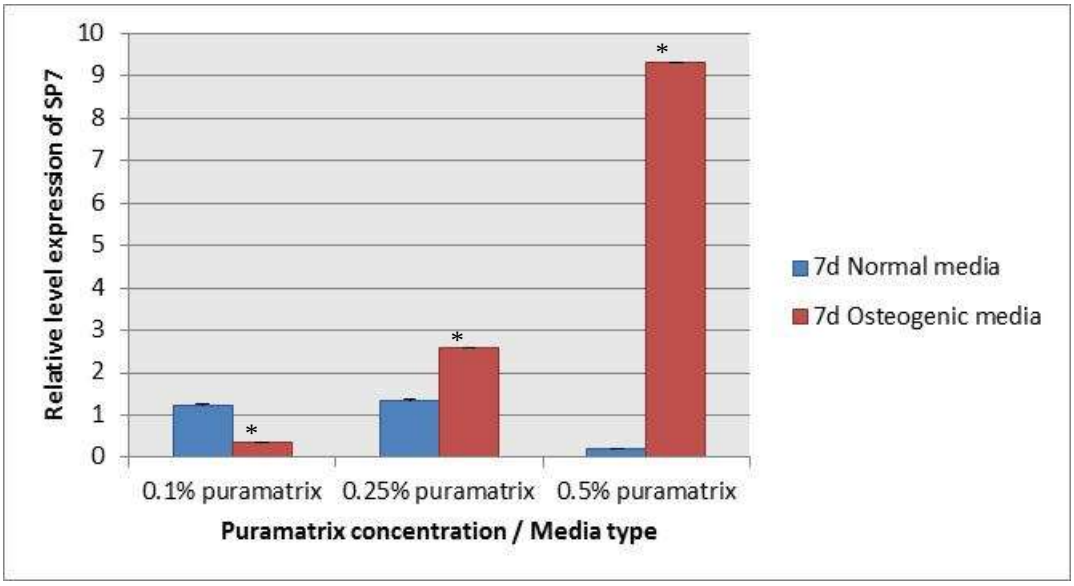

Figure 5.47 *SP7 relative expression level in encapsulated calvaria cells at 7days, the data represents the mean ± standard error of the mean n=9, a statistical significant was considered when P value ≤ 0.05 where (*) indicates significance compared to normal media.*

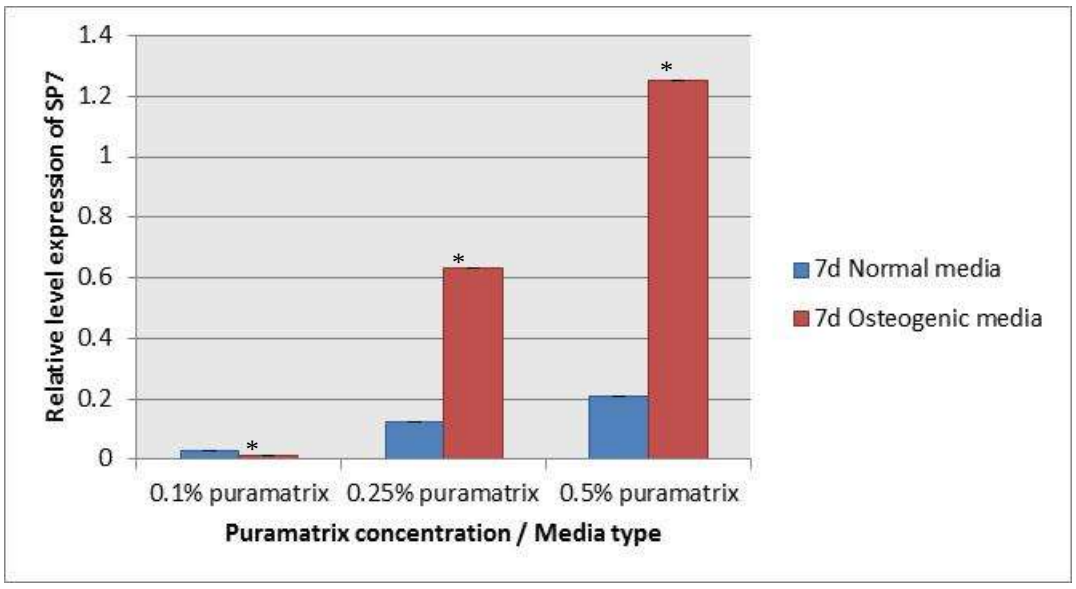

Figure 5.48 *SP7 relative expression level in encapsulated MSCs at 7days, the Data represents the mean ± standard error of the mean n=9, a statistical significant was considered when P value ≤ 0.05 where (*) indicates significance compared to normal media.*

As seen in Figure 5.49 Cx43 was expressed significantly by calvarial cells embedded in 0.1% Puramatrix compared to 0.25% and 0.5%. Whereas in MSCs there was no significant differences in Cx43 expression in all three concentrations, though it was higher on cells grown in normal media [figure 5.50].

Cx43 expression at 72hr increased significantly in calvarial cells within 0.1% Puramatrix compared to 0.25% and 0.5%, this rise was in both normal and osteogenic media though it was more in former [figure 5.51]. In MSCs, Cx43 expression level was almost the same as 24hr under normal and osteogenic media in cells embedded in 0.1% and 0.5% respectively, while it increased significantly under normal and osteogenic media in 0.5% and 0.1% respectively. The expression also increased in 0.25% in both normal and osteogenic media [Figure 5.52].

At 7days the expression in calvarial cells dropped significantly in 0.1% concentration under both normal and osteogenic media [Figure 5.53]. Interestingly, Cx43 increased significantly in cells within 0.25% grown in normal media while it decreased in osteogenic media [Figure 5.53]. On the other hand, MSCs in 0.1% and 0.25% Puramatrix showed Cx43 expression dropping in both normal and osteogenic media and in 0.5% Puramatrix and normal media [figure 5.54]. However, a significant high expression level of Cx43 was noted in MSCs encapsulated in 0.5% Puramatrix grown in osteogenic media [figure 5.54].

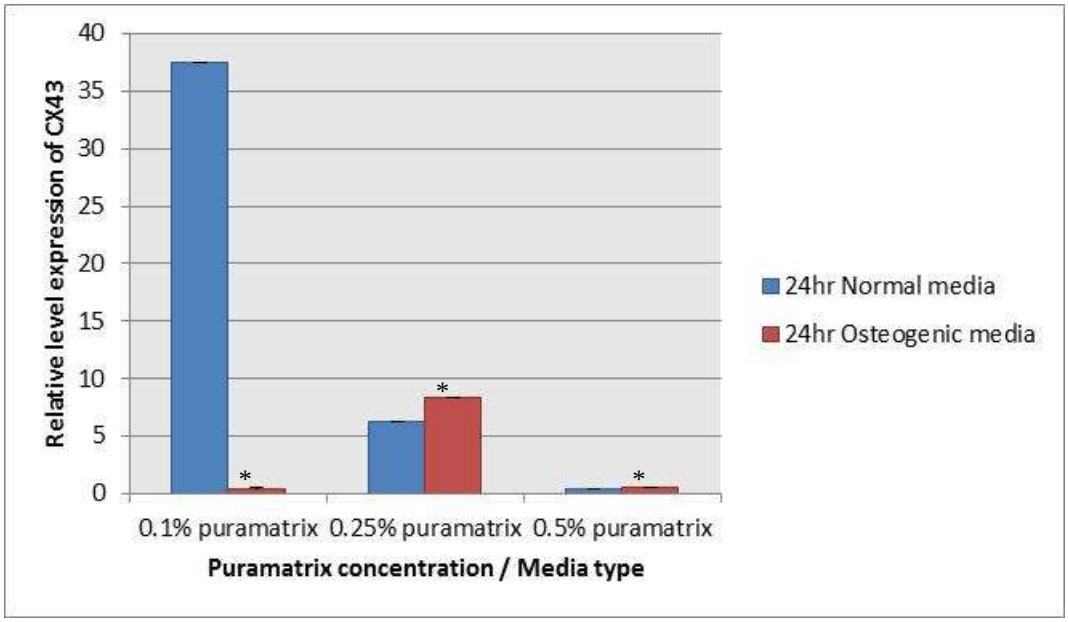

Figure 5.49 *CX43 relative expression level in encapsulated calvarial cells after 24hr, the Data represents the mean ± standard error of the mean n=9, a statistical significant was considered when P value ≤ 0.05 where (*) indicates significance compared to normal media.*

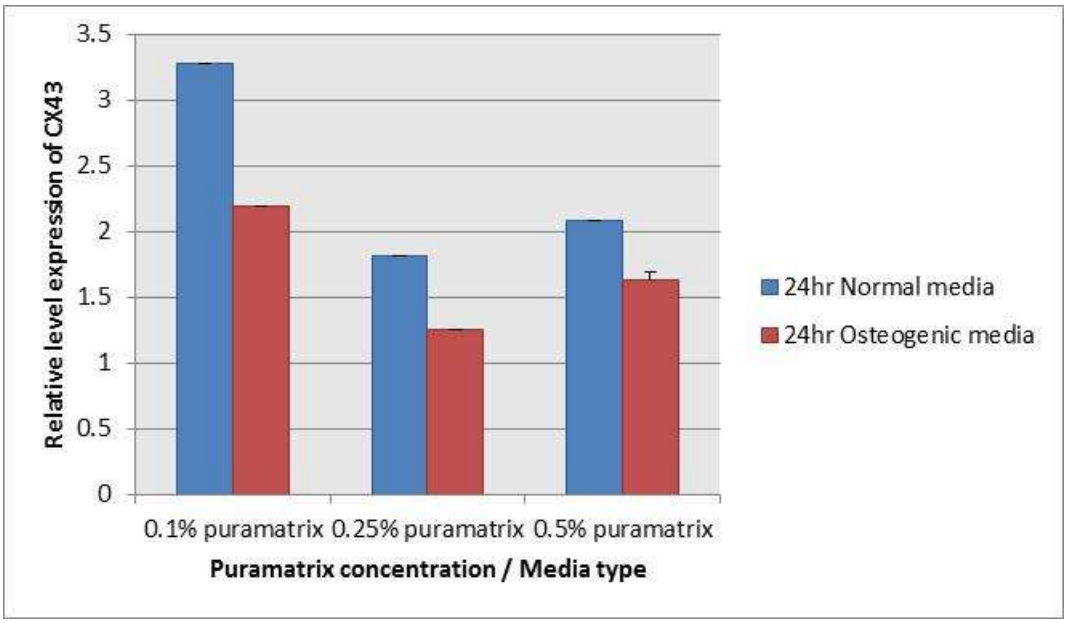

Figure 5.50 *CX43 relative expression level in encapsulated MSCs after 24hr, the data represents the mean ± standard error of the mean n=9, a statistical significant was detected here*

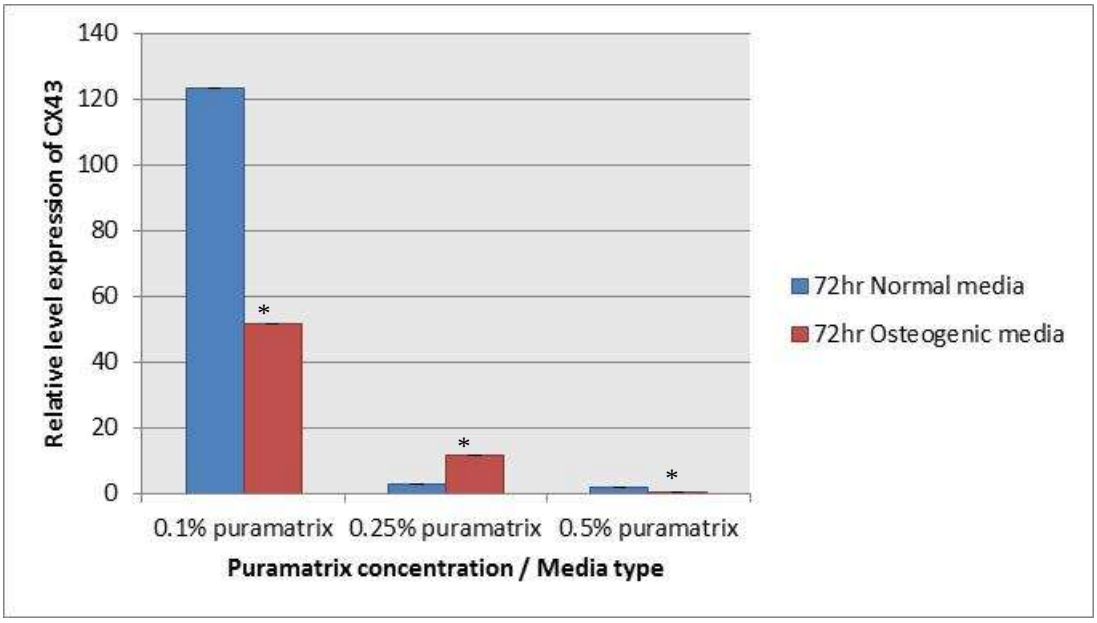

Figure 5.51 *CX43 relative expression level in encapsulated calvarial cells at 72hr, the data represents the mean ± standard error of the mean n=9, a statistical significant was considered when Pvalue ≤ 0.05 where (*) indicates significance compared to normal media.*

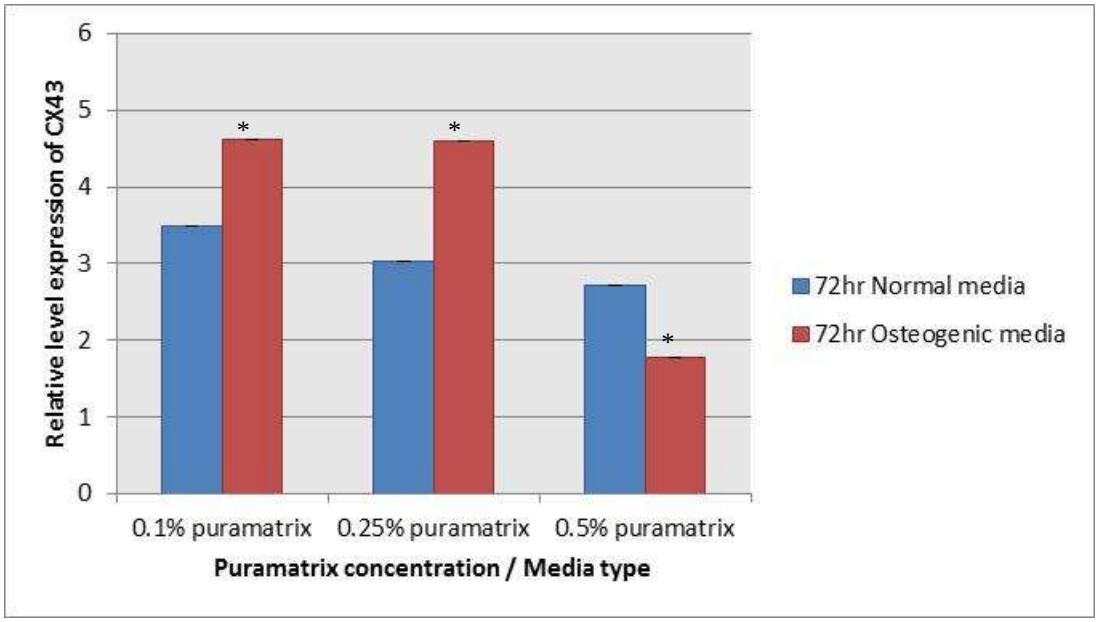

Figure 5.52 *CX43 relative expression level in encapsulated MSCs at 72hr, the data represents the mean ± standard error of the mean n=9, a statistical significant was considered when P value ≤ 0.05 where (*) indicates significance compared to normal media.*

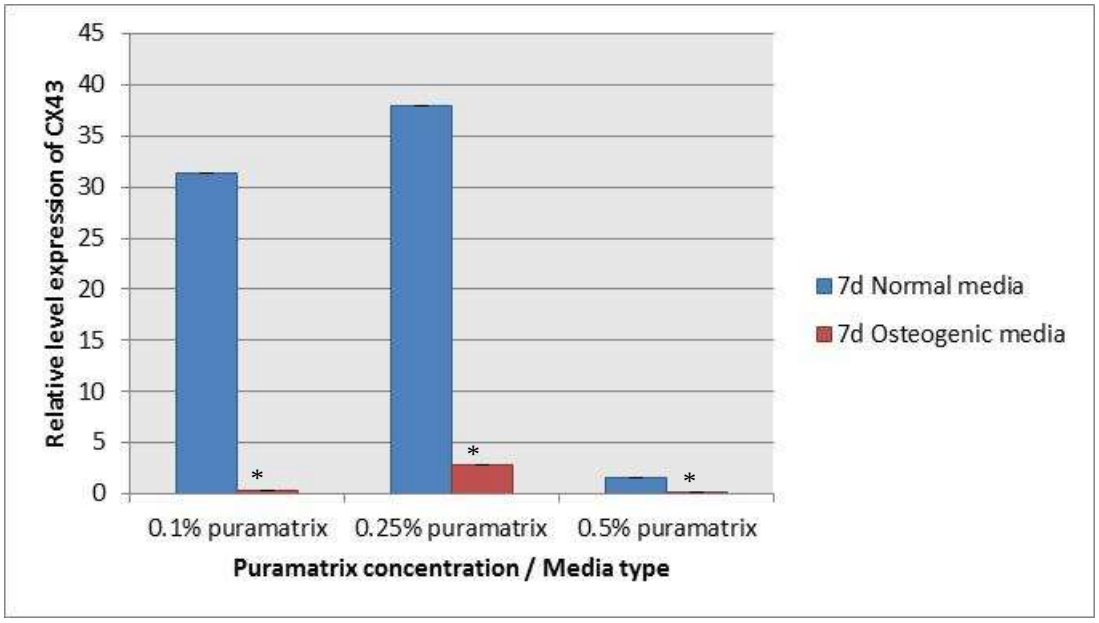

Figure 5.53 *CX43 relative expression level in encapsulated calvarial cells at 7days, the data represents the mean ± standard error of the mean n=9, a statistical significant was considered when P value ≤ 0.05 where (*) indicates significance compared to normal media.*

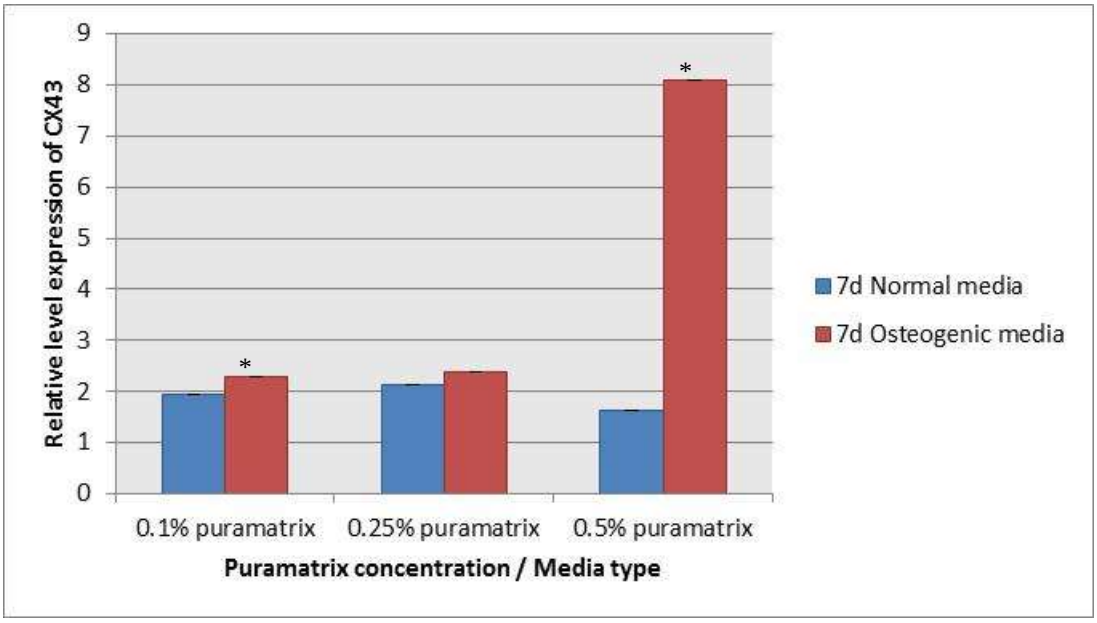

Figure 5.54 *CX43 relative expression level in encapsulated MSCs at 7days, the data represents the mean ± standard error of the mean n=9, a statistical significant was considered when P value ≤ 0.05 where (*) indicates significance compared to normal media.*

Calvaria cells ephrin B1 gene expression was significantly high in 0.1% and 0.25% under normal and osteogenic media respectively compared to other groups [figure 5.55]. But the expression was significantly higher in MSCs in 0.25% Puramatrix grown in osteogenic media [Figure 5.56].

Ephrin B1 expression continued to increase in 0.1% Puramatrix but in both normal and osteogenic media and in 0.25% under osteogenic conditions, whereas it decreased in 0.25% Puramatrix under normal conditions [Figure 5.57]. It also decreased in calvarial cells within 0.5% Puramatrix in both normal and osteogenic media [Figure 5.57]. Although the expression of ephrin B1 increased in MSCs embedded in all three Puramatrix concentrations, the expression was significantly higher in 0.25% Puramatrix grown in osteogenic media [Figure 5.58].

At 7 days the expression of the gene dropped significantly in calvarial cells encapsulated within 0.1% Puramatrix in both normal and osteogenic media and 0.25% Puramatrix and osteogenic media, while in 0.25% normal media the expression increased significantly [Figure 5.59]. In MSCs the expression dropped significantly in 0.25% Puramatrix and osteogenic media, conversely, it increased significantly in 0.5% under osteogenic conditions [Figure 5.60].

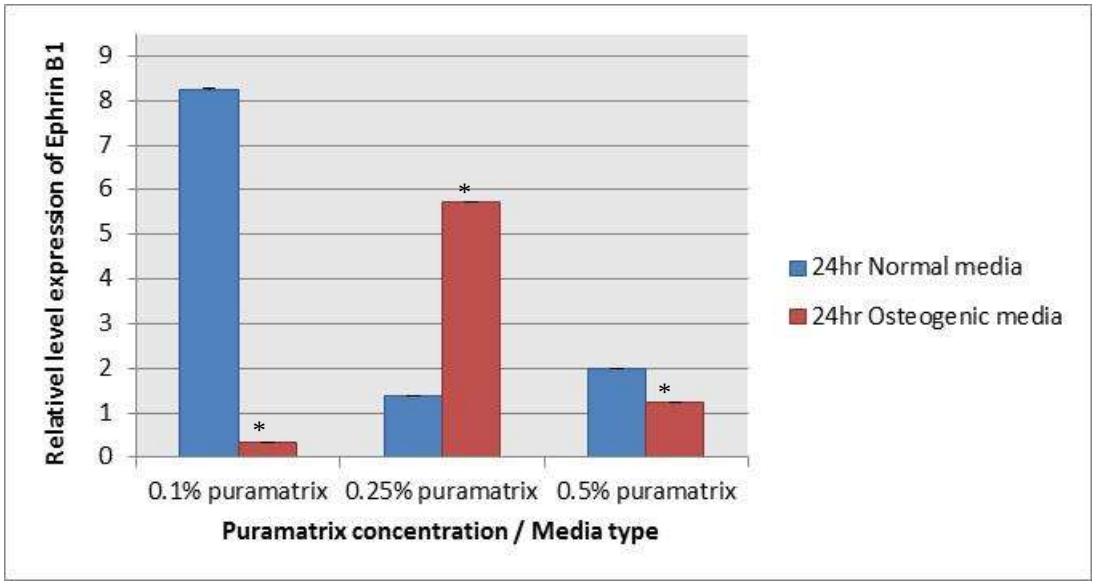

Figure 5.55 *Ephrin B1 relative expression level in encapsulated calvarial cells after 24hr, the Data represents the mean ± standard error of the mean n=9, a statistical significant was considered when P value ≤ 0.05 where (*) indicates significance compared to normal media.*

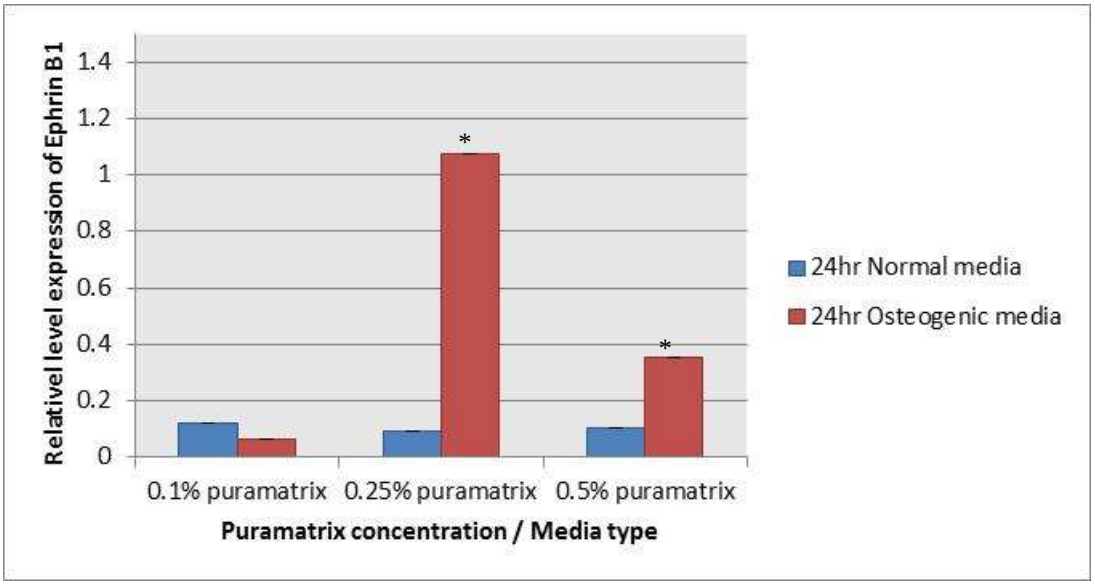

Figure 5.56 *Ephrin B1 relative expression level in encapsulated MSCs after 24hr, the data represents the mean ± standard error of the mean n=9, a statistical significant was considered when P value ≤ 0.05 where (*) indicates significance compared to normal media.*

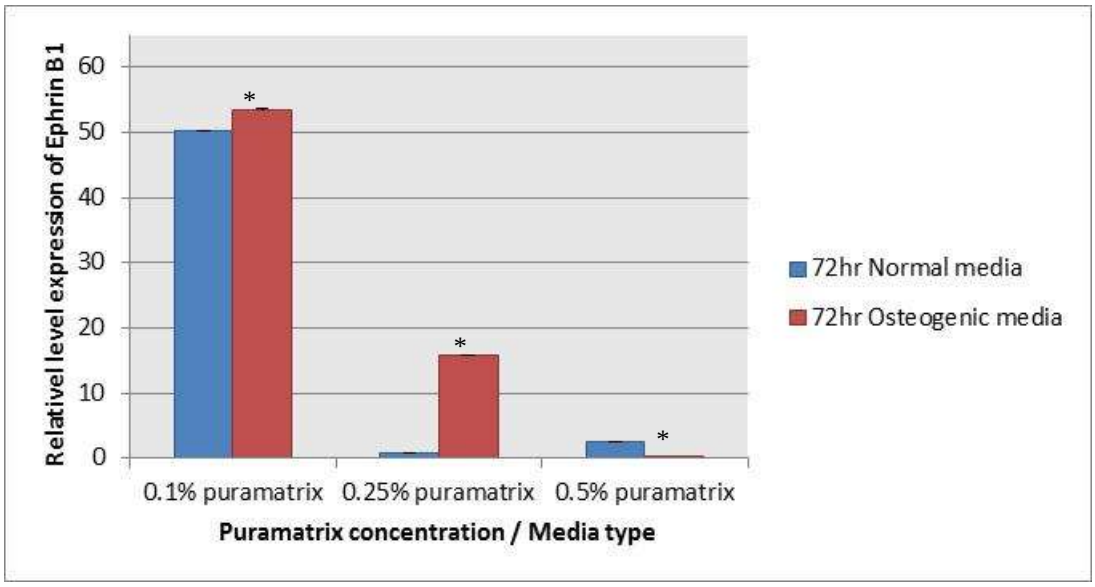

Figure 5.57 *Ephrin B1 relative expression level in encapsulated calvarial cells at 72hr, the data represents the mean ± standard error of the mean n=9, a statistical significant was considered when P value ≤ 0.05 where (*) indicates significance compared to normal media.*

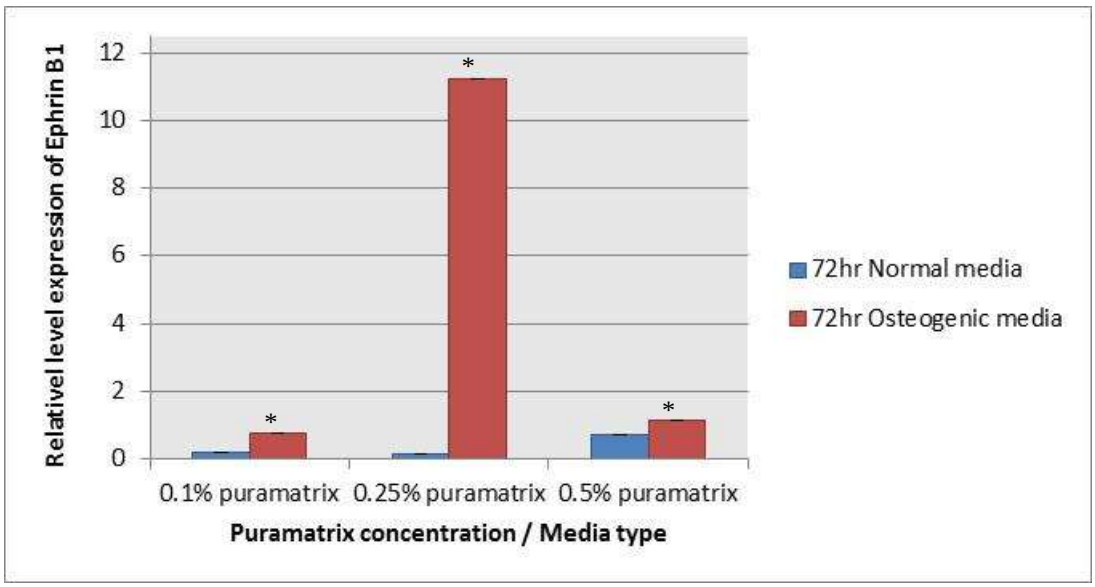

Figure 5.58 *Ephrin B1 relative expression level in encapsulated MSCs at 72hr, the data represents the mean ± standard error of the mean n=9, a statistical significant was considered when P value ≤ 0.05 where (*) indicates significance compared to normal media.*

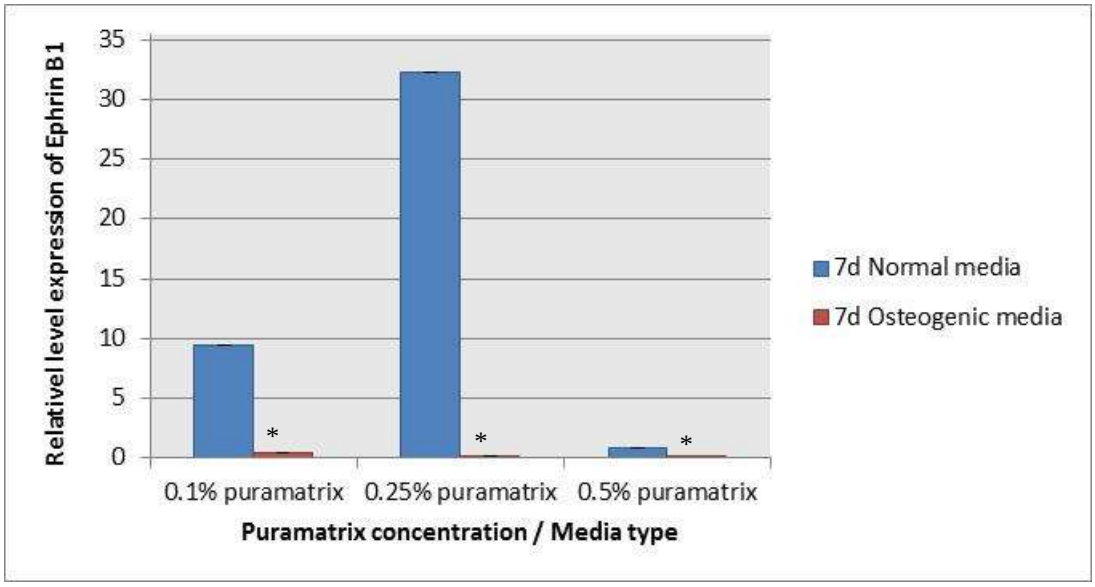

Figure 5.59 *Ephrin B1 relative expression level in encapsulated calvarial cells at 7days, the data represents the mean ± standard error of the mean n=9, a statistical significant was considered when P value ≤ 0.05 where (*) indicates significance compared to normal media.*

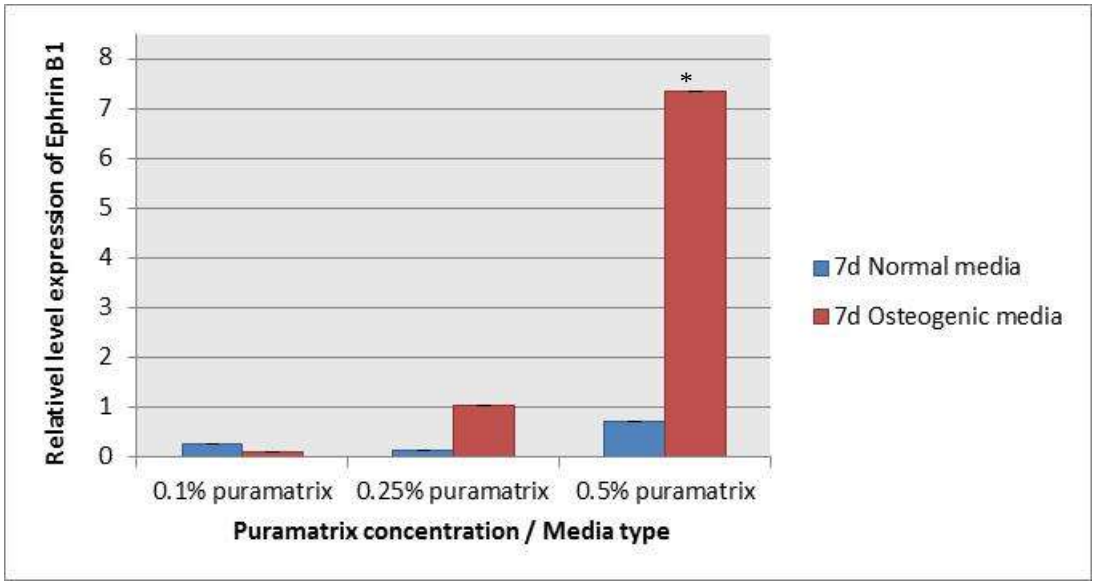

Figure 5.60 *Ephrin B1 relative expression level in encapsulated MSCs at 7days, the data represents the mean ± standard error of the mean n=9, a statistical significant was considered when P value ≤ 0.05 where (*) indicates significance compared to normal media.*

A significantly high level of ephrin B2 mRNA transcripts was identified in calvarial cells encapsulated with 0.1% and 0.25% Puramatrix in normal and osteogenic media respectively [Figure 5.61]. Whereas the level of the gene was slightly more in 0.5% Puramatrix and normal media compared to osteogenic media [Figure 5.61]. On the other hand, the expression of the gene in MSCs was significantly high when encapsulated in 0.5% Puramatrix and grown in osteogenic media [Figure 5.62].

At 72hr the gene expression increased significantly in calvarial cells encapsulated within 0.1% Puramatrix and normal and osteogenic media and it increased also in 0.25% osteogenic media [Figure 5.63]. Whilst in MSCs a significant difference in gene expression was noted, with an increase in the gene expression level recorded in both 0.1% and 0.25% Puramatrix in osteogenic media [Figure 5.64]. Though, the level of the gene decreased at 72hr in MSCs encapsulated within 0.5% Puramatrix and osteogenic media it was still higher than those in 0.5% Puramatrix and normal media [Figure 5.64].

At 7days the expression of ephrin B2 dropped in calvarial cells embedded in 0.1% and 0.5% Puramatrix in normal and osteogenic media and in 0.25% Puramatrix in osteogenic media alone, but increased in 0.25% normal media [Figure 5.65]. Significant differences in the expression of the gene was recorded in MSCs, where it increased in 0.5% Puramatrix in normal and osteogenic media, and in 0.1% and 0.25% Puramatrix in normal media only but decreased in osteogenic media [Figure 5.66].

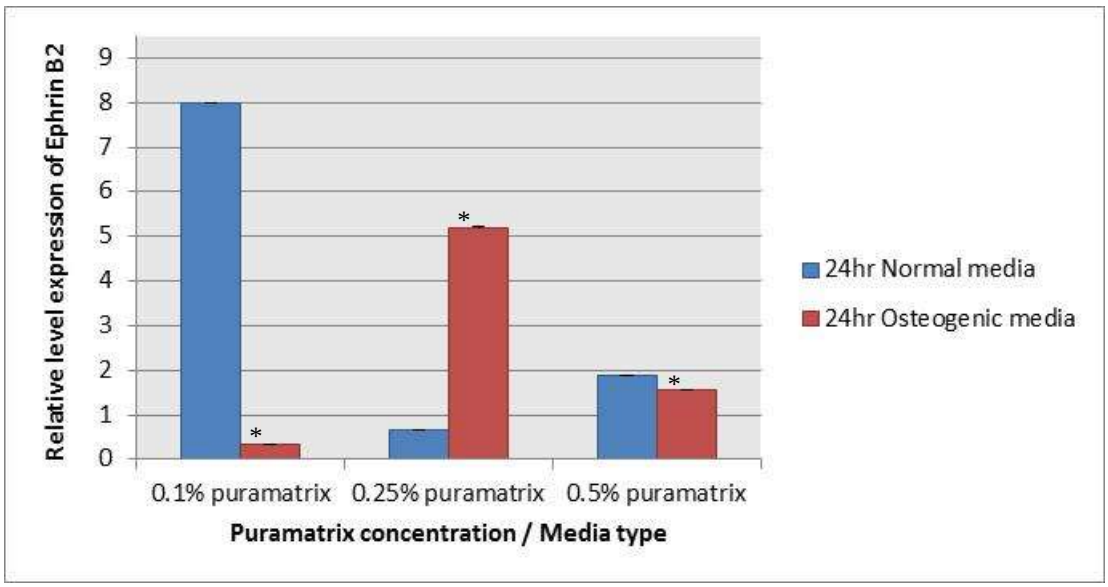

Figure 5.61 *Ephrin B2 relative expression level in encapsulated calvarial cells after 24hr, the data represents the mean ± standard error of the mean n=9, a statistical significant was considered when P value ≤ 0.05 where (*) indicates significance compared to normal media.*

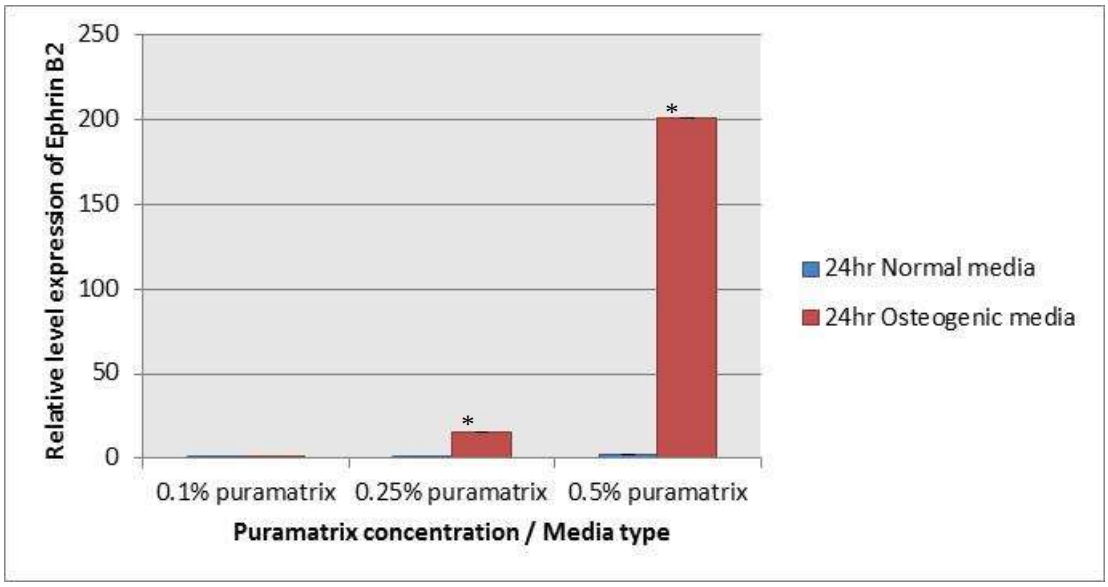

Figure 5.62 *Ephrin B2 relative expression level in encapsulated MSCs after 24hr, the data represents the mean ± standard error of the mean n=9, a statistical significant was considered when P value ≤ 0.05 where (*) indicates significance compared to normal media.*

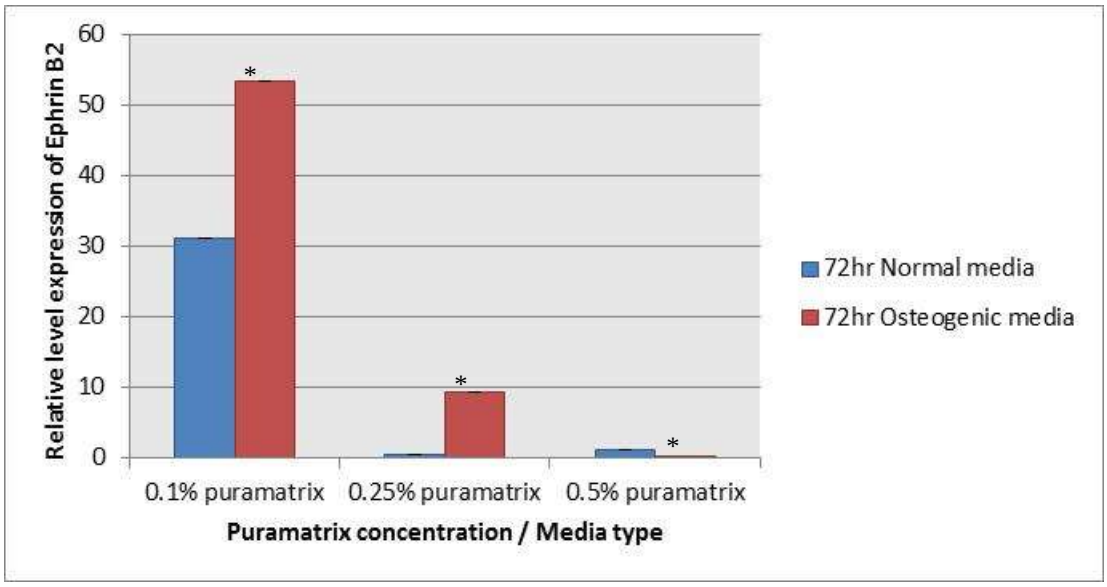

Figure 5.63 *Ephrin B2 relative expression level in encapsulated calvarial cells at 72hr, the data represents the mean ± standard error of the mean n=9, a statistical significant was considered when P value ≤ 0.05 where (*) indicates significance compared to normal media.*

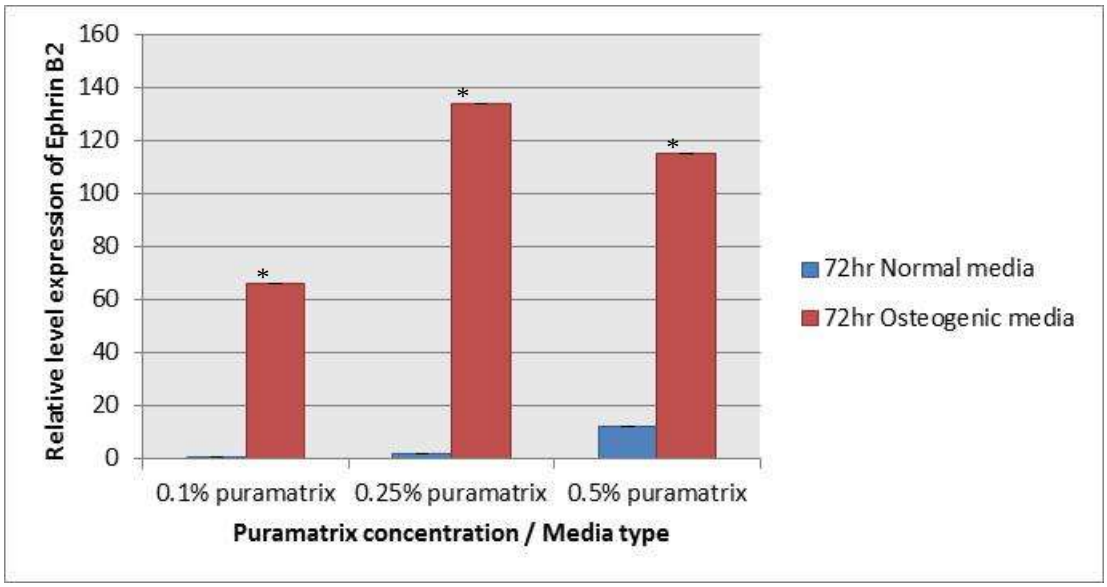

Figure 5.64 *Ephrin B2 relative expression level in encapsulated MSCs at 72hr, the Data represents the mean ± standard error of the mean n=9, a statistical significant was considered when P value ≤ 0.05 where (*) indicates significance compared to normal media.*

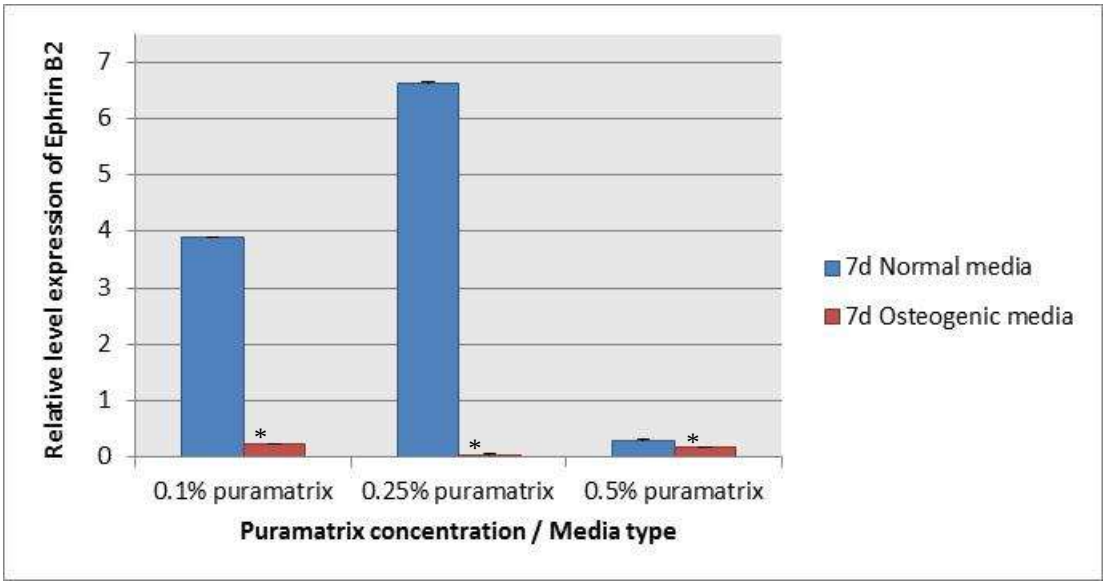

Figure 5.65 *Ephrin B2 relative expression level in encapsulated calvarial cells at 7days, the data represents the mean ± standard error of the mean n=9, a statistical significant was considered when P value ≤ 0.05 where (*) indicates significance compared to normal media.*

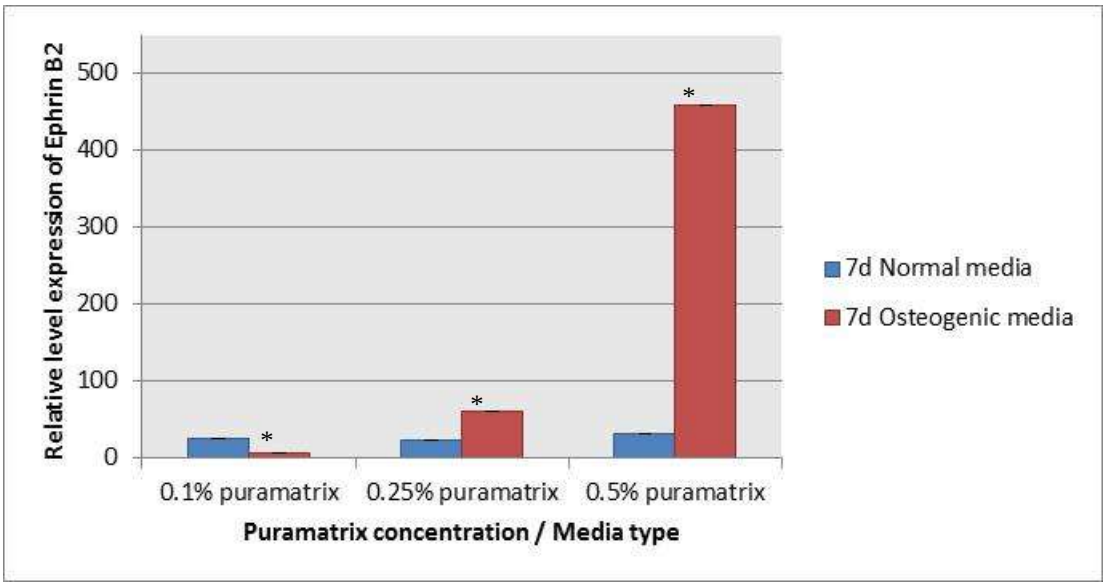

Figure 5.66 *Ephrin B2 relative expression level in encapsulated MSCs at 7days, the data represents the mean ± standard error of the mean n=9, a statistical significant was considered when P value ≤ 0.05 where (*) indicates significance compared to normal media.*

Ephrin B4 gene expression in calvarial cells was high in 0.5% Puramatrix and normal media compared to 0.1% and 0.25% Puramatrix [Figure 5.67]. While in MSCs the expression was high in 0.25% Puramatrix and osteogenic media, and an almost equal expression level was recorded in 0.1% Puramatrix in normal and osteogenic media [Figure 5.68].

In contrast at 72 hrs, the level of the gene increased in calvarial cells within 0.1% Puramatrix plus normal and osteogenic media, and in 0.25% osteogenic media [Figure 5.69]. While it decreased in 0.25% Puramatrix and normal media, and in 0.5% Puramatrix in both normal and osteogenic media [Figure 5.70]. The expression of ephrin B4 was significantly increased an MSCs encapsulated in 0.1%, 0.25% and 0.5% Puramatrix grown in osteogenic media and in 0.25% Puramatrix grown in normal media [Figure 5.71].

At 7days ephrin B4 expression decreased significantly in calvarial cells within 0.1% Puramatrix plus normal and osteogenic media and in 0.25% Puramatrix and osteogenic media while it increased in 0.25% Puramatrix with normal media [Figure 5.72]. In MSCs the expression was also decreased in 0.1% Puramatrix with normal and osteogenic media, likewise in 0.25% Puramatrix in osteogenic media but increased under normal media [figure 5.73]. Whereas the expression increased significantly in 0.5% Puramatrix and normal media accompanied with a slight increase in osteogenic media [figure 5.73].

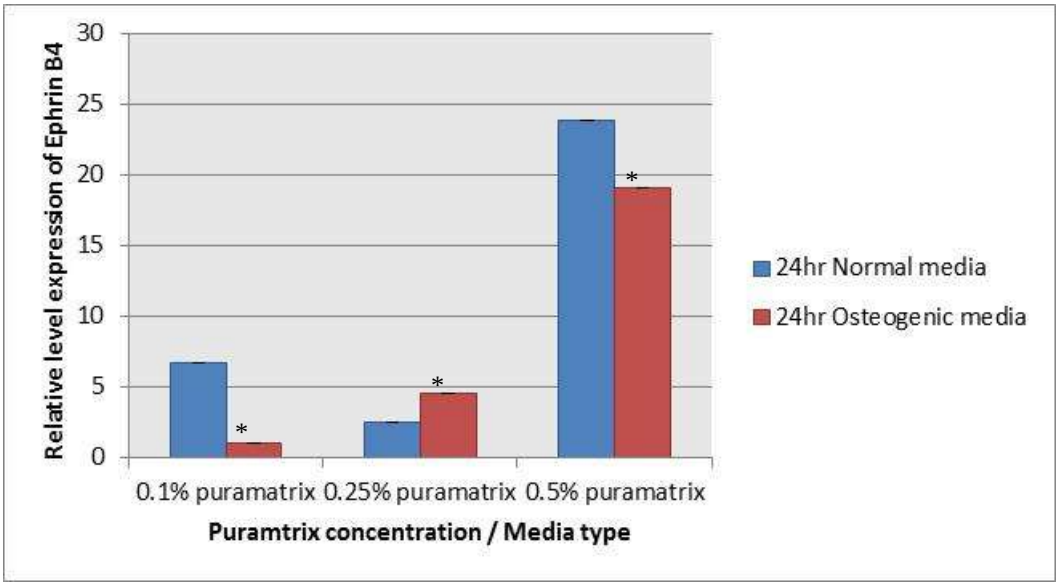

Figure 5.67 *Ephrin B4 relative expression level in encapsulated calvaria cells after 24hr, the data represents the mean ± standard error of the mean n=9, a statistical significant was considered when P value ≤ 0.05 where (*) indicates significance compared to normal media.*

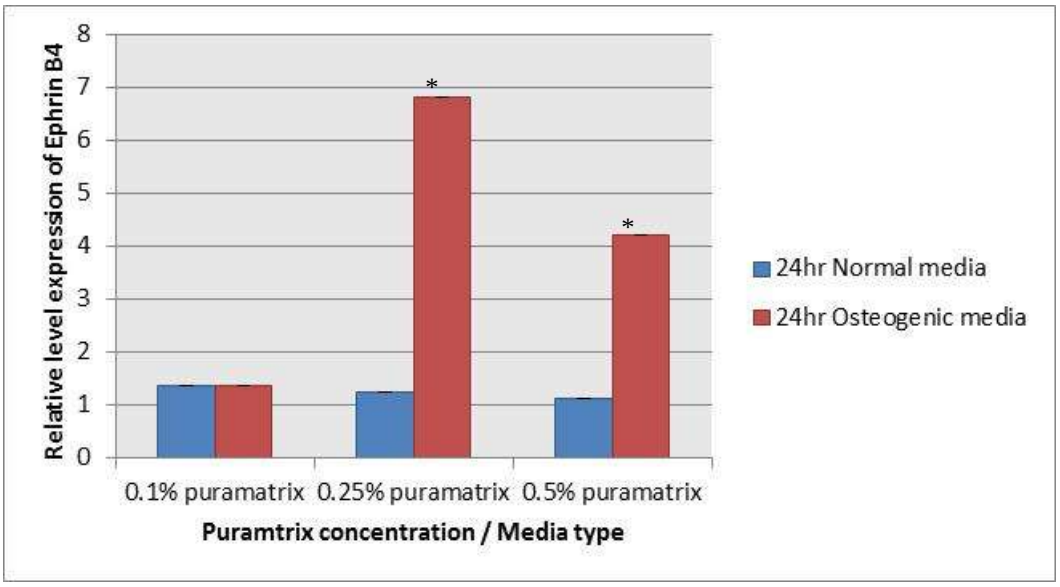

Figure 5.68 *Ephrin B4 relative expression level in encapsulated MSCs after 24hr, the data represents the mean ± standard error of the mean n=9, a statistical significant was considered when P value ≤ 0.05 where (*) indicates significance compared to normal media.*

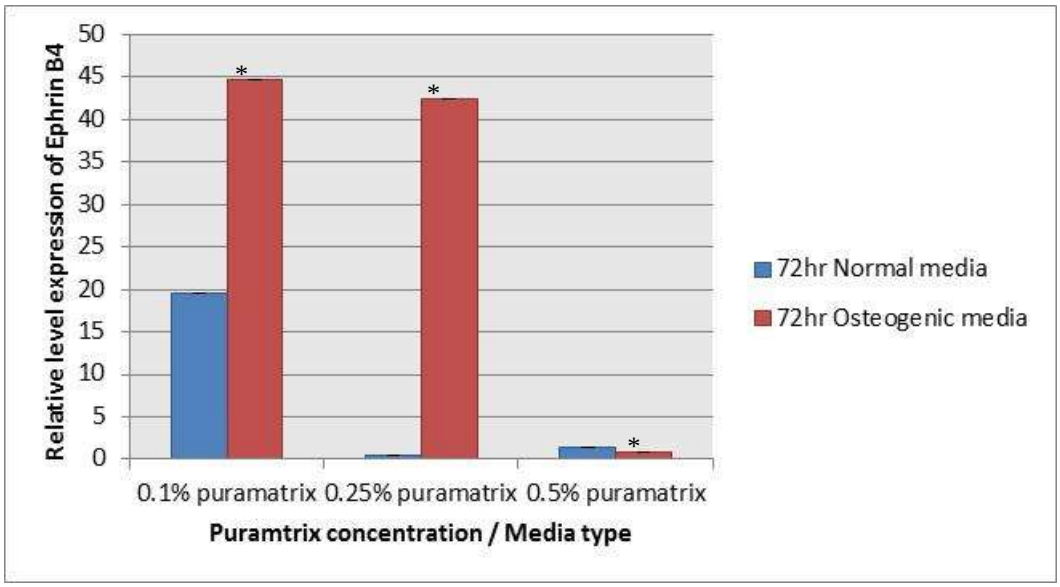

Figure 5.69 *Ephrin B4 relative expression level in encapsulated calvarial cells at 72r, the data represents the mean ± standard error of the mean n=9, a statistical significant was considered when P value ≤ 0.05 where (*) indicates significance compared to normal media.*

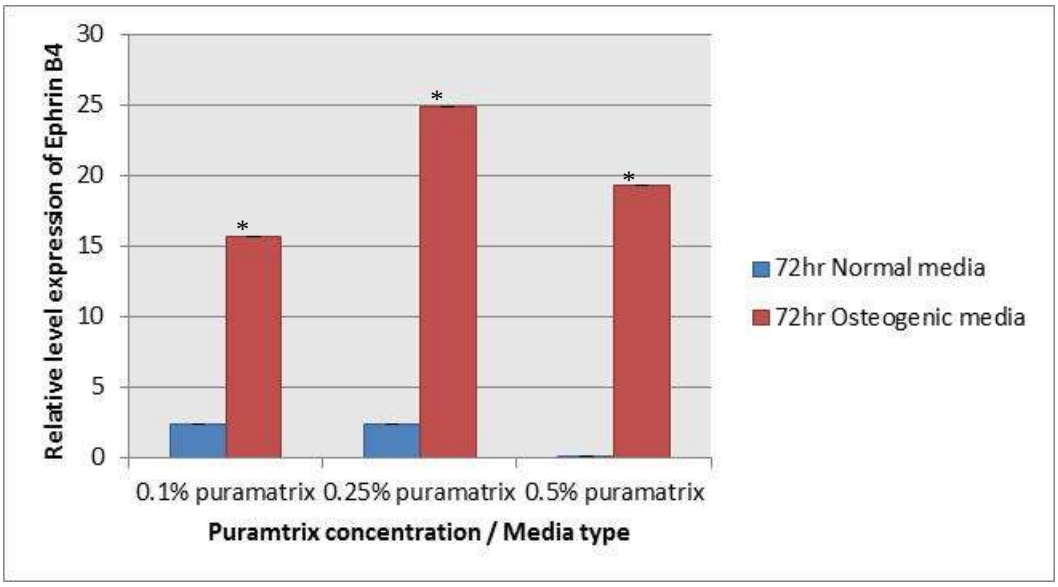

Figure 5.70 *Ephrin B4 relative expression level in encapsulated MSCs at 72hr, the data represents the mean ± standard error of the mean n=9, a statistical significant was considered when P value ≤ 0.05 where (*) indicates significance compared to normal media.*

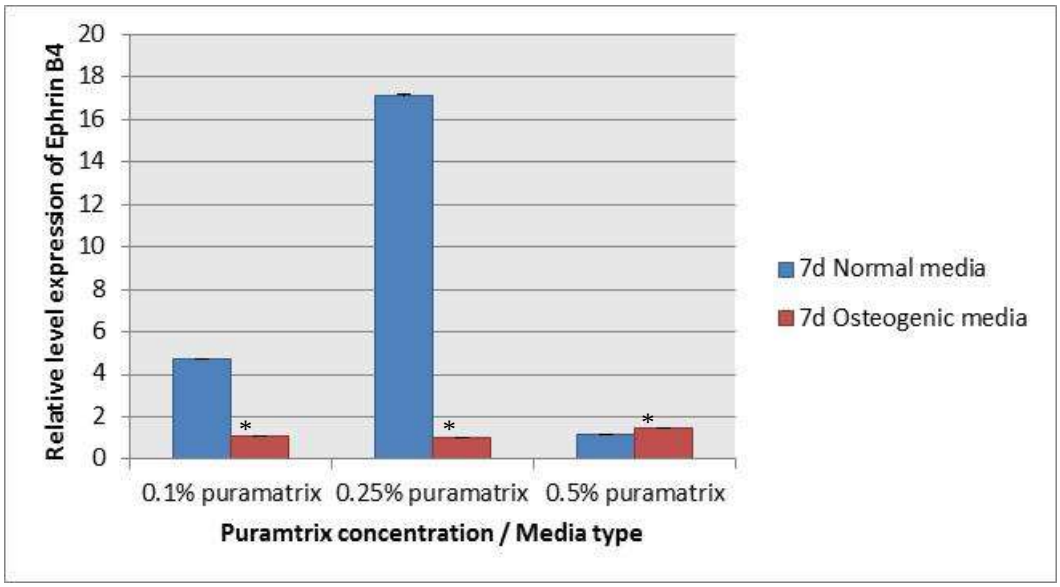

Figure 5.71 *Ephrin B4 relative expression level in encapsulated calvarial cells at 7days, the data represents the mean ± standard error of the mean n=9, a statistical significant was considered when P value ≤ 0.05 where (*) indicates significance compared to normal media.*

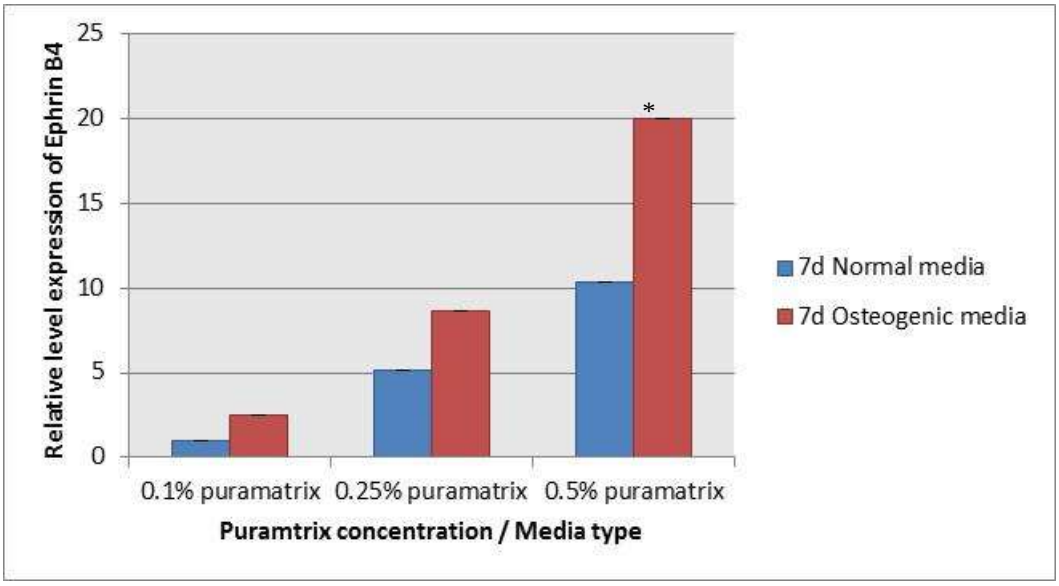

Figure 5.72 *Ephrin B4 relative expression level in encapsulated MSCs at 7days, the data represents the mean ± standard error of the mean n=9, a statistical significant was considered when P value ≤ 0.05 where (*) indicates significance compared to normal media.*

5.4 Discussion:

Hydrogel scaffolds have been the subject of intensive research interest as candidates in tissue engineering due to their similarities to natural ECM and their ability to be modified (Haycock 2011; El-Sherbiny and Yacoub 2013). In the present study different concentrations of Puramatrix peptide hydrogel was tested assessed for their ability to influence osteogenesis and also alter the balance of cell-cell and cell-ECM interactions both in 2D and 3D.

Puramatrix is a self- assembling peptide that forms a hydrogel scaffold of nanofibers (McGrath, Novikova et al. 2010). According to the manufacturers, cells can be either seeded on top of the hydrogel surface or encapsulated within the hydrogel. In this study the first attempt was to seed cells on the surface of the Puramatrix. The results revealed the difficultly to obtain a durable layer of the scaffold which remained intact throughout the experimental period. A significant contribution to this is undoubtedly the weak physical properties of the scaffold (Akiyama, Yamamoto-Fukuda et al. 2013) but mechanical tearing of the gel by the contractility of the cells cannot be ruled out. Consequently because of the hydrogel breaking some cells formed clusters while others adhered to what is likely to be the well plate surface (as viewed under phase contrast microscopy). However, when examined under scanning electron microscope a thin layer of biomaterial was seen where cells adhered to it. In this case it is likely that the stiffness of the underlying plastic contributes to reinforce the mechanical properties of the Puramatrix. In addition, SEM studies showed the formation of nanofibers mesh in all Puramatrix concentrations but this was denser at high concentrations. The structures of these fibres has previously been examined but by using atomic force microscopy where it was shown that at low Puramatrix concentration 0.1% and 0.25%, homogenous single and

bundle fibers were formed, while at higher concentrations a very dense nanofiber network was formed (Ortinau, Schmich et al. 2010).

An initial objective of the study was to examine and compare cells grown as a monolayer on the surface of a culture plate and on a Puramatrix hydrogel surface. However since it was difficult to obtain an intact layer of Puramatrix to which cells could unequivocally attach we had to focus our studies on cells encapsulated in Puramatrix. The work presented here found that with 0.1% Puramatrix the cell/hydrogel mixture was homogenous compared to 0.25% and 0.5%. Also, in all three concentrations cells were seen to communicate with each other as well as the surrounding material. This communication would likely allow cells to coordinate their activity through cell-cell interactions and secretion of paracrine molecules (Yoshida and Teramoto 2007).

The ability of Puramatrix to facilitate bone regeneration has previously been reported by (Misawa, Kobayashi et al. 2006). This is affected by cell viability and ability to produce osteogenic markers. In the current study when comparing the viability of the cells between rat calvaria cells and human MSCs it was found that at low concentration (0.1%) of Puramatrix and at high concentration (0.5%) the viability of MSCs was elevated. But when using 0.25% Puramatrix concentration the viability of calvaria cells was increased. These results suggest that undifferentiated cells respond differently to different concentrations of Puramatrix. This was confirmed by alkaline phosphatase enzyme activity measurement where it was greater in MSCs at 0.1% and 0.5% of the Puramatrix. However, when measuring the relative level expression of ALP it was found that calvarial cells grown in normal media expressed more ALP while it was higher in MSCs grown in osteogenic media in all concentrations. A possible explanation for this conflict between ALP colorimetric assay and qRt-PCR results could be due to the

sensitivity of the colorometric assay to different factors such as light (van Meerloo, Kaspers et al. 2011). However, this result has not previously been described.

On the other hand, effects of Puramatrix hydrogel concentration on osteogenic gene expression were examined. The results of the study showed that overall the expression of Runx2, Cx43, SP7, ephrinB1, ephrinB2, and ephrinB4 was greater in calvarial cells grown in normal media and in MSCs grown in osteogenic media. This suggested that, not only the concentration of Puramatrix may affect osteoblastogeneisis but also media composition as well.

The differential effects of Puramatrix concentration on cell activity could likely be mediated through the different mechanical properties of the gels. Evidence suggests that the compliance of the interacting material will influence the biology of cells with for example MSCs differentiating to fat cells on a soft substrate whilst moving towards the osteoblast lineage on stiffer materials (Engler, Sen et al. 2006). In addition, our system could also influence the way in which cells interact with each other with cells within a high concentration of Puramatrix likely finding it more difficult to form cell-cell interactions in this environment.

In conclusion, Puramatrix hydrogel enhances cells osteogenesis in all three concentrations even though two cell lines behaved differently to different concentrations of hydrogel. Thus it is preferable to test the optimal concentration when using different cell lines.

Chapter 6: Final conclusions and future work

This study set out to address three aims: the first was to optimize the formation of spheroids in vitro and then assess spheroid viability and potential towards osteogenesis in comparison to cells grown in conventional monolayer [2D]; the second aim used rat calvarial cells and human mesenchymal stem cells and the spheroid culture system to examine cell/cell interactions and finally the last aim used RAD16-1 which is known commercially as Puramatrix™ and MAPTrix as a scaffold to create 3D environments for the cells and so manipulate the balance of cell-cell and cell-ECM interactions.

As tissue culture plastic is a topologically flat surface that poorly reproduces the complex architecture observed *in vivo*, 3D culture systems have been the subject of intense study (Page, Flood et al. 2013). Spheroid cells aggregates are the most widely used 3D culture system (Mueller-Reichert 2010). Since spontaneous cell aggregation occurs only in a few cancerous cell lines 3D culture systems ranging from simple to a more complex methods have been developed for other cell types (Page, Flood et al. 2013). In work presented here, the efficiency of spheroid formation was investigated using different simple approaches and different cells densities for culturing cells in 3D. The results concluded that with the cell types investigated in these studies that using an anti-adhesive material, PolyHEMA to prevent cells adherence was as an effective simple and cost-efficient method for the production of spheroids. However, the limitation of this method is that the size of the spheres initially formed is less controllable, athough the size and number will change anyway over time. It has been suggested that neither a too low or a too high cell density should be used in initially setting up the cultures as the resulting spheroids may exhibit poor intercellular communication and transport limitation respectively (Goldstein 2001). The findings of the work presented here support the idea of

using high cell density for the production of spheroids as previously described (Langenbach, Berr et al. 2011). Moreover, high alkaline phosphatase activity and more mineralization was observed in dense cultures (Goldstein 2001).

In addition, the viability of the cells was measured using MTT assay which seemed a suitable choice during the research. However, other work suggests that measuring total DNA is the most reliable method in 3D culture and when seeding at high cell density (Ng, Leong et al. 2005). Therefore the limitation of various methods available for measuring cells proliferation should be taking in to consideration (Ng, Leong et al. 2005). Our rationale for using MTT was to assess only viable cells in the culture system.

Osteoblastogenesis and mesenchymal stem cell differentiation was investigated and contrasted between traditional tissue culture and in 3D spheroids. It was reported previously that gene expression by cells grown in 3D correlates more closely with the *in vivo* scenario in comparison to 2D cell culture (Sivaraman, Leach et al. 2005). Furthermore, the ability of spheroids to differentiate to osteogenic tissue spontaneously has been previously reported using human unrestricted somatic stem cells (Langenbach, Berr et al. 2011). The results of this study revealed that alkaline phosphatase activity appeared more elevated in 2D cultures compared to 3D. However, it was noted that there were contrasting results between the two types of cells with expression of osteogenic genes; higher when MSCs were grown in osteogenic media while with calvarial osteoblasts significant expression was also observed when grown in normal media. It is therefore important to consider the phenotype of the cells, their environment and the chemical cues given to the cells when interpreting these findings. The rat osteoblast cultures are enriched pools of osteogenic cells that are committed to that lineage while the mesenchymal stem cell populations are heterogeneous and contain cells that are multipotent as well as some that have begun to make fate decisions. The mechanical

environment and cytoskeletal tension is a strong regulator of differentiation and therefore it is of little surprise that rat osteoblasts grown on stiff tissue culture plastic need little encouragement to further differentiate. Whilst for MSCs they would be significantly responsive to the osteogenic media and find the 3D spheroid environment more analogous to the soft marrow pericellular environment, with not only matrix, but also direct contact from other cells influencing their activity.

Because of the potential regulatory cues delivered by cell-cell interactions such as gap junctions, experiments were performed to determine their role. Cx43 in bone has been widely studied where it was found that it releases bone modulators affecting bone remodelling under mechanical stimuli (Batra and Jiang 2012). Also Cx43 is required for the anabolic effect of Parathyroid hormone [PTH] (Loiselle, Paul et al. 2013). Where osteoblasts lacking Cx43 do not respond to PTH causing decrease in bone mineral content, they exhibit altered response to mechanical forces (Plotkin and Bellido 2013). Moreover, previous studies note an up-regulation of Cx43 during fracture healing (Loiselle, Paul et al. 2013). The results of the experiments presented here reveal that Cx43 localization in 2D was different under normal conditions compared to osteogenic media with its redistribution to the cell surface and formation of cell-cell plaques as the cells differentiate. But in 3D culture it was difficult to study Cx43 localization by microscopy, which is considered one of the challenges accompanied with the use of 3D culture systems (Mueller-Reichert 2010), however puntate staining could be observed that may have been of increased intensity at the cell surface. There was certainly evidence of increased immunoreactivity in rat spheroids compared to the ones derived from human MSCs. This was supported by the qRT-PCR data which showed elevated levels of transcripts for Cx43 in rat cells compared to human MSCs. Trends for the expression of Cx43, Ephrin B1 and Ephrin B2 were similar for each cell type in a given condition

showing that regulation of these proteins that are responsible for cell-cell interactions is likely to be coordinated. Interestingly Cx43 expression seemed to increase over the 7 days in human MSCs cultured in 3D perhaps reflecting the formation of durable gap junction structures.

Finally, identifying an optimal scaffold to aid tissue repair in regenerative medicine treatment strategies is a key challenge (Chatterjee, Lin-Gibson et al. 2010). Spheroids provide a way of delivering large numbers of viable cells in a controlled environment to help facilitate regeneration of diseased or damaged tissues. Experiments were therefore performed to investigate if spheroids could be reinforced with biomolecular scaffolds and investigate how this affects cell function. So, mainly we aimed to examine two types of hydrogel MAPTrix and Puramatrix. However due to the poor mechanical properties of MAPTrix, Puramatrix only was used in this study. Puramatrix is a sequence of peptide that builds a hydrogel scaffold of nano-fibers based on bottom-up assembly (Ye, Zhang et al. 2008). An initial attempt to seed cells directly on the surface of Puramatrix and cell drop technique was used to create 3D aggregates. In this study, three concentration of Puramatrix was used. The results showed that Puramatrix enhanced cells osteogenesis overall however, calvarial cell viability in 0.25% of Puramatrix was high compared to other concentrations, while in MSCs the viability was greater in 0.5% Puramatrix. Similarly, alkaline phosphatase activity in calvarial cells was high in 0.25% whereas MSCs favoured 0.5% of Puramatrix. It is interesting that cell osteogenesis was enhanced in Puramatrix hydrogel, although, previous studies reported that osteoblasts favour stiffer materials (McCauley and Somerman 2012; Eyckmans and Chen 2014).

Recently Pannaxins gap junction have interested researchers where studies have shown that osteoblastic cells express pannexins 1 and 3, the former is believed to effect

cell mechanotransduction whereas the latter is a Runx2 signalling target (Plotkin and Bellido 2013). Moreover, these junctions drive cells aggregation through a signalling cascade which remodels actin cytoskeleton (Bao, Lai et al. 2012). In addition, it was found that Pannexin 1 determines the degree of compaction of the spheroids (Fennema, Rivron et al. 2013). Therefore, a further study with more focus on Pannaxins role on cells aggregation and their role on osteogenesis is suggested.

Overall, spheroids form a more complex cell/cell and cell/ECM interaction, however, there is still doubt whether spheroids [3D] is significantly closer to cells in vivo than cells in thin monolayer [2D] because of the challenges associated with culturing spheroids (Achilli, Meyer et al. 2012). For example, it is difficult to control spheroids in culture, microscopy and assays techniques to analyse spheroids are also difficult (Achilli, Meyer et al. 2012) and a high-throughput confocal structural analysis of 3D cultures has not yet been established (Fennema, Rivron et al. 2013).

References:

3DBiomatrix. (2012). "3D Cell Culture 101: An Introduction to 3D Cell Culture Tools and Techniques." Retrieved 8/01/2015, 2015, from www.3DBiomatrix.com.

Abdi, R., P. Fiorina, et al. (2008). "Immunomodulation by mesenchymal stem cells: a potential therapeutic strategy for type 1 diabetes." Diabetes **57**(7): 1759-1767.

Achilli, T. M., J. Meyer, et al. (2012). "Advances in the formation, use and understanding of multi-cellular spheroids." Expert Opin Biol Ther **12**(10): 1347-1360.

Adams, D. S. (2003). Lab Math: A Handbook of Measurements, Calculations and Other Quantitative Skills for Use at the Bench, Cold Spring Harbor Laboratory Press,U.S.

Aggeli, A., N. Boden, et al., Eds. (2001). Self-Assembling Peptide Systems in Biology, Medicine and Engineering Springer.

Akiyama, N., T. Yamamoto-Fukuda, et al. (2013). "In situ tissue engineering with synthetic self-assembling peptide nanofiber scaffolds, PuraMatrix, for mucosal regeneration in the rat middle-ear." Int J Nanomedicine **8**: 2629-2640.

Aranda, R. t., S. M. Dineen, et al. (2009). "Comparison and evaluation of RNA quantification methods using viral, prokaryotic, and eukaryotic RNA over a 10(4) concentration range." Anal Biochem **387**(1): 122-127.

Arora, M. (2013) "Cell Culture Media: A Review." DOI: http://dx.doi.org/10.13070/mm.en.3.175.

Arvanitis, D. and A. Davy (2008). "Eph/ephrin signaling: networks." Genes Dev **22**(4): 416-429.

Atala, A. and B. Lanza, Eds. (2001). Methods of Tissue Engineering Academic Press Inc.

Atala, A. and R. Lanza, Eds. (2001). Methods of Tissue Engineering, Academic Press.

Baharvand, H., S. M. Hashemi, et al. (2006). "Differentiation of human embryonic stem cells into hepatocytes in 2D and 3D culture systems in vitro." Int J Dev Biol **50**(7): 645-652.

Bajaj, P., R. M. Schweller, et al. (2014). "3D Biofabrication Strategies for Tissue Engineering and Regenerative Medicine." Annual review of biomedical engineering **16**: 247-276.

Bao, B. A., C. P. Lai, et al. (2012). "Pannexin1 drives multicellular aggregate compaction via a signaling cascade that remodels the actin cytoskeleton." J Biol Chem **287**(11): 8407-8416.

Bao, J., J. E. Fisher, et al. (2013). "Serum-free medium and mesenchymal stromal cells enhance functionality and stabilize integrity of rat hepatocyte spheroids." Cell Transplant **22**(2): 299-308.

Batra, N. and J. X. Jiang (2012). ""INTEGRINating" the connexin hemichannel function in bone osteocytes through the action of integrin alpha5." Commun Integr Biol **5**(5): 516-518.

Baum, O., R. Hlushchuk, et al. (2007). "Increased invasive potential and up-regulation of MMP-2 in MDA-MB-231 breast cancer cells expressing the beta3 integrin subunit." Int J Oncol **30**(2): 325-332.

Bellows, C. G., J. N. Heersche, et al. (1990). "Determination of the capacity for proliferation and differentiation of osteoprogenitor cells in the presence and absence of dexamethasone." Dev Biol **140**(1): 132-138.

Benson, M. D., L. A. Opperman, et al. (2012). "Ephrin-B stimulation of calvarial bone formation." Dev Dyn **241**(12): 1901-1910.

Bogner, A., P. H. Jouneau, et al. (2007). "A history of scanning electron microscopy developments: Towards “wet-STEM” imaging." Micron **38**(4): 390-401.

Bozzola, J. J. (1998). Electron Microscopy: Principles and Techniques for Biologists, Jones and Bartlett Publishers.

Breslin, S. and L. O'Driscoll (2013). "Three-dimensional cell culture: the missing link in drug discovery." Drug Discov Today **18**(5-6): 240-249.

Chapdelaine, J. M. (1989). "MTT reduction: a tetrazolium-based colorimetric assay for cell survival and proliferation."

Chatterjee, K., S. Lin-Gibson, et al. (2010). "The effect of 3D hydrogel scaffold modulus on osteoblast differentiation and mineralization revealed by combinatorial screening." Biomaterials **31**(19): 5051-5062.

Choi, Y., Ed. (2012). Osteoimmunology: Interactions of the Immune and skeletal systems II. Advances in Experimental Medicine and Biology, Springer.

Cree, I. A., Ed. (2011). Cancer Cell Culture: Methods and Protocols. Methods in Molecular Biology, Humana Press.

Cukierman, E., R. Pankov, et al. (2002). "Cell interactions with three-dimensional matrices." Curr Opin Cell Biol **14**(5): 633-639.

Dang, S. M., M. Kyba, et al. (2002). "Efficiency of embryoid body formation and hematopoietic development from embryonic stem cells in different culture systems." Biotechnol Bioeng **78**(4): 442-453.

de Feijter, A. W., D. F. Matesic, et al. (1996). "Localization and function of the connexin 43 gap-junction protein in normal and various oncogene-expressing rat liver epithelial cells." Mol Carcinog **16**(4): 203-212.

Debruyne, D., M. Mareel, et al. (2009). "Cell aggregation on agar as an indicator for cell-matrix adhesion: effects of opioids." In Vitro Cell Dev Biol Anim **45**(8): 473-482.

Del Duca, D., T. Werbowetski, et al. (2004). "Spheroid preparation from hanging drops: characterization of a model of brain tumor invasion." J Neurooncol **67**(3): 295-303.

Dhandayuthapani, B., Y. Yoshida, et al. (2011). "Polymeric scaffolds in tissue engineering application: a review." International Journal of Polymer Science **2011**.

Dhawan, D., A. B. Jeffreys, et al. (2008). "Cyclooxygenase-2 dependent and independent antitumor effects induced by celecoxib in urinary bladder cancer cells." Mol Cancer Ther **7**(4): 897-904.

Drury, J. L. and D. J. Mooney (2003). "Hydrogels for tissue engineering: scaffold design variables and applications." Biomaterials **24**(24): 4337-4351.

Duval, R. E., I. Clarot, et al. (2012). "Interest of designed cyclodextrin-tools in gene delivery." Annales Pharmaceutiques Françaises **70**(6): 360-369.

Dvir-Ginzberg, M., I. Gamlieli-Bonshtein, et al. (2003). "Liver tissue engineering within alginate scaffolds: effects of cell-seeding density on hepatocyte viability, morphology, and function." Tissue Eng **9**(4): 757-766.

Edwards, C. M. and G. R. Mundy (2008). "Eph receptors and ephrin signaling pathways: a role in bone homeostasis." Int J Med Sci **5**(5): 263-272.

El-Sherbiny, I. M. and M. H. Yacoub (2013). "Hydrogel scaffolds for tissue engineering: Progress and challenges." Global Cardiology Science and Practice **2013**(3): 38.

Engler, A. J., S. Sen, et al. (2006). "Matrix elasticity directs stem cell lineage specification." Cell **126**(4): 677-689.

Eyckmans, J. and C. S. Chen (2014). "Stem cell differentiation: Sticky mechanical memory." Nat Mater **13**(6): 542-543.

Fairman, R. and K. S. Akerfeldt (2005). "Peptides as novel smart materials." Curr Opin Struct Biol **15**(4): 453-463.

Farrell Jr, R. E. (2010). Chapter 2 - RNA Isolation Strategies. RNA Methodologies (4th Edition). R. E. Farrell. San Diego, Academic Press**:** 45-80.

Fennema, E., N. Rivron, et al. (2013). "Spheroid culture as a tool for creating 3D complex tissues." Trends Biotechnol **31**(2): 108-115.

Fichman, G. and E. Gazit (2014). "Self-assembly of short peptides to form hydrogels: Design of building blocks, physical properties and technological applications." Acta biomaterialia **10**(4): 1671-1682.

Firestein, G. S., R. C. Budd, et al. (2008). Kelley's Textbook of Rheumatology, Saunders.

Folkman, J. and A. Moscona (1978). "Role of cell shape in growth control." Nature **273**(5661): 345-349.

Fujita, T., Y. Azuma, et al. (2004). "Runx2 induces osteoblast and chondrocyte differentiation and enhances their migration by coupling with PI3K-Akt signaling." The Journal of cell biology **166**(1): 85-95.

Gelain, F., D. Bottai, et al. (2006). "Designer self-assembling peptide nanofiber scaffolds for adult mouse neural stem cell 3-dimensional cultures." PLoS One **1**: e119.

Gelain, F., A. Horii, et al. (2007). "Designer Self-Assembling Peptide Scaffolds for 3-D Tissue Cell Cultures and Regenerative Medicine." Macromolecular Bioscience **7**(5): 544-551.

Ghosh, S. (2006). Role of tumor architecture in elicitation of effector functions of human cytotoxic T-lymphocytes recognizing melanoma associated antigens. Faculty of Natural Sciences. Basel, Switzerland, The University of Basel. **PhD**.

Goldstein, A. S. (2001). "Effect of seeding osteoprogenitor cells as dense clusters on cell growth and differentiation." Tissue Eng **7**(6): 817-827.

Gross, L. (2006). "Disrupted Intercellular Communication Causes a Disfiguring Birth Defect." PLoS Biol **4**(10): e335.

Haasper, C., J. Zeichen, et al. (2008). "Tissue engineering of osteochondral constructs in vitro using bioreactors." Injury **39 Suppl 1**: S66-76.

Haycock, J. W. (2011). "3D cell culture: a review of current approaches and techniques." Methods Mol Biol **695**: 1-15.

Ho, W. Y., S. K. Yeap, et al. (2012). "Development of multicellular tumor spheroid (MCTS) culture from breast cancer cell and a high throughput screening method using the MTT assay." PLoS One **7**(9): e44640.

Holder, N. and R. Klein (1999). "Eph receptors and ephrins: effectors of morphogenesis." Development **126**(10): 2033-2044.

Hsiao, A. Y., Y. C. Tung, et al. (2012). "384 hanging drop arrays give excellent Z-factors and allow versatile formation of co-culture spheroids." Biotechnol Bioeng **109**(5): 1293-1304.

Hutmacher, D. W., J. C. Goh, et al. (2001). "An introduction to biodegradable materials for tissue engineering applications." Annals of the Academy of Medicine, Singapore **30**(2): 183-191.

Jensen, P. L. (2000). "Eph Receptors and Ephrins." STEM CELLS **18**(1): 63-64.

Jing, Y. and Y. Jian-Xiong (2011). "3-D spheroid culture of bone marrow mesenchymal stem cell of rhesus monkey with improved multi-differentiation potential to epithelial progenitors and neuron in vitro." Clin Experiment Ophthalmol **39**(8): 808-819.

Kadono, H., J. Kido, et al. (1999). "Inhibition of osteoblastic cell differentiation by lipopolysaccharide extract from Porphyromonas gingivalis." Infect Immun **67**(6): 2841-2846.

Kang, H. G., J. M. Jenabi, et al. (2007). "E-cadherin cell-cell adhesion in ewing tumor cells mediates suppression of anoikis through activation of the ErbB4 tyrosine kinase." Cancer Res **67**(7): 3094-3105.

Karadzic, I., V. Vucic, et al. (2014). "Effects of novel hydroxyapatite-based 3D biomaterials on proliferation and osteoblastic differentiation of mesenchymal stem cells." Journal of Biomedical Materials Research Part A.

Karamuk, Z. E. (2001). "Embroidered Textiles for Medical Applications: New Design Criteria with Respect to Structural Biocompatibility."

Kaveh, K., R. Ibrahim, et al. (2011). "Mesenchymal stem cells, osteogenic lineage and bone tissue engineering: a review." Journal of Animal and Veterinary Advances **10**(17): 2317-2330.

Kawai, K., H. Hayashi, et al. (2001). "Assessment of the number of local cytotoxic T lymphocytes required for degradation of micrometer-size tumor spheroids." Cytotechnology **37**(1): 31-40.

Ke, N., A. Albers, et al. (2004). "One-week 96-well soft agar growth assay for cancer target validation." Biotechniques **36**(5): 826-828, 830, 832-823.

Khang, G., M. S. Kim, et al., Eds. (2007). MANUAL FOR BIOMATERIALS/SCAFFOLD FABRICATION TECHNOLOGY. Manuals in Biomedical Research, World Scientific Publishing.

Khoei, S., B. Goliaei, et al. (2004). "Differential thermo-resistance of multicellular tumor spheroids." Iranian Journal of Science and Technology **28**: 107-116.

Kim, S. M., Y. G. Kim, et al. (2013). "The effects of dexamethasone on the apoptosis and osteogenic differentiation of human periodontal ligament cells." J Periodontal Implant Sci **43**(4): 168-176.

Kresse, G.-B. (2003) "Cell Proliferation and Viability Measurement – Delicate Tasks Require Precise Solutions." **3**, 26-28.

Kubota, K., H. D. Preisler, et al. (1981). "Comparison between agar and methylcellulose cultures of human leukemic cells." Cancer Res **41**(8): 3052-3057.

Kullander, K. and R. Klein (2002). "Mechanisms and functions of Eph and ephrin signalling." Nat Rev Mol Cell Biol **3**(7): 475-486.

Kunz-Schughart, L. A. and J. P. Freyer (2002). "Phosphorous metabolites and steady-state energetics of transformed fibroblasts during three-dimensional growth." Am J Physiol Cell Physiol **283**(4): C1287-1297.

Kurioka, D., A. Takagi, et al. (2011). "Multicellular Spheroid Culture Models: Applications in Prostate Cancer Research and Therapeutics." Journal of Cancer Science & Therapy **3**(3).

Kutz, M., Ed. (2009). Biomedical Engineering & Design Handbook, McGraw-Hill Professional.

Kwan Tat, S., J. P. Pelletier, et al. (2008). "Activation of the receptor EphB4 by its specific ligand ephrin B2 in human osteoarthritic subchondral bone osteoblasts." Arthritis Rheum **58**(12): 3820-3830.

Kwan Tat, S., J. P. Pelletier, et al. (2009). "Treatment with ephrin B2 positively impacts the abnormal metabolism of human osteoarthritic chondrocytes." Arthritis Res Ther **11**(4): R119.

Langenbach, F., K. Berr, et al. (2011). "Generation and differentiation of microtissues from multipotent precursor cells for use in tissue engineering." Nat Protoc **6**(11): 1726-1735.

Langenbach, F., C. Naujoks, et al. (2013). "Scaffold-free microtissues: differences from monolayer cultures and their potential in bone tissue engineering." Clin Oral Investig **17**(1): 9-17.

Lanza, R., R. Langer, et al., Eds. (2007). Principles of Tissue Engineering Academic Press.

Le Beyec, J., S.-Y. Xu R Fau - Lee, et al. (2007). "Cell shape regulates global histone acetylation in human mammary epithelial cells." (0014-4827 (Print)).

Lee, S., Ed. (2005). Encyclopedia of Chemical Processing CRC Press.

Lee, W. G., D. Ortmann, et al. (2010). "A hollow sphere soft lithography approach for long-term hanging drop methods." Tissue Eng Part C Methods **16**(2): 249-259.

Li, S., J. Pan, et al. (1999). "Agar coating in multicellular spheroids culture of rat hepatocytes." Chinese Science Bulletin **44**(24): 2246-2249.

Lin, R. Z. and H. Y. Chang (2008). "Recent advances in three-dimensional multicellular spheroid culture for biomedical research." Biotechnol J **3**(9-10): 1172-1184.

Lin, S.-J., W.-C. Hsiao, et al. (2006). "THE EFFECT OF SERUM CONCENTRATION ON THE SPHEROID FORMING ACTIVITY AND CELL GROWTH OF HUMAN MELANOCYTES ON CHITOSAN SURFACE." Biomedical Engineering: Applications, Basis and Communications **18**(01): 42-46.

Ling, T.-Y., Y.-L. Liu, et al. (2014). "Differentiation of lung stem/progenitor cells into alveolar pneumocytes and induction of angiogenesis within a 3D gelatin–Microbubble scaffold." Biomaterials **35**(22): 5660-5669.

Liu, J., L. Ma, et al. (2013). "Spheroid body-forming cells in the human gastric cancer cell line MKN-45 possess cancer stem cell properties." Int J Oncol **42**(2): 453-459.

Loiselle, A. E., E. M. Paul, et al. (2013). "Osteoblast and osteocyte-specific loss of Connexin43 results in delayed bone formation and healing during murine fracture healing." J Orthop Res **31**(1): 147-154.

Longati, P., X. Jia, et al. (2013). "3D pancreatic carcinoma spheroids induce a matrix-rich, chemoresistant phenotype offering a better model for drug testing." BMC Cancer **13**: 95.

Lu, W. and C. M. Lieber (2007). "Nanoelectronics from the bottom up." Nature materials **6**(11): 841-850.

Mark, H. F. (2004). Encyclopedia of Polymer Science and Technology, Wiley-Interscience.

Martin, B. M. (1994). Tissue Culture Techniques: An Introduction, Birkhäuser.

Martinez, E. F., T. A. Donato, et al. (2012). "In vitro effects of ascorbic acid and beta-glycerophosphate on human gingival fibroblast cells." Tissue Cell **44**(5): 325-331.

Matsubara, T., K. Kida, et al. (2008). "BMP2 regulates Osterix through Msx2 and Runx2 during osteoblast differentiation." Journal of biological chemistry **283**(43): 29119-29125.

Matsuo, K. and N. Irie (2008). "Osteoclast-osteoblast communication." Arch Biochem Biophys **473**(2): 201-209.

Mayer, R. J., J. H. Walker, et al., Eds. (1988). Immunochemical Methods in Cell and Molecular Biology Biological Techniques Series, Academic Press Inc

McCauley, L. K. and M. J. Somerman, Eds. (2012). Mineralized Tissues in Oral and Craniofacial Science: Biological Principles and Clinical Correlates, Wiley-Blackwell

McGrath, A. M., L. N. Novikova, et al. (2010). "BD™ PuraMatrix™ peptide hydrogel seeded with Schwann cells for peripheral nerve regeneration." Brain research bulletin **83**(5): 207-213.

Meilander, N. J. and R. V. Bellamkonda (2004). "Biomaterials to promote tissue regeneration." Handbook of Biomedical Engineering and Design.

Mihic, A., J. Li, et al. (2014). "The effect of cyclic stretch on maturation and 3D tissue formation of human embryonic stem cell-derived cardiomyocytes." Biomaterials **35**(9): 2798-2808.

Mirkin, C. A. and C. M. Niemeyer, Eds. (2007). Nanobiotechnology II: More Concepts and Applications Wiley VCH.

Misawa, H., N. Kobayashi, et al. (2006). "PuraMatrixTM facilitates bone regeneration in bone defects of calvaria in mice." Cell transplantation **15**(10): 903-910.

Mueller-Reichert, T., Ed. (2010). Electron Microscopy of Model Systems. Methods in Cell Biology, Academic Press.

Mundy, G. R. and F. Elefteriou (2006). "Boning up on ephrin signaling." Cell **126**(3): 441-443.

Nakamura, H. (2007). "morphology, function, and differentiation of bone cells." Journal of Hard Tissue Biology **16**(1): 15-22.

Ng, K. W., D. T. Leong, et al. (2005). "The challenge to measure cell proliferation in two and three dimensions." Tissue Eng **11**(1-2): 182-191.

Ortinau, S., J. Schmich, et al. (2010). "Effect of 3D-scaffold formation on differentiation and survival in human neural progenitor cells." Biomed Eng Online **9**(1): 70.

Ortinau, S., J. Schmich, et al. (2010). "Effect of 3D-scaffold formation on differentiation and survival in human neural progenitor cells." Biomed Eng Online **9**: 70.

Ozeki, M., S. Kuroda, et al. (2011). "Differentiation of bone marrow stromal cells into osteoblasts in a self-assembling peptide hydrogel: in vitro and in vivo studies." J Biomater Appl **25**(7): 663-684.

Page, H., P. Flood, et al. (2013). "Three-dimensional tissue cultures: current trends and beyond." Cell Tissue Res **352**(1): 123-131.

Pallua, N. and C. V. Suschek (2010). Tissue Engineering: From Lab to Clinic, Springer.

Pampaloni, F., E. G. Reynaud, et al. (2007). "The third dimension bridges the gap between cell culture and live tissue." Nature reviews Molecular cell biology **8**(10): 839-845.

Pease, J. C., M. Brewer, et al. (2012). "Spontaneous spheroid budding from monolayers: a potential contribution to ovarian cancer dissemination." Biol Open **1**(7): 622-628.

Phelan, M. C. (2007). "Basic Techniques in Mammalian Cell Tissue Culture." **36**: 1.1.1–1.1.18.

Phung, Y. T., D. Barbone, et al. (2011). "Rapid generation of in vitro multicellular spheroids for the study of monoclonal antibody therapy." J Cancer **2**: 507-514.

Pietrzak, W. S., Ed. (2008). Musculoskeletal Tissue Regeneration: Biological Materials and Methods Orthopedic Biology and Medicine, Humana Press.

Plotkin, L. I. and T. Bellido (2013). "Beyond gap junctions: Connexin43 and bone cell signaling." Bone **52**(1): 157-166.

Pratap, J., M. Galindo, et al. (2003). "Cell growth regulatory role of Runx2 during proliferative expansion of preosteoblasts." Cancer research **63**(17): 5357-5362.

Rajagopal, K. and J. P. Schneider (2004). "Self-assembling peptides and proteins for nanotechnological applications." Curr Opin Struct Biol **14**(4): 480-486.

Raptis, L., Ed. (2001). SV40 Protocols. Methods in Molecular Biology, Humana Press.

Razali, N. M. and Y. B. Wah (2011). "Power comparisons of shapiro-wilk, kolmogorov-smirnov, lilliefors and anderson-darling tests." Journal of Statistical Modeling and Analytics **2**(1): 21-33.

Riss, T. (2014). "Overview of 3D Cell Culture Model Systems & Validating Cell-based Assays for Use with 3D Cultures." Retrieved 13/03/2014, 2014, from http://www.promega.co.uk/resources/webinars/worldwide/archive/overview-of-3d-cell-culture-model-systems/?utm_source=blog&__utma=1.1534540607.1394738021.1394738021.1394738021.1&__utmb=1.1.10.1394738021&__utmc=1&__utmx=-&__utmz=1.1394738021.1.1.utmcsr=promega.wordpress.com|utmccn=(referral)|utmcmd=referral|utmcct=/2014/03/12/3d-cell-culture-models-challenges-for-cell-based-assays/&__utmv=-&__utmk=77314197.

Rivron, N. C., C. C. Raiss, et al. (2012). "Sonic Hedgehog-activated engineered blood vessels enhance bone tissue formation." Proc Natl Acad Sci U S A **109**(12): 4413-4418.

Robinson, J. P., J. Sturgis, et al. (2009). Immunofluorescence. Immunohistochemical Staining Methods Education Guide, Dako.

Roskams, J. and L. Rogers (2002). Lab Ref, Cold Spring Harbor Laboratory Press.

Rouwkema, J., J. de Boer, et al. (2006). "Endothelial cells assemble into a 3-dimensional prevascular network in a bone tissue engineering construct." Tissue Eng **12**(9): 2685-2693.

Rudisch, A., H. v. d. Kuip, et al. (2012). Molecular Characterization of the Tumour-Stroma Crosstalk Using a Novel 3D Co-Culture In Vitro Model. conference 3D Cell Culture Advanced Model Systems, Applications & Enabling Technologies. Zurich/Switzerland.

Rungarunlert, S., M. Techakumphu, et al. (2009). "Embryoid body formation from embryonic and induced pluripotent stem cells: Benefits of bioreactors." World J Stem Cells **1**(1): 11-21.

Rungarunlert, S., M. Techakumphu, et al. (2009). "Embryoid body formation from embryonic and induced pluripotent stem cells: Benefits of bioreactors." World Journal of Stem Cells **1**(1): 11-21.

Ryadnov, M. G. (2007). "Peptide alpha-helices for synthetic nanostructures." Biochem Soc Trans **35**(Pt 3): 487-491.

Saha, K., J. F. Pollock, et al. (2007). "Designing synthetic materials to control stem cell phenotype." Curr Opin Chem Biol **11**(4): 381-387.

Saleh, F. A., M. Whyte, et al. (2011). "Effects of endothelial cells on human mesenchymal stem cell activity in a three-dimensional in vitro model." Eur Cell Mater **22**: 242-257; discussion 257.

Schwartz, M. A., C. Lechene, et al. (1991). "Insoluble fibronectin activates the Na/H antiporter by clustering and immobilizing integrin alpha 5 beta 1, independent of cell shape." Proceedings of the National Academy of Sciences **88**(17): 7849-7853.

Shaohong, C., K. Chandrasekhar, et al. (2013). "Transgenic Overexpression of Ephrin B1 in Bone Cells Promotes Bone Formation and an Anabolic Response to Mechanical Loading in Mice." PLoS One **8**(7).

Shapiro, S. S. and M. B. Wilk (1964). "An analysis of variance test for normality(complete samples)."

Shi, C. J., J. Gao, et al. (2011). "CD133(+) gallbladder carcinoma cells exhibit self-renewal ability and tumorigenicity." World J Gastroenterol **17**(24): 2965-2971.

Shidham, V. B. and B. F. Atkinson (2007). Cytopathologic Diagnosis of Serous Fluids, Saunders.

Shui, C., T. C. Spelsberg, et al. (2003). "Changes in Runx2/Cbfa1 expression and activity during osteoblastic differentiation of human bone marrow stromal cells." J Bone Miner Res **18**(2): 213-221.

Sivaraman, A., J. K. Leach, et al. (2005). "A microscale in vitro physiological model of the liver: predictive screens for drug metabolism and enzyme induction." Curr Drug Metab **6**(6): 569-591.

Song, I. H., A. I. Caplan, et al. (2009). "Dexamethasone inhibition of confluence-induced apoptosis in human mesenchymal stem cells." J Orthop Res **27**(2): 216-221.

Souza, G. R., J. R. Molina, et al. (2010). "Three-dimensional tissue culture based on magnetic cell levitation." Nature nanotechnology **5**(4): 291-296.

Stachowiak, A. (2010). "Standards in Scientific Communities II Cell Viability." Laboratory Fundamentals in Biological Engineering Retrieved 18/03/2014, 2014, from http://ocw.mit.edu/courses/biological-engineering/20-109-laboratory-fundamentals-in-biological-engineering-spring-2010/lecture-notes/MIT20_109S10_lec_m3d4.pdf.

Sutherland, R., J. Carlsson, et al. (1981). "Spheroids in cancer research." Cancer Research **41**(7): 2980-2984.

TAKEI, J. (2005). "Self-Assembling 3-Dimensional Scaffold Peptide Hydrogel for Bone and General Tissue Regeneration." Journal of Oral Tissue Engineering **3**(2): 71-79.

Taylor, P. (2013). "Product Focus: Microplates, Assay Reagents, Screening Consumables, and Kits." Journal of Biomolecular Screening **18**(4): 504-506.

Triffitt, J. T., R. O. Oreffo, et al. (2001). "Osteogenic stem-cell characterization and development: potentials for cytotherapy." Cytotherapy **3**(5): 413-416.

Tsukada, T., T. Kouki, et al. (2013). "Reassembly of anterior pituitary organization by hanging drop three-dimensional cell culture." Acta Histochem Cytochem **46**(4): 121-127.

Ulrich, T. A., A. Jain, et al. (2010). "Probing cellular mechanobiology in three-dimensional culture with collagen-agarose matrices." Biomaterials **31**(7): 1875-1884.

van Meerloo, J., G. J. L. Kaspers, et al. (2011). Cell sensitivity assays: the MTT assay. Cancer Cell Culture, Springer**:** 237-245.

Vernon-Parry, K. D. (2000). "Scanning electron microscopy: an introduction." III-Vs Review **13**(4): 40-44.

Wang, H., B. Pang, et al. (2012). "Dexamethasone has variable effects on mesenchymal stromal cells." Cytotherapy **14**(4): 423-430.

Wang, W., K. Itaka, et al. (2009). "3D spheroid culture system on micropatterned substrates for improved differentiation efficiency of multipotent mesenchymal stem cells." Biomaterials **30**(14): 2705-2715.

Wilson, K. and J. Walker, Eds. (2000). Principles and Techniques of Practical Biochemistry, Cambridge University Press.

Wirth, C., V. Comte, et al. (2005). "Nitinol surface roughness modulates in vitro cell response: a comparison between fibroblasts and osteoblasts." Materials Science and Engineering: C **25**(1): 51-60.

Xiao, L. and T. Tsutsui (2013). "Characterization of human dental pulp cells-derived spheroids in serum-free medium: stem cells in the core." J Cell Biochem **114**(11): 2624-2636.

Xing, W., J. Kim, et al. (2010). "Ephrin B1 regulates bone marrow stromal cell differentiation and bone formation by influencing TAZ transactivation via complex formation with NHERF1." Mol Cell Biol **30**(3): 711-721.

Yarlagadda, P. K., M. Chandrasekharan, et al. (2005). "Recent advances and current developments in tissue scaffolding." Biomed Mater Eng **15**(3): 159-177.

Ye, Z., H. Zhang, et al. (2008). "Temperature and pH effects on biophysical and morphological properties of self-assembling peptide RADA16-I." J Pept Sci **14**(2): 152-162.

Yoshida, D. and A. Teramoto (2007). "The use of 3-D culture in peptide hydrogel for analysis of discoidin domain receptor 1-collagen interaction." Cell Adh Migr **1**(2): 92-98.

Yoshida, S., S. Shimmura, et al. (2005). "Serum-free spheroid culture of mouse corneal keratocytes." Invest Ophthalmol Vis Sci **46**(5): 1653-1658.

Yu, X., G. P. Dillon, et al. (1999). "A laminin and nerve growth factor-laden three-dimensional scaffold for enhanced neurite extension." Tissue Eng **5**(4): 291-304.

Yusuf, B., R. Gopurappilly, et al. (2013). "Embryonic fibroblasts represent a connecting link between mesenchymal and embryonic stem cells." Dev Growth Differ **55**(3): 330-340.

Zhang, S. (2003). "Building from the bottom up." materials today **6**(5): 20-27.

Zhang, S. and A. Rich (1997). "Direct conversion of an oligopeptide from a β-sheet to an α-helix: a model for amyloid formation." Proceedings of the National Academy of Sciences **94**(1): 23-28.

Zhang, S., X. Zhao, et al. (2005). "PuraMatrix: self-assembling peptide nanofiber scaffolds." Scaffolding in tissue engineering: 217-238.

Zhang, X., L. H. Xu, et al. (2010). "Cell aggregation induces phosphorylation of PECAM-1 and Pyk2 and promotes tumor cell anchorage-independent growth." Mol Cancer **9**: 7.

Zhang, Y., C. Chai, et al. (2006). "Co-culture of umbilical cord blood CD34+ cells with human mesenchymal stem cells." Tissue Eng **12**(8): 2161-2170.

Zhang, Z.-G., Z.-H. Li, et al. (2011). "Advances in bone repair with nanobiomaterials: mini-review." Cytotechnology **63**(5): 437-443.

Zhao, C., N. Irie, et al. (2006). "Bidirectional ephrinB2-EphB4 signaling controls bone homeostasis." Cell metabolism **4**(2): 111-121.

Zhao, X. and S. Zhang (2006). Self-Assembling Nanopeptides Become a New Type of Biomaterial. Polymers for Regenerative Medicine. C. Werner, Springer Berlin Heidelberg. **203:** 145-170.

Appendix A: Dulbecco's Modified Eagle Medium (DMEM) High glucose Media Formulations

Components	Molecular Weight	Concentration (mg/L)	mM
Amino Acids			
Glycine	75	30	0.4
L-Arginine hydrochloride	211	84	0.398
L-Cystine 2HCl	313	63	0.201
L-Glutamine	146	580	3.97
L-Histidine hydrochloride-H2O	210	42	0.2
L-Isoleucine	131	105	0.802
L-Leucine	131	105	0.802
L-Lysine hydrochloride	183	146	0.798
L-Methionine	149	30	0.201
L-Phenylalanine	165	66	0.4
L-Serine	105	42	0.4
L-Threonine	119	95	0.798
L-Tryptophan	204	16	0.0784
L-Tyrosine	181	72	0.398
L-Valine	117	94	0.803
Vitamins			
Choline chloride	140	4	0.0286
D-Calcium pantothenate	477	4	0.00839
Folic Acid	441	4	0.00907
Niacinamide	122	4	0.0328
Pyridoxine hydrochloride	204	4	0.0196
Riboflavin	376	0.4	0.00106
Thiamine hydrochloride	337	4	0.0119

i-Inositol	180	7.2	0.04
Inorganic Salts			
Calcium Chloride (CaCl2-2H2O)	147	264	1.8
Ferric Nitrate (Fe(NO3)3"9H2O)	404	0.1	0.000248
Magnesium Sulfate (MgSO4-7H2O)	246	200	0.813
Potassium Chloride (KCl)	75	400	5.33
Sodium Bicarbonate (NaHCO3)	84	3700	44.05
Sodium Chloride (NaCl)	58	6400	110.34
Sodium Phosphate monobasic (NaH2PO4-2H2O)	154	141	0.916
Other Components			
D-Glucose (Dextrose)	180	4500	25
Phenol Red	376.4	15	0.0399

Appendix B: Dulbecco's Modified Eagle Medium (DMEM) Low glucose Media Formulations

Components [g/L]	Concentration
Inorganic Salts	
CaCl2	0.2
Fe(NO3)3 • 9H2O	0.0001
MgSO4	0.09767
KCl	0.4
NaHCO3	3.7
NaCl	6.4
NaH2PO4	0.109
Amino Acids	
L-Alanyl-L-Glutamine	-
L-Arginine • HCl	0.084
L-Cysteine • 2HCl	0.0626
L-Glutamine	-
Glycine	0.03
L-Histidine • HCl • H2O	0.042
L-Isoleucine	0.105
L-Leucine	0.105
L-Lysine • HCl	0.146
L-Methionine	0.03
L-Phenylalanine	0.066
L-Serine	0.042
L-Threonine	0.095
L-Tryptophan	0.016
L-Tyrosine • 2Na • 2H2O	0.10379
L-Valine	0.094
Vitamins	

Choline Chloride	0.004
Folic Acid	0.004
myo-Inositol	0.0072
Niacinamide	0.004
D-Pantothenic Acid • ½Ca	0.004
Pyridoxal • HCl	-
Pyridoxine • HCl	0.004
Riboflavin	0.0004
Thiamine • HCl	0.004
Other	
D-Glucose	1.0
HEPES	-
Phenol Red • Na	0.0159
Pyruvic Acid • Na	0.11
ADD	
Glucose	-
L-Glutamine	0.584
NaHCO3	-